Extent and chronology of the Pleistocene permafrost in France : database of periglacial structures and OSL dating of sand wedges.

Eric Andrieux

THESE

présentée à

L'UNIVERSITE DE BORDEAUX

Ecole doctorale Sciences et Environnements

par

Eric Andrieux

Pour obtenir le grade de

DOCTEUR

Spécialité : Préhistoire et Géologie du Quaternaire

Extent and chronology of the Pleistocene permafrost in France: database of peri-glacial structures and OSL dating of sand-wedges.

Sous la direction de : Pascal Bertran

le 16 Juin 2017

Après avis de :

Jef Vandenberghe, Professeur émérite, Université d'Amsterdam
Norbert Mercier, Directeur de recherche, CNRS, CRP2A (UMR 5060)

Devant la commission d'examen formée de:

M. **Pascal Bertran**, Ingénieur chargé de recherche, Inrap/PACEA (UMR5199)	Examinateur
M. **Pierre Antoine**, Directeur de recherche, CNRS, LGP (UMR 8591)	Examinateur
M. **Mark Bateman**, Professeur, Université de Sheffield	Examinateur
M. **Julian Murton**, Professeur, Université du Sussex	Examinateur
Mme **Maria Sachez-Goni**, Directeur d'études, EPHE, EPOC (UMR 5805)	Examinateur
Mme **Christelle Lahaye**, Maitre de conférence, Université Bordeaux Montaigne	Examinateur
M. **Jef Vandenberghe**, Professeur émérite à l'Université d'Amsterdam	Rapporteur
M. **Norbert Mercier**, Directeur de recherche, CNRS, CRP2A (UMR 5060)	Rapporteur

Abstract

During the Mid to Late Pleistocene, the land area affected by periglacial conditions expanded and contracted repeatedly over large surfaces in mid-latitude Western Europe. In such environments, permafrost or deep seasonal freezing of the ground formed typical features, which have been the subject of abundant research by geomorphologists. In particular, researchers attempted to reconstruct the maximal extent of Pleistocene permafrost based on field evidence. Although most reconstructions suggest that permafrost spread over part of France during the coldest periods of the Pleistocene, there is no agreement regarding the land surface affected. This is mainly due to the scarcity of field data used for mapping and to the questionable palaeoclimatic significance of certain periglacial features. In addition, permafrost modelling during the Last Glacial Maximum using Global Climate Models does not seem consistent with field data. To solve these issues, a database of Pleistocene periglacial features has been compiled from a review of academic literature and unpublished reports, the analysis of aerial photographs and new field surveys. Polygons, soil stripes, ice-wedge pseudomorphs, sand wedges and composite wedge pseudomorphs were included in the database together with their geographic coordinates, geological context, description and references. The distribution of the identified features was analysed with a GIS software and clearly indicates that large areas in France were affected by periglaciation, apart from the southwesternmost part of France and the Languedoc. Ice-wedge pseudomorphs do not extend south of 47°N which indicates that widespread discontinuous permafrost did not affect the land south of the Paris basin. The exclusive presence of sand wedges with primary infill between 45 and 47°N, mainly in the periphery of coversands, suggests that thermal contraction cracking of the ground occurred together with sand drifting in a context of deep seasonal frost or sporadic discontinuous permafrost, unfavourable for the growth of significant ground-ice bodies. However, the description of composite-wedge pseudomorphs below 47°N indicates that at least locally ice veins formed probably during exceptionally cold winters. To provide a chronological framework for thermal contraction cracking single-grain OSL measurements were performed on 33 samples taken in the sandy infilling of sand-wedges and composite-wedge pseudomorphs. Results suggest that multiple events were recorded within wedges. The extraction of the datasets using the Finite Mixture Model, which was developed to analyse statistically data comprising multiple components, allowed calculating 86 ages. These age estimates show that wedge activity in France occurred at least 11 times over the last 100 ka. The most widespread events of thermal contraction cracking occurred between ca. 30 and 24 ka (Last Permafrost Maximum) and are concomitant with periods of high sand availability (MIS 2). Although most phases

of sand-wedge growth correlate well with known Pleistocene cold periods, the identification of wedge activity during late MIS 5 and the very beginning of the Holocene strongly suggests that sand-wedges do not only indicate permafrost but also deep seasonal ground freezing in the context of low winter insolation. The previously published young ages yielded by North-European sand-wedges likely result from poor record of periglacial periods concomitant with low sand availability and/or age averaging inherent to standard luminescence methods. This work allowed us to propose a map of the maximum extent of Late Pleistocene permafrost in France, which partially reconciles field data with palaeoclimatic simulations. The remaining discrepancies may be linked with a potential time lag between the Last Permafrost Maximum (c. 31–24 ka) and the Last Glacial Maximum (21 ka) and to the already identified warm winter bias of the models.

Résumé

De nombreuses tentatives de reconstruction de l'étendue du paléo-pergélisol à partir de données de terrain montrent que de grandes parties de la France ont été affectées à la fin du Pléistocène. Cette étendue maximale a été attribuée au Dernier Maximum Glaciaire (DMG). Néanmoins, des contradictions existent entre les différentes reconstructions qui ont été réalisées pendant près d'un siècle ; elles résident en partie dans l'absence de consensus sur la signification paléoclimatique de certaines structures périglaciaires. De plus, le cadre chronologique utilisé pour ces reconstructions est principalement basé sur des datations relatives et/ou sur l'hypothèse que le maximum de froid durant le dernier glaciaire a été atteint pendant le DMG. Dans ce contexte, il était nécessaire de réévaluer les structures déjà décrites à la lumière de notre connaissance actuelle des processus périglaciaires et d'en chercher de nouvelles pour datation. L'approche développée pour résoudre ces problèmes a été divisée en trois parties. Tout d'abord, une base de données homogène fournissant un accès simple aux structures périglaciaires répertoriées sur le territoire français a été constituée. Celle-ci permet de remettre un site ou une structure dans un contexte régional pour éviter les interprétations simplistes et favorise une vision à l'échelle nationale. Cette base de données est accessible en ligne (https://afeqeng.hypotheses.org/48). Les données en coupe concernant les coins sableux, les pseudomorphoses de coin de glace et les coins composites ainsi que les données obtenues à partir de photos aériennes sur les polygones et les sols striés ont été compilées. Dans la deuxième partie de notre travail, nous nous sommes attachés à traiter les données recueillies. L'analyse à l'aide d'un SIG nous a apportée des informations sur l'influence de différents facteurs sur le développement des structures périglaciaires. Des comparaisons avec un ensemble de données du Nord de l'Europe a rendu possible la proposition d'une nouvelle carte des limites du pergélisol lors de son extension maximale en Europe de l'Ouest. La carte a ensuite été comparée avec des simulations du pergélisol issues de Modèles Globaux du Climat. Enfin, la troisième partie de cette thèse fournit le premier cadre chronologique pour la fissuration par contraction thermique du sol en France, en s'appuyant sur la datation par luminescence optiquement stimulée (OSL) du remplissage sableux des coins.

Extension géographique des structures périglaciaires en France

La distribution des structures identifiées indique clairement que de larges zones en France ont été affectées par des phénomènes périglaciaires, sauf l'extrême Sud-Ouest et le Languedoc. Les structures périglaciaires sont principalement situées dans des bassins sédimentaires, en particulier dans des dépôts alluviaux datant du début ou du milieu du Pléistocène.

Les pseudomorphoses de coin de glace se situent uniquement au nord de la latitude 47°N, préférentiellement dans des terrains mal drainés. Leur présence prouve que les régions localisées au nord de cette latitude ont été affectées *a minima* par du pergélisol discontinu étendu, qui se développe dans des environnements actuels lorsque la température moyenne annuelle de l'air (TMAA) est inférieure ou égale à -4/-5°C. La distribution des pseudomorphoses de coin de glace est fortement corrélée avec celle des dépôts lœssiques. Néanmoins, leur absence en dessous de 47°N ne peut pas être expliquée uniquement par des difficultés d'identification dans des terrains plus hétérogènes. Elle suggère plutôt que la croissance de corps de glace significatifs n'était pas possible au sud de cette latitude. Les coins composites qui ont été décris à une latitude inférieure à 47°N possèdent un remplissage secondaire limité, ce qui témoigne que, au moins localement, des veines de glace se sont formées à des latitudes plus basses, mais probablement pendant des hivers exceptionnellement froids.

Les coins sableux épigénétiques fossiles sont principalement situés entre 47 et 43.5°N au voisinage de sables de couverture dans la vallée de Loire, le nord de l'Aquitaine et dans la basse vallée du Rhône. L'analyse de ces structures à l'aide d'un SIG montre qu'elles sont présentes essentiellement dans des terrains bien drainés, souvent à une altitude plus élevée que celle des terrains environnants. Leur interprétation est plus controversée dans la mesure où ces structures sont rares dans les environnements actuels et où elles ont été décrites principalement dans des zones arides à pergélisol continu où la déflation est active, notamment en Antarctique. Au Pléistocène, dans un contexte caractérisé par une forte aridité aux latitudes moyennes et par l'extension des déserts froids, ces coins ne doivent probablement être considérés que comme des indicateurs de la contraction thermique puisque le transport éolien de sable était bien plus important que dans des milieux arctiques actuels. C'est notamment le cas en France, comme le suggère la localisation des coins sableux sur les marges de sables de couverture ou à proximité de vieilles formations sableuses soumises à la déflation. La contraction thermique du sol se produit de façon habituelle dans des zones qui sont affectées soit par un gel saisonnier profond, soit par du pergélisol, à des TMAA inférieures ou égales à -1/0°C et jusqu'à 2°C dans des zones hyper-continentales. La fissuration est favorisée par de fortes chutes de température et un gradient thermique moyen dans la couche active supérieur à -10°C/m. L'interprétation de ces structures comme des témoins de pergélisol continu telle qu'elle était admise auparavant est probablement une des principales raisons des différences entre les reconstructions de l'extension du pergélisol qui ont été proposées.

Aucune structure de pingo en système fermé n'a été observée en France. Dans des environnements actuels, ces structures sont limitées au pergélisol continu, c'est-à-dire dans des zones où les TMAA sont

inférieures à -6°C/-8°C. En se basant sur cette observation, il n'y a pour le moment aucune preuve que du pergélisol continu ait affecté la France. Des récentes recherches dans le nord de la France ont néanmoins permis d'identifier les traces d'un potentiel pingo en système ouvert dans des alluvions du dernier glaciaire. Ces structures se forment actuellement *a minima* dans des milieux à pergélisol discontinu étendu. Des déformations thermokarstiques liées à la fonte d'un pergélisol riche en glace (lithalses ?) ont également été identifiées. Leur datation pourrait potentiellement apporter des données pour mieux contraindre les phases de froids extrêmes du dernier glaciaire.

La plupart des sols en tâches et des sols striés sont situés au nord de la latitude 47°N, ce qui correspond à la limite sud de la distribution des pseudormorphoses de coin de glace. Ces structures peuvent dès lors être interprétées comme des déformations d'une couche active dans des milieux à pergélisol.

Aucune corrélation n'a été trouvée entre la taille des polygones, qui sont interprétés comme des réseaux de fissures de contraction thermique et d'autres paramètres tels que la composition du sol. La taille moyenne du diamètre des polygones suggère plutôt que les polygones en France ont atteint un état d'équilibre après leur subdivision durant de multiples ou de longues périodes d'activité.

L'étendue du pergélisol qui a été définie à partir de ces résultats est en accord avec les résultats sur les aquifères profonds d'Europe de l'ouest qui montrent que leur recharge n'a pas été interrompue pendant les phases les plus froides de la fin du Pléistocène dans la majeure partie de la France. La carte proposée est également en accord avec les précédentes reconstructions considérées comme les plus « chaudes ». La reconstruction de l'étendue du pergélisol obtenue par les simulations climatiques montre néanmoins des différences avec les données de terrain. Une des raisons invoquées peut être un décalage dans le temps entre le DMG (21 ka) utilisé pour la modélisation et l'âge de l'extension maximale du pergélisol au dernier glaciaire (31-24 ka), ou également un biais chaud pour les températures hivernales dans les modèles comme déjà identifié par certains auteurs.

Cadre chronologique

Les données chronologiques disponibles sur les structures périglaciaires en France étaient quasi-inexistantes et ce travail constitue un apport significatif à ce sujet.

Dans les dépôts lœssiques du nord de la France, six niveaux principaux de pseudomorphoses de coin de glace ont été décrits. A l'exception de quelques dates OSL, ces structures sont principalement datées par corrélation avec d'autres coupes. Les niveaux de pseudomorphoses de coin de glace indiquent

que de multiples phases d'aggradation et de dégradation du pergélisol se sont produites au cours du Pléistocène récent. L'histoire du pergélisol reconstituée à partir des coupes de lœss diffère fortement de celle suggérée par les âges obtenus dans le Nord de l'Europe sur des coins sableux. Ces derniers indiquent au contraire une phase principale d'activité à la fin du Pléniglaciaire. Les quelques dates précédemment réalisées sur des coins sableux en France ont donné des âges plus anciens que pour ceux du Nord de l'Europe. Des coins appartenant à un même réseau polygonal ont par ailleurs livré des âges différents. Ces résultats suggéraient donc que la croissance des coins de sable a été asynchrone et contrôlée par des facteurs locaux plutôt que globaux. Néanmoins, des datations récentes faites au Canada ont montré que la présence de multiples populations de paléodoses dans des coins sableux pourrait témoigner de plusieurs périodes d'activité. De plus amples recherches étaient donc nécessaires pour établir si c'était le cas ou non. L'étude et la datation des coins sableux français a donné cette opportunité et nous a permis d'établir la première chronologie de la fissuration par contraction thermique en France.

Trois zones ont été prospectées pour trouver de nouveaux coins sableux en vue de leur datation : le nord de l'Aquitaine, la vallée de la Loire et la basse vallée du Rhône. Ces régions sont situées dans le voisinage de sables de couverture ou de sables alluviaux qui ont pu fournir suffisamment de matériel par déflation pour la formation de remplissages primaires sableux pendant le Pléistocène. La recherche dans la basse vallée du Rhône n'a pas permis d'identifier de nouvelles structures, mais 17 échantillons ont été pris dans 5 coins dans le Nord de l'Aquitaine et 16 échantillons dans 8 coins de la vallée de la Loire. L'analyse en OSL *single grain* des échantillons collectés nous a permis d'identifier plusieurs phases d'activité dans chaque échantillon. Les 86 âges obtenus définissent 11 périodes de fissuration par contraction thermique, ce qui est plus en accord avec l'apparente complexité et le nombre de phases à pseudomorphoses de coin de glace dans le Nord de la France. La croissance des coins étaient plus importante pendant les phases de refroidissement de la fin du Pléistocène lorsque la contraction thermique était concomitante avec la mise en place des sables de couverture. La principale période de contraction thermique identifiée, que ce soit pour les coins sableux ou les coins de glace, s'est produite entre 30 et 24 ka, ce qui correspond très probablement à l'étendue maximale du pergélisol. De façon plus surprenante, il apparait que des coins ont fonctionné pendant la fin du SIM 5 et le début de l'Holocène, c'est-à-dire au cours de périodes pendant lesquelles d'autres proxys (insectes, pollen) montrent clairement que les TMAA étaient trop élevées pour que du pergélisol puisse se développer. Ces périodes sont caractérisées par une faible insolation hivernale, qui cause une forte saisonnalité et un gel saisonnier profond en hiver. Les coins sableux pouvaient se former dans de telles conditions.

Les dates précédemment obtenues sur les coins sableux tombent principalement pendant les SIM 3/2 dans le Nord de l'Aquitaine, ou à la fin du SIM 2 – Dryas récent dans le nord de l'Europe. Ces âges se corrèlent bien avec la principale période de mise en place des sables de couverture dans chacune de ces régions et expliquent donc l'apparente divergence observées entre les deux zones pour la croissance des coins sableux. Par ailleurs, dans la mesure où des méthodes de datation par luminescence conduisant à des âges moyennés ont été utilisées pour dater ces coins, l'identification de plusieurs périodes d'activité est impossible et fournit une explication aux âges variables livrés par des coins appartenant à un même réseau polygonal.

Extent and chronology of the Pleistocene permafrost in France: database of periglacial structures and OSL dating of sand wedges.

Table of Contents

1. Introduction

During the Pleistocene, the low temperatures and the large extent of ice sheets caused 40 to 50% of the earth's land surface to experience multiple phases of periglacial conditions (French, 2007). The repetitive development and thaw of ground ice bodies and the formation of wedges due to thermal contraction cracking of the ground are amongst the processes that shaped, formed and/or deformed the mid-latitudes landscapes during this period. Numerous periglacial relict features that include wedge structures and large involutions have been widely observed in France in the last 80 years which led to the assumption that large parts of France was affected by frost-action during the Pleistocene. In recent years, the development of rescue archaeology has greatly increased the number of features described. Remote sensing and online databases of aerial photographs (Geoportail, Google Earth) have also eased the recognition of patterned ground and large polygonal networks. In modern environments, such features reflect specific cold climate conditions, therefore their relict counterpart should indicate similar past environments. Their study can lead to a better understanding of the periglaciation history in France and Europe. However, the weak agreement between the reconstitutions of past permafrost previously attempted highlights the different interpretations that have been made upon the occurrence of certain periglacial features, and the lack of well-described data. Within this framework, the first goal of this thesis was to create a database that gathers the French undisputable Pleistocene periglacial features. In order to achieve this goal it was necessary not only to re-evaluate the literature, including articles, PhD theses, unpublished dissertations and geology reports from rescue archaeology, in the light of our present understandings of periglacial processes but also to gather new features from field surveys and from the analysis of aerial photographs. GIS-based analysis of the database and placing the French data in a broader context allowed a better understanding of the environmental conditions during the Late Pleistocene. The second goal of the thesis was to provide a chronology of the periglacial events in France by dating sand-wedges with optically stimulated luminescence (OSL).

This work raised many questions that have been addressed in this thesis:

- What are the environmental parameters that influence the formation of the periglacial features studied?

- What are the reasons behind the different interpretations of the field evidence for periglaciation? Which periglacial features were strictly formed under permafrost conditions?

- What was the maximum extent of the permafrost during the Late Pleistocene? Does the

maximum extent of the features correspond to the Last Glacial Maximum?

- What are the techniques that should be used when considering the dating of sand-wedges? Are the previously acquired ages on sand-wedges reliable?

- When did thermal contraction cracking of the ground occur in France during the Late Pleistocene?

This thesis consists of an introductory chapter (2) that aims at providing the scientific background necessary for the understanding of the terms further used. It is followed by chapter 4, which contains the research methodologies and details on the material used that were not developed at length in the papers published in international journals.

Chapter 4 presents the French database of periglacial features and has been published in the journal Quaternaire (Andrieux et al., 2016a; https://afeqeng.hypotheses.org/48). It reports on the selection criteria of the features added to the database, and on the main limits that should be considered when using the data for interpretations.

Chapter 5 deals with the GIS analysis of the database, and was published in the journal Permafrost and Periglacial Processes (Andrieux et al., 2016b). By accommodating different layers of information the main factors that influenced the development of periglacial features in France were elucidated. The geographic distribution of the georeferenced features added to those from northern Europe also allowed us to propose a map of the permafrost boundaries in Western Europe during the Last Permafrost Maximum (LPM). The field data were also compared to the permafrost distribution according to a model downscaled for France to delineate the advances and issues in reconstruction methodologies.

Chapter 6 contains a paper submitted to Earth and Planetary Science Letters (Andrieux et al., submitted). The chronology of thermal contraction cracking in France was investigated thanks to the optical luminescence dating of 33 samples taken in French sand-wedges. The results reflect that the primary sand-filled features have a complex multi-phased activity history, which calls into question our understanding of how periglaciation occurred in Western Europe during the Late Pleistocene.

In chapter 7, results and discussions of the papers are synthesized. It also provides a discussion about the implication of this work and the further research that could be considered to improve our understanding of the Pleistocene periglacial palaeoenvironments in Europe.

2. Scientific background

This paragraph aims at defining the basics of periglacial processes, landforms and terms that will be further discussed.

2.1. Permafrost and deep seasonal freezing of the ground

The most prominent processes in periglacial environment are due to the frost action in the ground. In such environments, the land areas experience either perennially frozen ground, or seasonal frost.

The ground that remains frozen (at temperature at or below 0°C) for at least two consecutive years is termed permafrost (French, 2007). It is topped by a seasonally frozen layer named active layer, i.e. which freezes in winters and thaw in summers. The distribution and thickness of permafrost and the active layer is determined by many factors such as air temperature, thermal conductivity of the ground, ground texture, aspect, vegetation and snow cover, etc. (Mackay, 1993). Permafrost highly impacts the circulation of water in the ground, and is usually classified depending on the percentage of the land area it covers (French, 2007). It is considered as continuous when it underlies more than 90% of an area, as widespread discontinuous when it underlies 50 to 90% and sporadic (or "scattered" sensu Allard and Seguin, 1987) when it underlies between 10 to 50% of the area. This classification is used in this thesis. Continuous permafrost indicates areas with thick permafrost where only localized thawed zones or taliks exist beneath lakes or river channels. Discontinuous permafrost is used for areas that have large unfrozen zones, and sporadic permafrost indicates only patches of perennially frozen ground (Figure 1). A relationship exists between Mean Annual Air Temperatures (MAATs) and the type of permafrost, however the MAATs proposed for the southernmost permafrost boundary and the continuous-to-discontinuous boundary vary according to the authors. In this thesis the MAATs for the permafrost boundaries were chosen following Romanovskij (1976), Vandenberghe and Pissart (1993) and Huijzer and Vandenberghe (1998) and have been taken with caution since the relationship between permafrost and temperatures may have been slightly different in the past (Murton and Kolstrup, 2003).

The degree of differentiation between perennially and seasonally frozen sediment depends largely upon the time over which the permafrost existed (French, 2007). Only few features provide unequivocal proof of periglaciation and their recognition has often proved difficult and led to debate in the scientific community (e.g. Péwé, 1966; Black, 1976; Kasse and Vandenberghe, 1998; Bockheim et al., 2009; Christiansen et al., 2016). Distinguishing nowadays relict or inactive features that

formed under those conditions during the Pleistocene is thus even more complex. Not only the relict features may be deformed or eroded by thermokarst or pedogenesis, but can also relate to multiple events of deep seasonal freezing and/or permafrost. This is why the recognition of frost-action features requires caution and a good understanding of the processes involved in their formation.

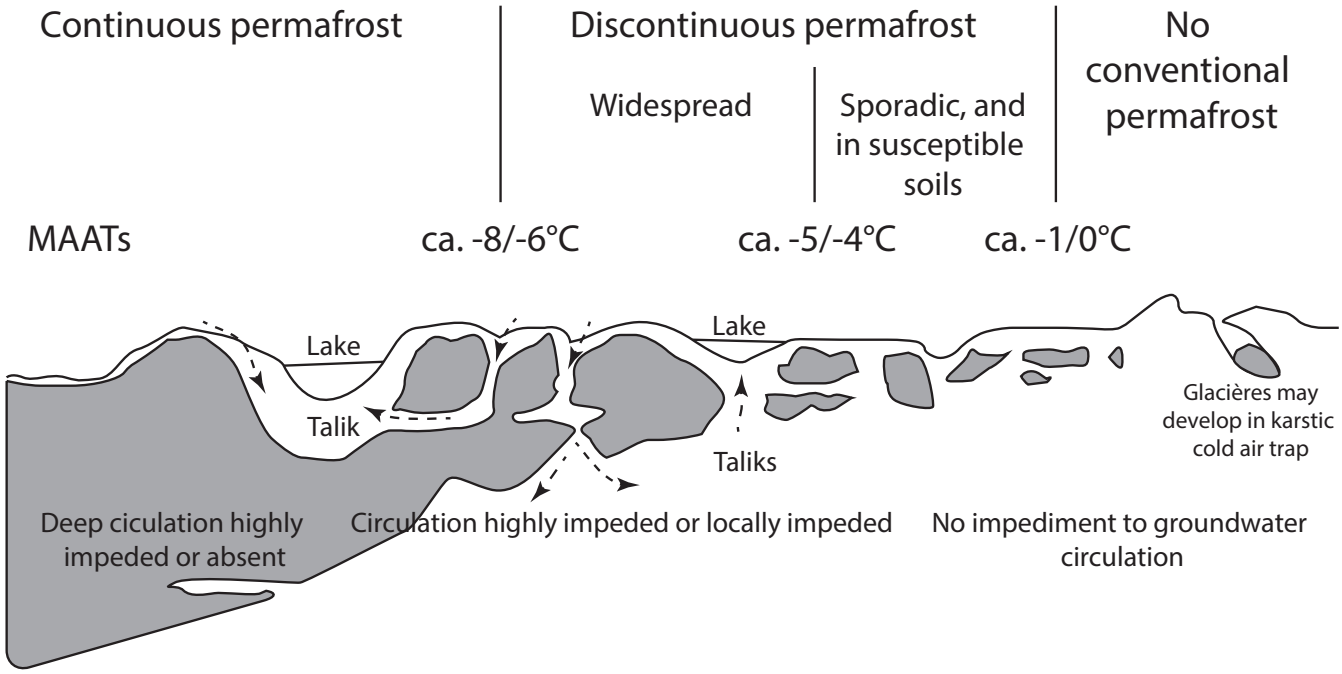

Figure 1: Schematic diagram illustrating the permafrost boundaries and circulation of water. Mean Annual Air Temperatures of the different permafrost types were chosen following Romanovskij (1976), Vandenberghe and Pissart (1993) and Huijzer and Vandenberghe (1998); grey: permafrost; modified from Ford (1993).

2.2. Thermal contraction cracking

The rapid cooling and the lowering of temperatures of the ground can lead to its contraction and subsequent cracking (Lachenbruch, 1962, 1966). This process also known as thermal contraction cracking, occurs in areas that undergo deep freezing of the ground either within permafrost or not, therefore it is one of the most indicative markers for periglaciation. Thermal contraction cracking forms polygonal networks of fissures reaching 5 to 30 m in diameter that were mapped using aerial photographs in France (see chapter 5). These should not be confused with the decimetric cryo-desiccation polygons that are ubiquitous in environment experiencing seasonal freezing (Washburn, 1979). Repeated thermal contraction cracking and filing of the narrow fissures by ice and mineral material builds structures termed veins when they are <10 cm wide or wedges when they are >10 cm (Murton et al., 2000; Murton, 2013) (Figure 2).

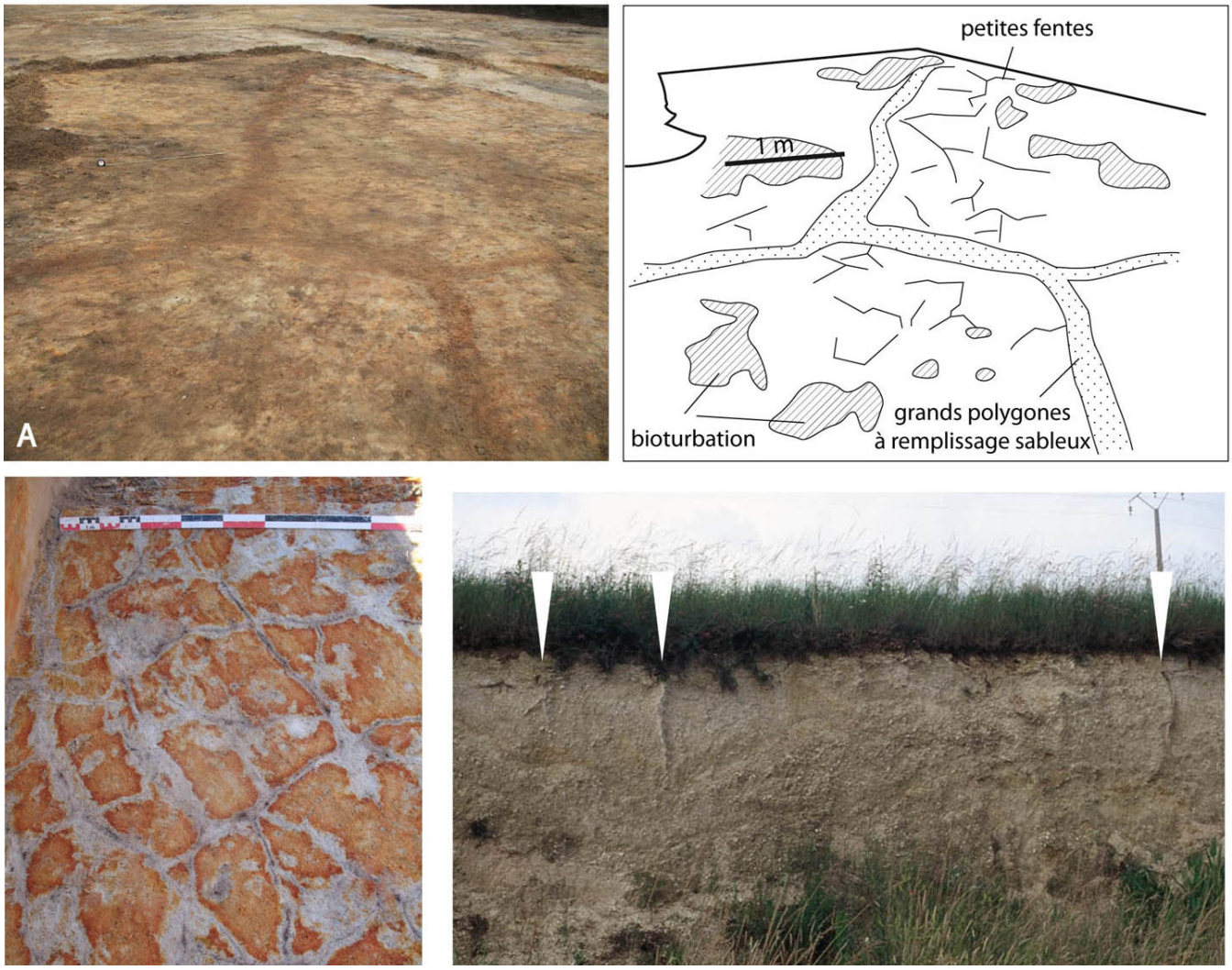

Figure 2: A – Large polygonal network of thermal contraction cracks, subdivided by small cryo-desiccation cracks (Veyrac, France); B – Cryo-desiccation polygons affected by redox processes, in clayey sand (Gironde, France); C – Network of wedges in cross-section (Le Thor, France). Photos P. Bertran.

According to the geomorphological context, three sub-types of wedges can be distinguished. Epigenetic wedges develop in stable host materials and grow sideways. Syngenetic wedges grow upward in environments characterised by a high rate of sedimentation (e.g. in loess deposits). Anti-syngenetic wedges grow downward on surfaces subject to erosion (Murton, 2013) (Figure 3).

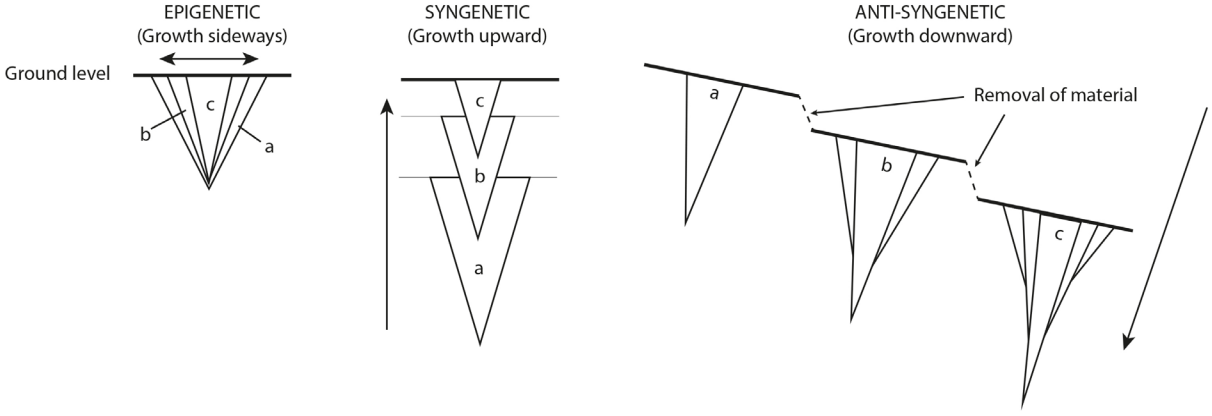

Figure 3: Classification of wedges according to growth direction

In current environments, wedges are classified depending on their infilling that can vary based on suface conditions:

- In a permafrost milieu, snow or melt-water may fill the cracks during the summer and freeze at depth. The repetition of this process forms V-shaped ice-wedges (Murton, 2013) (Figure 4A). During phases of permafrost degradation, the void left by the ice-body may be filled by overlying sediment or host material. This is distinguished as a 'secondary infilling'. Ice-wedge thaw usually led to host material deformations and micro-faulting (Harris et al., 2005) and relict structures bear little resemblance with active ice-wedges. They are called ice-wedge pseudomorphs. Many ice-wedge pseudomorphs have been identified in northern France, essentially in the loess deposits.

- The primary infilling of wedges by ground material forms soil wedges. The most distinctive of these are sand-wedges (Figure 4B). They are formed by the progressive infilling of thermal contraction cracks by aeolian sand (Péwé, 1959; Murton et al., 2000). In modern environments, active sand-wedges have been mostly described in polar deserts in continuous permafrost (e.g. in Antarctica; Bockheim et al., 2009) but they may form in seasonally frozen ground (Wolffe et al., 2016). Sand wedges have a high preservation potential as they are not composed of ice, and therefore do not get deformed during permafrost thaw. Relict sand-wedges have been described in French Quaternary sediments and are valuable geochronological proxies that can be dated (see chapter 6).

- The infilling of both ice and ground-material lead to the formation of composite-wedges (Figure 4C). Therefore, these wedges in a relict state present both primary and secondary infillings. Composite-wedge pseudomorphs were identified in France, but difficulties in the recognition of secondary infillings may have led to their classification as sand-wedges (see chapter 4).

Figure 4: A - Ice-wedge (Canadian Arctic, photo A. Pissart). Scale is 2 m long; B - Inactive primary sand wedge in ice-rich clay and pebbly sand (Mackenzie Delta, Canada; from Murton et al., 2000); C - Inactive primary sand wedge on the left, and composite sand-ice wedge on the right in massive ice and icy sediments (Mackenzie Delta, Canada; from Murton et al., 2000).

2.3. Patterned ground, involutions and other periglacial features

In periglacial environments, repeated frost heave and thaw consolidation together with other processes such as load casting cause ductile deformation of the ground that in turn form patterned ground. These can be associated or not with the sorting of material, and are classified into small polygons (<10 m in diameter), circles or nets, hummocks and mudboils (Washburn, 1979). The patterned ground features are mostly present in the active layer of permafrost, but can also form in areas affected by deep seasonal freezing of the ground. On slopes nets, polygons and circles tend to stretch, which results in the formation of soil stripes (Büdel 1960; Bertran et al., submitted) (Figure 5).

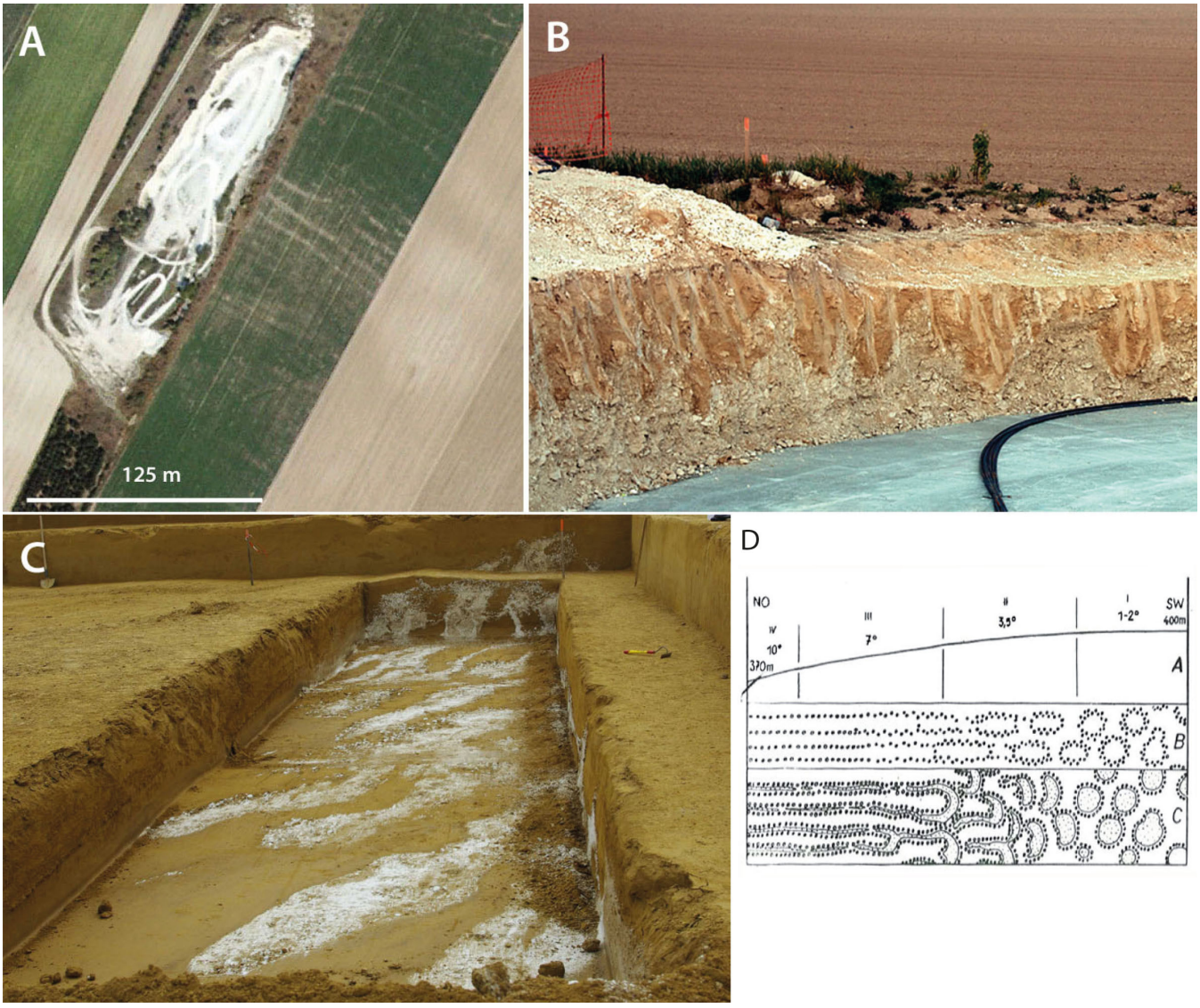

Figure 5: A – soil stripes in aerial photograph (IGN/Google Earth) and B – in cross-section (photo P. Benoit), Champfleury_3 (3.99°E, 48.60°N); C – soil stripes in vertical and horizontal cross-section, Havrincourt (3.07°E, 50.12°N) (photo P. Antoine); D - Stretching of nets into soil stripes on slopes, from Büdel (1960)

Small nets and soil stripes were identified in France thanks to geological surveys, re-evaluation of the French literature and investigation of aerial photographs (see chapter 4, and 5). Cross-sections in patterned grounds showed involutions (sensu French, 2007). Multiple mechanisms interacting between each others are cited to explain the genesis of involutions and patterned ground features, and it is often difficult or impossible to assign a particular process to their formation. Although it is likely that the involutions spotted in France are of periglacial origin (i.e. cryoturbations; Bertran et al., submitted), they were referenced but not fully studied in this thesis.

Beside ice-wedges, one of the most indicative markers of permafrost is the occurrence of pingos. These are large domes formed of injection ice that can reach up to 500 m in diameter and 70 m in height, and that require the conservation of large ice bodies. Two types of pingos are distinguished. The closed-system pingos form only in continuous permafrost above drained lakes and water-rich sediment, whereas open-system pingos are linked with the resurgence of groundwater (Figure 6; Figure 7A). As the water freezes in the permafrost, it is forced upward forming ice mounds. Lithalsas are cryogenic mounds composed of segregation ice that form in discontinuous permafrost (Pissart, 2002; Calmels et al., 2007) (Figure 7B). Both the pingos and lithalsas create distinctive crater-shaped scars when thawed. Palsas are ice-cored peat mounds, which are characteristics of sporadic permafrost areas and that form where abundant segregation ice accumulates near the ground surface (Figure 6; Figure 7C). They may reach up to 50 m in diameter and 7 m in height (Washburn, 1979; French, 2007).

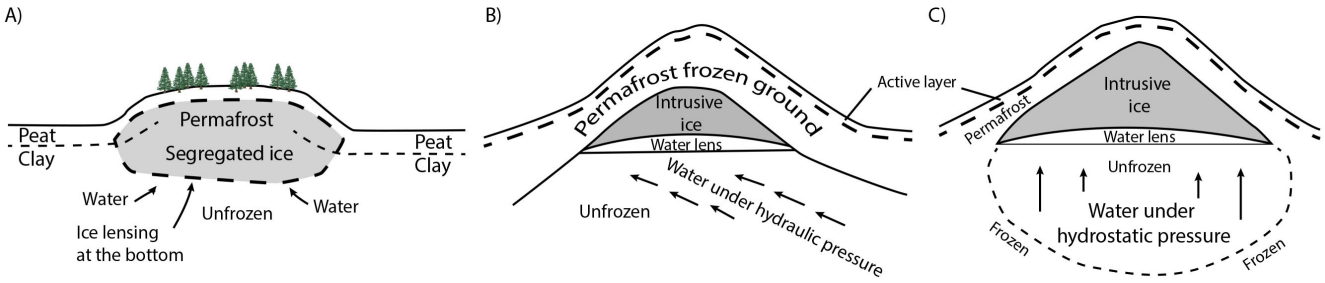

Figure 6: Schematic diagram of A – a palsa, B – an open-system pingo, and C – a closed-system pingo; from French, 2007.

Despite the investigation of several potential examples in the literature, no pingo or lithalsa scars have been identified so far with certainty in France (Boyé, 1958; Michel, 1967; Courbouleix and Fleury, 1996; Lécolle, 1998) whereas convincing examples are described in The Netherlands (Kasse and Bohncke, 1992) and in the United Kingdom (Watson and Watson, 1974; Ballantyne and Harris, 1994; Ross et al., 2011).

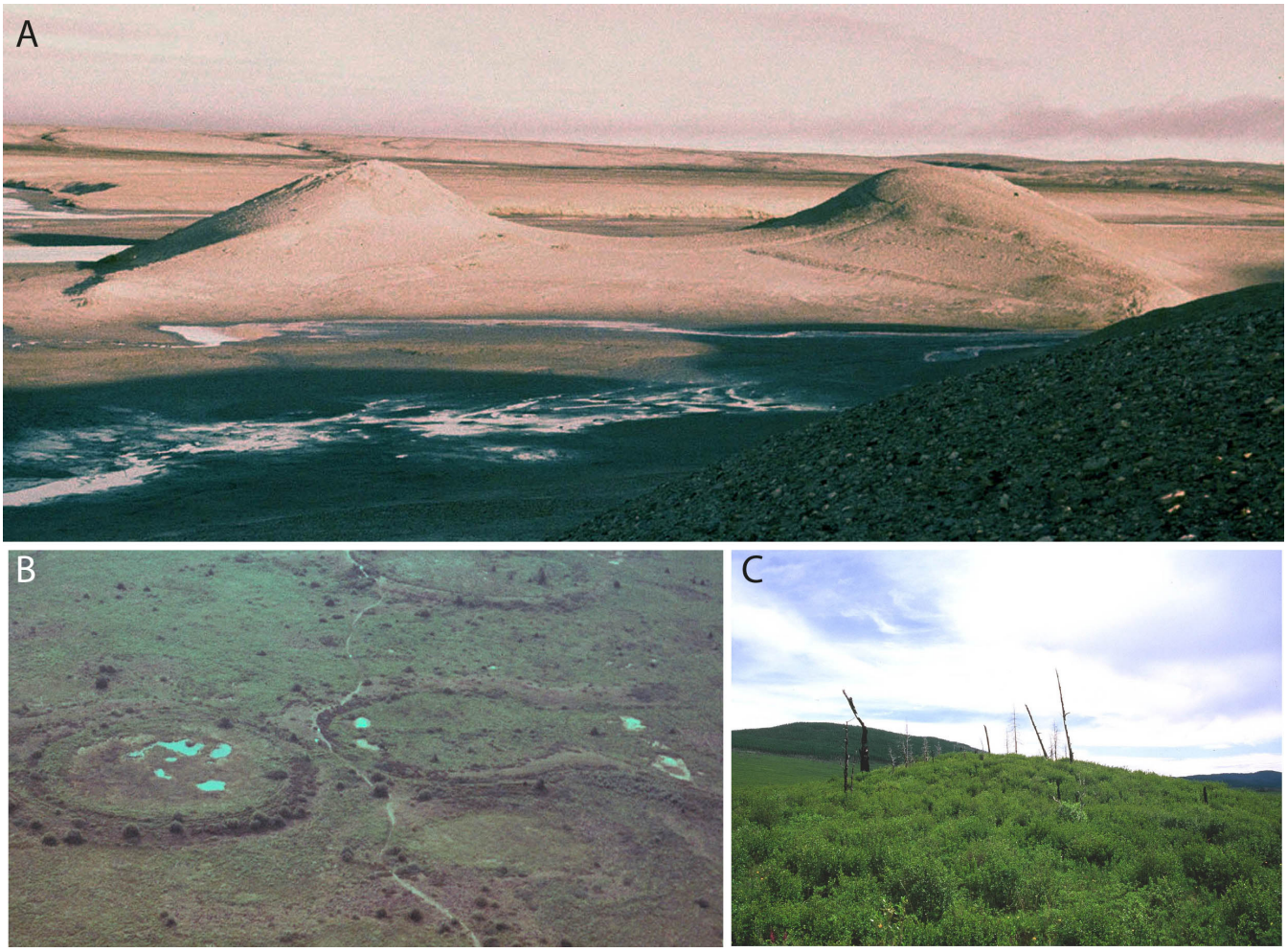

Figure 7: A - Pingos (Canadian Arctic, Photo A. Pissart); B - Lithalsa scars (Hautes-Fagnes, Photo A. Pissart); C – Palsa in peatland (Mongolia, Photo P. Bertran).

2.4. Permafrost reconstructions

Based on field evidence, several regional and national overviews aiming at reconstructing the extent of Pleistocene permafrost in France have been published, namely by Cailleux (1948), Poser (1948), Tricart (1956), Maarleveld (1976), Lautridou and Sommé (1981), Velichko (1982), Texier and Bertran (1993), Courbouleix and Mouroux (1994), Lautridou and Coutard (1995), Van Vliet-Lanoe (1989, 1996), Huijzer and Vandenberghe (1998), Van Vliet-Lanoe and Hallégouet (2001), Lenoble et al. (2012), Vandenberghe et al. (2014) (Figure 8). Although these reconstructions differ significantly, they all agree that permafrost extended over large parts of north-eastern France during the coldest periods of the Pleistocene (particularly the Last Glacial). The southern limit of the permafrost extent is more controversial and the differences between the reconstructions have to be linked with divergences in the interpretation of the scarce periglacial features, particularly sand-wedges.

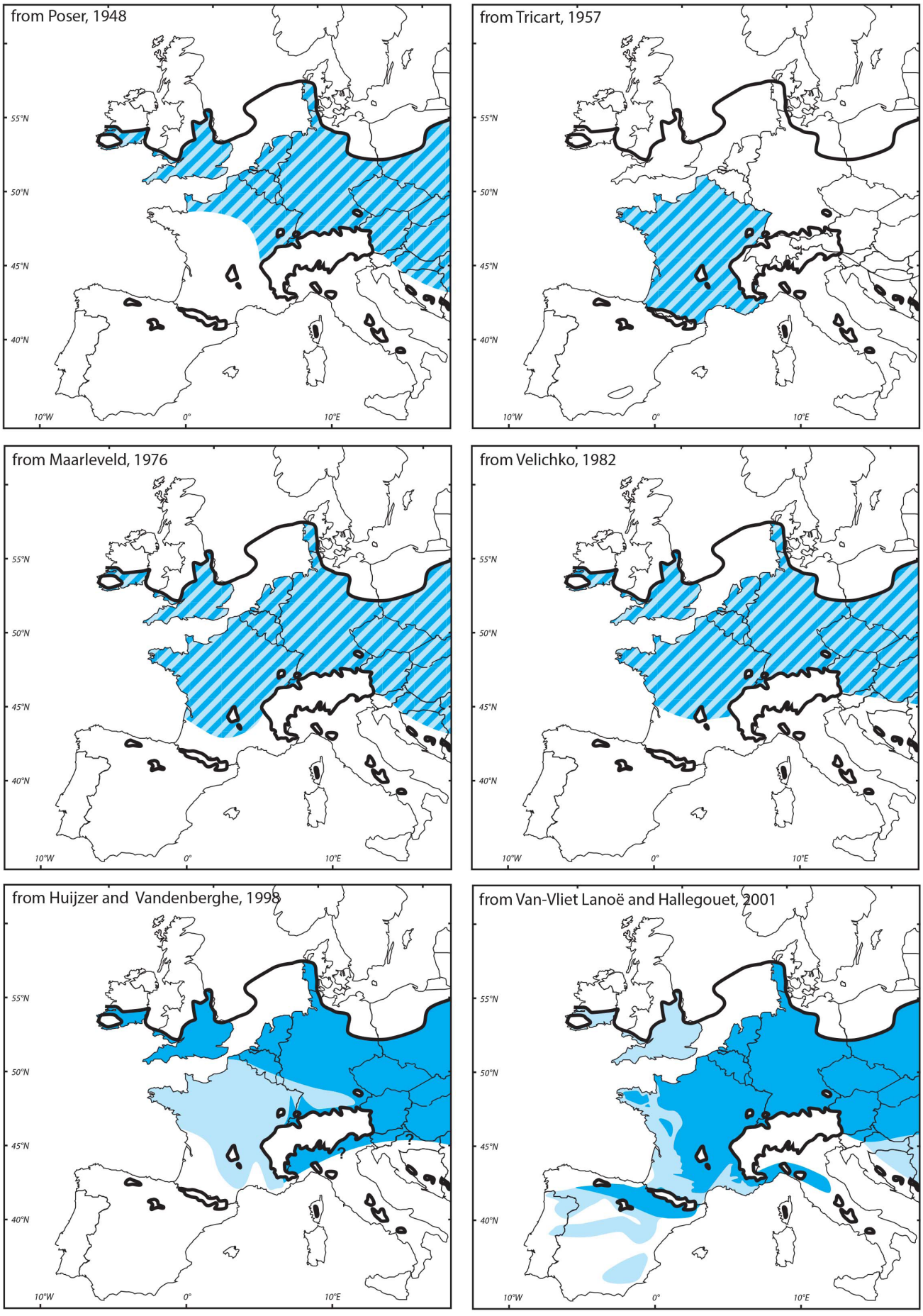

Figure 8: Reconstitutions of the Pleistocene permafrost extent in Western Europe from Pöser (1948), Tricart (1957), Maarleveld (1976), Velichko (1982), Huijzer and Vandenberghe (1998) and Van-Vliet Lanoë and Hallegouet (2001)

In the last decade, modelling of past permafrost has provided new data on this issue using different approaches (e.g. Renssen and Vandenberghe, 2003; Levavasseur et al. 2011; Vandenberghe et al., 2012; Saito et al., 2013; Kitover et al., 2013) (Figure 9, Figure 10). These models successfully reconstructed current permafrost but the simulations of permafrost extent during the Last Glacial Maximum (LGM, ca. 21 ka) show large discrepancies. Models predict the absence of permafrost in areas where geological features forming in discontinuous or continuous permafrost have been described (Levavasseur et al., 2011). In addition, large uncertainties emerged in the modelled extension for the LGM, for example the southern limit of discontinuous permafrost is located either in France or in Poland for respectively the 'cold' and 'warm' extremes (Vandenberghe et al., 2012).

In this context, it is critical to provide a database with geo-located features in France, similar to previous work done in Northern Europe (Isarin et al., 1998). The GIS-analysis of such databases can provide keys to understand the factors involved in the distribution of periglacial features.

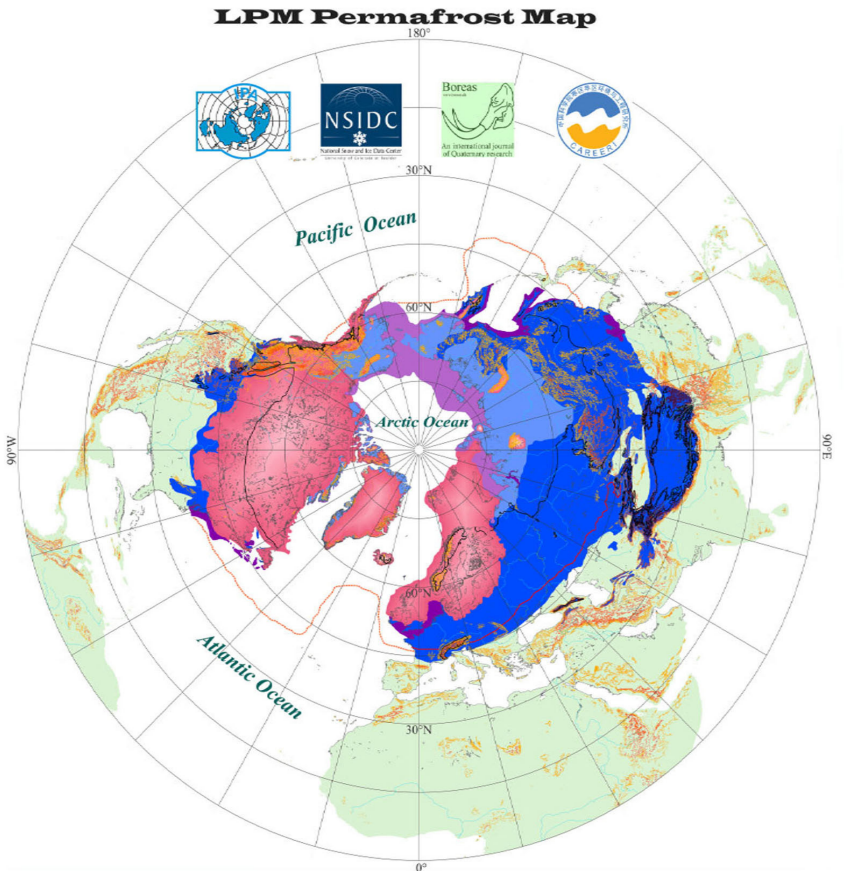

Figure 9: Last Permafrost Extent (LPM) according to Vandenberghe et al. (2014). Blue: Permafrost; red line: approximate boundary between continuous and discontunuous permafrost; dashed orange line: approximate limit of LPM winter sea ice extent

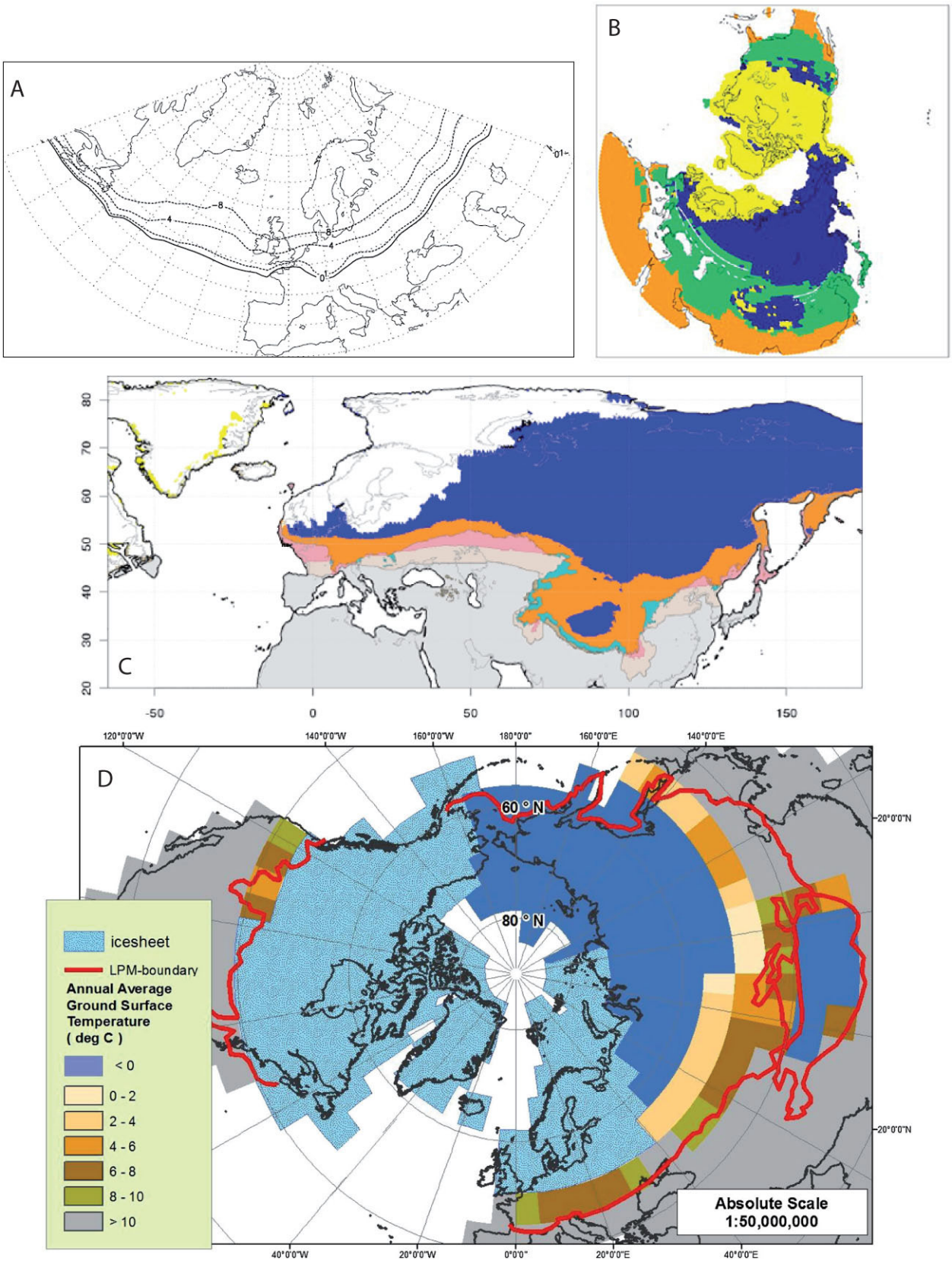

Figure 10: Simulations of the LGM permafrost extent. A – Renssen and Vandenberghe (2003), the 0°C isotherm show the area covered by permafrost; B – Saito (2013), yellow: ice, blue: permafrost, green: deep seasonal freezing of the ground; C – Levavasseur et al. (2011), blue: continuous permafrost, orange: discontinuous permafrost; D – Kitover et al. (2015), dark blue areas show the extent of permafrost.

2.5. Chronological data

One of the issues encountered by the researchers for their reconstructions is the lack of dating since the periglacial features observed may have formed during different periods. The main chronological markers currently available in France are based on stratigraphy in loess sequences, but a few dating have been made in direct relation with periglacial features.

2.5.1. Loess chronostratigraphy

The correlation of the different cross-sections from northern France and the available datings made it possible to subdivide the sequences and find different periglacial events (Antoine and Locht, 2015; Antoine et al., 2016) (Figure 11):

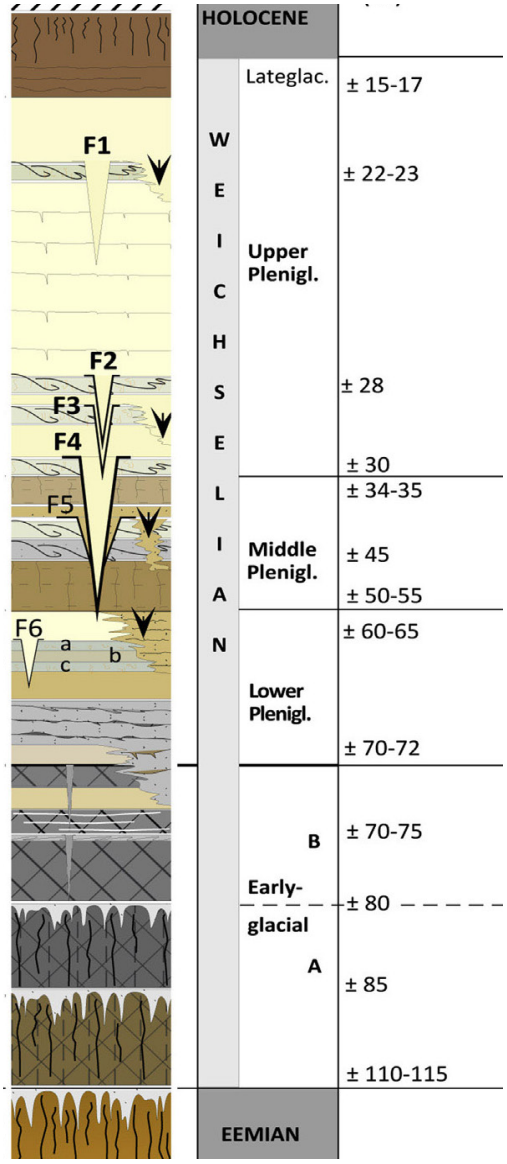

Figure 11: Summary of Northern France pedo-lithostratigraphic sequences. F1-F6: ice-wedge pseudomorphs levels (Antoine et al., 2016)

- The Early glacial stretches from ca. 112 to 78 ka (OIS 5c to 5a). The fossil soils show evidence for deep seasonal freezing. Flint tools associated with this phase have been dated between 91 to 105 ka by thermoluminescence (Fresnoy-au val: 106 ± 12 ka BP, Goval and Locht., 2009; Villiers-Adam: 105 ± 12 ka BP, Locht et al., 2003; Seclin: 91 ± 11 à 95 ± 11 ka BP, Tuffreau et al., 1994). The first local aeolian deposits are found within the end of this sequence in the OIS 5-4 around 78 to 70 ka and characterize an environment with greater aridity.

- The Lower Pleniglacial (ca.70 to 55 ka) shows the first widespread loess deposits associated with ice wedge pseudomorphs (Villiers-Adams, Loch et al., 2003). This sequence is rarely preserved in northern France because of erosion, which is attributed to permafrost degradation. The sequence is better represented in the Rhine valley where it has been dated by OSL to 65 ± 5 ka (Antoine et al., 2001).

- The Middle Pleniglacial (ca. 55 to 35 ka) is characterized by the development of palaeosoils ('Saint-Acheul and Villiers-Adam Soil Complexes'), which reflect long

interstadials (Antoine et al., 2016). The Middle Pleniglacial sequence is marked at its beginning by an erosive event that led to the deposition of laminated and cryoturbated colluvium dated to 55-50 ka cal BP. Erosion is thought to reflect thermokarst gullies linked at Villiers-Adam with the degradation of ice-wedge pseudomorphs, which developed between 45 to 55 ka (Antoine et al., 2001) (Figure 12).

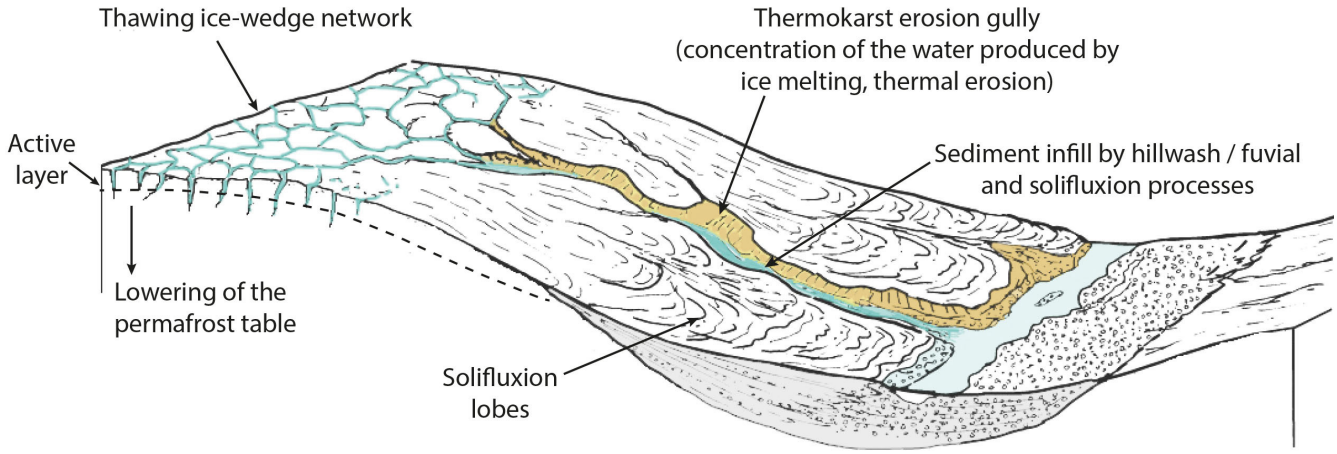

Figure 12: Incision of a thermokarstic gully on a slope (source P. Antoine, drawing L. Deschodt)

- The Upper Pleniglacial (ca.30 to 15 ka) is characterized by thicker loess deposits. In the lower part, several levels of ice wedge pseudomorphs associated with soliflucted 'tundra gleys' (i.e. Haplic Cryosols according to Kadereit et al., 2013) have been identified. A major level of ice wedge pseudomorphs has been described at the transition between the Middle and the Upper Pleniglacial at ca. 30 ka. Above this level, a thick cryoturbated tundra gley associated with two levels of ice wedge pseudomorphs, which are rarely preserved, is described as the 'Santerre Horizon'. The sequence continues with laminated loess marked by small syngenetic wedges and dated in most cross-sections from northern Europe between 22 and 27 ka. At the top of this level a tundra gley associated with ice wedge pseudomorphs is observed (e.g. Sourdon, Antoine, 1989). This tundra gley is thought to be the French equivalent of the 'Nagelbeek tongue horizon' or 'Kesselt level' described in Belgium, which has been dated around 22 ka ^{14}C BP or 27-26 cal ka BP (Haesaerts et al., 1981; Lautridou, 1985; Van Vliet-Lanoë, 1996). More recent relative datings in Onnaing (France) yielded younger ages close to 22 ka cal BP (Antoine and Locht, 2015). A last level of small ice wedge pseudomorphs, or soil wedges, has been identified at the summit of the loess deposits in Saint-Hilaire-sur-Helpe (Feray et al., 2013) and would stratigraphically be situated between 15 and 20 ka.

This approach based on stratigraphic markers to provide relative ages has proven useful for the loess areas thanks to the homogeneity of the deposits and their high sedimentation rates (e.g. Vandenberghe, 1983; Haesaerts et al., 2016). In other areas with heterogeneous Quaternary sediments, or low sedimentation rates, it is often impossible to get a chronological framework (e.g. Pleistocene terraces with epigenetic wedges). Although the temporal history of sediment infillings in wedges may be complicated, attempts to dating these features have been made in the last 30 years.

2.5.2. Ice-wedge pseudomorph dating

Despite stratigraphic markers that give relative ages, only few reliable dating were made in direct association with ice-wedge pseudomorphs in cross-sections from Northern France, Belgium, Netherlands and Germany. At Grouw (Netherlands), in a milieu characterised by high sedimentation rates of loess, Vandenberghe (1993) was able to bring to light seven phases of syngenetic ice-wedge development using ^{14}C dating, i.e. 3 formed between 43.3 ka and 35.3 ka, one is older than 43.3 ka and 3 are younger than 35.3 ka. At Hermignies (Belgium) a level of ice-wedge pseudomorphs is intercalated between two levels of loess dated to 21.5 ± 2.5 and 25.9 ± 3 ka by thermoluminescence (Frechen et al., 2001). Two levels of ice wedge pseudomorphs were also dated in Germany at Ostrau between respectively 25.7 ± 3.6 ka and 28.0 ± 3.8 ka and between 29.1 ± 4 ka and 30.3 ± 4.2 ka (Kreutzer et al., 2012; Meszner et al., 2013). In Poland and NW Ukraine, at least three events are dated between 30 and 12 ka (Zielinski et al., 2014) and an ice-wedge pseudomorph was dated between 40 ± 4 and 41 ± 3.5 ka (Kostrup, 2007). In France, at Savy, a tundra gley associated with a level of ice wedge pseudomorphs yielded an U/Th Electron Spin Resonance (ESR) age of 30 ± 2 ka on a horse bone and dental enamel (Locht et al., 2006), and at Havrincourt six levels of ice-wedge pseudomorphs have been identified (F1, F2, F3, F4, F5, F6; Antoine et al., 2014) and dated with Single-Aliquot Regenerative-dose Optically Stimulated Luminescence (SAR OSL). F1 was not dated but is stratigraphically anterior to F2 and F3 that were formed within two tundra gleys slotted together and dated at 28.4 ± 1.8 ka (Figure 12). Another tundra gley formed in association with F4 yielded an age of 31.4 ± 2.0 ka. F5 identified at the interface between two soil complexes was dated between 42.1 ± 2.8 and 51.5 ± 3.2 ka. Finally, small pseudomorphs (F6) were identified in a tundra gley bracketed between 61.7 ± 4 and 65 ± 3.8 ka.

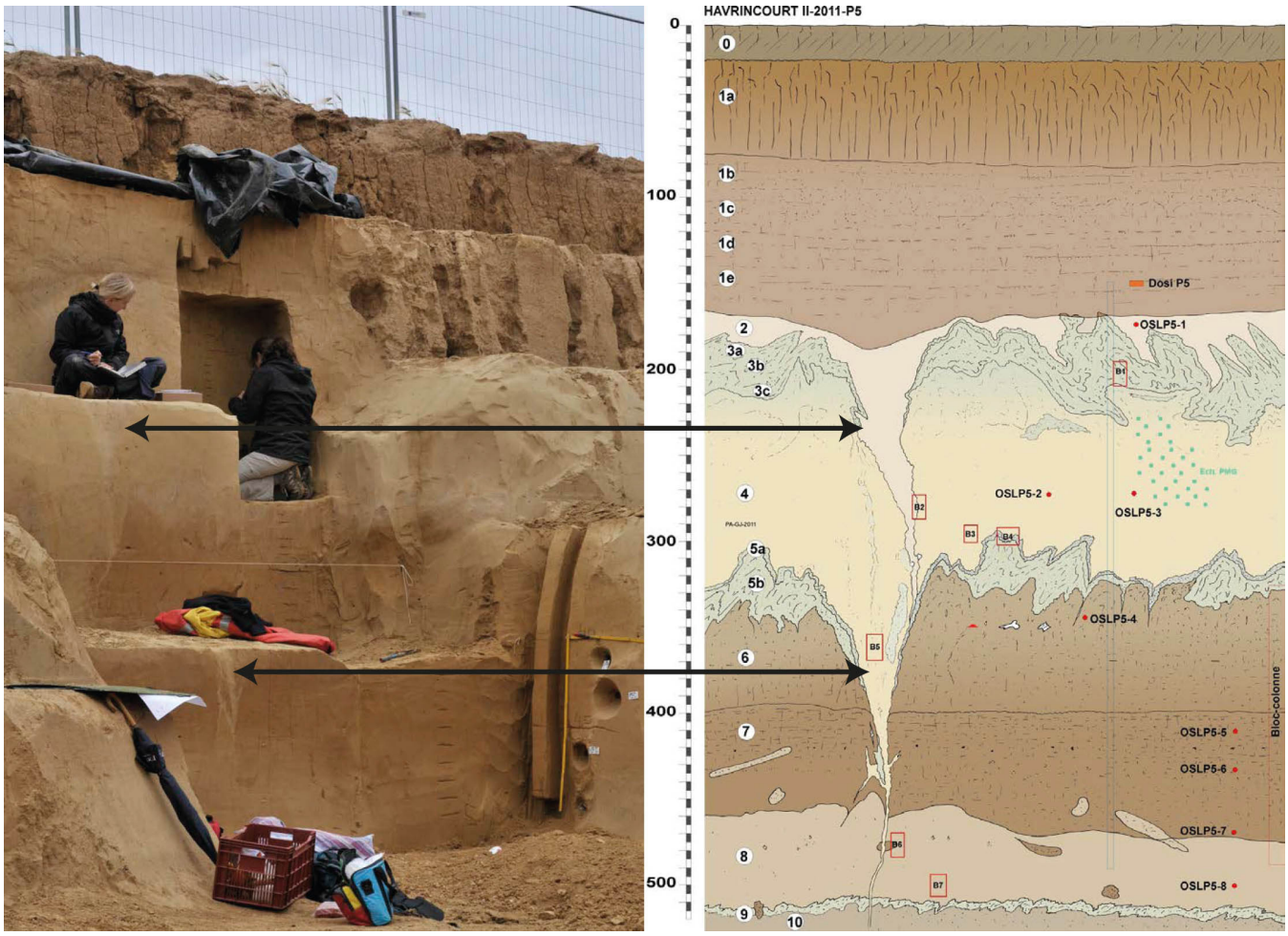

Figure 13: Loess cross-section Hav.2-P5 in Havrincourt (France) showing two ice-wedge levels (F2 and F3), from Antoine et al. (2014) (Photo P. Antoine)

2.5.3. Dating of sand-wedges and composite-wedge pseudomorphs

The sand wedges and the primary sandy infilling of the composite wedge pseudomorphs that have been preserved with little sediment disturbance are suitable for luminescence dating. With the recent advances in luminescence techniques and protocols, some of the dating may appear obsolete but provide useful information that can be used for comparisons.

Kolstrup and Mejdahl (1986) were the first to apply thermoluminescence (TL) on K-feldspars collected from the sand filling of two sand wedges and a composite-wedge pseudomorph in Jutland (Denmark). This returned ages of 39 ± 5, 24 ± 3 and 17 ± 3 ka. The oldest age coming from the composite-wedge pseudomorph exceeded the expected age and was attributed to partial bleaching due to sediment mixing during secondary infilling. These ages were later corrected by Christiansen (1998) for the effect of shallow traps (Mejdhal et al., 1992) and gave estimates of 24 ± 2 ka, 33 ± 3 ka, and 53 ± 5 ka. Böse (1992) used both TL (Mejdhal 1988, 1991) and infrared-stimulated luminescence (IRSL; Duller, 1991)

on a sand wedge from the Brandenburg region in Germany yielding respectively ages of 19.4 ± 1.5 and 19.3 ± 1.5 ka. Multiple-aliquot additive-dose infrared-stimulated luminescence (IRSL MAAD) was applied on K-feldspars grains and polymineral fine grains collected from two sand wedges infillings found at Crumbling Point in the Mackenzie Delta area (Canada) by Murton et al. (1997) giving a mean age of 14 ± 1 ka (n = 7) and another sample yielded a fading-corrected IRSL age of 16.1 ± 0.2 ka (Murton and Bateman, 2007). Christiansen (1998) also dated a sand-wedge at Emmerleve Klev (Denmark) using TL on K-feldspars, and optically stimulated luminescence (OSL) on quartz, which age estimates are respectively 34 ± 3 ka and 32 ± 3 ka. Owen et al. (1998) used IRSL and OSL MAAD on polymineral fraction collected within the fill of a sand wedge found in the Gobi Desert (Mongolia). The sample returned an age of 15.7 ± 3.0 ka. Böse (2000) dated sand wedges at two sites in western Poland using single-aliquot regeneration and added-dose (SARA procedure, Mejdahl and Bøtter-Jensen, 1994) on feldspars, which gave mean ages of 12.9 ± 1.3 ka (n=4) on feldspars and 14.3 ± 1.4 ka (n=3) on quartz. French et al. (2003) applied multiple-aliquot OSL on quartz taken from the fill of three sand wedges to show two separate periods of wedge formation in Pine Barrens (New Jersey, USA) of 15-18 ka and 55-65 ka. Kolstrup (2004) found single-aliquot regenerative-dose (SAR) OSL ages from the sandy infill of a composite-wedge pseudomorph in Tjaereborg (Denmark) of 270 ka which is much older than the host sediments (which gave an age of 150 ka). The wedge samples showed poor equivalent dose (De) reproducibility and single grain measurement confirmed the existence of multiple-dose populations within the sample. This was attributed to partial bleaching but it could also reflect by part a multiple-phased wedge growth. Briant et al. (2005) reported two SAR OSL ages on quartz coming from a sand wedge in Pode Hole Quarry (England) of 31.1 ± 2.1 and 10.5 ± 1.2. Kjaer et al (2006) dated a sand-wedge in Sölvegatan (Sweden) yielding a SAR OSL age on quartz of 16 ± 1 ka. Kovacs et al. (2007) published two SAR OSL ages from a sand wedge in Mogyorod (Hungary) of 20.75 ± 2.3 and 22.66 ± 2.86 ka. The ages were later recalculated by Fàbiàn et al. (2014) including different values of paleomoisture and yielded estimates of 15.7 ± 1.8 ka and 17.2 ± 2.2 ka. Kasse et al. (2007) dated two units in the Netherlands containing sand wedges which give their relative ages. The sand wedges have formed between 28.8 ± 2.4 to 24.4 ± 1.8 ka in unit A and between 25.2 ± 2 ka to 17.2 ± 1.2 ka in unit B. Buylaert et al. (2009) dated with SAR OSL 14 sand wedges in Flanders (Belgium) and included single grain measurements which show that the sediment within the cracks was bleached prior burial. The wedges in Vrasene yielded the ages of 13.9 ± 1.0, 18 ± 1.3, 14.4 ± 0.9 ka, in Sint-Niklaas 16.4 ± 1.1, 129 ± 11, 36.4 ± 4.1 ka, in Ruddervoorde 21.0 ± 1.2, 19.3 ± 1.1, 15.4 ± 1.0 ka, in Aalter 14.8 ± 0.9, 20.4 ± 1.2, 15.5 ± 1.0 ka, and in Belsele 15.5 ± 1.0, 14.0 ± 0.9 ka. Guhl et al. (2012) dated two features with sandy infills in Jonzac (France). The authors applied SAR OSL on quartz from the sand

wedges and used the Central Age Model (CAM) for the calculation of age estimates, yielding the age of 26.6 ± 4.4 ka. The investigation of the OSL results from the second feature revealed contamination of the sample by host material. The use of single grain measurement and Finite Mixture Model (FMM) for the calculation of the age estimates provided an age of 27.4 ± 5.5 ka for the second feature by isolating the different age components. In the southwest of France, OSL dating was carried out on numerous sand wedges. Lenoble et al. (2012) published the SAR OSL ages on quartz of two sand wedges in Cap-de-Bos (24.3 ± 2.8 ka) and Leognan (25.5 ± 2.2 ka). Bertran et al. (2014) reported two ages of a sand wedge in Salaunes (26.7 ± 1.5 ka on feldspars and 24.3 ± 1.7 ka on quartz), and two ages on quartz from another sand wedge found in Cussac-Fort-Médoc (26.6 ± 1.8 and 27.7 ± 1.7 ka). Other datings on sand wedges were done in 2013 and yielded the SAR OSL ages on quartz of 21.1 ± 1.1 ka in Mérignac, 30.0 ± 1.5 ka in Saint-André-de-Cubzac, 46.4 ± 2.2 and 93 ± 4.2 ka in Durtal, and unexpected ages that were considered as incoherent of 95.4 ± 5.9 and 121.1 ± 6.2 ka on a sand wedge found in Jau-Dignac-et-Loirac. Rémillard et al. (2015) dated the sandy infills of two composite-wedge pseudomorphs and a sand wedge found on the Magdalen Islands (Canada) with a SAR OSL technique on quartz. This returned the ages of 10.1 ± 0.7 and 10.7 ± 0.7 ka for the sand infills in the composite wedge pseudormophs, and 9.8 ± 0.7 ka for the sand wedge. In Poland, Ewertowski et al. (2016) dated the sandy infill of a composite-wedge pseudomorph in Kaszczor which returned the OSL ages of 18.1 ± 0.1, 17.5 ± 0.9, 18.3 ± 0.8, 18.6 ± 0.9 ka, and a sand-wedge in Wloszakowice that yielded estimates of 14.9 ± 0.8, and 14.6 ± 0.9 ka.

3. Research methodologies

In view of the broad objectives of this study, namely to assess the chronology and extent of the Late Pleistocene permafrost in France, and to comply with the timing and limited funds available to conduct this project, it was necessary to define cost and time-effective methodologies.

3.1. Data acquisition

A thorough search of the literature, which includes articles in journals, PhD and master theses, archaeological survey reports, geology reports, and the explanatory notes of the geological maps of France, was conducted to gather data on periglacial features. Since the investigated literature covers the last 80 years, the features were re-evaluated to the light of our present knowledge and understanding of periglacial processes and environments. Although the initial data gathered were abundant, all the features from the literature that were not accompanied by drawings, photographs, or good descriptions

and all the data that could give raise to doubts were not added to the published version of the database (see chapter 4).

New field surveys were necessary not only to check the features described in the literature, but also because it was essential to find new features to describe, analyse, sample and date. France is a country of almost 650,000 km². Obviously it was not possible to prospect the whole territory in order to find periglacial evidence. To restrain the study area we focused our work on the regions located at altitudes lower than 500 m. This allowed us to exclude from the database the features mentioned in mountainous areas, and for which it was complicated to infer a Pleistocene origin since deep seasonal freezing or permafrost still occur at present time. Despite such a limitation, the study area remained large, so that we organised our survey into two parts:

- The analysis and interpretation of the aerial photographs available in Google Earth and Geoportail made it possible to cover large areas. Search was initiated in regions where periglacial features had already been described in the literature, and was then extended to neighbouring areas or regions that share similar geological characteristics. Regions were then tested when features were expected. Feature visibility is highly dependent on local conditions such as ground moisture or vegetation, so it was necessary to review all archival photographs taken over the last 10-20 years to improve the chance to spot features (Figure 14). The features observed comprise polygonal networks, soil stripes, potential thermokarst, small nets and other undetermined patterned ground. The geographic coordinates and an image of each periglacial evidence identified were stored (see chapter 5). A site was considered to represent a single land parcel or a few adjacent parcels where periglacial features were spotted. Only the indisputable features were added in the published version of the database, and only the image with the most clearly visible features were selected for analysis. 242 sites of small nets and 90 of involutions were analysed in Bertran et al. (submitted).

Figure 14: Local conditions impact on features visibility. Polygons St Rémy en Provence in A – 2013, B – 2015.

- New field data and samples were collected from cross-sections either during rescue archaeology investigations or during our own geological surveys. The latter required the identification of potential sites where both cross-sections and periglacial features could be visible. The Loire valley, Northern Aquitaine, and the lower valley of the Rhône were prospected for this purpose to check the presence of wedges that were previously identified in aerial photographs as polygonal networks. To gather the data presented in this thesis, hundreds of sites that include quarries, building constructions, drainage ditches and trenches were inspected in each of the area selected. In the Bordeaux region this work was initiated by different authors (P. Bertran, A. Lenoble, L. Sitzia) and was continued during my PhD.

3.2. Geological setting

The Loire valley, Northern Aquitaine and the lower Rhône valley were surveyed to find periglacial features (Figure 15). Despite an extensive search, no periglacial evidence was found in the lower Rhône valley. In contrary, many features were discovered in Northern Aquitaine, and in the Loire valley.

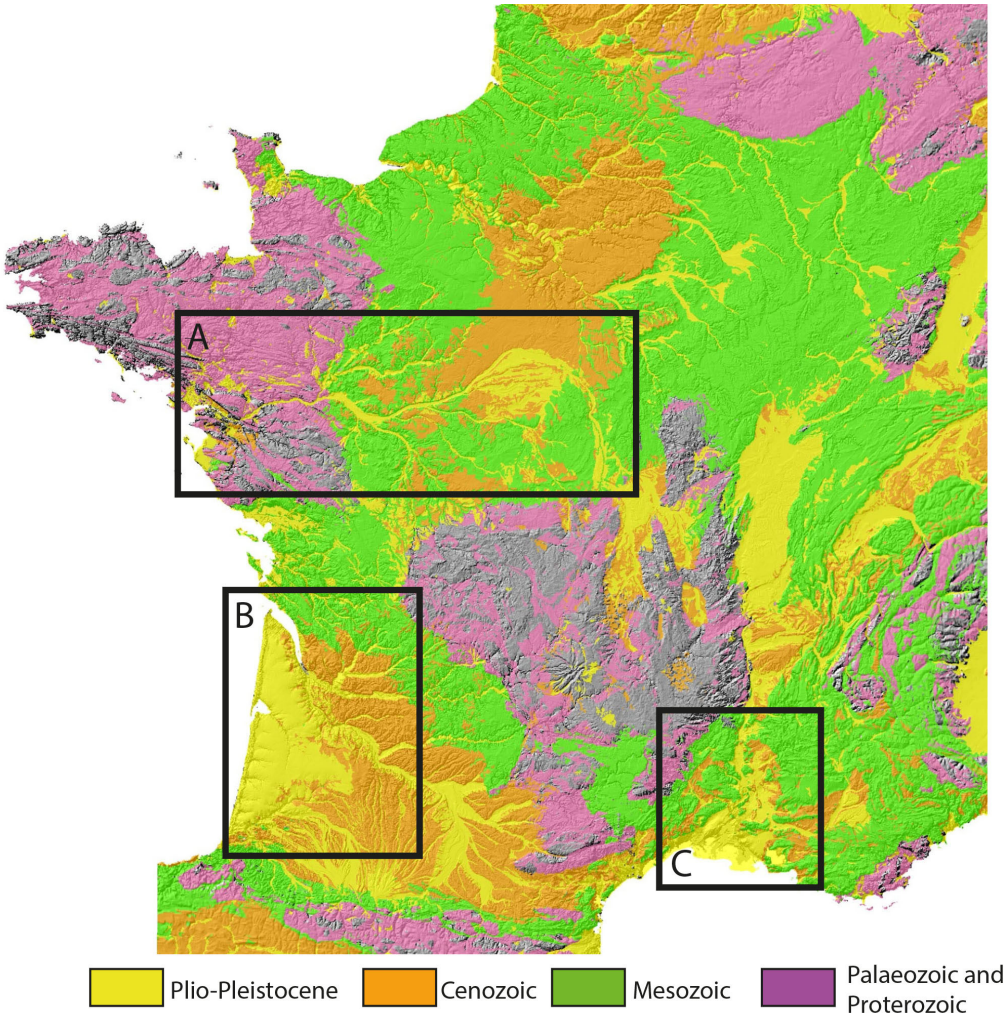

Figure 15: Simplified Geological map of France (BRGM), and surveyed areas: A - Loire valley, B - Northern Aquitaine and C - Lower valley of the Rhône River

A total of 33 samples were taken within the sandy infills of sand wedges and composite wedge pseudomorphs located in these areas for dating purposes. Although numerous periglacial features were described during the course of the PhD, the emphasis is placed here on the sampled ones.

3.2.1. Northern Aquitaine

The surveyed area in northern Aquitaine is located in the Aquitaine sedimentary basin which is mostly composed by Jurassic, Cretaceous, Tertiary and Quaternary deposits. From the Late Miocene to the Middle Pleistocene the basin was filled by fluvial deposits coming from the Massif Central and the Pyrenees mountains and carried by the Dordogne and Garonne rivers, setting up complex terrace systems (Dubreuilh, 1976; Sitzia, 2014). Most epigenetic relict sand-wedges were found in the Middle to Lower Pleistocene Garonne terraces. These features are located in close proximity to the Landes coversands that accumulated during the Late Pleistocene and could have provided sufficient sand for the infilling of the wedges (Sitzia et al., 2015) (Figure 16). Most sand-wedges in this area develop

in gravel or sand of alluvial origin that show sometimes cryoturbations. Sand wedges usually open below decimetre thick coversands with ventifacts, have massive sandy infillings with faint laminations, are V-shaped, 1 to 2 m in depth, and 0.3 to 0.6 m in width. A few develop within alluvial loam and show deformation. In total, 16 samples were gathered from 5 sand-wedges in Northern Aquitaine.

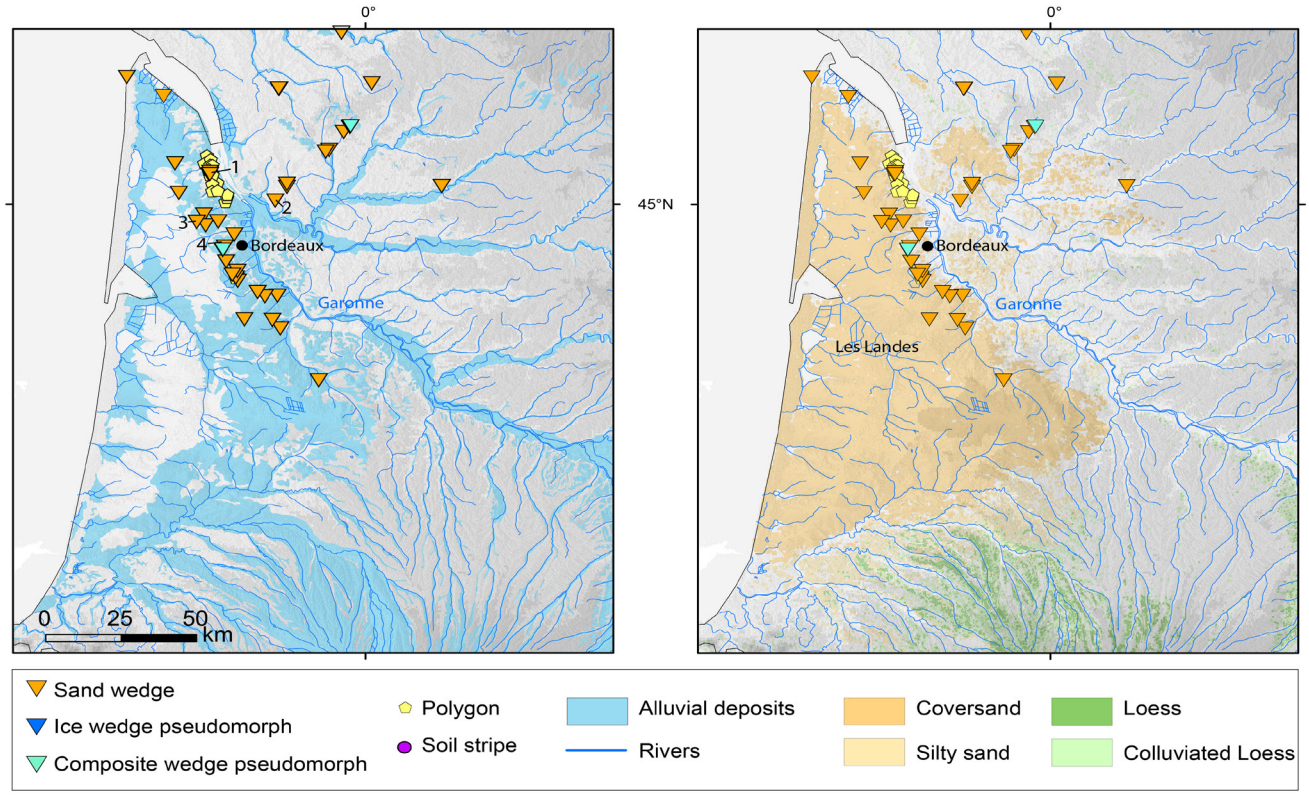

Figure 16: Spatial distribution of the periglacial features described in Northern Aquitaine. Numbered wedges were dated: 1=Cussac-Fort-Médoc, 2=St-André-de-Cubzac, 3=Salaunes (Château Montgaillard), 4=Mérignac (Parking Chronopost)

3.2.1.1. Salaunes (Château Montgaillard)

At Salaunes (Château Montgaillard, latitude 44.935°N, longitude 0.821°W, altitude 49 m a.s.l.), a heterogeneous sequence of lower Pleistocene sandy gravel (Fxa on the geological map of France) is overlain by thin coversand (< 30 cm) within which centimetric ventifacts are visible. Multiple sand wedges were found in the sections that also contains involutions (Figure 17B). Although the sand wedges have a massive sandy infill and are about the same length (ca.1 m) their width varies significantly from a few centimetres to 50 cm. Four samples were taken laterally within a sand wedge that is 1.1 m in depth and 0.5 m in width (Shfd14011, Shfd14012, Shfd14013, Shfd14014) (Figure 17A).

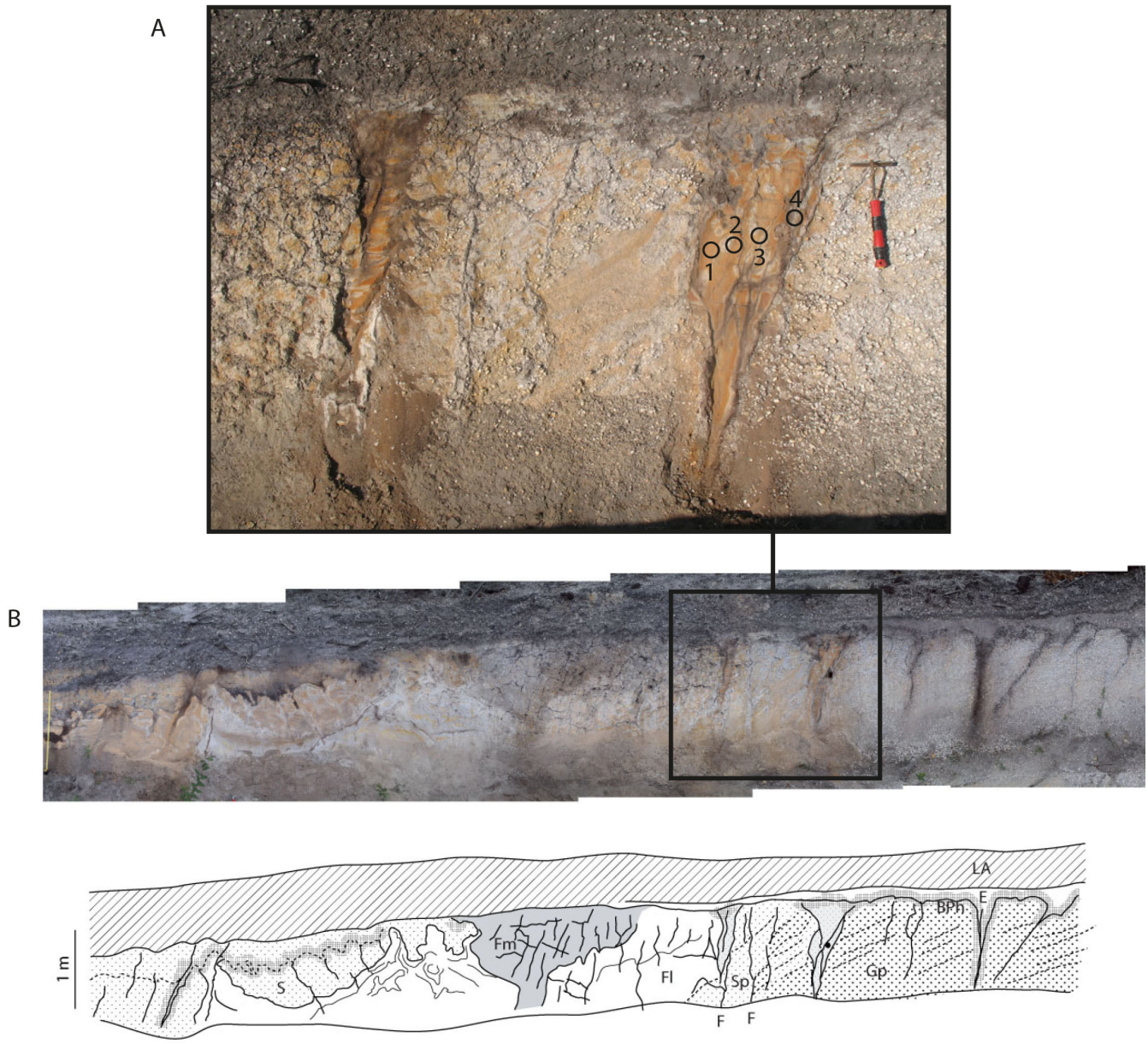

Figure 17: Sand-wedges in sandy gravel at Salaunes (Château Montgaillard; 44.935°N, 0.821°W). A - Close-up of the sampled wedge, 1=Shfd14011, 2=Shfd14012, 3=Shfd14013, 4=Shfd14014. B - Cross-section of the site showing involutions. LA: ploughed horizon, E: eluvial horizon, Bth: spodic horizon, Fm: massive silt and clay, Fl: laminated silt, Sp: planar cross-stratified sediment, Gp: planar cross-stratified gravel, F: Fault

3.2.1.2. Cussac-Fort-Médoc (Parcelle Lagrange)

At Cussac-Fort-Médoc (Parcelle Lagrange, latitude 45.114°N, longitude 0.750°W, altitude 38 m a.s.l.), several sand wedges were observed in ditches. They form a large polygonal network (12 to 15 m in diameter) visible on aerial photographs and described by Lenoble et al. (2012) (Figure 18). The sand wedges in this area are found in Lower Pleistocene sandy gravel (Fxb1) and are sometimes overlain with coversand which width varies from a few centimetres to 20 cm. The sand wedges are generally about 0.8 m in length and 0.3 to 0.7 m in width and are characterized by a massive sandy infilling. The wider sand wedge was sampled (Shfd14021, Shfd14022, Shfd14023, Shfd14024, Shfd14025, Shfd14025; Figure 18C).

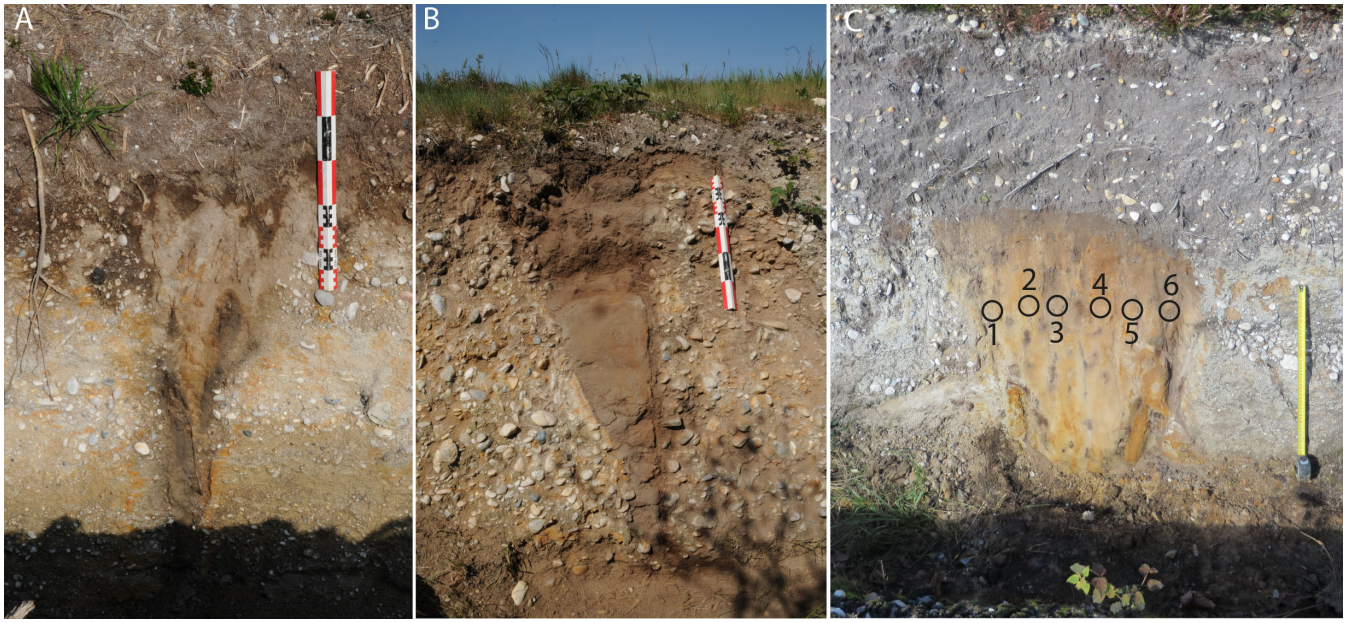

Figure 18: Sand-wedges in sandy-gravel (45.114°N, 0.75°W) A and B - Cussac-Fort-Médoc “le Moule” (Photos A. Lenoble) and C - Cussac-Fort-Médoc “Parcelle Lagrange” 1=Shfd14021, 2=Shfd14022, 3=Shfd14023, 4=Shfd14024, 5=Shfd14025, 6=Shfd14026. Scales are 50 cm.

3.2.1.3. Mérignac (Parking Chronopost)

At Mérignac (Parking Chronopost, latitude 44.827°N, longitude 0.689°W, altitude 47 m a.s.l.), multiple sand wedges and a composite wedge pseudomorph were found in a 250 m long cross-section (Figure 19; Figure S1). They formed in Lower Pleistocene alluvial gravel and loam (Fxbg) and can attain 1 to 2 m in depth. The sand wedges in the alluvial loam show deformation and have a 0.3 to 0.6 m width whereas the ones in the gravel are not deformed and are thinner (0.2 to 0.4 m). The wedges are associated with networks of small fissures without distinguishable infill. These fissures cross-cut the wedges and are therefore posterior to their development. They are generally 0.2 m in length and are more visible in the loam where they can reach their maximum depth (up to 1.5 m).

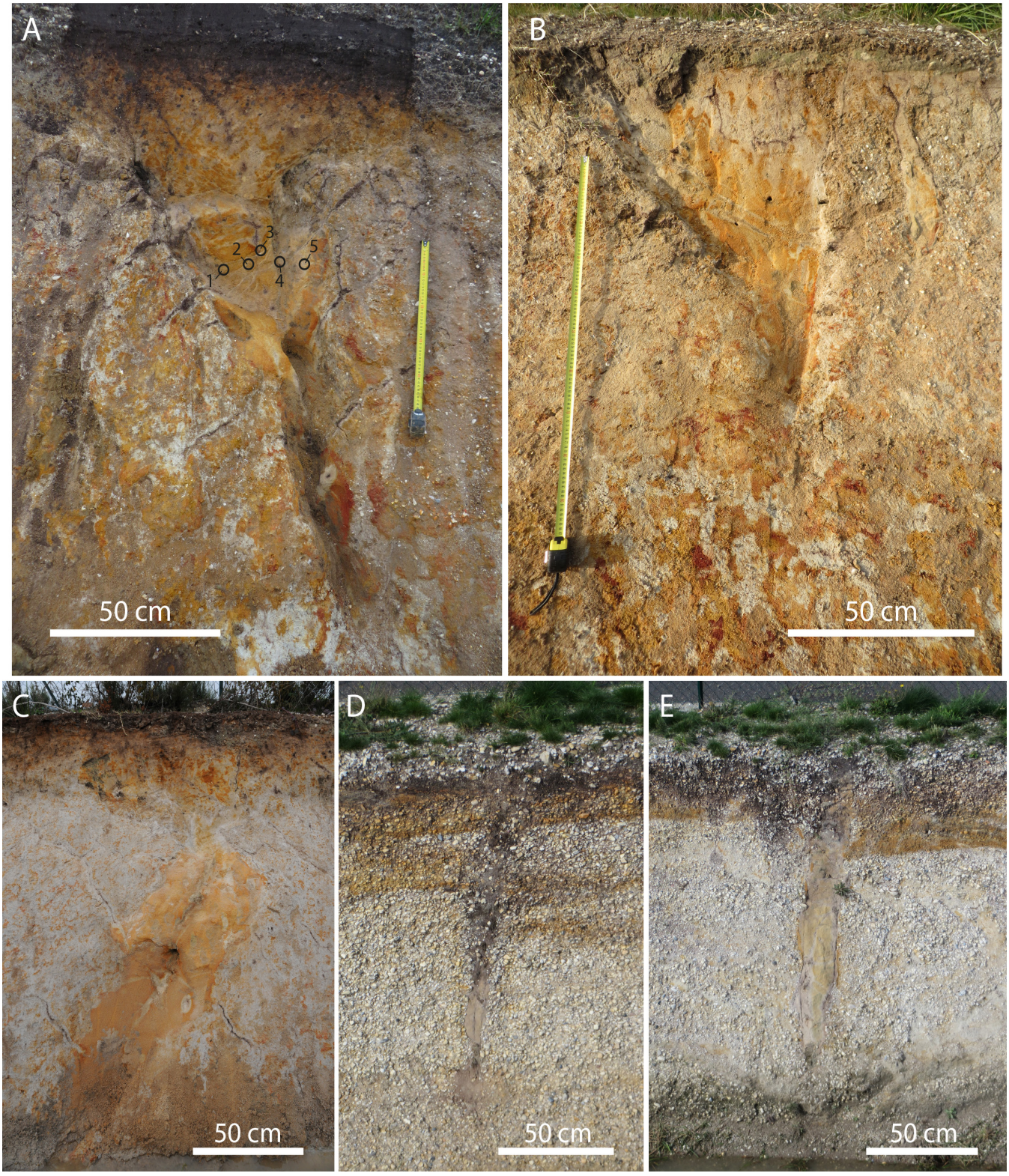

Figure 19: Mérignac (Parking Chronopost) A and B - massive sand-wedges in alluvial loam, C - deformed sand-wedge with a bulbous shape in alluvial loam, D - small composite-wedge in gravel and E - laminated sand-wedge in gravel 1=Shfd14015, 2=Shfd14016, 3=Shfd14017, 4=Shfd14018, 5=Shfd14019

Ductile deformation and reverse faults were identified within the gravel. Similar deformations were identified during simulations of collapsing magma chambers (Geyer et al., 2006). In our context they were interpreted as resulting from the collapse of a karstic cavity in the underlying limestone (Jolivel et al., 2016) (Figure 20).

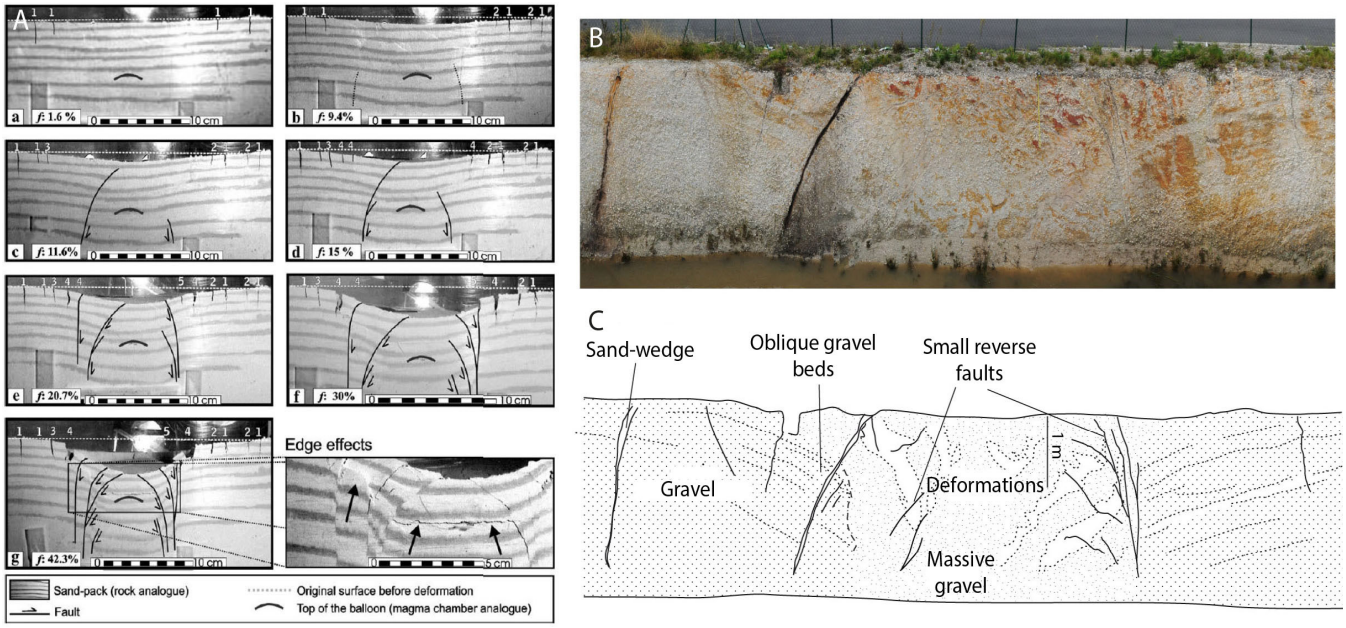

Figure 20: Ductile deformations in Mérignac (Parking Chronopost; 44.827°N, 0.689°W) B and C similar to deformations identified during experimentation of a caldera collapse (A; Geyer et al., 2006)

A sand wedge from this site was sampled and dated in 2012 using small aliquots SAR OSL (Shfd12099). For comparison, it was dated in this study using single grain OSL (shfd12099-2) along with 5 other samples taken in a different sand wedge (Shfd14015, Shfd14016, Shfd14017, Shfd14018, Shfd14019) (Figure 18A).

3.2.1.4. Saint-André-de-Cubzac (ZAC parc d'Aquitaine)

At Saint-André-de-Cubzac (ZAC Parc d'Aquitaine; 45°N, 0.43°W, 60 m a.s.l.), numerous sand wedges where observed below 30 to 50 cm thick coversand in a Tertiary clay or clayey sand substratum (RCFx). In the clayey sand, the sand wedges have a massive infill with faint laminations. They have a classic V shape, open just below the coversand, are 10 to 30 cm wide, and 1.6 m deep. In the clay, the wedges are deformed and have sometimes bulbous shapes. These sand wedges are clearly visible only below the first 50 to 60 cm of cryoturbated clay substratum. Single-aliquot SAR OSL was applied on a sample taken within a sand wedge in 2012 (Shfd12098), and for comparison in this study we used single grain SAR OSL to acquire the age estimates from the same sample (Shfd12098-2) (Figure 21).

Figure 21: Sand wedges in Oligocene clayey sand, Saint-André-de-Cubzac (45°N, 0.43°W; Photos P. Bertran). Scales are 50 cm long.

3.2.2. Loire valley

In the Loire valley, the study area stretches over 400 km from the Sologne region to the mouth of the river Loire nearby Nantes. Sand-wedges, composite-wedge pseudomorphs, ice-wedge pseudomorphs and involutions were found in this area in several alluvial terraces, noted Fv, Fw, Fx, and Fy-z on the geological map of France, and in chalk deposits (Figure 22). These terraces overlay Miocene limestones, sands or marls, or the Plio-Pleistocene Sologne sandy and silty alluvial deposits (Tissoux et al., 2017; Liard et al., 2017). The Loire valley is also characterised by thin sandy aeolian deposits that were listed on few maps (Haase et al., 2007) and are thought to have originated either from the reworking by the wind of sandy alluvial deposits during the Mid to Late Pleistocene or from the surrounding plateaus.

The sites of Olivet and Sainte-Geneviève-des-Bois (Les Bézards) are located in the Loire valley nearby the Sologne coversands. La-Chapelle-aux-Choux, Durtal, Challans and La Louverie are also in the Loire valley downstream in areas within which thin coversands are widespread (Figure 22).

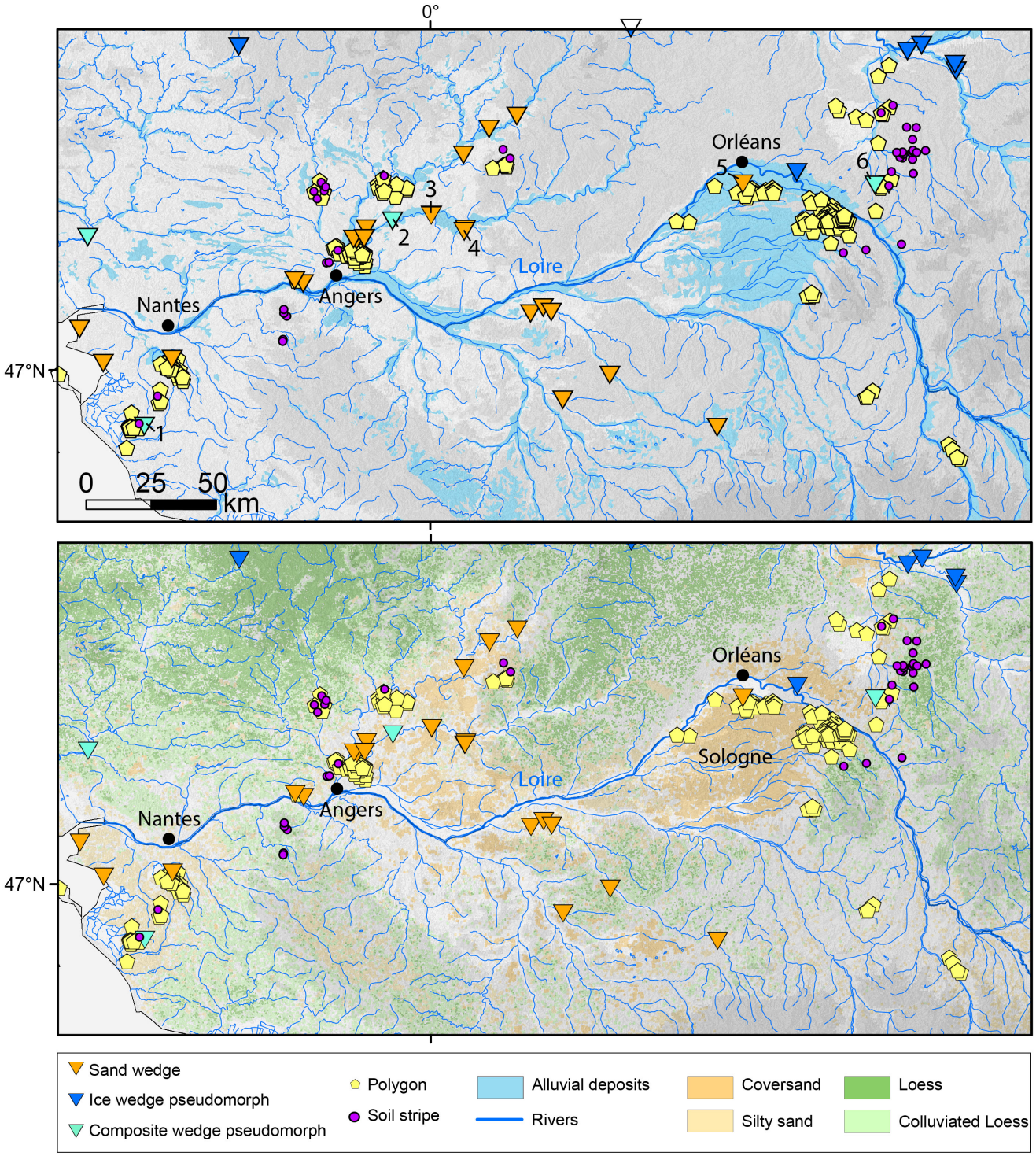

Figure 22: Spatial distribution of the periglacial features described in the Loire valley. Numbered wedges were dated: 1=Saint-Christophe-du-Ligneron (Challans), 2=Les Rairies (Durtal), 3=La Flèche (La Louverie), 4=La Chapelle aux Choux, 5=Olivet, 6=Sainte-Geneviève-des-Bois (Les Bézards)

3.2.2.1. Olivet

At Olivet (Latitude 47.815° N, longitude 1.927° E, altitude 114 m a.s.l.), a sand wedge within which laminations were observed has been sampled (Shfd15085, Shfd15086). The wedge develops in a Lower Pleistocene sandy alluvial terrace of the Loire River (Fw). Its opening is deformed by cryoturbation and it is 0.8 m wide, 1.8 m in depth (Figure 23A).

3.2.2.2. Sainte Geneviève des Bois (Les Bézards)

At Sainte-Geneviève-des-Bois (Les Bézards, latitude 47.810° N, longitude 2.742° E, altitude 145 m a.s.l.) a composite wedge pseudomorph grew within Tertiary silty sand (e-g). The deformed wedge is characterized by a primary massive coarse sand infill within which 4 samples were taken (Shfd15087, Shfd15088, Shfd15089, Shfd15090) and a secondary silt infill in its centre where U-shaped laminations are visible (Figure 23B).

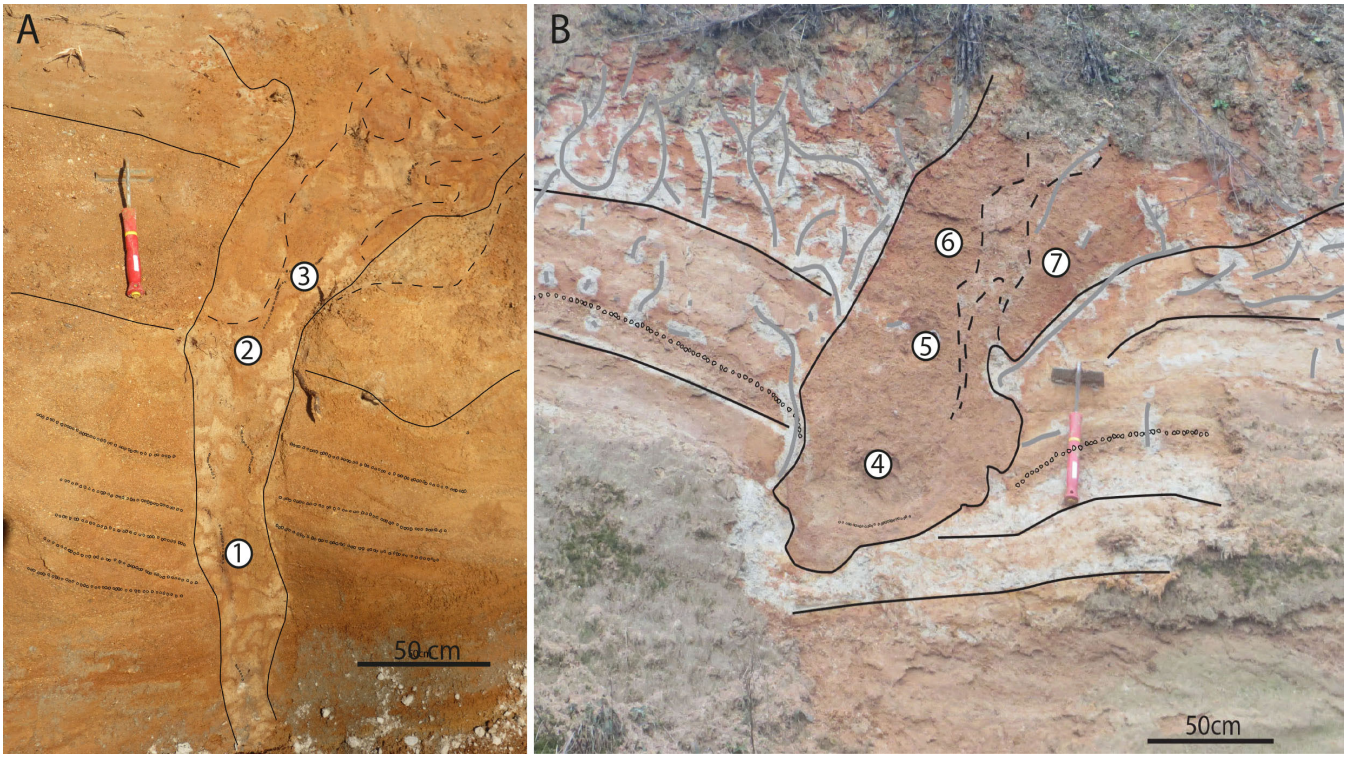

Figure 23: A - Sand wedge in lower Pleistocene alluvial sand (Olivet, 47.815°N, 1.927°E), 1=Shfd15085, 2=Shfd15086. Its opening is deformed by cryoturbations, the sample 3 was not dated. B - Composite-wedge pseudomorph in Tertiary silty sand, 4=Shfd15087, 5=Shfd15088, 6=Shfd15089, 7=Shfd15090

3.2.2.3. La Chapelle aux Choux

At La-Chapelle-aux-Choux (Latitude 47.617°N, longitude 0.211°E, altitude 69 m a.s.l), three sand wedges found in gravel and sandy gravel were sampled (Fx, Fw). The wedges share a similar classic V shape but different size characteristics. The first sand wedge that was sampled appears below 30 cm of cryoturbated gravel, and is 0.35 m wide and 1 m in length (Shfd15076) (Figure 24A). Three samples were taken in another wedge found in gravel (Shfd15077, Shfd15078, Shfd15079). It is 0.5 m wide and 0.7 m in depth, but its top part may have been eroded (Figure 24B). Two samples were taken in another sand wedge that develops in sandy gravel (Shfd15083, Shfd15084). It is 0.35 m wide, 1 m in depth. While the other two wedges sampled in this area have a massive sand infilling this one shows laminations of more or less coarse sand and is characterized by a centimetre-wide crack extending downward out of the wedge toe (Figure 24C).

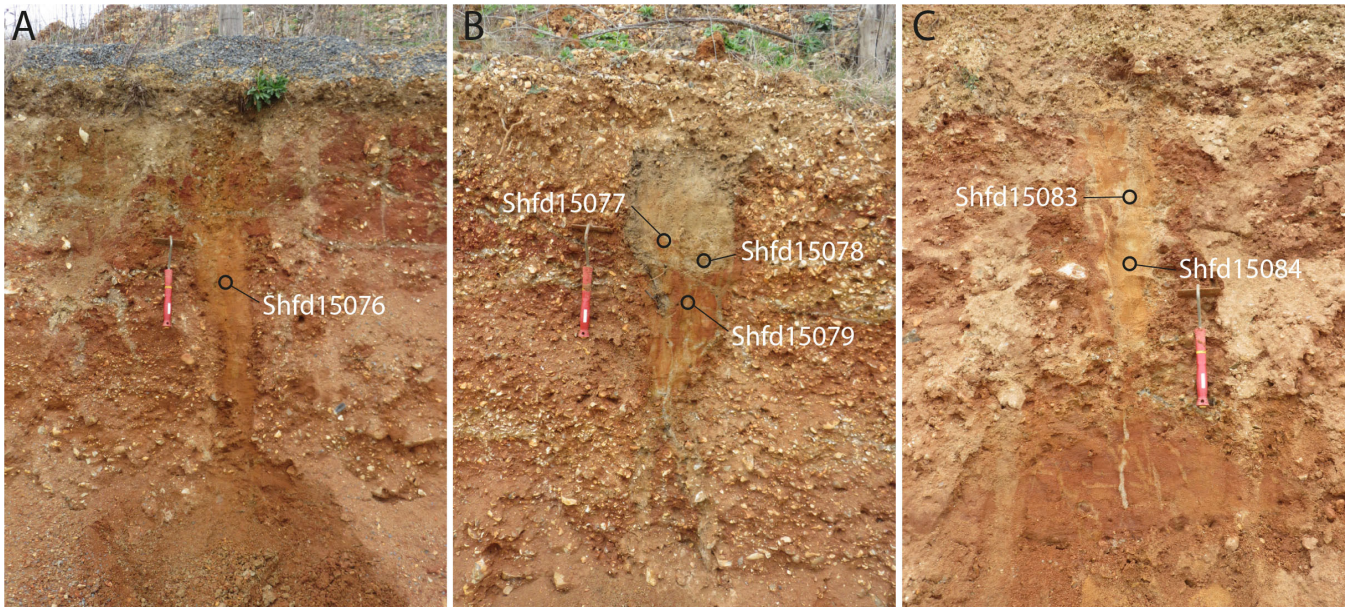

Figure 24: Sand-wedges in Midlle Pleistocene gravel and sandy gravel (La Chapelle aux Choux, 47,61°N, 0.21°E). The scraper is 35 cm long.

3.2.2.4. Les Rairies (Durtal)

At Les Rairies (Durtal, latitude 47.660° N, longitude 0.231° W, altitude 39 m a.s.l.), a composite wedge pseudomorph has been identified within sandy gravel deposits (Fx). Unlike other composite wedge pseudomorphs observed, the wedge sampled has a late primary sandy infill with laminations (30 cm wide, 1.7 m depth) which cross-cuts a wider secondary infill composed of massive sandy gravel (1 m wide, 2 m in depth). Vertical laminations are visible in the infilling of the sand wedge where 2 samples were taken: Shfd13040 was dated using both single aliquot SAR OSL and single grain SAR OSL (Shfd13040-2) and Shfd14028 with single grain SAR OSL. A sample taken in the secondary infilling returned incoherent ages (Figure 25A).

3.2.2.5. Saint-Christophe-du-Ligneron (Challans)

At Saint-Christophe-du-Ligneron (Challans, latitude 46.8° N, longitude 1.76° E, altitude 32 m a.s.l.), a sand wedge has been described within gravel (P2) and sampled (Shfd14020). It is 0.4 m in width and 1.4 m in depth. The first 30 cm of the host material show a platy structure which testifies to numerous freezing and thawing cycles. In the wedge the upper 30 cm are composed of a sandy gravel whereas the lower part of the infilling is massive silty sand (Figure 25B). It is likely that this wedge is a composite-wedge pseudomorph.

3.2.2.6. La Flèche (La Louverie)

At La Flèche (La Louverie, latitude 47.685° N, longitude 0.010° W, altitude 34 m a.s.l.), a forked sand wedge was identified. It opens in sand and gravel (Fx) where upward bending of the strata is visible. The top part of the wedge is deformed, 0.5 m wide, and affected by redox and soil formation processes. The wedge is 1.7 m and its silty sand infilling shows a laminated part where a sample was taken (Shfd14027) (Figure 25C).

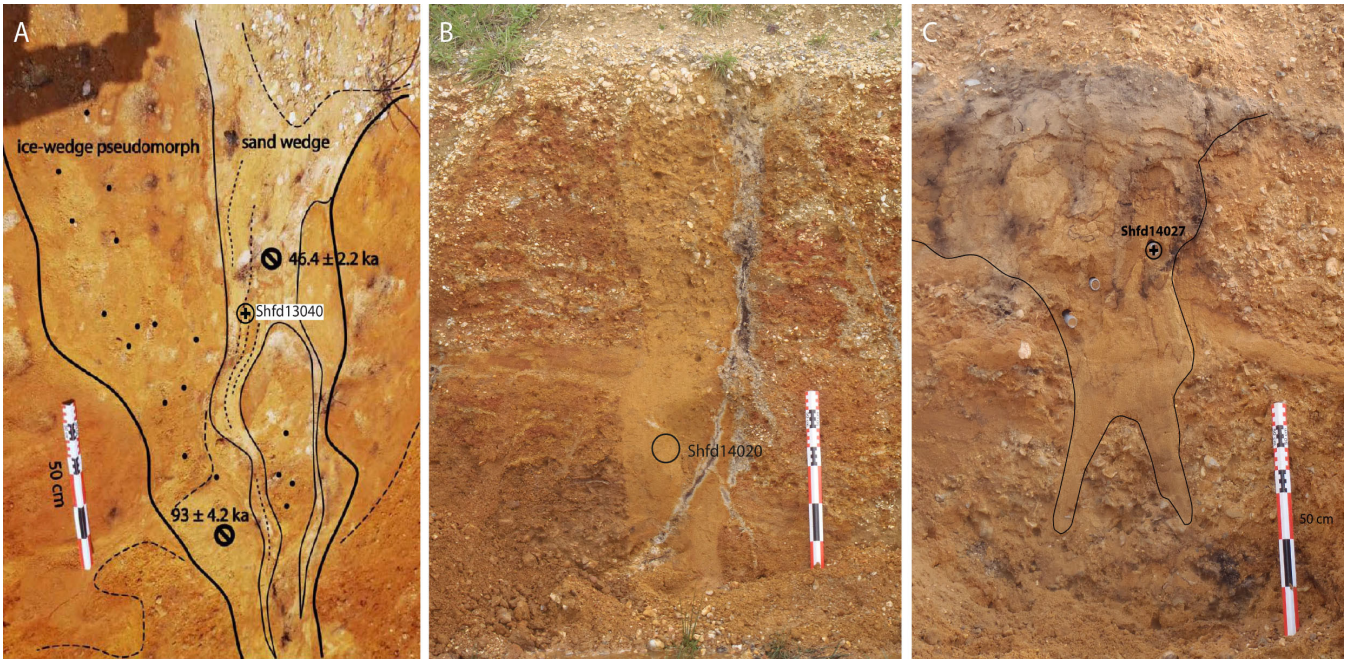

Figure 25: A - Composite-wedge pseudomorph in Midlle Pleistocene sandy gravel (Durtal, 47,66°N, 0.231°E); B - Sand-wedge in Pliocene gravel (Challans, 46.8°N, 1.76°E); C - A forked sand-wedge in Middle Pleistocene sand and gravel (La Louverie, 47.685°N, 0.01°W)

3.3. Luminescence Dating

The dating of relict periglacial wedges yields palaeoclimatic and geomorphological information. Emphasis was placed on the dating of primary sand infill, deposited in thermal contraction cracks, because it can provide age estimates of the timing of wedge growth. Optically Stimulated Luminescence (OSL) dating was considered the most adequate method to derive an absolute chronology for thermal contraction cracking in France.

After burial the sediment is exposed to a low level of radiations coming from both cosmic radiations (cosmic rays) and the decay of naturally-occurring radionuclides, principally Uranium (U), Thorium (Th), Rubidium (Rb) and Potassium (K). They are present in the surrounding sediment matrix or are constituents of some minerals, and emit alpha particles (α), beta particles (β) and gamma rays (ɣ). Most crystals contain lattice defects or impurities where electrons get trapped when excited by these ionizing

radiations. Since this occurs at a certain rate, the crystals act as storage units of energy which intensity is related to the time of accumulation. Eviction of electrons from shallow traps may occur by vibration of the lattice during burial of the sample (Aitken, 1998). This makes the shallow traps unstable and not adequate for dating. Deeper traps require a higher amount of energy to be emptied and thus are stable over geological time-scales. Energy coming from sunlight during transport, from an external light or thermal source is required to remove the electrons out of deeper traps and make it return to its equilibrium state (i.e bleaching, zeroing or reset; Figure 26A). In the case of optically stimulated luminescence, light is used to release the electrons from the traps. Once the electrons are evicted, they can be trapped again, or recombine in defects attractive to electrons (luminescence centres). The recombination of the electrons result in the emission of light, termed optically stimulated luminescence. The intensity of the light signal emitted is proportional to the amount of electrons stored in the defects. This allows for the stored charge to be quantified, i.e. the equivalent dose (De) measured in Gray (Gy). It can be used in combination with the data on the total dose rate received while buried (Gy/ka) to calculate the age since the last light or heat exposure following (Aitken, 1998):

Age (ka) = Equivalent dose (De) (Gy) / Dose rate (Gy/ka)

The luminescence measurements were performed in Sheffield (England) under the supervision of Mark Bateman (Departement of Geography, University of Sheffield) on a Risø reader TL-DA-15 equipped with a 90Sr/90Y beta source for irradiation (Figure 26B). Quartz was chosen over feldspars because it is ubiquitous in sand-wedge infilling. It can provide age estimates up to 350 ka (Murray and Olley, 2002). Preparation of the samples and dating methodologies are described in chapter 6.

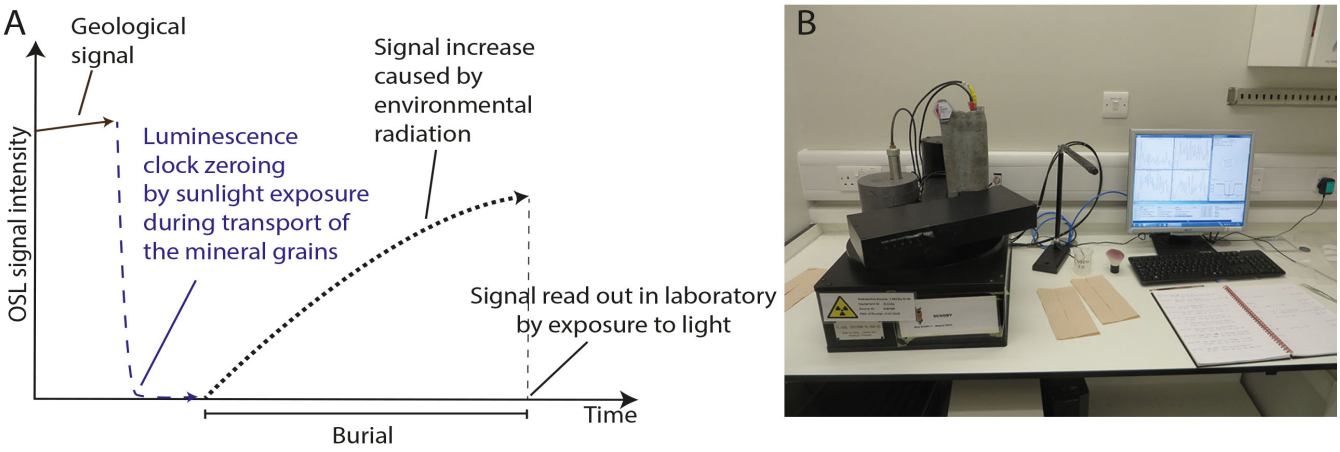

Figure 26: A - Luminescence principle. B - Risø reader TL-DA-15 equipped with a 90Sr/90Y beta source for irradiation used for the OSL measurements in this PhD, aka Scooby

4. Database of Pleistocene periglacial features in France: description of the online version

Eric Andrieux, Pascal Bertran, Pierre Antoine, Laurent Deschodt, Arnaud Lenoble, Sylvie Coutard, et collaborateurs*

* Aurélie Ajas, Quentin Borderie, Jean-Pierre Coutard, François Didierjean, Bertrand Dousteyssier, Catherine Ferrier, Philippe Gardère, Thierry Gé, Morganne Liard, Jean-Luc Locht, Henri-Georges Naton, Mathieu Rué, Luca Sitzia, Brigitte Van Vliet-Lanoë, Gérard Vernet

Andrieux, E., Bertran, P., Antoine, P., Deschodt, L., Lenoble, A., Coutard, S., 2016b. Database of pleistocene periglacial features in France: description of the online version », *Quaternaire*, 27/4, 329-339.

Quaternaire, **27**, (4), *2016*, p. 329-339

DATABASE OF PLEISTOCENE PERIGLACIAL FEATURES IN FRANCE: DESCRIPTION OF THE ONLINE VERSION

■

Eric ANDRIEUX[1], Pascal BERTRAN[2, 1], Pierre ANTOINE[3], Laurent DESCHODT[4], Arnaud LENOBLE[1], Sylvie COUTARD[5] & collaborators*

ABSTRACT

A database of Pleistocene periglacial features in France has been compiled from a review of academic literature and reports of rescue archaeology, the analysis of aerial photographs and new field surveys. Polygons, soil stripes, ice-wedge pseudomorphs, sand wedges and composite wedge pseudomorphs are included in the database together with their geographic coordinates, geological context, description and associated references. It is hoped that this database, which aim is to be integrated in broader studies, will stimulate further work on past permafrost reconstruction and will favour greater understanding of the climatic events that lead to the formation of the periglacial features. The database is available online on the AFEQ-CNF INQUA website (https://afeqeng.hypotheses.org/487). A folder that contains photographs and sketches of the features is also available on request.

Keywords: permafrost, ice-wedge pseudomorphs, sand wedges, composite wedge pseudomorphs, polygons, soil stripes, France

RÉSUMÉ

BASE DE DONNÉES DES STRUCTURES PÉRIGLACIAIRES PLÉISTOCÈNES EN FRANCE : DESCRIPTION DE LA VERSION ACCESSIBLE EN LIGNE

Une base de données des structures périglaciaires pléistocènes de France a été créée à partir d'une revue de la littérature scientifique, de rapports d'archéologie préventive, de l'analyse de photographies aériennes et de nouvelles prospections de terrain. Les polygones, les sols striés, les pseudomorphoses de coin de glace, les coins de sable et les pseudomorphoses de coin composite ont été répertoriés dans la base de données avec leurs coordonnées géographiques, le contexte géologique, leur description et les références bibliographiques associées. Nous espérons que cette base de données, dont le but est d'être intégrée dans des études plus larges, stimulera de prochains travaux sur la reconstitution du pergélisol pléistocène et favorisera une plus grande compréhension des événements climatiques qui ont conduit à la formation de ces structures périglaciaires. La base de données est disponible en ligne sur le site de l'AFEQ-CNF INQUA (https://afeqeng.hypotheses.org/487). Un dossier contenant les photographies et dessins des structures périglaciaires est également disponible sur demande.

Mots-clés : pergélisol, pseudomorphoses de coin de glace, coins de sable, pseudomorphoses de coin composite, polygones, sols striés, France

1 - INTRODUCTION

During the Pleistocene, periglacial landscapes have formed over large surfaces in mid-latitude Western Europe. The Mid to Late Pleistocene climate oscillations caused the land area affected by periglacial conditions to expand and contract repeatedly. Many relict periglacial features bear witness of these events and raised abundant research by geologists and geomorphologists. Aside from the engineering aspects of these discoveries, the scientific community focused on the climatic significance of the features, the reconstruction of past environments, and finally, the possible impact of the periglacial milieus on Palaeolithic populations.

Reconstructions of the previous extent of permafrost in Western Europe have been proposed for over 60 years (Poser, 1948; Büdel, 1951; Kaiser, 1960; Maarleveld, 1976; Lautridou & Sommé, 1981; Velichko, 1982). Further improvements were later made using increasingly available observations on present-day permafrost

[1] PACEA, UMR 5199 Université de Bordeaux – CNRS, Bâtiment B18, Allée Geoffroy-Saint-Hilaire, CS 50023, FR-33615 Pessac cedex. *Courriel* : andrieux.e@gmail.com
[2] INRAP, 140 avenue du Maréchal Leclerc, FR-33130 Bègles. *Courriel* : pascal.bertran@inrap.fr
[3] LGP, UMR 8591 Université Paris 1 – CNRS, 1 place A. Briand, FR-92195 Meudon cedex. *Courriel* : pierre.antoine@cnrs-bellevue.fr
[4] INRAP, 11 rue des champs, ZI de la Pilaterie, FR-59650 Villeneuve-d'Ascq. *Courriel* : laurent.deschodt@inrap.fr
[5] INRAP, 518 rue Saint-Fuscien, FR-80090 Amiens. *Courriel* : sylvie.coutard@inrap.fr

* Aurélie AJAS, Quentin BORDERIE, Jean-Pierre COUTARD, François DIDIERJEAN, Bertrand DOUSTEYSSIER, Catherine FERRIER, Philippe GARDÈRE, Thierry GÉ, Morgane LIARD, Jean-Luc LOCHT, Henri-Georges NATON, Mathieu RUÉ, Luca SITZIA, Brigitte VAN VLIET-LANOË, Gérard VERNET.

Manuscrit reçu le 18/05/2016, accepté le 20/07/2016

(Péwé, 1966; Romanovskij, 1985; Mackay & Burn, 2002; Murton, 2013), and sporadic, discontinuous and continuous Pleistocene permafrost was differentiated in the proposed maps (Vandenberghe & Pissart, 1993; Van Vliet-Lanoë, 1989, 1996; Huijzer & Vandenberghe 1998; Isarin *et al.*, 1998; Van Vliet & Hallégouët, 2001; Renssen and Vandenberghe, 2003; Vandenberghe *et al.*, 2014). Despite the lack of agreement between these reconstructions, these studies agree that permafrost extended over large parts of France during the Pleistocene.

Most of the datasets available have been published in French language with limited circulation, and unfortunately remains largely inaccessible to the international community. During the last decade, the launch of online databases of aerial photographs (Google earth, Géoportail) has eased the recognition of periglacial features, adding a lot of new data. The huge development of rescue archaeology also increased significantly the number of identified features.

This paper serves as an introduction to an online database aiming at gathering as exhaustively as possible the features related to past permafrost in France, to give easier access to a homogenised and reliable dataset. It also reports on the main limits that should be considered when using the map or the data to make interpretations. The establishment of such a database is of the outmost importance to progress towards a better general understanding of periglacial environments.

The database was first introduced by Bertran *et al.* (2014), who focused on the geographic distribution of the georeferenced features and reviewed the available chronological data. Periglacial features and their characteristics were entered into a GIS to elucidate the different factors that influenced the development of periglacial features and to propose a new map of the main Pleistocene permafrost boundaries in Western Europe (Andrieux *et al.*, 2015). We propose here an improved online version of the database illustrating and explaining identification criteria of the periglacial features gathered.

2 - DATA COLLECTION, DATABASE STRUCTURE

The selected items comprise features observed from aerial photographs and classified in (i) polygonal networks and (ii) soil stripes, and features observed in cross-section and classified in (iii) sand wedges, (iv) ice-wedge pseudomorphs, and (v) composite wedge pseudomorphs. Involutions, patterned grounds other than soil stripes, pingo and lithalsa scars, which are also considered potentially testifying to past permafrost, have not been integrated into the database, since re-evaluation of the features mentioned in the literature is still under progress. They will be added to the database at the end of this process. Similarly, mountain permafrost features were not included in the database.

Multi-user tests were performed on the photographs to be sure that only indisputable features were added to the database. When different features were present on the same site, it appears in the file of the most represented type. Search for periglacial features in aerial photographs have been made primarily in areas where some had been previously reported in the literature. Search was then extended to neighbouring regions. In this process, it became rapidly obvious that many features were preferentially associated with specific substrates, for example old (Lower Pleistocene and Tertiary) alluvial sand and gravel deposits for polygons, chalk with a thin loess cover for soil stripes… Blind tests in other regions were also made but were most of the time unsuccessful.

We also conducted a thorough search of the published literature on periglacial features in France, including articles in journals, PhD theses, other dissertations (often unpublished) and geology reports of rescue archaeology. These data were rigorously selected and all entries not accompanied by drawings, photographs or good descriptions were rejected from the database. We were forced to exclude a significant amount of features because the sources did not document them enough (lack of description or figure) or did not give satisfying geographic information (e.g. coordinates, grid references).

The investigated literature covers the last 60 years, and during such a time span the overall understanding and classification of the periglacial processes changed significantly. In the 50's, the research community lead by A. Cailleux and J. Tricart (Bastin & Cailleux, 1941; Cailleux, 1948, 1956; Tricart, 1963; Tricart & Cailleux, 1967) described abundant features assumed to be of periglacial origin in France, proving that Pleistocene frost-induced processes played a major role in shaping the landscape. Many were also mentioned in the explanatory notes accompanying the sheets of the geological map of France. "Fente de gel" (i.e. frost crack) and "fente en coin" (i.e. wedge) were used as general terms for wedges and cracks regardless their filling and width. As a consequence, with few exceptions (e.g. Michel, 1975; Yvard, 1968; Nury & Roux, 1969; Arnal, 1971), the "frost crack" data remains hardly usable within the frame of the current database.

A total of 615 sites have been identified. In aerial photographs, a site corresponds to a single land parcel or a few adjacent parcels.

The database consists of 5 CSV (Comma-Separated Values) files each dedicated to a single type of feature. The CSV format was chosen because of its simple use and the possibility of easy transformation into an attribute table in a GIS. Each CSV file is accompanied with a folder that contains photographs and sketches of the features when available. The ID number allows linking the listed features and corresponding pictures, drawings, or aerial photographs.

The basic fields documented are as follows:

– ID, the identification number of the feature;

– Longitude and Latitude in decimal degrees in the EPSG:4326 (WGS84) coordinate reference system;

– Altitude, derived from the DEM Aster GDEM 30 m;

– Site, the name of the place;

– City, the municipality;

– Region, the administrative region;

– Geol_code, the code of the geological substrate as shown in the 1:50,000 geological map of France (infoterre.brgm.fr);

– Substrat, the (simplified) lithology of the geological substrate as indicated in the explanatory note of the 1:50,000 geological map. "/" stands for "above";

– Reference, the bibliographic references when available;

– Photo_credit, the author of the photograph(s) or drawing(s) when available.

Additional fields are also provided for each type of features. They include:

– Size, the average size of the polygons calculated with the software ImageJ (see Andrieux *et al*., 2015, for detailed explanation of the measurement protocol);

– Spacing, the average spacing of the soil stripes calculated with the software ImageJ;

– Slope, the average slope gradient (in degrees) of the soil stripes derived from the DEM Aster GDEM 30 m;

– Expo, the orientation of the soil stripes (in degrees) measured on Google earth with the "ruler" tool;

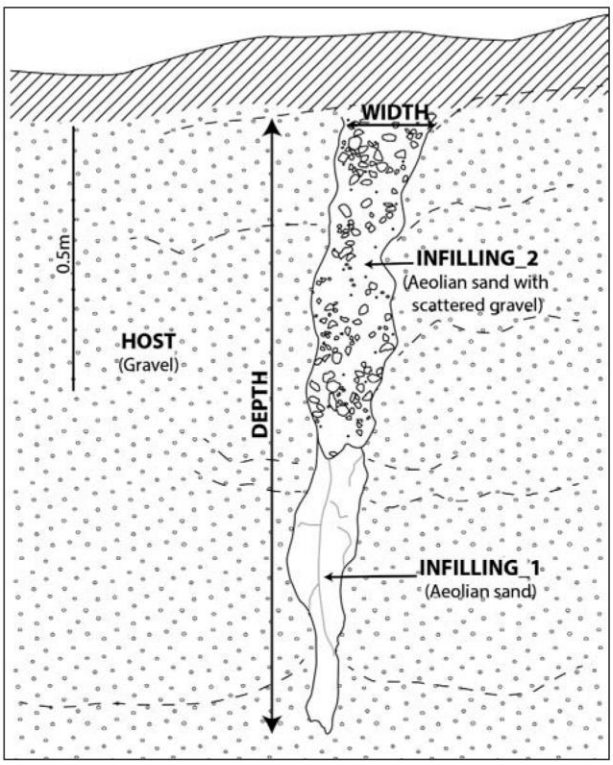

Fig. 1: Terms used for wedge description.
This composite wedge pseudomorph is located in Mérignac (Chronopost, 44°49'37.2"N, 0°41'23.999"W).
Fig. 1 : Termes utilisés pour la description des coins. La pseudomorphose de coin composite représentée provient du site de Chronopost à Mérignac (44°49'37.2"N, 0°41'23.999"W).

– Host, the lithology of the host material of the wedges determined from the description of the cross-section (fig. 1);

– Filling_1, the lithology of the main filling of the wedge;

– Filling_2, in case of different types of filling;

– Depth and Width, the dimensions of the wedges (Depth = null if the apex of the wedge is not visible).

Most of the features remain non dated at the moment. The chronological data have not been included in the database, they are accessible through the cited references.

3 - FEATURES DESCRIPTION

3.1 - POLYGONS

When frozen ground cools down rapidly, it contracts and cracks if the tensile stress is not relieved by creep (Lachenbruch, 1962, 1966). Thermal contraction cracking occurs widely in areas subjected to deep freezing where snow and vegetation covers are thin (Mackay, 1993; Mackay & Burn, 2002; Fortier & Allard, 2005), with or without permafrost (Washburn *et al*., 1963; Friedman *et al*., 1971; Romanovskij, 1985). Thermal contractions cracking forms large polygonal networks of fissures, evolving into V shaped wedges as a consequence of repeated filling by ice or sediment. The 284 fossil polygon sites listed in the database and found in aerial photographs are between 8 and 20 m in diameter (mean = 15 m, Andrieux *et al*., 2015). Most of the polygons observed in the lower Loire and Rhône valleys have sharp edges and thin walls, which appear darker than the surrounding land in aerial photographs (fig. 2A, B). Cross-sections discovered in the vicinity of a few sites suggest that the walls correspond to sand wedges or composite wedges. In the Paris basin and the north of France, some polygons have more rounded outlines and walls of irregular width (fig. 2C, D). They are thought to correspond to former ice-wedge polygons that have undergone thermokarstic degradation. Polygons in vineyards such as those in the Médoc region, southwest France, are often hardly visible in aerial photographs. Although not very conclusive by themselves, some photographs have been kept in the database because of the discovery of sand wedges in nearby cross-sections (Lenoble *et al*., 2012; Bertran *et al*., 2014). Aerial photographs also revealed fields of irregular and rounded "polygonal" features showing more heterogeneous sizes than typical ice or sand wedge polygons (fig. 3). Although a periglacial origin seems probable, their classification as thermal contraction features rather than very large patterned grounds remains doubtful (see aerial photographs and cross-sections in Agache, 1963, 1970) and needs further confirmation by field survey. As a consequence, this kind of features was not added to the database.

Fig. 2: Polygons.
Polygons with sharp edges and thin walls at (A) Marcilly-en-Villette (47°47'49.2"N, 1°58'15.6"E) and (B) Le Plessis-Grammoire (47°29'13.2"N, 0°26'16.799"W); polygons with rounded outlines due to thermokarstic degradation of the wedges at (C) Cantenay-Epinard (47°32'31.2"N, 0°26'16.799"W) and (D) Sainte-Geneviève-des-Bois (47°48'3.6"N, 2°46'37.2"E).
Fig. 2 : Réseaux polygonaux. Polygones avec des cloisons nettes et étroites à (A) Marcilly-en-Villette (47°47'49.2"N, 1°58'15.6"E) et (B) Le Plessis-Grammoire (47°29'13.2"N, 0°26'16.799"W) ; polygones avec des contours arrondis liés à la dégradation thermokarstique de coins de glace à (C) Cantenay-Epinard (47°32'31.2"N, 0°26'16.799"W) et (D) Sainte-Geneviève-des-Bois (47°48'3.6"N, 2°46'37.2"E).

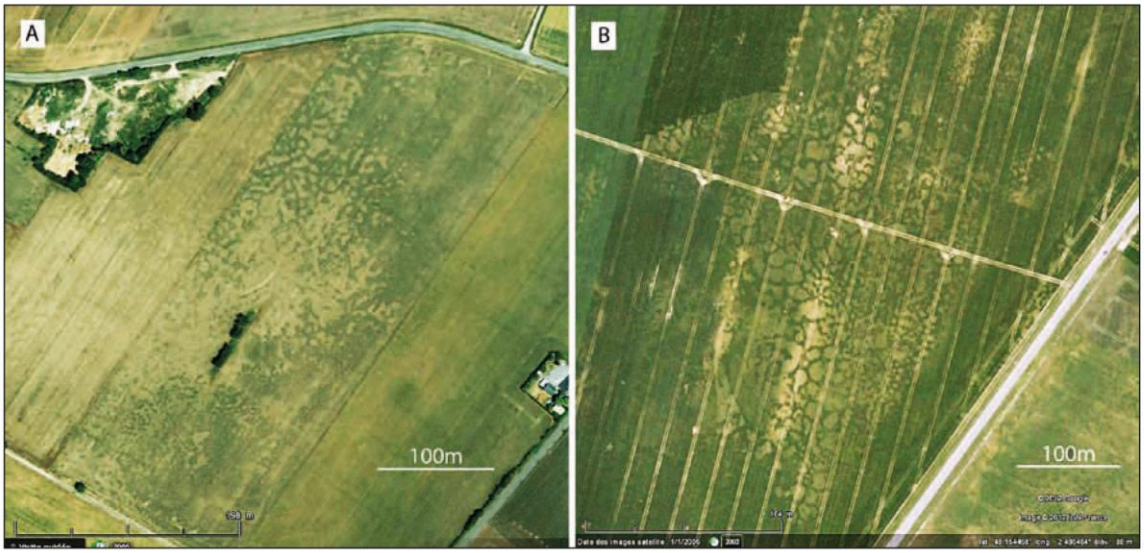

Fig. 3: Irregular polygonal patterns.
A/ Beaumont-du-Gâtinais (48°9'10.8"N, 2°29'20.399"E). B/ Poillé-sur-Vègre (47°55'22.8"N, 0°16'22.8"W).
Fig. 3 : Réseaux polygonaux irréguliers. A/ Beaumont-du-Gâtinais (48°9'10.8"N, 2°29'20.399"E). B/ Poillé-sur-Vègre (47°55'22.8"N, 0°16'22.8"W).

Small-scale polygons up to 1 m in diameter have been widely reported during field surveys but were not included in the database. They are assumed to reflect mostly (cryo-) desiccation fissures (Washburn, 1979; Van Vliet-Lanoë & Langohr, 1981).

3.2 - ICE-WEDGE PSEUDOMORPHS

Ice-wedge pseudomorphs, i.e. the features left by the melt of an ice-wedge, have been widely reported in France. Severe selection was made among the reported features, 90 ice wedge pseudomorphs are listed in the database. According to Black (1976), Washburn (1979), Vandenberghe (1983), Gozdzik (1994) and Murton (2013), the main criteria for their identification and consideration in the database are: (1) a V shape showing collapse structures due to the replacement of ice; these consist in block faulting (common in the coversands of northern Europe, Murton, 2013; no example has been found in France so far, fig. 4C), downturned strata in the host material or folding of the strata toward the wedge, vertically aligned clasts along the walls of the pseudomorph (mainly in gravel); (2) a minimum size of 0.2 m in width and 1.5 m in height, (3) deformation of the host material (upturned strata, vertical gravel pebbles) due to wedge growth, (4) evidence for a polygonal pattern from cross-sections or aerial photographs. The filling may be massive or show steeply dipping or U-shaped layers. Blocks of sediment may be present within the filling (fig. 4B). In loess deposits ice-wedge pseudomorphs are usually associated with a cryoturbated bleached layer with small ferruginous spots, interpreted as a former gley soil over permafrost (Gullentops, 1954; Haesaerts & Van Vliet-Lanoë, 1973; Antoine *et al.*, 2009, fig. 4A). Thermokarstic degradation of permafrost may lead to the erosion and deformation of the wedge, the formation of tunnels, ponds and gullies so that the relict ice-wedges are no longer identifiable or visible. The distribution of ice wedge pseudomorphs is therefore probably significantly underestimated in our dataset.

Not included in the database are many wedge structures described in France in the literature. They are narrow and lack any clear indication of host material collapsed in the wedge after the melt of an ice body (fig. 5). These features may represent either incipient ice wedges (ice veins) or soil wedges in seasonally frozen ground (Friedman *et al.*, 1971; Romanovskij, 1973; Murton, 2013).

3.3 - SAND-WEDGES

The primary filling of thermal contraction cracks by wind-blown sand forms sand wedges (Péwé, 1959; Black, 1976; Washburn, 1979; Kolstrup, 1986; Gozdzik, 1986; Murton, 1996; Bockheim *et al.*, 2009). Sand wedges do not show evidence of host material slumped in the wedge. They are usually V-shaped but may be irregular with multiple elementary sand veins extending out of the toe of the wedge into the host material (this typically occurs in sands, Romanovskij, 1976; Murton *et al.*, 2000) (fig. 6A), or have a "bulbous" shape (fig. 6B). The origin of the bulbous shape, illustrated by Murton *et al.* (2000) in Poland, remains uncertain. In our dataset, they were observed only in fine-grained substrates and may reflect deformation during the thawing of an ice-rich host sediment or deformation of the seasonally frozen layer due to frost heave (Jetchick & Allard, 1990; Van Vliet-Lanoë, 2005). Deformation of the host material induced by wedge growth is usually poorly developed and upward bending of strata occurs only occasionally. Field exposures generally show multiple sand wedges a few metres apart, which testifies to a polygonal pattern. The sand wedges identified in France have generally a massive filling (fig. 6C) but show sometimes vertical laminations (fig. 6D). According to Péwé (1959) and Murton & Bateman (2007), the lack of vertical lamination does not necessarily imply a secondary perturbation caused by the thaw of ice veins. Small eolised gravels may occasionally be present in the upper part of the filling and have probably felt into the fissures during the opening of the wedges (Péwé, 1959) (fig. 6E).

In the database, 82 sand wedges are listed. Only the wedges with a minimum width of 0.2 m and 0.5 m in height were added to the database to be sure to not consider possible desiccation or extension cracks filled by sand.

3.4 - COMPOSITE-WEDGE PSEUDOMORPHS

Composite wedges are thermal contraction cracks filled both by wind-blown sand and ice (Kolstrup, 1986; Murton, 1996; Murton *et al.*, 2000, 2007; Antoine *et al.*, 2005). The composite wedges share therefore common features with ice-wedge pseudomorphs and (primary) sand wedges. The most diagnostic feature is the evidence of a secondary filling occupying a significant part of the wedge. This filling appears typically either as cross-stratified to U-shaped beds of sand or gravel material (fig. 7A, B) or as a mixture of well-sorted (aeolian) sand with scattered gravel in the whole mass. Only wedges with a significant part of the filling showing U-shaped stratification were considered as composite wedge pseudomorphs since simple sand wedges may exhibit such a stratification in the upper decimetres as shown by Péwé (1959). In many cases, however, the wedges show different types of filling cross-cutting each other, suggesting a succession of dominantly icy or sandy phases (fig. 7C). One example (fig. 7D) corresponds to a gully overlying a truncated sand wedge. The gully is thought to be of thermokarstic origin and, therefore, suggests that the wedge filling contained a significant amount of ice. Overall, 10 composite-wedge pseudomorphs are listed in the database. However, this number may be underestimated because of difficulties in identifying secondary sandy fillings. Potential composite wedge pseudomorphs may, therefore, be classified here as sand-wedges.

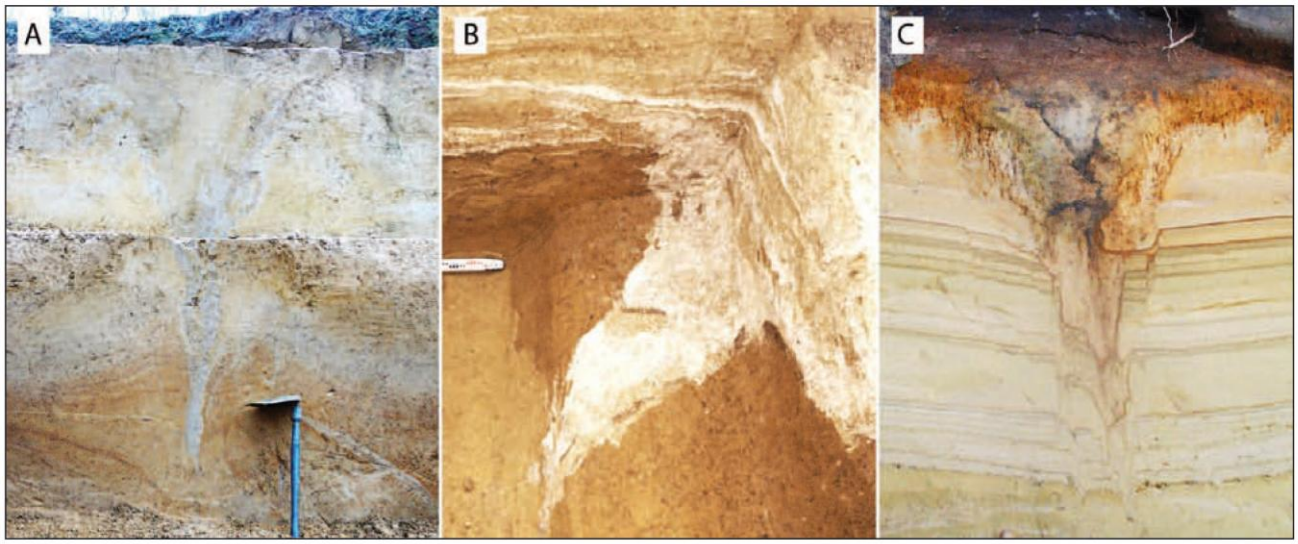

Fig. 4: Ice-wedge pseudomorphs.
A/ Pseudomorph filled by gleyed loess, Saint-Hilaire-sur-Helpe (50°7'12"N, 3°53'5.999"E; photo P. Antoine); the shovel is 50 cm long. B/ Collapsed blocks of loess in a pseudomorph, Corbie (49°55'48"N, 2°28'47.999"E; photo P. Antoine). C/ Pseudomorph with faulted blocks along the walls in coversands, Lutterzand, the Netherlands.
Fig. 4: Pesudomorphoses de coin de glace. A/ Pseudomorphose remplie par des læss gleyifiés à Saint-Hilaire-sur-Helpe (50°7'12"N, 3°53'5.999"E; photo P. Antoine) ; la pelle fait 50 cm de long. B/ Blocs de læss effondrés dans une pseudomorphose à Corbie (49°55'48"N, 2°28'47.999"E; photo P. Antoine). C/ Pseudomorphose de coin de glace avec des blocs glissés le long des parois dans des sables de couverture à Lutterzand, Pays-Bas.

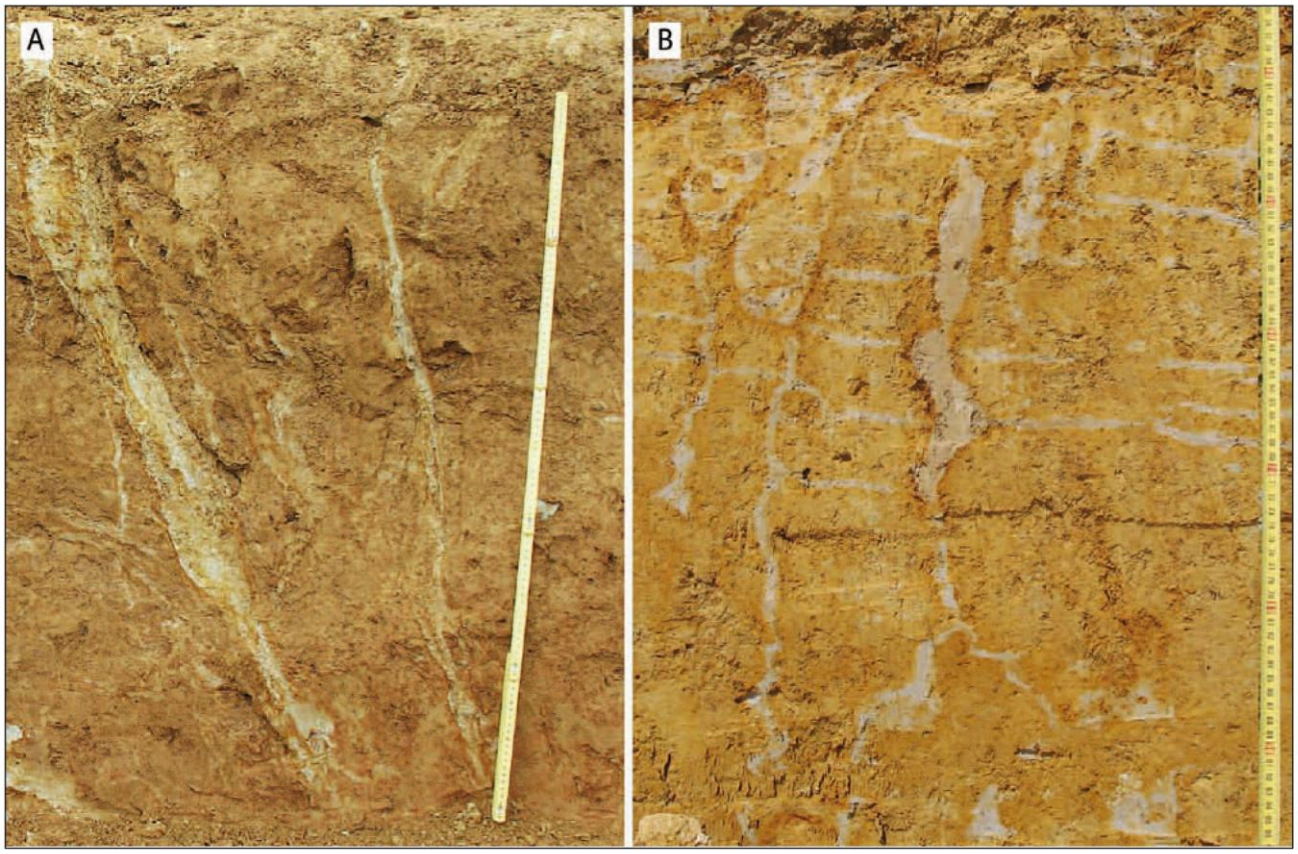

Fig. 5: Fissures interpreted as (cryo-)desiccation or thermal contraction cracks in a seasonally frozen ground.
A/ Combebrune 2 and B/ Romentères. The host material is colluviated aeolian silt. Both features located in the southwest of France form small-scale polygons in plan view (0.5 to 1 m in diameter). Although the digitations suggest repeated cracking, no evidence for ice melt and subsequent filling is visible. The fissures were secondarily affected by redox processes and bleaching due to waterlogging. In photo B, bleached horizontal fissures suggest that ice lenses formed in connection with the vertical fissures. The scale is 1 m long.
Fig. 5 : Fentes interprétées comme des fissures de (cryo-)dessiccation ou de contraction thermique dans un sol gelé saisonnièrement. A/ Combebrune 2 et B/ Romentères. Le matériel encaissant est composé de limons éoliens colluvionnés. Ces structures, situées dans le sud-ouest de la France, forment en plan des petits polygones de 0,5 à 1 m de diamètre. Bien que les digitations suggèrent une fissuration répétée, aucun indice de la fonte d'un corps de glace n'est visible. Les fissures ont été affectées secondairement par des processus d'oxydoréduction et un blanchiment lié à un engorgement temporaire. Dans la photo B, les fissures horizontales blanchies suggèrent que des lentilles de glace se sont formées en connexion avec les fissures verticales. L'échelle fait 1 m de long.

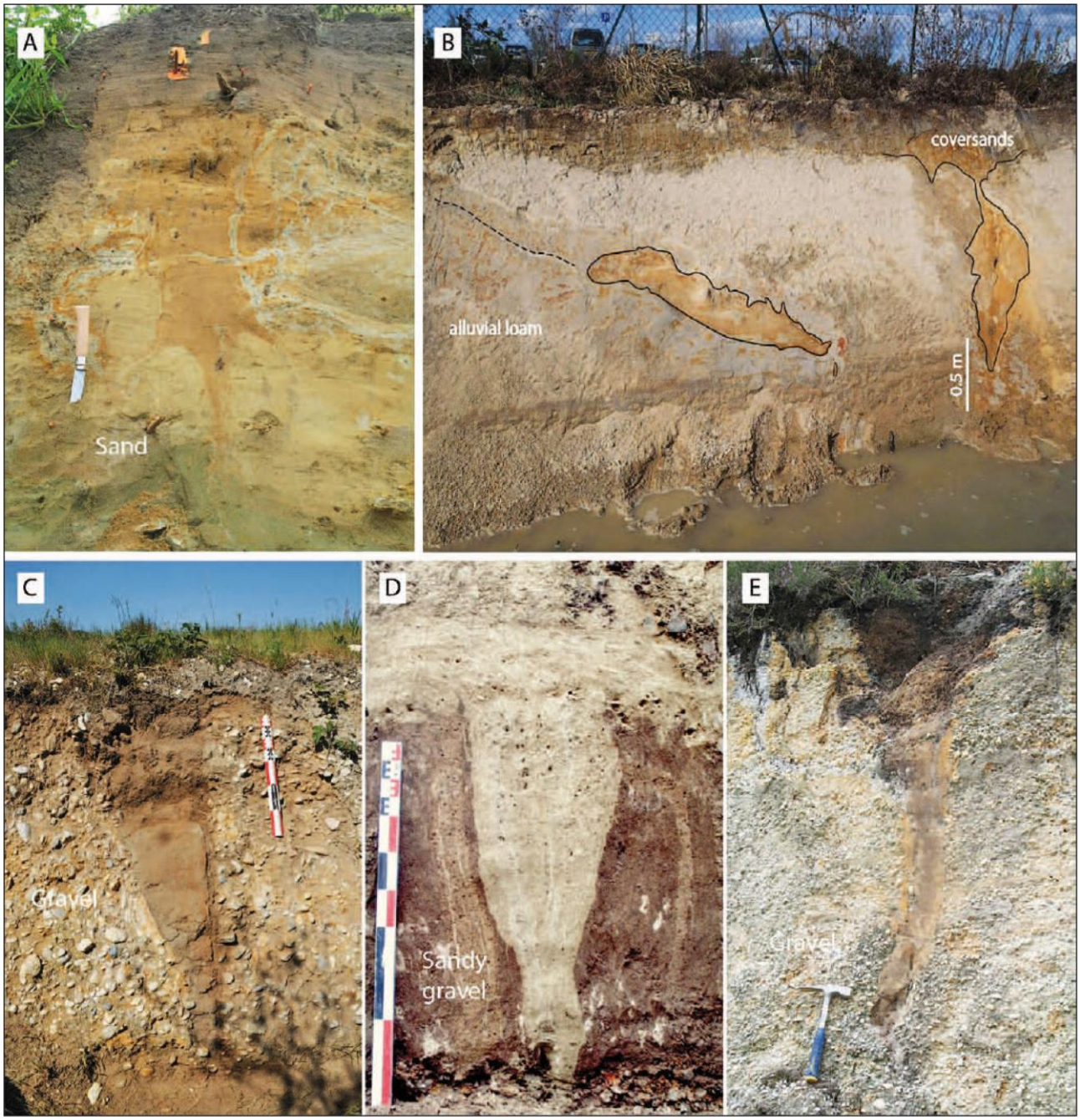

Fig. 6: Sand wedges.
A/ Sand wedge with multiple elementary sand veins extending out of the toe in Saint-Amand-les-Eaux (Mont-des-Bruyères, 50°26'16.8"N, 3°26'34.8"E); the knife is ca. 20 cm long. B/ Sand wedges with a bulbous shape in Mérignac (Chronopost 1, 44°49'37.2"N, 0°41'23.999"W). C/ Sand wedge with massive sand filling in Cussac-Fort-Médoc (Déchetterie, 45°7'19.2"N, 0°45'3.6"W); the scale is 50 cm long. D/ Sand wedge with vertical lamination in Joze (45°52'12"N, 3°17'24"E; photo G. Vernet); the scale is 1 m long. E/ Small eolised gravels in the top part of a sand wedge in Léognan (Lac Bleu 44°43'15.6"N, 0°37'29.999"W); the hammer is ca. 35 cm long.
Fig. 6 : Coins sableux. A/ Coin sableux avec de multiples veines élémentaires dans le prolongement de l'apex du coin à Saint-Amand-les-Eaux (Mont-des-Bruyères, 50°26'16.8"N, 3°26'34.8"E) ; le couteau fait 20 cm de long. B/ Coins sableux avec une forme en bulbe à Mérignac (Chronopost 1, 44°49'37.2"N, 0°41'23.999"W). C/ Coin sableux à remplissage primaire massif à Cussac-Fort-Médoc (Déchetterie, 45°7'19.2"N, 0°45'3.6"W) ; l'échelle fait 50 cm de long. D/ Coin sableux avec des laminations verticales à Joze (45°52'12"N, 3°17'24"E; photo G. Vernet) ; l'échelle fait 1 m de long. E/ Petits graviers éolisés dans la partie supérieure du remplissage d'un coin sableux à Léognan (Lac Bleu 44°43'15.6"N, 0°37'29.999"W); le marteau fait 35 cm de long.

3.5 - STRIPES

Stripes appearing in aerial photographs of ploughed fields are regularly spaced stripes of different colours, some of which are branched. They reflect alternating bands of light coloured (usually chalky) debris and darker loess or clay loam material or uneven plant growth due to contrasts in water content (fig. 8A, B). A small number of aerial photographs show spotted patterned ground on flat surfaces stretching into stripes on slopes (fig. 8D, C). A total of 149 sites of relict soil stripes have been identified in France, mostly in the Paris basin. The spacing between the stripes range from 2 to 13 m, but the distribution can be adjusted to two Gaussian functions peaking at 4.6 and

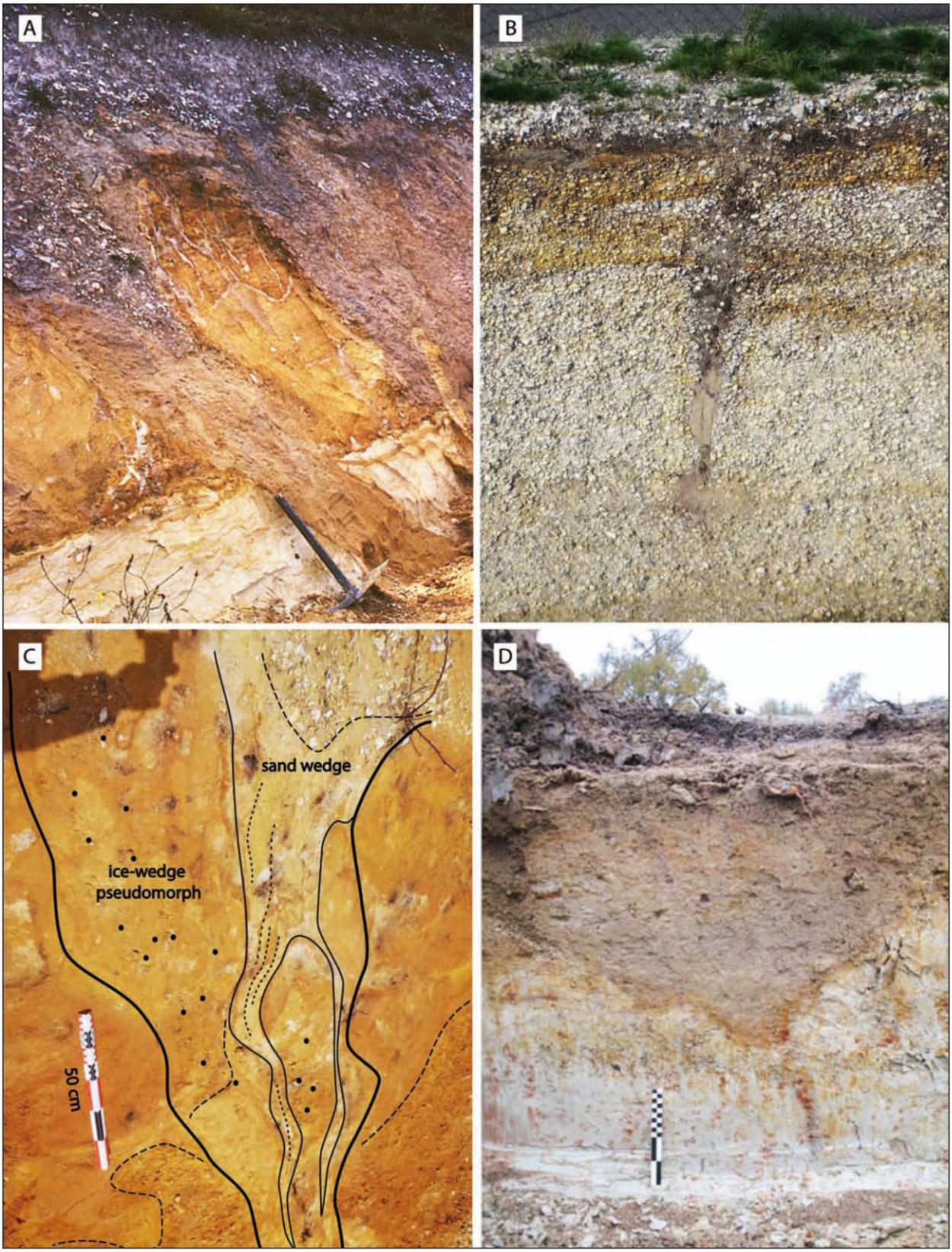

Fig. 7: Composite wedge pseudomorphs.
A/ Pseudomorph with a two-phase filling (sand, gravel) in Lessay (49°12'42.84"N, 1°31'52.859"W; photo J. P. Coutard); the pickaxe is 1 m long. B/ Same as A, Mérignac (Chronopost 2, 44°49'37.2"N, 0°41'16.799"W); the height of the wedge is 1.4 m. C/ Pseudomorph with different types of filling cross-cutting each other suggesting a first dominantly icy phase then a sandy one in Durtal (47°39'36"N, 0°13'51.6"W). D/ Thermokarstic gully truncating a sand wedge suggesting the melt of a former ice body in Saint-Vallier (LGV section 19-T244, 45°17'38.4"N, 0°4'19.199"W); the scale is 40 cm long.

Fig. 7 : Pseudomorphoses de coin composite. A/ Pseudomorphose avec un remplissage biphasé (sable, gravier) à Lessay (9°12'42.84"N, 1°31'52.859"W) ; la pioche fait 1 m de long. B/ Figure similaire à la précédente, Mérignac (Chronopost 2, 44°49'37.2"N, 0°41'16.799"W), la hauteur du coin est de 1,4 m. C/ Pseudomorphose avec deux générations successives de remplissage suggérant une première phase de type coin de glace, recoupée par une phase plus récente de type coin sableux à Durtal (47°39'36"N, 0°13'51.6"W). D/ Ravin probablement d'origine thermokarstique tronquant un coin à remplissage sableux suggérant la fonte d'un ancien corps de glace à Saint-Vallier (LGV section 19-T244, 45°17'38.4"N, 0°4'19.199"W) ; l'échelle fait 40 cm de long.

Fig. 8: Soil stripes.
A/ Airon-Saint-Vaast (50°26'24"N, 1°40'30"E). B/ Le Crotoy (50°12'10.8"N, 1°49'12"E). C/ Small patterned ground (rounded cells) stretching into stripes on slopes in Fontenay (48°6'36"N, 2°46'51.6"E) and D/ Triguères (47°56'34.8"N, 2°58'12"E).
Fig. 8 : Sols striés. A/ Airon-Saint-Vaast (50°26'24"N, 1°40'30"E). B/ Le Crotoy (50°12'10.8"N, 1°49'12"E). C/ Petits sols structurés (cellules arrondies) s'étirant en stries sur versant à Fontenay (48°6'36"N, 2°46'51.6"E) et D/ Triguères (47°56'34.8"N, 2°58'12"E).

7.9 m, which seem to be mostly related to the nature of the substrate (Andrieux *et al*., 2015). The largest stripes are found north of 49°N. Similar features were described previously in the UK amongst others by Williams (1964, 1968) and Ballantyne & Harris (1994). In modern periglacial environments, soil stripes form in the ground layer subjected to freezing and thawing cycles. They are found in seasonally frozen grounds, but are most developed over permafrost (Washburn, 1979; Ballantyne & Harris, 1994).

4 - CONCLUSIONS

The aim of this database is to be integrated in broader studies and to be progressively completed with the implementation of new field evidence of periglacial features. The data presented here should not be viewed as fully exhaustive; because of limited time and funds all the potential areas where periglacial features could be found in cross-sections have not been prospected yet. This is particularly the case for large areas of northeast France. Updating the database will make it possible to reconstruct more reliably past permafrost and to shed new light on some questions, such as the controlling factors of the gaps in deep aquifer recharge during the Late Pleistocene (Jiraková *et al*., 2011), the gaps in speleothem growth (Genty *et al*., 2010), and fluctuations of the peopling of vast regions of northern Europe during the Palaeolithic (Miller, 2012; Tallavaara *et al*., 2015). Conflicts and discrepancies may remain as shown by Andrieux *et al*. (2015) and few data exist with regard of the age of the features. To solve these issues further research on the origin and palaeoclimatic significance of some features and more thorough dating is needed. The online database can be downloaded at https://afeqeng.hypotheses.org/487 and used provided that this paper is cited in the references. The file of photographs and drawings is available on request from the first two authors (E. A. and P. B.).

ACKNOWLEDGMENTS

This work benefitted from funds provided by the INRAP, the Lascarbx (program of the Agence Nationale de la Recherche ANR-10-LABX-52), the University of Bordeaux and the UMR-5199 PACEA. C. Kasse and J. Vandenberghe presented to the authors the section illustrated in fig. 4A. We also acknowledge M. Bateman and J. Vandenberghe whose remarks have improved the manuscript.

REFERENCES

AGACHE R., 1963 - Informations archéologiques. Compte-Rendu de directeur de la circonscription préhistorique de Lille. *Gallia Préhistoire VI*, 165-180.

AGACHE R., 1970 - Détection aérienne de vestiges protohistoriques, gallo-romains et médiévaux dans le bassin de la Somme et ses abords. *Bulletin de la Société de Préhistoire du Nord,* **n° spécial 7**, 230 p.

ANDRIEUX E., BERTRAN P. & SAITO K., 2015 - Spatial analysis of the French Pleistocene permafrost by a GIS database. *Permafrost and Periglacial Processes*, **27** (1), 17-30.

ANTOINE P., MARCHIOL A., BROCANTEL M. & GROS Y., 2005 - Découverte de structures périglaciaires (sand-wedges et composite-wedges) sur le site de stockage de déchets radioactifs de l'Aube (France). *Comptes Rendus Géosciences*, **337** (16), 1462-1473.

ANTOINE P., ROUSSEAU D. D., MOINE O., KUNESCH S., HATTÉ C., LANG A., TISSOUX H. & ZÖLLER L., 2009 - Rapid and cyclic aeolian deposition during the Last Glacial in European loess: a high-resolution record from Nussloch, Germany. *Quaternary Science Reviews*, **28** (25-26), 2955-2973.

ARNAL H., 1971 - Les sols polygonaux étirés et sols striés d'âge würmien de Laudun (Gard). *Bulletin de l'Association Française pour l'Etude du Quaternaire*, **8** (3), 151-160.

BALLANTYNE C.K. & HARRIS C., 1994 - *The periglaciation of Great Britain*. Cambridge, Cambridge University Press, 330 p.

BASTIN A. & CAILLEUX A., 1941 - Action du vent et du gel au Quaternaire dans la region bordelaise. *Bulletin de la Société Géologique de France*, *série 5,* **11**, 259-266.

BERTRAN P., ANDRIEUX E., ANTOINE P., COUTARD S., DESCHODT L., GARDÈRE P., HERNANDEZ M., LEGENTIL C., LENOBLE A., LIARD M., MERCIER N., MOINE O., SITZIA L. & VAN VLIET-LANOË B., 2014 - Distribution and chronology of Pleistocene permafrost features in France: database and first results. *Boreas*, **43** (3), 699-711.

BLACK R.F., 1976 - Periglacial features indicative of permafrost: ice and soil wedges. *Quaternary Research*, **6** (1), 3-26.

BOCKHEIM J.G., KURZ M.D., SOULE S.A. & BURKE A., 2009 - Genesis of active sand-filled polygons in lower and central Beacon Valley, Antarctica. *Permafrost and Periglacial Processes,* **20** (3), 295-308.

BÜDEL J., 1951 - Die klimazonen des Eiszeitalters. *Eiszeitalters und Gegenwart*, **1**, 16-26.

CAILLEUX A., 1948 - Carte des actions périglaciaires quaternaires en France. *Bulletin du Service de la Carte Géologique de France*, **224**, 33-39.

CAILLEUX A., 1956 - Mares, mardelles et pingos. *Comptes Rendus, Académie des Sciences, Paris*, **242**, 1912-1914.

FORTIER D. & ALLARD M., 2005 - Frost-cracking conditions, Bylot Island, eastern Canadian Arctic archipelago. *Permafrost Periglacial Processes*, **16** (2), 145–161.

FRIEDMAN J.D., JOHANSSON C.E., OSKARSSON N., SVENSSON H., THORARINSSON S. & WILLIAMS J.R., 1971 - Observations on Icelandic polygon surfaces and palsa areas, photo interpretation and field studies. *Geografiska Annaler*, **53A** (3-4), 115-145.

GENTY D., COMBOURIEU-NEBOUT N., PEYRON O., BLAMART D., WAINER K., MANSURI F., GHALEB B., ISABELLO L., DORMOY I., VON GRAFENSTEIN U., BONELLI S., LANDAIS A. & BRAUER A., 2010 - Isotopic characterization of rapid climatic events during OIS3 and OIS4 in Villars Cave stalagmites (SW-France) and correlation with Atlantic and Mediterranean pollen records. *Quaternary Science Review*, **29** (19-20), 2799-2820.

GOZDZIK J.S., 1986 - Structures de fentes à remplissage primaire sableux du Vistulien en Pologne et leur importance paléogéographique. *Biuletyn Peryglacjalny*, **31**, 71-105.

GOZDZIK J.S., 1994 - Etudes des fentes de gel en Pologne centrale. *Biuletyn Peryglacjalny*, **33**, 49-78.

GULLENTOPS F., 1954 - *Contributions à la chronologie du Pléistocène et des formes du relief en Belgique.* Mémoire de l'Institut de Géologie de l'Université de Louvain, **18**, Louvain, Belgique, 125–252.

HAESAERTS P. & VAN VLIET-LANOË B., 1973 - Evolution d'un permafrost fossile dans les limons du dernier glaciaire à Harmignies (Belgique). *Bulletin de l'Association Française pour l'Etude du Quaternaire*, **10** (3), 151-164.

HUIJZER A.S. & VANDENBERGHE J., 1998 - Climatic reconstruction of the Weichselian Pleniglacial in northwestern and central Europe. *Journal of Quaternary Science*, **13** (5), 391-417.

ISARIN R.F.B., HUIJZER A.S. & VAN HUISSTEDEN J., 1998 - Time-slice oriented multi-proxy database (MPDB) for palaeoclimate reconstruction. *In CAPS (Circumpolar Active-Layer Permafrost System) CD-ROM, Version 1.0, National Snow and Ice Data Center*. CIRES, University of Colorado.

JETCHICK E. & ALLARD M., 1990 - Soil wedge polygons in northern Québec: description and paleoclimatic significance. *Boreas*, **19** (4), 353–365.

JIRAKOVÁ H., HUNEAU F., CELLE-JEANTON H., HRKAL Z. & LE COUSTUMER P., 2011 - Insights into palaeorecharge conditions for European deep aquifers. *Hydrology Journal,* **19** (8), 1545-1562.

KAISER K., 1960 - Klimazeugen des periglazialen Dauerfrostbodens in Mittel-und West-Europa. *Eiszeitalter und Gegenwart*, **11** (1), 121-141.

KOLSTRUP E., 1986 - Reappraisal of the upper Weichselian Periglacial environment from Danish frost wege casts. *Palaeogeography, Palaeoclimatology, Palaeoecology*, **56** (3-4), 237-249.

LACHENBRUCH A.H., 1962 - *Mechanics of thermal contraction cracks and ice-wedge polygons in permafrost.* Geological Society of America, Special Paper **70**, 69 p.

LACHENBRUCH A.H., 1966 - Contraction theory of ice-wedge polygons; a qualitative discussion. *In Proceedings, First International Permafrost Conference. National Academy of Science*, National Research Council of Canada, Publication **1287**, 63-71.

LAUTRIDOU J.P. & SOMMÉ J., 1981 - L'extension des niveaux repères périglaciaires à grandes fentes de gel de la stratigraphie du Pléistocène récent dans la France du Nord-Ouest. *Biuletyn Peryglacjalny*, **28**, 179-185.

LENOBLE A., BERTRAN P., MERCIER N. & SITZIA L., 2012 - Le site du Lac Bleu et la question de l'extension du pergélisol en France au Pléistocène supérieur. *Quaternaire continental d'Aquitaine : un point sur les travaux récents*. Livret-guide de l'excursion AFEQ-ASF 2012, Université de Bordeaux, AFEQ, 107-121.

MAARLEVELD G.C., 1976 - Periglacial phenomena and the mean annual temperature during the Last Glacial Time in the Netherlands. *Biuletyn Peryglacjalny*, **26**, 57-58.

MACKAY J.R., 1993 - Air temperature, snow cover, creep of frozen ground, and the time of ice-wedge cracking, western Arctic coast. *Canadian Journal of Earth Sciences,* **30** (8), 1720-1729.

MACKAY J.R. & BURN C.R., 2002 - The first 20 years (1978-1979 to 1998-1999) of ice-wedge growth at the Illisarvik experimental drained lake site, western Arctic coast, Canada. *Canadian Journal of Earth Science,* **39** (12), 95-111.

MICHEL J.P., 1975 - Périglaciaires des environs de Paris. *Biuletyn Peryglacjalny*, **24**, 259-352.

MILLER R., 2012 - Mapping the expansion of the Northwest Magdalenian. *Quaternary International,* **272-273**, 209-230.

MURTON J.B., 1996 - Morphology and paleoenvironmental significance of Quaternay sand veins, sand wedges and composite wedges, Tuktoyaktuk Coastlands, Western Arctic Canada. *Journal of Sedimentary Research*, **66** (1), 17-25.

MURTON J.B., 2013 - Permafrost and Periglacial Features. Ice Wedges and Ice-Wedge Casts. *In Encyclopedia of Quaternary Science (Second Edition),* Elsevier, Amsterdam, 436-451.

MURTON J.B. & BATEMAN M.D., 2007 - Syngenetic sand veins and anti-syngenetic sand wedges, Tuktoyaktuk Coastlands, western Arctic Canada. *Permafrost Periglacial Processes*, **18** (1), 33-47.

MURTON J.B., WORSLEY P. & GOZDZIK J., 2000 - Sand veins and wedges in cold Aeolian environments. *Quaternary Science Reviews*, **19** (9), 899-922.

NURY D. & ROUX R.M., 1969 - Présence de cryoturbation et de cailloutis quaternaires à l'ouest de Martigues (Bouches-du-Rhône). *Bulletin de l'Association Française pour l'Etude du Quaternaire*, **6** (2), 139-143.

PÉWÉ T.L., 1959 - Sand-wedge polygons (tessellations) *in* the McMurdo Sound Region, Antarctica a progress report. *American Journal of Science*, **257**, 545-552.

PÉWÉ T.L., 1966 - Palaeoclimatic significance of fossil ice wedges. *Biuletyn Peryglacjalny*, **5**, 65-72.

POSER H., 1948 - Boden-und Klimaverhältnisse im Mittle-und Westeuropa während der Würmeiszeit. *Erdkunde,* **2**, 53-68.

RENSSEN H. & VANDENBERGHE J., 2003 - Investigation of the relationship between permafrost distribution in NW Europe and extensive winter sea-ice cover in the North Atlantic Ocean during the cold phases of the Last Glaciation. *Quaternary Science Reviews,* **22** (2/4), 209-223.

ROMANOVSKIJ N.N., 1973 - Regularities in formation of frost-fissures and development of frost-fissure polygons. *Biuletyn Peryglacjalny,* **23**, 237-277.

ROMANOVSKIJ N.N., 1976 - The scheme of correlation of polygonal wedge structures. *Biuletyn Peryglacjalny,* **26**, 287-294.

ROMANOVSKIJ N.N., 1985 - Distribution of recently active ice and soil wedges in the USSR. *In* M. Church, & O. Slaymaker, (eds.), *Field and Theory - Lectures in Geocryology*. University of British Columbia Press, Vancouver, 154-165.

TALLAVAARA M., LUOTO M., KORHONEN N., JÄRVINEN H. & SEPPÄ H., 2015 - Human population dynamics in Europe over the Last Glacial Maximum. PNAS, **112** (27), 8232-8237.

TRICART J., 1963 - *Géomorphologie des régions froides.* Presse universitaire de France, Paris, 389 p.

TRICART J. & CAILLEUX A., 1967 - *Le modelé des régions périglaciaires*. SEDES, Paris, 512 p.

VANDENBERGHE J., 1983 - Ice-wedge casts and involutions as permafrost indicators and their stratigraphic position in the Weichselian. *Proceedings of the 4th International Conference on Permafrost, Fairbanks, Alaska*, **1**, 1298-1302.

VANDENBERGHE J. & PISSART A., 1993 - Permafrost changes in Europe during the last glacial. *Permafrost and Periglacial Process*, **4** (2), 121-135.

VANDENBERGHE J., FRENCH J., GORBUNOV A., MARCHENKO S., VELICHKO A.A., JIN H., CUI Z., ZHANG T. & WAN W., 2014 - The Last permafrost Maximum (LPM) map of the Northern Hemisphere: permafrost extent and mean annual air temperatures, 25-17 ka. *Boreas*, **43**, 652-666.

VELICHKO A.A., 1982 - *Palaeogeography of Europe during the Last One Hundred Thousand Years.* Nauka, Moscow, 156 p.

VAN VLIET-LANOË B., 1989 - Dynamics and extent of the Weichselian permafrost in western Europe (substage 5e to stage 1). *Quaternary International*, **3-4**, 109-113.

VAN VLIET-LANOË B., 1996 - Relations entre la contraction thermique des sols en Europe du Nord-Ouest et la dynamique de l'inlandsis weichselien. *Comptes-rendus de l'Académie des Science Paris*, **322** (série IIa), 461-468.

VAN VLIET-LANOË B., 2005 - Deformation in the active layer related with ice/soil wedge growth and decay in present day Arctic. Paleoclimatic implications. *Annales de la Société Géologique du Nord,* **13**, 81-95.

VAN VLIET-LANOË B. & HALLÉGOUËT B., 2001 - European permafrost at the LGM and at its maximal extent. The geological approach. *In* R. Paepe, & V. Melnikov (eds.), *Permafrost Response on Economic Development, Environmental Security and Natural Resources*. Kluwer Academic Publishers, Dordrecht, 195-213.

VAN VLIET-LANOË B., & LANGOHR R., 1981 - Correlation between fragipans and permafrost with special reference to Weischel silty deposits in Belgium and Northern France. *Catena*, **8**, 137-154.

WASHBURN A.L., 1979 - *Geocryology. A Survey of Periglacial Processes and Environments*. Edward Arnold, London, 406 p.

WASHBURN A.L., SMITH D. & GODDARD R., 1963 - Frost cracking in a Middle Latitude climate. *Biuletyn Peryglacjalny*, **12**, 175-189.

WILLIAMS R.B.G., 1964 - Fossil patterned ground in eastern England. *Biuletyn Peryglacjalny*, **22**, 337-349.

WILLIAMS R.B.G., 1968 - *Periglacial climate and its relation to landforms: a study of southern and eastern England during the Last Glacial Period*. PhD Thesis, University of Cambridge.

YVARD J.C., 1968 - Fentes de gel périglaciaire de la région de Tours. *Bulletin de l'Association Française pour l'Etude du Quaternaire*, **3**, 175-179.

5. Spatial analysis of the French Pleistocene permafrost by a GIS database

Eric Andrieux, Pascal Bertran, Kazuyuki Saito

Résumé:

L'analyse à l'aide d'un SIG de la base de données compilant les figures périglaciaires de France permet une meilleure évaluation de l'étendue maximale du pergélisol passé. La distribution des pseudomorphoses de coin de glace ne descend pas sous la latitude 47°N, ce qui suggère que le pergélisol discontinu étendu n'a pas affecté les régions au sud du Bassin parisien. La présence exclusive de coins de sable avec un remplissage primaire entre les latitudes 45 et 47°N, principalement à la périphérie de sables de couverture, indique que la fissuration par contraction thermique du sol s'est produite dans un contexte à la fois de déflation et de gel saisonnier profond ou de pergélisol sporadique, dans des milieux qui ne sont pas favorables à la croissance de corps de glace significatifs. La variation latitudinale de la taille des coins de sable montre clairement que ces structures se sont formées au niveau de la marge sud affectée par la contraction thermique. La carte de l'extension maximale du pergélisol Pléistocène en France proposée ici réconcilie en partie les données de terrain avec les simulations paléoclimatiques. Les contradictions restantes entre ces données peuvent être liées à un décalage dans le temps entre la dernière extension maximale du pergélisol (LPM, c. 31-24 ka) et le Dernier Maximum Glaciaire (DMG, 21 ka).

Mots clés: Pléistocène; pergélisol; SIG; Modélisation paléoclimatique; France

Andrieux, E., Bertran, P., Saito K., 2016a. Spatial analysis of the French Pleistocene permafrost by a GIS database. *Permafrost and Periglacial Processes*, 27 (1), 17-30.

PERMAFROST AND PERIGLACIAL PROCESSES
Permafrost and Periglac. Process. (2015)
Published online in Wiley Online Librar

Spatial analysis of the French Pleistocene permafrost by a GIS database

Eric Andrieux,[1]* *Pascal Bertran*[1,2] *and Kazuyuki Saito*[3]

[1] University of Bordeaux, PACEA, Pessac, France
[2] INRAP, Pessac, France
[3] International Arctic Research Center, University of Fairbanks, Fairbanks, Alaska, USA

ABSTRACT

GIS analysis of the French database of Pleistocene periglacial features allows an improved evaluation of the maximum extent of past permafrost. The distribution of typical ice-wedge pseudomorphs does not extend south of 47°N and therefore suggests that widespread discontinuous permafrost did not affect the regions south of the Paris Basin. The exclusive presence of sand wedges with primary infill between 45 and 47°N, mainly in the periphery of coversand areas, suggests that thermal contraction cracking of the ground occurred together with sand drifting in a context of deep seasonal frost or sporadic discontinuous permafrost, unfavourable for the growth of significant ground-ice bodies. The latitudinal variation of the wedge dimensions clearly shows that the sand wedges were located in the southern margin of the area affected by thermal contraction. The proposed map of Pleistocene permafrost in France partially reconciles field data with palaeoclimatic simulations. The remaining discrepancies may arise primarily from the time lag between the Last Permafrost Maximum (*c*. 31–24 ka) and the Last Glacial Maximum (21 ka).

KEY WORDS: Pleistocene; permafrost; GIS; palaeoclimatic modelling; France

INTRODUCTION

The extent of Pleistocene permafrost in France has been reconstructed several times based on field evidence (e.g. (Poser, 1948; Tricart, 1956; Maarleveld, 1976; Velichko, 1982; Huijzer and Vandenberghe, 1998; Van Vliet-Lanoë and Hallégouët, 2001)). Although these reconstructions differ significantly, largely because available data are scarce, they agree that permafrost spread over part of France during the coldest periods of the Pleistocene. During the last decade, modelling of past permafrost has provided new data on this issue using different approaches ((Renssen and Vandenberghe, 2003); Levavasseur *et al*., 2011; (Vandenberghe et al., 2012; Saito et al., 2013; Kitover et al., 2013)). The resulting estimates of permafrost extent at 21 ka (Last Glacial Maximum, LGM) still show, however, rather poor agreement. Within this framework, more field data are critical to evaluate the accuracy of the models and their ability to reconstruct the Last Glacial climate. To improve such an approach, the French database of Pleistocene periglacial features was set up in 2012 by several institutions (Laboratoire PACEA – université de Bordeaux, Laboratoire de Géographie Physique – CNRS Meudon, Institut National de Recherches Arquéologiques Préventives). This database benefitted particularly from the recent development of rescue archaeology, which has yielded a large amount of new field data. The database was presented by Bertran *et al*. (2014), who focused on the geographic distribution of the georeferenced features and their main characteristics, and reviewed the available chronological data.

The present paper adds to the database a GIS, which accommodates different layers of information and elucidates the factors that influence the development of periglacial features. In order to place the French data in a broader context, data from the northern Europe database (Isarin et al., 1998) have been integrated and make it possible to propose a new map of the main permafrost boundaries in Western Europe during its maximal extent. The field data were also compared with an improved set of modelled permafrost distributions, derived from LGM simulations by state-of-the-art global climate models (GCMs) and downscaling for France on a 2 km resolution, to delineate advances and issues in both reconstruction methodologies.

*Correspondence to: E. Andrieux, Université Bordeaux, PACEA, allée Geoffroy-Saint-Hilaire, 33600 Pessac, France.
E-mail: andrieux.e@gmail.com

Received 26 January 2015
Accepted 28 May 2015

MATERIAL AND METHODS

Data Acquisition and Selection

Numerous periglacial structures have been described in France. Many of the data collected in this study come from journals, doctoral theses and archaeological survey reports. These data were rigorously selected, and all entries not accompanied by drawings, photographs or descriptions were rejected from the database.

The analysis and interpretation of aerial photographs available in Google Earth and Geoportail (http://www.geoportail.gouv.fr/accueil) identified hundreds of periglacial features (Bertran et al., 2014). They were classified as: (1) polygonal networks; (2) soil stripes; and (3) small nets, usually appearing as adjacent irregular circles. Photographs were strictly selected to show only indisputable features. These appear mainly on aerial photographs taken in late summer and in years of severe drought, because of differential growth of vegetation or contrasting water content of the ground. They were sought primarily in areas where periglacial features had been previously reported in the literature. Searches were then extended to neighbouring regions with a similar substrate.

New field data were also collected from trenches made during rescue archaeology investigations and from cross-sections in key areas such as Bordeaux, Nantes and Angers ((Lenoble et al., 2012; Bertran et al., 2014), unpublished data). Structures observed in cross-sections were classified as: (1) sand wedges (i.e. wedges with a primary infill of sand, including possible composite wedges); (2) ice-wedge pseudomorphs (i.e. wedge structures wider than 0.2 m, with a secondary infill and either subsidence structures or upturned host strata); and (3) cryoturbation structures (minimum height of 0.5 m). For each feature observed in the field, the width, height and spacing were measured and the nature of the host material and the infilling was determined. When several features were juxtaposed, the largest values were considered as representative of the site, having removed the values of apparent width obtained on ice-wedge pseudomorphs and sand wedges observed obliquely to the cross-sections.

All the data were stored in a GIS developed with ArcGIS (ESRI Redlands, California, USA). In order to place the French data in a broader context, we included in our database information on sand wedges (N = 22), composite wedges (N = 5), ice-wedge pseudomorphs (N = 33), cryoturbations (N = 36) and pingo scars (N = 7) from the database Paleo-periglacial phenomena in Northwestern Europe developed by Isarin *et al.* (1998). This database is accessible on the website of the National Snow and Ice Data Center (http://nsidc.org/data/ggd248.html).

Dimension Measurement from Aerial Photographs

The good quality and resolution of the geolocalised aerial photographs provided by the French National Geographical Institute (IGN http://www.ign.fr/) allowed us to measure the dimensions and spacing of numerous features. This operation was performed in a standardised way using ImageJ software in order to obtain reliable values. ImageJ is an open-source image processing software (US National Institute of Health, http://imagej.nih.gov/ij/). The images were acquired from screenshots of Google Earth and Geoportail. For each image, the information about scale and location was retained. The images with the most clearly visible features were selected for analysis. A total of 94 images of polygonal networks, 83 of soil stripes and three of small nets were analysed. The images were previously converted to greyscale and the contrast was increased.

The grey-level values of profiles intersecting the features were measured. On the graphs obtained, the lowest (darkest) values are usually provided by the sides of the polygons (higher ground moisture, more developed vegetation) and form clearly identifiable peaks (Figure 1). Depending on the case, the margins of the soil stripes appear to have a lighter colour (e.g. on chalklands) or a darker colour than the stripe centres. The concordance of the peaks with the polygon sides or the margins of the soil stripes and not with artefacts such as ditches or gullies was checked every time and any dubious peak was ignored. Several profiles have been made in the most suitable areas for each photograph. The spacing between the peaks has then been averaged over all the profiles. The widths obtained in this way are comparable to the spacing of the polygon sides such that it can be measured from cross-sections. They are also similar to the values used in the simulations by Plug and Werner (Plug and Werner, 2002). The measurements of soil stripes are perpendicular to their orientation.

This technique has the advantage of being standardised, replicable and easy to implement. But it may slightly underestimate the actual size of the polygons because the profiles pass at a more or less great distance from the centre of gravity of each polygon. The distribution of the values was finally adjusted to a Gaussian function or a combination of Gaussian functions using the software Fitik 0.9.8 (Wojdyr, 2010) to define precisely the modal value(s).

Geographic Processing

ArcGIS has been used to combine information from the databases and the digital elevation model (DEM), and to map the results. The DEM Aster GDEM was used, which has a 30 m resolution (http://gdem.ersdac.jspacesystems.or.jp/).

The nature of the substrate for each feature was extracted from the geological map of France (scale 1:50 000) established by the Bureau de Recherches Géologiques et Minières (BRGM) (http://infoterre.brgm.fr/). Owing to the scale of the map, imprecision remains high and the thinner and less extensive geological formations are not specified, thus leading to possible misidentification. Data on soil texture are available in the database GIS Sol from the Institut National de la Recherche Agronomique (http://www.gissol.

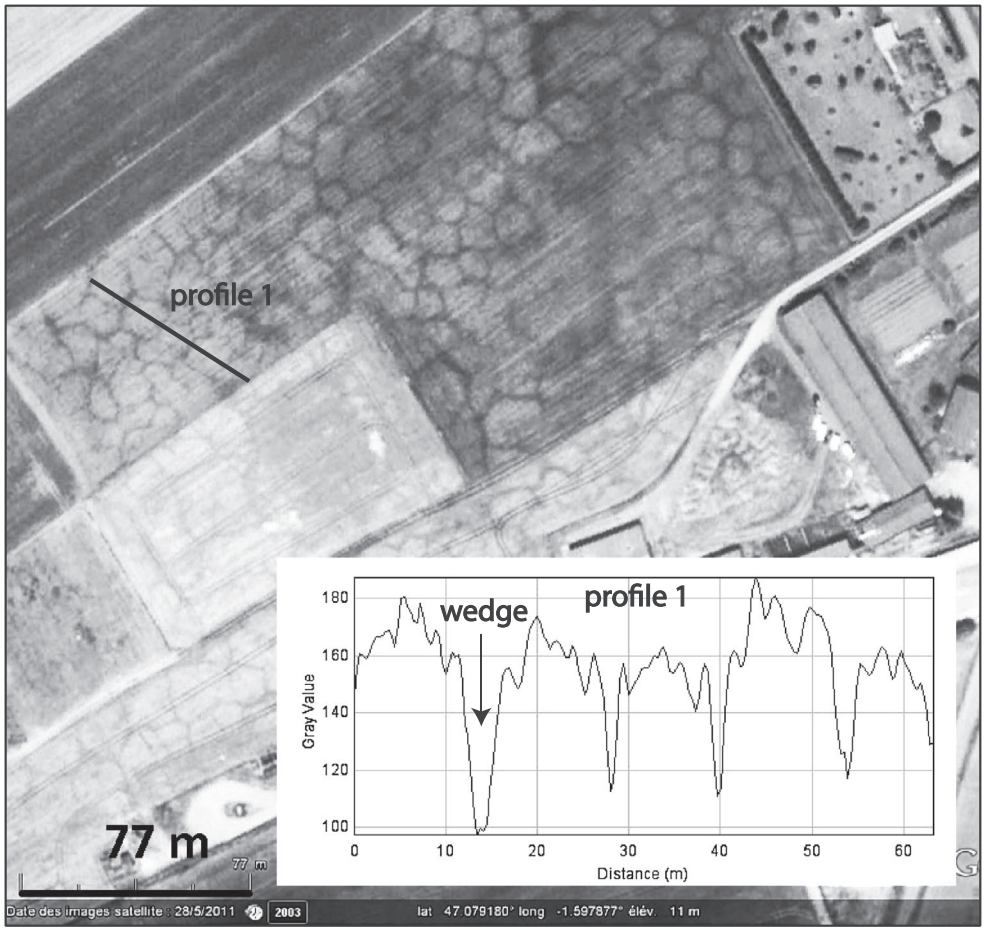

Figure 1 Aerial view of polygons (Google Earth/National Geographical Institute) and analysis of the grey levels along a profile with ImageJ to measure the polygon width.

fr/outil/outils.php). The percentage of sand, silt and clay in the topsoil is measured in samples and averaged for geographic areas corresponding to the agricultural area of a township (1 to 45 546 ha, averaging 1 sample for 115 ha). Therefore, the resolution remains low and may also generate significant bias in some areas.

Altitude, slope gradient and slope orientation were derived from the DEM Aster GDEM. The 30 m resolution leads to mean values for surfaces of 900 m^2. Tests were performed to extract the orientation of soil stripes with the 50 m resolution DEM from the IGN for comparison. The orientation of soil stripes was also determined using the 'ruler' tool in Google Earth, which measures the angle in degrees between a line (a stripe) and the north azimuth.

The relative altitude of sand wedges and ice-wedge pseudomorphs to their surrounding land was analysed using ArcGIS tools. A buffer of 300 m in diameter was set around the features, then the average elevation of the area was calculated and compared to that of the features.

Modelled Palaeo-Permafrost Distributions

The distribution of the subsurface thermal regime at the LGM (21 ka) was reproduced using surface air temperature products from selected GCMs participating in the Paleoclimate Model Intercomparison Project Initiative III (Braconnot et al., 2012) and a statistical diagnosis developed by Saito *et al*. (2013) that utilises freezing and thawing indices. The derived frozen ground types roughly correspond to continuous and discontinuous permafrost, seasonally (longer than 2 weeks) and intermittently (shorter than 2 weeks) frozen ground, and no freezing.

The maps were further downscaled with a digital elevation model, ETOPO1 (Amante and Eakins, 2009), to a 1 arc-minute resolution, assuming the constant atmospheric lapse rate of 6.5 ºC/km (Saito et al., 2014). In producing topography at the LGM, change in sea level was set constantly to -127 m (Clark and Mix, 2002; Milne and Mitrovica, 2008), and glacial isostasy was not taken into account. The explanation of the frozen ground diagnosis, the downscaling methodology and

details of the models used in this study are given in Saito *et al.* (2014).

RESULTS

The French database has identified so far 914 georeferenced structures: 58 ice-wedge pseudomorphs, 75 sand wedges, 56 cryoturbations, 346 polygonal networks, 137 soil stripes and 242 small nets (Figure 2). The elevation of the features derived from the DEM is between 0 and 393 m asl. On average, the features visible on aerial photographs (polygons, patterned ground) are located at a slightly higher elevation than those observed in cross-sections (ice-wedge pseudomorphs, sand wedges, cryoturbations), but the difference is not statistically significant.

Polygons

The polygons occur mainly in Pleistocene or Neogene alluvial formations but they can also be found in marl, chalk and sandy or clayey weathering mantles (alterites). The southernmost polygons reach 43.4°N, but the majority of them are located in the Paris Basin north of 47°N. No polygon was observed on aerial photographs in the areas of northern France where loess deposits are thicker than 3 m (Lautridou, 1985), because of burial under post-LGM loess cover.

Polygon diameters range from 10 to 25 m. The size distribution can be adjusted to a Gaussian function with a mode equal to 15.1 m (quality of fit $R^2 = 0.810$) (Figure 3). No clear relationship appears in our data-set between the size of the polygons and the latitude, or with the lithology of the host material (Figure 4) or with the soil texture (Figure 5).

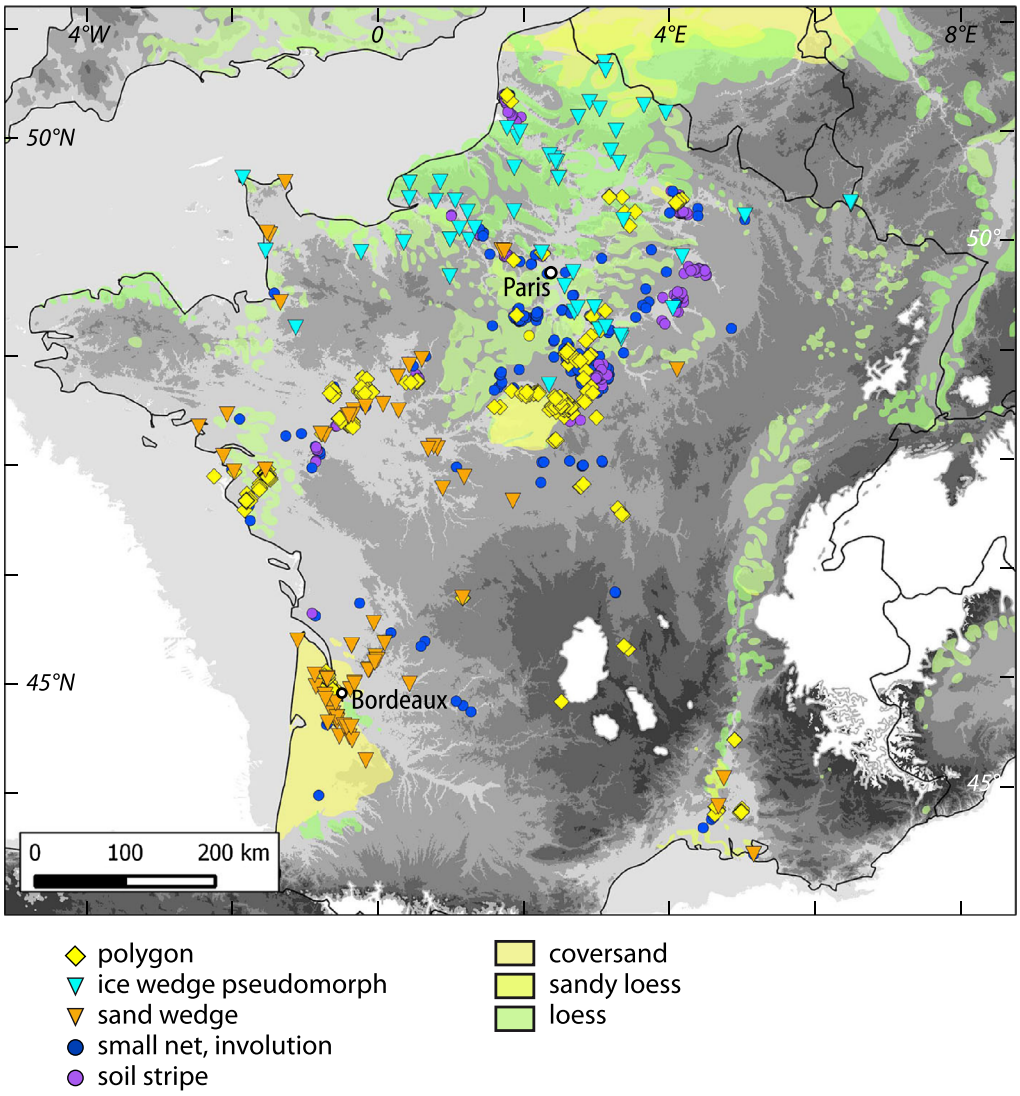

Figure 2 Map of periglacial features listed in the French database. This figure is available in colour online at wileyonlinelibrary.com/journal/ppp

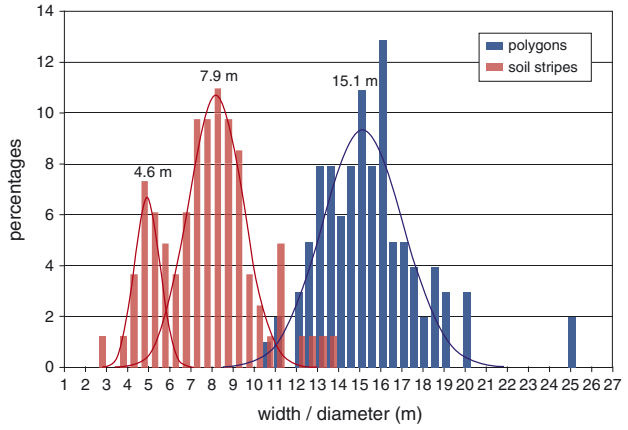

Figure 3 Distribution of the width of soil stripes and the diameter of polygons, and adjustment to Gaussian functions. This figure is available in colour online at wileyonlinelibrary.com/journal/ppp

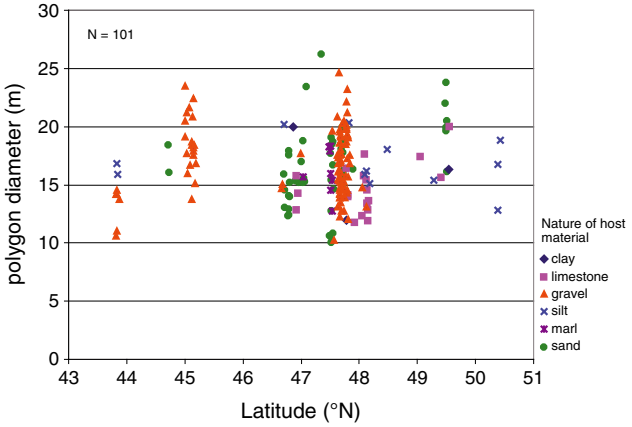

Figure 4 Distribution of the diameter of polygons as a function of latitude and the ground nature taken from the French 1:50 000 geological map (Bureau de Recherches Géologiques et Minières). This figure is available in colour online at wileyonlinelibrary.com/journal/ppp

Sand Wedges and Ice-Wedge Pseudomorphs

Several observations can be made from the spatial analysis of the distribution and size of sand wedges and ice-wedge pseudomorphs:

1. Ice-wedge pseudomorphs are abundant north of 49°N and present to 47°N (Figure 6). No typical ice-wedge pseudomorphs have been found south of 47°N, although a few composite wedges have been reported previously from the Bordeaux region, close to 45°N (Bertran et al., 2014). Most of the pseudomorphs have been described from loess sections in northern France. The distribution of ice-wedge pseudomorphs is strongly correlated with that of loess.
2. The area between 47 and 43°N includes the majority of the sand wedges. No sand wedge is recorded at a lower latitude. The wedges are located mainly on Neogene to Middle Pleistocene alluvial deposits, typically in the periphery of aeolian coversands as in Aquitaine and south of Orleans in the Paris Basin. Sand wedges have also been described on the margins of the great north European sand belt.
3. The maximum depth of the wedges in Europe clearly relates to the latitude (Figure 7). The depth range is large for a given latitude, but the maximum value decreases rapidly between 57 and 43°N. The southernmost wedges have a maximal depth of about 1.5 m.
4. The width of the wedges also relates to the latitude (Figure 8). The outliers are, however, more numerous than in the previous case.
5. Sand wedges are located in sites that are on average at a higher elevation than the surrounding terrain. Conversely, ice-wedge pseudomorphs are located on flat terrain (Figure 9).

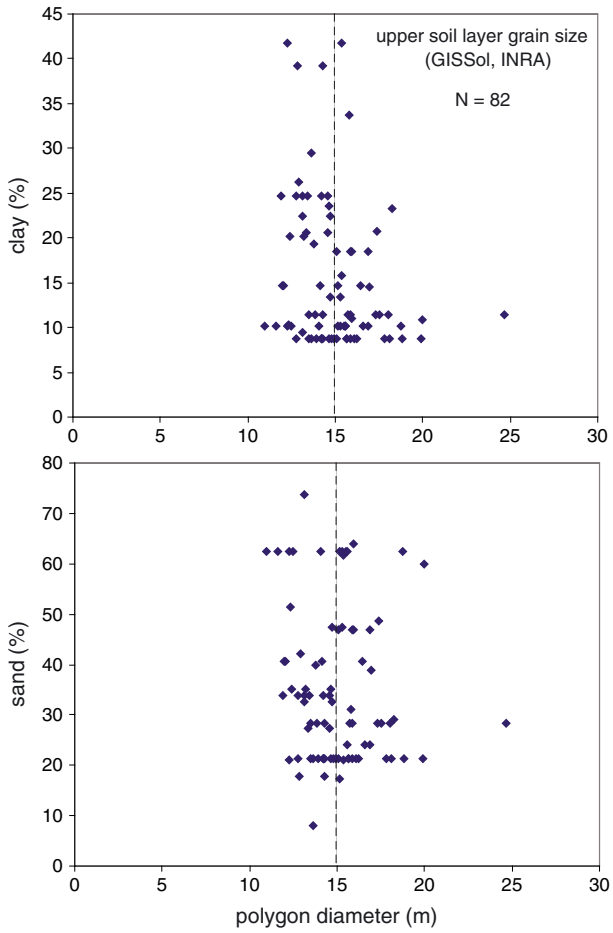

Figure 5 Distribution of the diameter of polygons as a function of the grain size of the topsoil layer, from GIS Sol data (Institut National de la Recherche Agronomique, INRA). This figure is available in colour online at wileyonlinelibrary.com/journal/ppp

Soil Stripes

Soil stripes in the database are primarily located in the Paris Basin, particularly in the border of coverloams, on

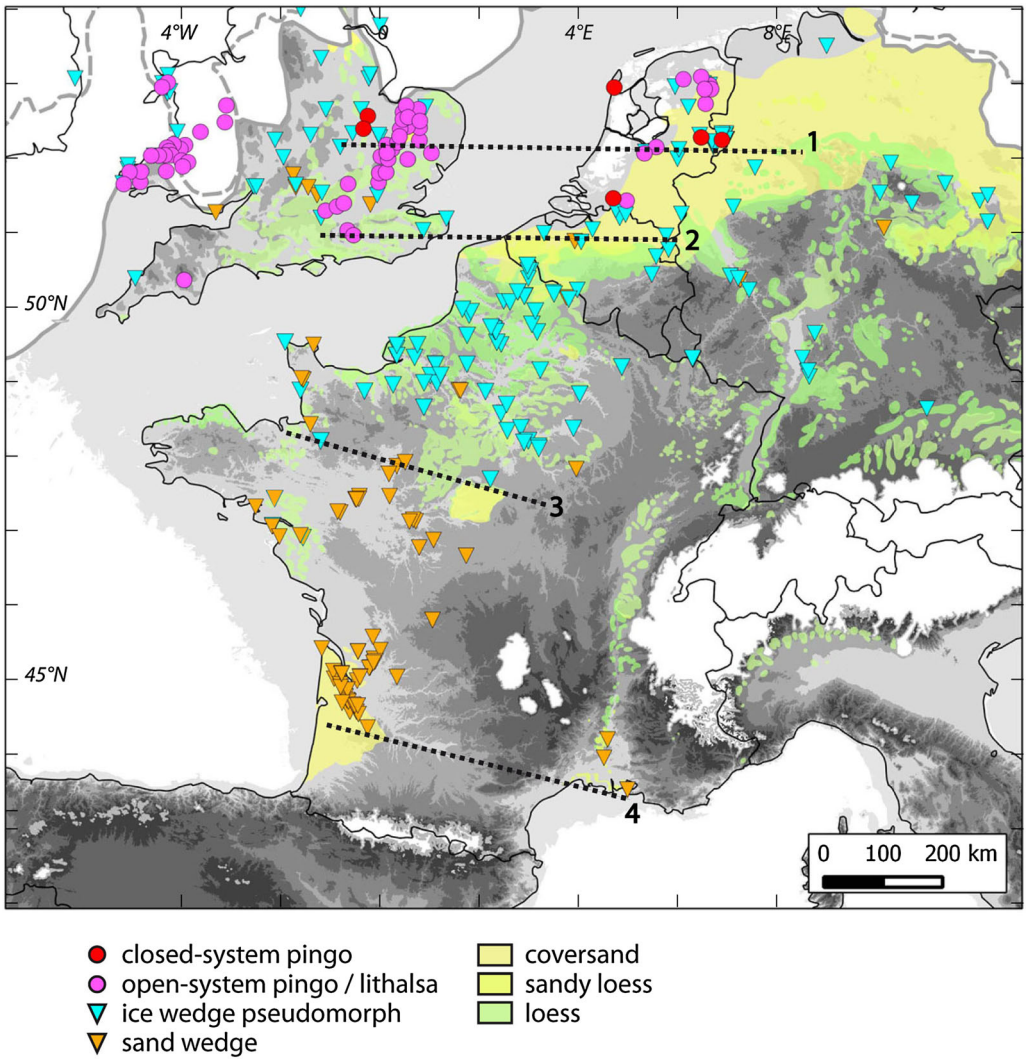

Figure 6 Distribution of pingo or lithalsa scars, ice-wedge pseudomorphs and sand wedges listed in the French and northern European (Isarin et al., 1998) databases. The distribution of pingo or lithalsa scars in Great Britain has been taken from Ballantyne and Harris (Ballantyne and Harris, 1994). The outlines of the Scandinavian and British ice sheets at 21 ka (solid line) and 19 ka (dashed line) are taken from Böse et al. (2012). The other ice sheets come from Ehlers and Gibbard (Ehlers and Gibbard, 2004). The -120 m sea level is taken from http://www.emodnet.eu/bathymetry. Southern limits of: 1 – closed-system pingo scars; 2 – open-system pingo or lithalsa scars; 3 – ice-wedge pseudomorphs; 4 – sand wedges. This figure is available in colour online at wileyonlinelibrary.com/journal/ppp

alluvial deposits or chalk. They have typically formed on a coarse substrate (gravel, fragmented chalk) covered by a metre-thick layer of loess that forms pockets in the coarse material. Few examples have been reported south of the Loire River.

Soil stripes have developed on a 6.3° mean slope gradient, with a maximum of 25° and a minimum of 0°. The latter value is clearly underestimated due to the low resolution of the DEM. The orientation distribution of the soil stripes obtained from the 30 m and 50 m DEMs, and that measured using the 'ruler' tool in Google Earth are significantly different (Figure 10). On account of the low resolution of the DEMs, only the values obtained from Google Earth are considered here as valid. Based on these data, a preferred direction appears along a NNW/SE axis, with a dominant NNW slope orientation (more than 50% of the soil stripes).

The average spacing of the stripes measured with ImageJ ranges from 2.5 to 13.3 m (Figure 3). The modal width calculated from adjustment of the distribution to a Gaussian function is 7.3 m, but the quality of the fit is poor ($R^2 = 0.813$). Insofar as the histogram of the values clearly shows the existence of distinct peaks, the distribution was then adjusted to a combination of two Gaussian functions. The quality of the fit improves significantly ($R^2 = 0.930$). Modal widths are respectively 4.6 and 7.9 m. The average spacing of the stripes is, thus, substantially less than the diameter of the polygons, and there is less than 10 per cent overlap between both features. No relationship was found

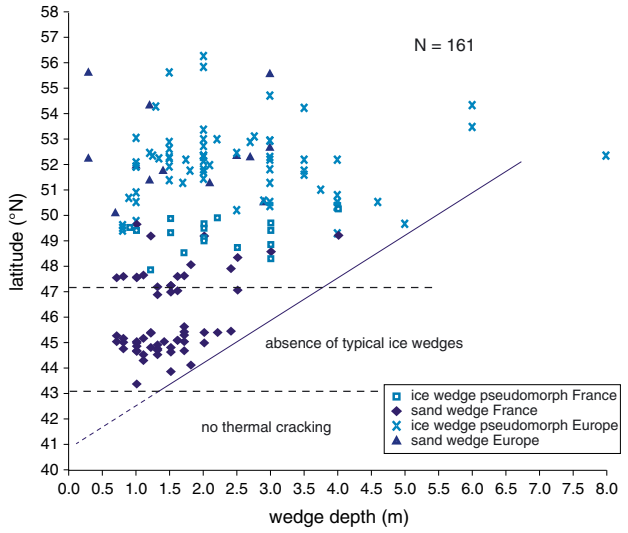

Figure 7 Distribution of the depth of ice-wedge pseudomorphs and sand wedges as a function of latitude. This figure is available in colour online at wileyonlinelibrary.com/journal/ppp

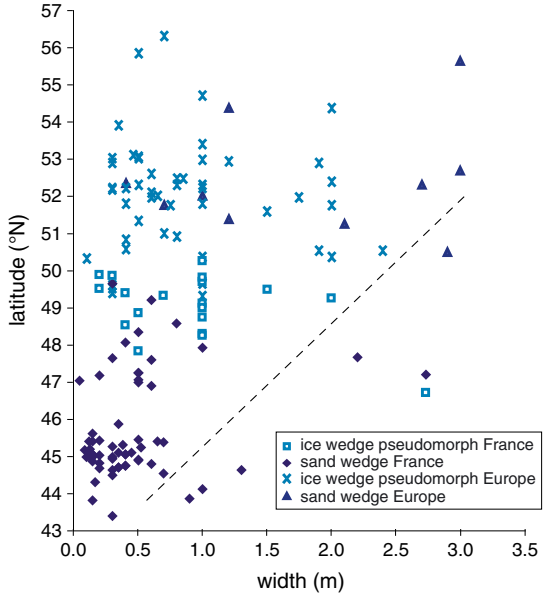

Figure 8 Distribution of the width of ice-wedge pseudomorphs and sand wedges as a function of latitude. This figure is available in colour online at wileyonlinelibrary.com/journal/ppp

between stripe width and orientation (Figure 11A). Stripe width as a function of latitude and the nature of the ground shows some interesting patterns (Figure 11B). In northern France, soil stripes in loess overlying chalk (shown as 'silt' when loess is indicated on the 1:50 000 geological map and otherwise as 'chalk') or on alluvial gravel ('gravel') have an average width close to 8 m. Further south, many soil stripes have developed in weathered clay ('clay') or colluvium derived from it. Such stripes have a width centred around 4.5 m. If we consider all the available data, the latitude does not seem to play an important role by itself, except that the loess belt occurs between 48 and 51°N. Overall, therefore, the composition of the sedimentary cover seems mainly to determine the width of the stripes.

Small Nets

The geographical distribution of small nets is generally similar to that of soil stripes and a gradual transition between the two features is locally observed. Small nets are, however, more rarely found on a chalk substrate, whereas they are abundant on plateaus of old detrital formations or weathered clays. Because of the frequent interruption of the walls (coalescent or partially eroded circles), few aerial photographs have been favourable for measuring their size. Three sites in the Paris Basin gave sizes between 6.2 and 10.7 m, comparable to those obtained on soil stripes. In a few cases, the attribution of large nets to cryoturbation within a former active layer rather than to networks of ice-wedge pseudomorphs remains uncertain without data in cross-section.

DISCUSSION

The Role of Local Factors in the Distribution and Characteristics of Periglacial Features

The distribution of the features recorded in the database indicates that a large part of France was affected by periglacial phenomena, as shown by Bertran *et al*. (2014). These features are mainly located in sedimentary basins, particularly in Cretaceous and Cenozoic terrains, as well as along the Pleistocene alluvial corridors. The southwesternmost part of France and the Languedoc are the only regions that did not yield any periglacial features, despite abundant field research.

In modern periglacial environments, many factors may control the formation of the investigated features (Washburn, 1979; French, 2007). They include the climate, but also local factors that greatly influence the thermal regime of the ground, such as vegetation, snow cover and topography. The nature of the ground and especially its frost susceptibility, thermal conductivity and mechanical behaviour as well as the water content are also key parameters.

As part of our study, the influence of some parameters has been assessed by combining several layers of information in a GIS. Although the resolution of the layers of the ground composition and topography remains low, their comparison with the distribution map of periglacial features and their dimensions highlights the following:

1. The soil stripes are interpreted to have developed in a former active layer (Goldthwait, 1976; Washburn, 1985) in thin (less than 2 m thick) fine-grained material overlying coarse deposits. This explains the lack of soil stripes in

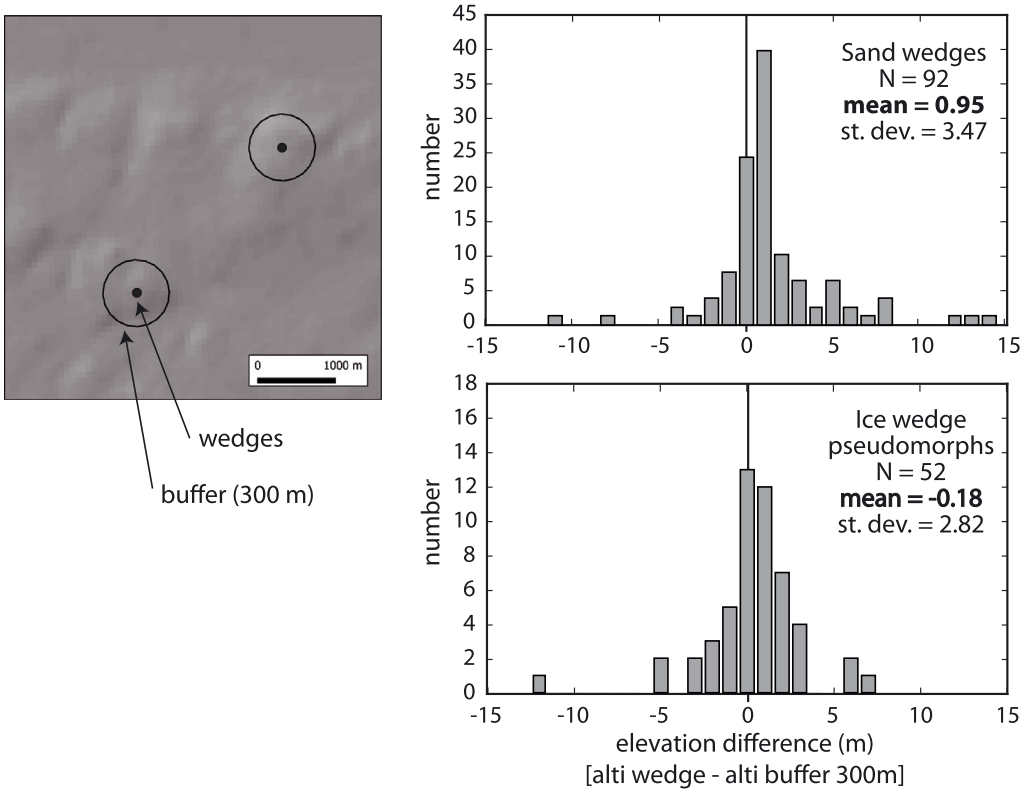

Figure 9 Distribution of the differences in elevation between the sites with ice-wedge pseudomorphs or sand wedges and the surrounding terrains within a circle 300 m in diameter. This figure is available in colour online at wileyonlinelibrary.com/journal/ppp

the plains of northern France with a thick loess cover, and their abundance in the Cretaceous aureole of the Paris Basin, especially in the periphery of plateaus where the silt cover is thin. However, this does not explain their scarcity in the Cretaceous terrains and the alluvial formations of the Aquitaine Basin. The width of the stripes is mainly influenced by the nature of the sedimentary cover, whereas the other parameters considered (latitude, slope gradient, slope orientation) do not play any identifiable role. The properties of this cover are therefore crucial to their formation (Ballantyne and Harris, 1994). The slope orientation also seems to control the presence/absence of soil stripes, since they are mostly oriented to the northwest and to a lesser extent, to the southeast.

2. The polygons are interpreted as networks of thermal contraction cracks (sand wedges or ice-wedge pseudomorphs) that developed in a wide variety of frost-susceptible substrates. No clear correlation has been found between their size and other parameters, including the ground composition. Similar findings were also made in active periglacial environments in Svalbard (Matsuoka and Hirakawa, 1993). This observation is quite unexpected insofar as the linear shrinkage coefficient of the ground is potentially correlated with its grain size (Lachenbruch, 1962; Romanovskij, 1985). This may be explained by the following phenomena: (1) the critical role played by the fine-grained matrix and/or the interstitial ice on contraction rather than by the coarse-grained component of the ground; and (2) a sufficiently long activity of the networks so that secondary cracks have subdivided them until a steady state was reached, which is relatively independent of the ground composition. According to the simulations made by Plug and Werner (Plug and Werner, 2002; Plug and Werner, 2008), a steady state appears after a few hundred years, with a strong variability associated with the frequency of extreme cold winter events. The size of the epigenetic networks in Neogene or Lower Pleistocene formations, particularly sand wedge networks, may result from repeated but very discontinuous activity during the cold stadials of the Pleistocene. The average spacing of the cracks (i.e. the polygon sides) measured in our dataset is around 15.3 m. It falls within the range of the steady-state values obtained by Plug and Werner (Plug and Werner, 2002) in their various scenarios. In the absence of accurate data on the age of the formations in which the polygons formed, it has not been possible to really test the possible influence of the exposure time to periglacial processes on the spacing of the cracks.
3. The distribution of ice-wedge pseudomorphs correlates strongly with that of loess in northern France. This correlation is not related to the fact that silts strongly favour thermal contraction cracking (Romanovskij, 1985), because sand wedges and polygons are present in a wide variety of substrates. Nor is it simply related to a

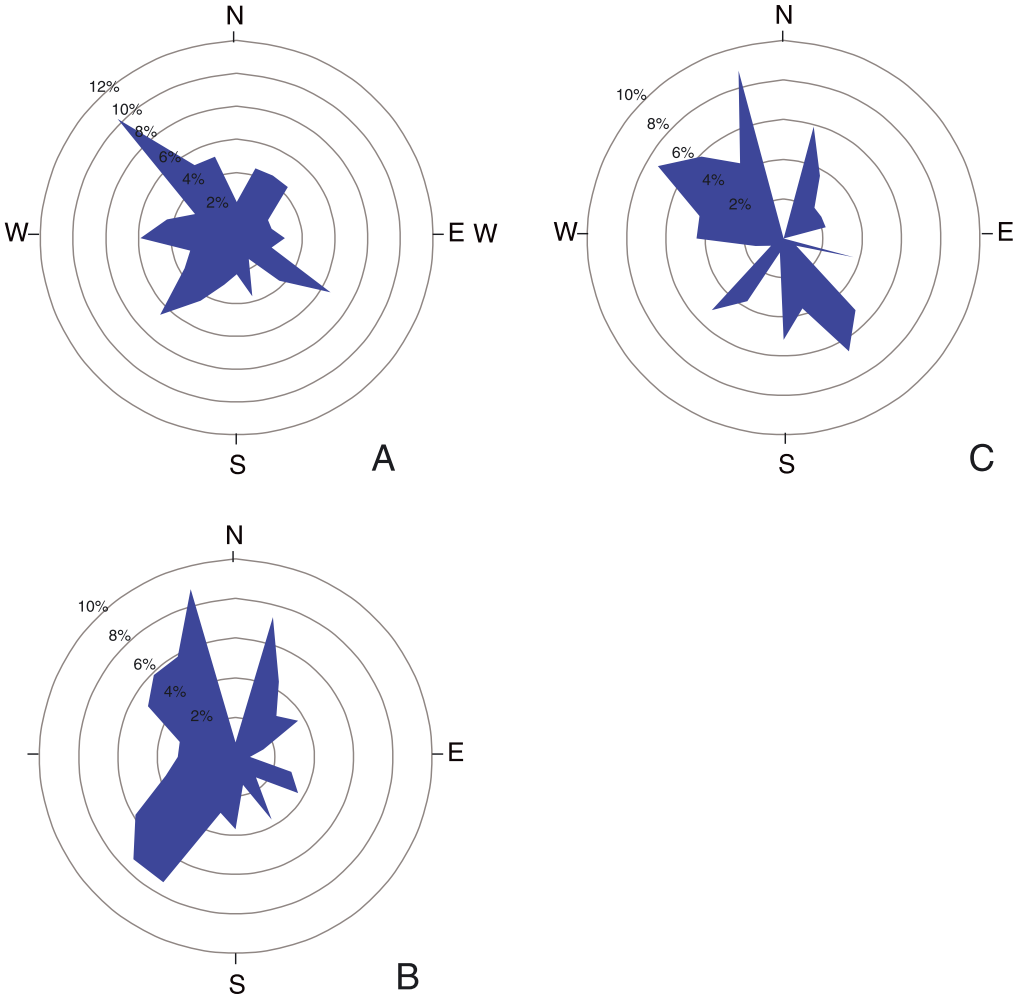

Figure 10 Orientation of the soil stripes, using (A) the 50 m digital elevation model (DEM); (B) the 30 m DEM; and (C) the 'ruler' tool in Google Earth. This figure is available in colour online at wileyonlinelibrary.com/journal/ppp

coincidence between the latitudinal extension of loess and that of ice wedges insofar as very few pseudomorphs have been described in the northeastern quarter of France outside the loess area although situated at similar latitude. The most likely assumption is that there is a bias due to poor preservation and recognition of ice-wedge pseudomorphs in heterogeneous materials.

4. The sand wedges have a very discontinuous distribution over France, limited to sandy or gravelly formations on plateaus and high terraces. The difference in altitude between the sand wedge sites and the surrounding terrains shows that they grew on prominences, that is, in well-drained contexts, unlike ice wedges. They also concentrate in the vicinity of coversands. Their formation thus appears to have been highly dependent on the capacity of the ground to provide enough sand for deflation to fill the cracks, and their distribution underestimates the areas that were affected by thermal contraction cracking.

Latitudinal Zonation of Periglacial Features

A latitudinal zonation of periglacial features across Europe clearly emerges from the map in Figure 6 and the size distribution of the wedges. The main points are as follows:

1. No pingo or lithalsa scars have been identified with certainty in France, although an extensive literature is devoted to possible examples (e.g. (Boyé, 1958; Michel, 1967; Courbouleix and Fleury, 1996; Lécolle, 1998)). The general lack of ramparts, observations in vertical cross-sections and chronological data casts doubt on the interpretation of many closed depressions as scars of perennial ice mounds. The features described in the coversands of Aquitaine by Boyé (Boyé, 1958) and Legigan (Legigan, 1979) have been recently reinterpreted as being of karstic origin (sinkholes) by Texier (Texier, 2011), following observations in

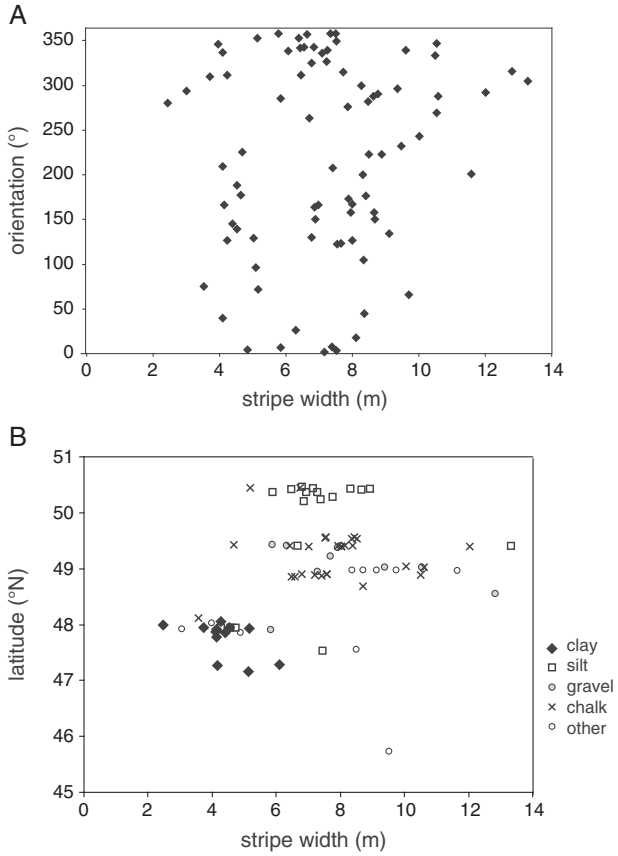

Figure 11 (A) Distribution of the width of soil stripes as a function of the slope orientation; (B) distribution of the width of soil stripes as a function of latitude and the composition of the substrate (Bureau de Recherches Géologiques et Minières).

trenches and radiocarbon dating. Convincing examples of pingos dated to the Pleniglacial have instead been described in The Netherlands (Kasse and Bohncke, 1992) and in the UK (Watson and Watson, 1974; Ballantyne and Harris, 1994; Ross et al., 2011). The majority of these examples are thought to have originated as open-system pingos or lithalsas and are, therefore, indicative of continuous or widespread discontinuous permafrost (Mackay, 1988; French, 2007; Pissart, 2000; Wolfe et al., 2014). According to Wolfe *et al.* (2014), the lithalsas are currently developing in Arctic environments at a mean annual air temperature (MAAT) close to -4 °C, with extremes at -2 and -7 °C, while Mackay (Mackay, 1988) suggested that open-system pingos are unable to grow at a MAAT higher than -5 to -6 °C. Closed-system pingos, typically associated with refreezing of a talik following the drainage of a lake, are the only periglacial features whose presence is limited to a continuous permafrost environment (Washburn, 1979; French, 2007). Some features in The Netherlands have been classified as closed-system pingo scars by Isarin *et al.* (1998).

2. No typical ice-wedge pseudomorphs have been described south of 47°N. This indicates that the growth of large ice bodies in thermal contraction cracks was not possible in more southern regions, either because of the absence of permafrost or the brevity of permafrost phases. The presence of composite wedges in southwest France suggests that, at least locally, ice veins formed at lower latitudes, possibly during some exceptionally cold winters (cf. (Murton and Kolstrup, 2003)). In current Arctic environments, ice wedges may grow where regional MAATs are lower than, or equal to -3.5 to -4 °C (Hamilton et al., 1983; Burn, 1990). According to M. Allard (personal communication), however, these values should be seen as extreme ones and a limit closer to -5 °C, as proposed by Péwé (Péwé, 1966) in Alaska, is probably more representative.
3. The southernmost sand wedges are located at 43.5°N in southwest France, and 43°N in the southeast (Provence). In modern periglacial environments, the distribution of sand wedges is restricted to very dry areas within continuous permafrost, particularly in Antarctica (Bockheim et al., 2009; Hallet et al., 2011), where thermal contraction cracking is associated with active sand drifting. During the Pleistocene, characterised by greater aridity than at present in mid-latitudes (Jost et al., 2005) and the extension of cold deserts (Kasse, 2002; Bertran et al., 2011), sand inputs may not have been a limiting factor for the formation of sand wedges as in modern Arctic regions and the southern boundary of these features is thought to reflect that of thermal contraction cracking. This is particularly the case in the periphery of coversands in southwest France. Thermal contraction cracking currently occurs where there is permafrost or deep seasonal frost, and the MAAT is lower or equal to -1/0 °C (Washburn et al., 1963; Friedman et al., 1971; Allard and Seguin, 1987) or even 2 °C in hypercontinental areas (Romanovskij, 1973, 1985).
4. The relationship between the maximal depth of ice-wedge pseudomorphs and sand wedges and latitude suggests that thermal contraction cracks propagate deeper in the ground as the ground temperature decreases, due to more brittle permafrost behaviour, enhanced thermal conductivity of the ground (Throop et al., 2012) and deepening of the depth of zero annual thermal amplitude (and, hence, thickening of the layer subject to stress) (Romanovskij, 1973). Figure 7 indicates that sand wedges in southwest France are located in an area unfavourable for deep thermal contraction cracking. The depth of the sand wedges at latitude 45°N is between 0.7 and 1.5 m, comparable with the depth of the active-layer soil wedges in discontinuous permafrost in sub-Arctic Québec (Jetchick and Allard, 1990), and to the cracks in deep seasonal frost in Iceland (Friedman et al., 1971). According to our database, the depth of ice-wedge pseudomorphs at latitude 50°N reaches 4 to 5 m, and approximately corresponds to the depths of ice wedges in widespread discontinuous permafrost in

Svalbard (MAAT = -6 °C; (Matsuoka and Hirakawa, 1993)).

5. The relationship between the width of the wedges and latitude can be explained by several factors: (i) the frequency of harsh winters that favoured thermal contraction cracking increased with latitude; (ii) the duration of the growth of ice bodies also increased with latitude, in conjunction with longer permafrost phases during the Pleistocene; and (iii) for sand wedges, which may have repeatedly grown during the coldest phases separated by long periods of inactivity, the cumulative number of growth episodes increased with latitude. The relationship between width and latitude is, however, less clear than that between depth and latitude, and the dispersion of the measurements is large. For ice-wedge pseudomorphs, the main factor involved is probably the subsidence of the host material that accompanied the melting of ice. The collapse of the walls may have caused significant variations in the width of the pseudomorphs. Other possible factors include the presence of anti-syngenetic wedges (Mackay, 1995) and non-representative measurements of the actual width of the wedges because of their obliquity to the cross-section.

Pleistocene Permafrost Extent: Synthesis and Comparison with Other Data

The field data allow approximate delineation of the areas affected by past permafrost (Figure 6). The configuration described here probably coincides with the Last Permafrost Maximum (LPM) according to the optically stimulated luminescence ages obtained on the infilling of sand wedges (Buylaert et al., 2009; Bertran et al., 2014, and references therein; E. Andrieux, unpublished data). The main points that can be drawn are:

1. France has probably never been affected by continuous permafrost. Based on the current state of knowledge, the southern limit of pingo and lithalsa scars crosses Belgium and the UK north of latitude 51°N.

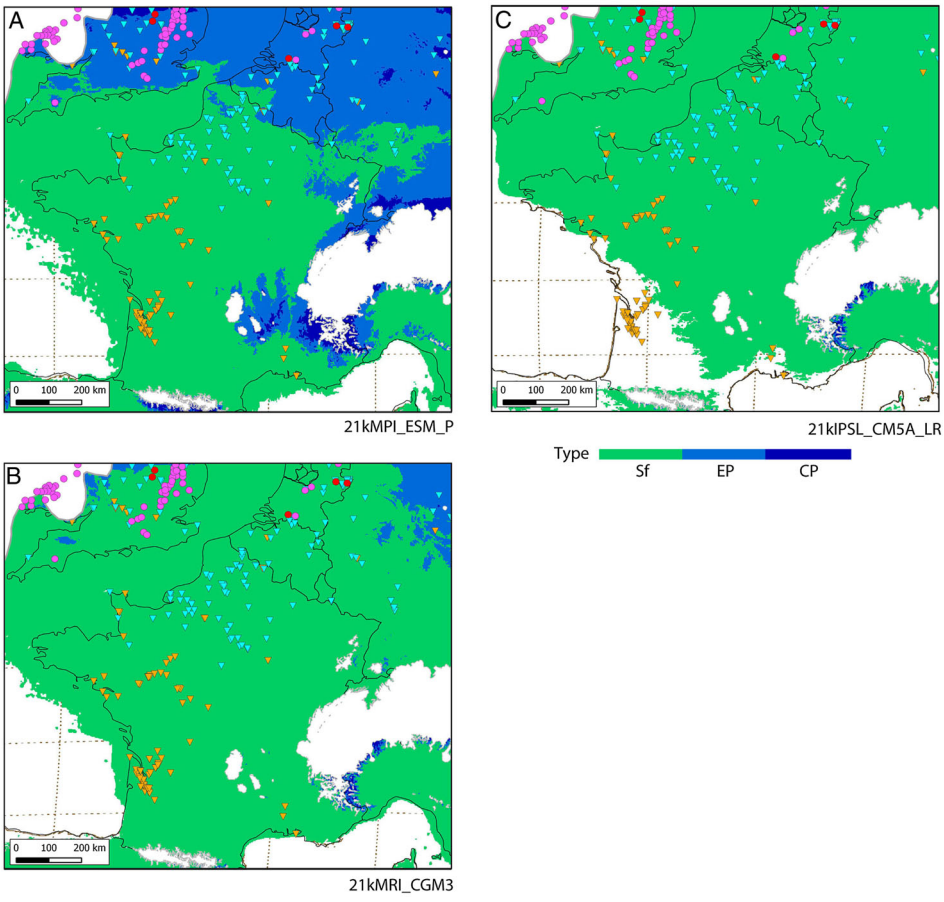

Figure 12 Frozen ground distribution at 21 ka (Last Glacial Maximum) derived from surface air temperatures simulated by global climate models participating in the Paleoclimate Model Intercomparison Project Initiative III, and downscaled to Western Europe. Here, (A) the coldest (MPI_ESM_P), (B) median (MRI_CGM3) and (C) warmest (IPSL_CM5A_LR) results are shown. Continuous (CP) and discontinuous (EP) permafrost are shown in dark and light blue, respectively, and seasonal (Sf) frost in green. See figure 6 for symbols. This figure is available in colour online at wileyonlinelibrary.com/journal/ppp

Unfortunately, most of the scars remain undated and some may have formed during the Younger Dryas Stadial. Nevertheless, an LGM age has been proposed for some pingo scars in The Netherlands (K. (Kasse and Bohncke, 1992)). At this latitude, the ice wedges may have reached about 6 m in depth.

2. The southern boundary of ice-wedge pseudomorphs is close to 47°N and approximately corresponds to the southern edge of the Paris Basin. According to the data from present-day ice-wedge environments, this limit would have been close to the MAAT isotherm of -3 to -4 °C. The area between 47 and 51°N was, therefore, affected by widespread discontinuous permafrost.
3. The southern boundary of the sand wedges, located around 43.5°N in southwest France, is assumed to reflect the limit of thermal contraction cracking, at a MAAT close to -1 to 0 °C. Therefore, the area between 43.5 and 47°N was probably affected by sporadic discontinuous permafrost or, at the southern margin of that area, by deep seasonal frost.

In comparison with many reconstructions of past permafrost extent based on field data ((Huijzer and Vandenberghe, 1998; Van Vliet-Lanoë and Hallégouët, 2001; Vandenberghe et al., 2014), and references therein), the one proposed here is among the less 'cold' (i.e. for which the permafrost extent was less important). The main reasons for this reconstruction are the observation that true ice-wedge pseudomorphs did not develop at latitudes south of 47°N, and the interpretation of sand wedges as features that were not necessarily related to permafrost conditions in contexts where sand drifting was widespread.

Studies on groundwater recharge of deep aquifers in Europe (Jiraková et al., 2011) provide new data for comparison. They show that the recharge associated with the watersheds of Provence, northern Aquitaine and the southern Paris Basin does not exhibit any interruption during the Late Pleistocene, whereas the recharge of aquifers in Normandy, the northern part of the Paris Basin and Lorraine (northeast France) displays a gap between *c*. 30 and 19 ka, which reflects the interruption of groundwater circulation by the growth of widespread permafrost. These data agree well with the reconstruction proposed here.

Comparison to Palaeoclimatic Simulations

A downscaling of the simulated distribution of permafrost during the LGM (21 ka) was made for Western Europe. The comparison between the simulation and the data shows a more or less important divergence according to the model used (Figure 12). Considering a median simulation such as 21kMRI_CGM3, the limits of continuous and discontinuous permafrost were located at least 3° to the north and 10° to the east of the limits implied by the field data. For the coldest simulation (21kMPI_ESM_P), the difference is reduced to about 2° in latitude and 5° in longitude. It places the southern limit of discontinuous permafrost near the Franco-Belgian border, whereas the continuous permafrost zone did not spread beyond the northeastern corner of Germany.

In agreement with Vandenberghe *et al*. (2014) and Bertran *et al*. (2014), the LPM (i.e. the coldest period of the Last Glacial) does not coincide strictly with the LGM and seems significantly older (*c*. 24–31 ka). This may partly explain the discrepancies observed between the simulated and field data. According to the latter, the difference between the LPM and LGM MAATs would have been in the order of 2 to 3 °C, a value which does not seem unrealistic.

CONCLUSION

The GIS analysis of the French and northern European databases of Pleistocene periglacial features has significantly clarified our understanding of the distribution of past permafrost. The distribution of indisputable ice-wedge pseudomorphs does not extend south of 47°N and, therefore, suggests that widespread discontinuous permafrost did not affect the regions south of the Paris Basin. The exclusive presence of primary sand wedges in a band located between 45 and 47°N reflects the association between active sand transport by the wind at the margins of the coversands and thermal contraction cracking of the ground subject to deep seasonal frost or sporadic discontinuous permafrost but unfavourable to the growth of large ground-ice bodies. The latitudinal evolution of the different types of wedges clearly demonstrates that the sand wedges were located in the southern margin of the area affected by thermal contraction. The distribution of pingo scars in Western Europe, which are restricted to the UK (however, many of them are thought to be lithalsa scars, J. Murton personal communication) and The Netherlands, strongly suggests that continuous permafrost never spread over France.

The proposed map of Pleistocene permafrost in France partially reconciles field data with palaeoclimatic simulations. A discrepancy between them may reflect a time lag between the LPM (probably about 31–24 ka) and the LGM (21 ka). This remains to be investigated thoroughly using simulations and improved dating of periglacial features.

ACKNOWLEDGEMENTS

This work benefitted from funds provided by the INRAP, the Lascarbx (the universities of Bordeaux) and PACEA. We acknowledge all the people who contributed to the database, particularly P. Antoine, S. Coutard, J. P. Coutard, L. Deschodt, B. Dousteyssier, P. Gardère, A. Lenoble, D. Millet and B. Van Vliet-Lanoë. We warmly thank B. Moulin and F. Prodeo for their assistance in the use of the GIS software. Some georeferenced data were provided by S. Zaragosi., M. Allard, M. Bateman, J. Kovacs, J. Murton and J. Vandenberghe also contributed to improve the first draft of the paper.

REFERENCES

Allard M, Seguin MK. 1987. Le pergélisol au Québec nordique: bilan et perspectives. *Géographie Physique et Quaternaire* **XLI** (1): 141–152.

Amante C, Eakins BW. 2009. ETOPO1 1 arc-minute global relief model: procedures, data sources and analysis. NOAA Technical Memorandum NESDIS NGDC-24.

Ballantyne CK, Harris C. 1994. The Periglaciation of Great Britain. Cambridge University Press: Cambridge.

Bertran P, Bateman M, Hernandez M, Lenoir M, Mercier N, Millet D, Tastet JP. 2011. Inland aeolian deposits of southwest France: facies, stratigraphy and chronology. *Journal of Quaternary Science* **26**: 374–388.

Bertran P, Andrieux E, Antoine P, Coutard S, Deschodt L, Gardère P, Hernandez M, Legentil C, Lenoble A, Liard M, Mercier N, Moine O, Sitzia L, Van Vliet-Lanoë B. 2014. Distribution and chronology of Pleistocene permafrost features in France: database and first results. *Boreas* **43**: 699–711.

Bockheim JG, Kurz MD, Soule SA, Burke A. 2009. Genesis of active sand-filled polygons in lower and central Beacon Valley, Antarctica. *Permafrost and Periglacial Processes* **20**: 295–308 DOI: 10.1002/ppp.661.

Böse M, Lüthgens C, Lee JR, Rose J. 2012. Quaternary glaciations of northern Europe. *Quaternary Science Reviews* **44**: 1–25.

Boyé M. 1958. Les lagunes du plateau landais. *Biuletyn Peryglacjalny* **26**: 195–225.

Braconnot P, Harrison SP, Kageyama M, Bartlein PJ, Masson-Delmotte V, Abe-Ouchi A, Otto-Bliesner B, Zhao Y. 2012. Evaluation of climate models using palaeoclimatic data. *Nature Climate Change* **2**: 417–424.

Burn CR. 1990. Implications for palaeoenvironmental reconstructions of recent ice-wedge development at Mayo, Yukon Territory. *Permafrost and Periglacial Processes* **1**: 3–14.

Buylaert JP, Ghysels G, Murray AS, Thomsen KJ, Vandenberghe D, De Corte F, Heyse I, Van den Haute P. 2009. Opticla dating of relict sand wedges and composite-wedge pseudomorphs in Flandders, Belgium. *Boreas* **38**: 160–175.

Clark PU, Mix AC. 2002. Ice sheets and sea level of the Last Glacial Maximum. *Quaternary Science Reviews* **21**: 1–7.

Courbouleix S, Fleury R. 1996. Mares, mardelles et pergélisol: exemple des dépressions circulaires de Sologne. *Environnements Périglaciaires* **3**: 63–70.

Ehlers J, Gibbard PL. 2004. *Quaternary Glaciations - Extent and Chronology*, *Part I*: *Europe*. In Developments in Quaternary Science, **2a**. Elsevier: Amsterdam.

French HM. 2007. The Periglacial Environment, 3rd edition. John Wiley & Sons: Chichester.

Friedman JD, Johansson CE, Oskarsson N, Svesson H, Thorarinsson S, Williams JR. 1971. Observations on Icelandic polygon surfaces and palsa areas, photo interpretation and field studies. *Geografiska Annaler* **53A**(3-4): 115–145.

Goldthwait RP. 1976. Frost-sorted patterned ground: a review. *Quaternary Research* **6**: 27–35.

Hallet B, Sletten R, Whilden K. 2011. Microrelief development in polygonal patterned ground in the Dry Valleys of Antarctica. *Quaternary Research* **75**: 347–355.

Hamilton TD, Ager TA, Robinson SW. 1983. Late Holocene ice wedges near Fairbanks, Alaska, U.S.A.: environmental setting and history of growth. *Arctic and Alpine Research* **15**: 157–168.

Huijzer B, Vandenberghe J. 1998. Climatic reconstruction of the Weichselian Pleniglacial in northwestern and central Europe. *Journal of Quaternary Science* **13**(5): 391–417.

Isarin R, Huijzer B, van Huissteden K. 1998. Time-slice oriented multiproxy database (MPDB) for palaeoclimatie reconstruction. National Snow and Ice Data Center, University of Boulder, Colorado. http://nsidc.org/data/ggd248.html

Jetchick E, Allard M. 1990. Soil wedge polygons in northern Québec: description and palaeoclimatic significance. *Boreas* **19**: 353–367.

Jiraková H, Huneau F, Celle-Jeanton H, Hrkal Z, Le Coustumer P. 2011. Insights into palaeorecharge conditions for European deep aquifers. *Hydrology Journal* **19**: 1545–1562.

Jost A, Lunt D, Kageyama M, Abe-Ouchi A, Peyron O, Valdes PJ, Ramstein G. 2005. High-resolution simulations of the Last Glacial Maximum climate over Europe: a solution to discrepancies with continental palaeoclimatic reconstructions? *Climate Dynamics* **24**: 557–590.

Kasse CK. 2002. Sandy aeolian deposits and environments and their relation to climate during the Last Glacial Maximum and Lateglacial in northwest and central Europe. *Progress in Physical Geography* **26**(4): 507–532.

Kasse CK, Bohncke S. 1992. Weichselian Upper Pleniglacial aeolian and ice-cored morphology in the southern Netherlands (Noord-Brabant, Groote Peel). *Permafrost and Periglacial Processes* **3**: 327–342.

Kitover DC, van Balen RT, Roche DM, Vandenberghe J, Renssen H. 2013. New estimates of permafrost evolution during the last 21 k years in Eurasia using numerical modelling. *Permafrost and Periglacial Processes* **24**: 286–303.

Lachenbruch AH. 1962. Mechanics of the thermal contraction cracks and ice-wedge polygons in permafrost. Geological Society of America Special Paper 70.

Lautridou JP. 1985. Le cycle périglaciaire pléistocène en Europe du nord-ouest et plus particulièrement en Normandie. Thèse de doctorat d'état, University of Caen, Caen, t. 1.

Lécolle F. 1998. Que faire des dépressions fermées. *Quaternaire* **9**: 101–104.

Legigan P. 1979. L'élaboration de la formation du Sables des Landes. Dépôt résiduel de l'environnement sédimentaire *Pliocène-Pléistocène centre aquitain*. Mémoires de l'Institut de Géologie du Bassin d'Aquitaine **9**.

Lenoble A, Bertran P, Mercier N, Sitzia L. 2012. Le site du Lac Bleu et la question de l'extension du pergélisol en France au Pléistocène supérieur. *Quaternaire continental d'Aquitaine*: *un point sur les travaux récents*. Guidebook of the field excursion AFEQ-ASF 2012. University of Bordeaux, **AFEQ**: 107–121.

Levavasseur G, Vrac M, Roche DM, Paillard D, Martin A, Vandenberghe J. 2011. Present and LGM permafrost from climate simulations: contribution of statistical downscaling *Climate of the Past, Discussions* **7**: 1647–1962.

Maarleveld GC. 1976. Periglacial phenomena and the mean annual air temperature during the last glacial time in The Netherlands. *Biuletyn Periglacjalny* **26**: 57–78.

Mackay JR. 1988. Pingo collapse and palaeoclimatic reconstruction. *Canadian Journal of Earth Sciences* **25**: 495–511.

Mackay JR. 1995. Ice wedges on hillslopes and landform evolution in the late Quaternary, western Arctic coast, Canada. *Canadian Journal of Earth Sciences* **32**: 1093–1105.

Matsuoka N, Hirakawa K. 1993. Critical polygon size for ice-wedge formation in Svalbard and Antarctica. In *Proceedings of the Sixth International Permafrost Conference*, Beijing. South China University of Technology Press: Lanzhou; vol. **1**, 449–454.

Michel JP. 1967. Dépressions fermées dans les alluvions anciennes de la Seine à 100 km au S-E de Paris. *Bulletin de l'Association Française pour l'Etude du Quaternaire* **2**: 131–134.

Milne GA, Mitrovica JX. 2008. Searching for eustasy in deglacial sea-level histories. *Quaternary Science Reviews* **27**: 2292–2302.

Murton JB, Kolstrup E. 2003. Ice-wedge casts as indicators of palaeotemperatures: precise proxy or wishful thinking? *Progress in Physical Geography* **27**(2): 153–170.

Péwé TL. 1966. Paleoclimatic significance of fossil ice wedges. *Biuletyn Peryglacjalny* **5**: 65–72.

Pissart A. 2000. Remnants of lithalsas of the Hautes Fagnes, Belgium: a summary of present-day knowledge. *Permafrost and Periglacial Processes* **11**: 327–355.

Plug LJ, Werner BT. 2002. Nonlinear dynamics of ice-wedge networks and resulting sensitivity to severe cooling events. *Nature* **417**: 929–932.

Plug LJ, Werner BT. 2008. Modelling of ice-wedge networks. *Permafrost and Periglacial Processes* **19**: 63–69.

Poser H. 1948. Boden- und Klimaverhältnisse im Mittle- und Westeuropa während der Würmeiszeit. *Erdkunde* **2**: 53–68.

Renssen H, Vandenberghe J. 2003. Investigation of the relationship between permafrost distribution in NW Europe and extensive winter sea-ice cover in the North Atlantic Ocean during the cold phases of the Last Glaciation. *Quaternary Science Reviews* **22**: 209–223.

Romanovskij NN. 1973. Regularities in formation of frost-fissures and development of frost-fissure polygons. *Biuletyn Peryglacjalny* **23**: 237–277.

Romanovskij NN. 1985. Distribution of recently active ice and soil wedges in the USSR. In Field and Theory: Lectures in Geocryology, Church M, Slaymaker O (eds). University of British Columbia Press: Vancover; 154–165.

Ross N, Harris C, Brabham PJ, Sheppard TH. 2011. Internal structure and geological context of ramparted depressions, Llanpumsaint, Wales. *Permafrost and Periglacial Processes* **22**: 291–305.

Saito K, Sueyoshi T, Marchenko S, Romanovsky V, Otto-Bliesner B, Walsh J, Bigelow N, Hendricks A, Yoshikawa K. 2013. LGM permafrost distribution: how well can the latest PMIP multi-model ensembles perform reconstruction? *Climate of the Past* **9**: 1697–1714.

Saito K, Marchenko S, Romanovsky V, Hendricks A, Bigelow N, Yoshikawa K, Walsh J. 2014. Evaluation of LPM permafrost distribution in northeast Asia reconstructed and downscaled from GCM simulations. *Boreas* **43**: 733–749.

Texier JP. 2011. Genèse des lagunes landaises: un point sur la question. In *De la lagune à l'airial*: *le peuplement de la Grande Lande*, Merlet JC, Bost JP (eds). Aquitania suppl. 24. Pessac; 23–42.

Throop J, Lewkowicz AG, Smith SL. 2012. Climate and ground temperature relations at sites across the continuous and discontinuous permafrost zones, northern Canada. *Canadian Journal of Earth Sciences* **49**: 865–876.

Tricart J. 1956. Carte des phénomènes périglaciaires quaternaires en France. Mémoire pour servir à l'explication de la carte géologique détaillée de la France. Ministère de l'Industrie et du Commerce: Paris.

Vandenberghe J, Renssen H, Roche DM, Goose H, Velichko AA, Gorbunov A, Levavasseur G. 2012. Eurasian permafrost instability constrained by reduced sea-ice cover. *Quaternary Science Reviews* **34**: 16–23.

Vandenberghe J, French H, Gorbunov A, Marchenko S, Velichko AA, Jin H, Cui Z, Zhang T, Wan X. 2014. The Last permafrost Maximum (LPM) map of the Northern Hemisphere: permafrost extent and mean annual air temperatures, 25-17 ka. *Boreas* **43**: 652–666.

Van Vliet-Lanoë B, Hallégouët B. 2001. European permafrost at the LGM and at its maximal extent. The geological approach. *In* Permafrost Response on Economic Development, Environmental Security and Natural Resources, Paepe R, Melnikov V (eds). Kluwer Academic Publishers: Dordrecht; 195–213.

Velichko AA. 1982. Palaeogeography of Europe during the Last One Hundred Thousand Years. Nauka: Moscow.

Washburn AL. 1979. Geocryology - A survey of periglacial processes and environment. Arnold Publications: London.

Washburn AL. 1985. Periglacial problems. *In* Field and Theory. Lectures in Geocryology, Church M, Slaymaker O (eds). University of British Columbia Press: Vancover; 167–202.

Washburn AL, Smith DD, Goddard RH. 1963. Frost cracking in a middle-latitude climate. *Biuletyn Peryglacjalny* **12**: 175–189.

Watson E, Watson S. 1974. Remains of pingos in the Cletwr basin, south-west Wales. *Geografiska Annaler* **56A**: 213–225.

Wojdyr MJ. 2010. Fityk: a general-purpose peak fitting program. *Journal of Applied Crystallography* **43**: 1126–1128.

Wolfe SA, Stevens CW, Gaandderse AJ, Oldenborger GA. 2014. Lithalsa distribution, morphology and landscape associations in the Great Slave Lowland, Northwest Territories, Canada. *Geomorphology* **204**: 302–313.

6. The chronology of Late Pleistocene thermal contraction cracking in France

Eric Andrieux, Mark D. Bateman, Pascal Betran

Résumé:

Une grande partie de la France est restée hors de l'emprise des calottes glaciaires durant la fin du Quaternaire, et a été soumise à des phases répétées d'activité périglaciaire. De nombreuses structures périglaciaires ont été décrites dans ces zones, mais la compréhension des conditions environnementales et climatiques qui ont présidé à leur formation, leur chronologie et la reconstitution de l'étendue du pergélisol étaient jusqu'à présent des objectifs difficiles à atteindre. Les remplissages primaires sableux fossiles et les pseudomorphoses de coins composites ont enregistré cette activité périglaciaire. Dans la mesure où ils contiennent du matériel riche en quartz bien blanchis, ces structures sont adaptées à la datation par Luminescence Stimulée Optiquement (OSL). Cette étude vise à reconstruire la chronologie de l'activité des coins dans deux régions: le nord de l'Aquitaine, et la vallée de la Loire. Les résultats des mesures en OSL *single-grain* permettent d'identifier plusieurs phases d'activité des coins sableux, au minimum 11 durant les derniers 100 ka. La phase de fissuration par contraction thermique la plus répandue s'est produite entre 30 et 24 ka (i.e. pendant la dernière phase d'extension maximale du pergélisol, LPM), qui est concomitante avec des périodes de grande disponibilité en sable éolien (SIM 2). Bien que la plupart des phases de croissance des coins sableux se corrèle bien avec les périodes froides du Pléistocène, l'identification de périodes d'activité vers la fin du SIM 5 et au début de l'Holocène suggère fortement que ces structures n'indiquent pas seulement la présence de pergélisol mais aussi un gel saisonnier profond dans un contexte de faible insolation hivernale. Ces données suggèrent également que les âges globalement plus jeunes obtenus à partir des coins sableux dans le nord de l'Europe résultent très certainement d'un enregistrement limité des périodes caractérisées par une déflation réduite, et/ou du calcul moyenné des âges qui est inhérent aux méthodes standard de datation par luminescence.

Mots clés : OSL, Datation par luminescence, Coin de sable, France

Andrieux, E., Bateman M., Bertran, P., 2017. The chronology of Late Pleistocene thermal contraction cracking in France. submitted

The chronology of Late Pleistocene thermal contraction cracking in France

Eric Andrieux[1], Mark D. Bateman[2], Pascal Bertran[1,3]

[1] PACEA, UMR 5199 Université de Bordeaux – CNRS, Bâtiment B18, Allée Geoffroy-Saint-Hilaire, CS 50023, 33615 Pessac cedex, France. *Email*: andrieux.e@gmail.com

[2] Department of Geography, University of Sheffield, Winter Street, Sheffield S10 2TN, UK. *Email*: m.d.bateman@sheffield.ac.uk

[3] INRAP, 140 avenue du Maréchal Leclerc, 33130 Bègles, France. *Email*: pascal.bertran@inrap.fr

Abstract

Much of France remained unglaciated during the Late Quaternary and was subjected to repeated phases of periglacial activity. Numerous periglacial features have been reported but disentangling the environmental and climatic conditions they formed under, the timing and extent of permafrost and the role of seasonal frost has up until now remained elusive. The primary sandy infillings of relict sand-wedges and composite-wedge pseudomorphs record periglacial activity. As they contain well-bleached quartz-rich aeolian material they are suitable for optically stimulated luminescence dating (OSL). This study aims to reconstruct when wedge activity took place in two regions of France; Northern Aquitaine and in the Loire valley. Results from single-grain OSL measurements identify multiple phases of activity within sand wedges which suggest that wedge activity in France occurred at least 11 times over the last 100 ka. The most widespread events of thermal contraction cracking occurred between ca. 30 and 24 ka (Last Permafrost Maximum) which are concomitant with periods of high sand availability (MIS 2). Although most phases of sand-wedge growth correlate well with known Pleistocene cold periods, the identification of wedge activity during late MIS 5 and the very beginning of the Holocene strongly suggests that these features do not only indicate permafrost but also deep seasonal ground freezing in the context of low winter insolation. These data also suggest that the overall young ages yielded by North-European sand-wedges likely result from poor record of periglacial periods concomitant with low sand availability and/or age averaging inherent with standard luminescence methods.

Keywords: OSL, Luminescence dating, Sand wedge, France

Introduction

Globally during the last glacial periglaciation extended from high to mid-latitude areas driven by overall climatic coolings. Areas beyond the ice limits experienced multiple periglacial phases and have records of these events preserved in the surficial sediments and landforms (Isarin et al., 1998; Andrieux et al., 2016a). A long-standing challenge has been to establish the relationship between preserved structures and periglacial processes and climate (e.g. Williams, 1968; Péwé, 1966; Vandenberghe, 1983; Kasse and Vandenberghe, 1998; Murton et al., 2000; Murton, 2013). This has led to attempt to model the style and extent of periglaciation in mid latitudes (e.g. Tricart, 1956; Maarleveld, 1976; Huijzer and Vandenberghe, 1998; Van Vliet-Lanoë and Hallégouët, 2001; Vandenberghe et al., 2014). A second challenge has been to understand the timing and extent of these relict periglacial features to enable linkages with other palaeoclimatic proxy records and to better understand spatial regional differences. Previous work (e.g. Buylaert et al., 2009) have undertaken this at the region scale but such studies are hampered by the often polycyclic nature of periglacial features.

The age of when ice and sand wedges formed remains uncertain so far in France and available data are often marred by large uncertainties. The secondary nature of the infilling of ice wedge pseudomorphs does not allow direct dating, and age estimates generally rely on bracketing dates obtained from host and cover sediments. Primary infillings are composed of quartz-rich aeolian sand, which is suitable for optically stimulated luminescence (OSL) dating. Sand wedges are, however, far from being readily datable features. Standard OSL methods applied to a sample of sandy infilling, i.e. a cylinder 5 cm in diameter and 20 cm long, make sense only if all the sand grains have a similar depositional history. Studies in modern arctic settings suggest that such an assumption is probably not true in most cases. As shown by Mackay (1993), thermal contraction cracking occurs episodically resulting in repetitive abandonment and reactivation of the wedges. The millimetre-thick vertical sand laminae may thus reflect successive, discrete episodes of cracking and filling, which are potentially separated by long phases of wedge inactivity.

Accordingly, recent studies by Bateman (2008) and Bateman et al. (2010) pointed that OSL dating of sand wedges shows sometimes palaeodose (De) scatter that cannot be explained by poor recycling, sensitivity changes, variable OSL components, recuperation problems, or large De uncertainties from dim grains. This scatter may be related to multiple De components as it would be the case in a multi-phase formation model for the wedges. Consequently, the ages calculated from luminescence values

yielded by aliquot measurement or/and Central Age Model analysis (CAM, Galbraith et al., 1999) may not necessarily represent the true ages of the features but rather averaged values. The use of high resolution single grain measurements and the extraction of the datasets with Finite Mixture Model (FMM, Galbraith and Green, 1990), which was developed to analyse statistically data comprising multiple components, allow for the calculation of more representative ages (Bateman et al., 2010, 2014; Guhl et al., 2013).

This present study aimed to establish for the first time a chronological framework for periglacial wedge formation in France during the Late Pleistocene. Following the approach proposed by Bateman et al. (2010), single grain OSL measurements and FMM analysis were applied to a comprehensive suite of 33 samples taken from the infillings of French sand-wedges and composite-wedge pseudomorphs in order to better understand the chronology of Late Pleistocene thermal contraction cracking events. The features selected are from a number of sites located within two regions, one in Northern Aquitaine which is one of the southernmost areas of sand-wedge occurrence in France (~45°N), the other in the Loire valley in a more northern region (~47°N) (Figure 1).

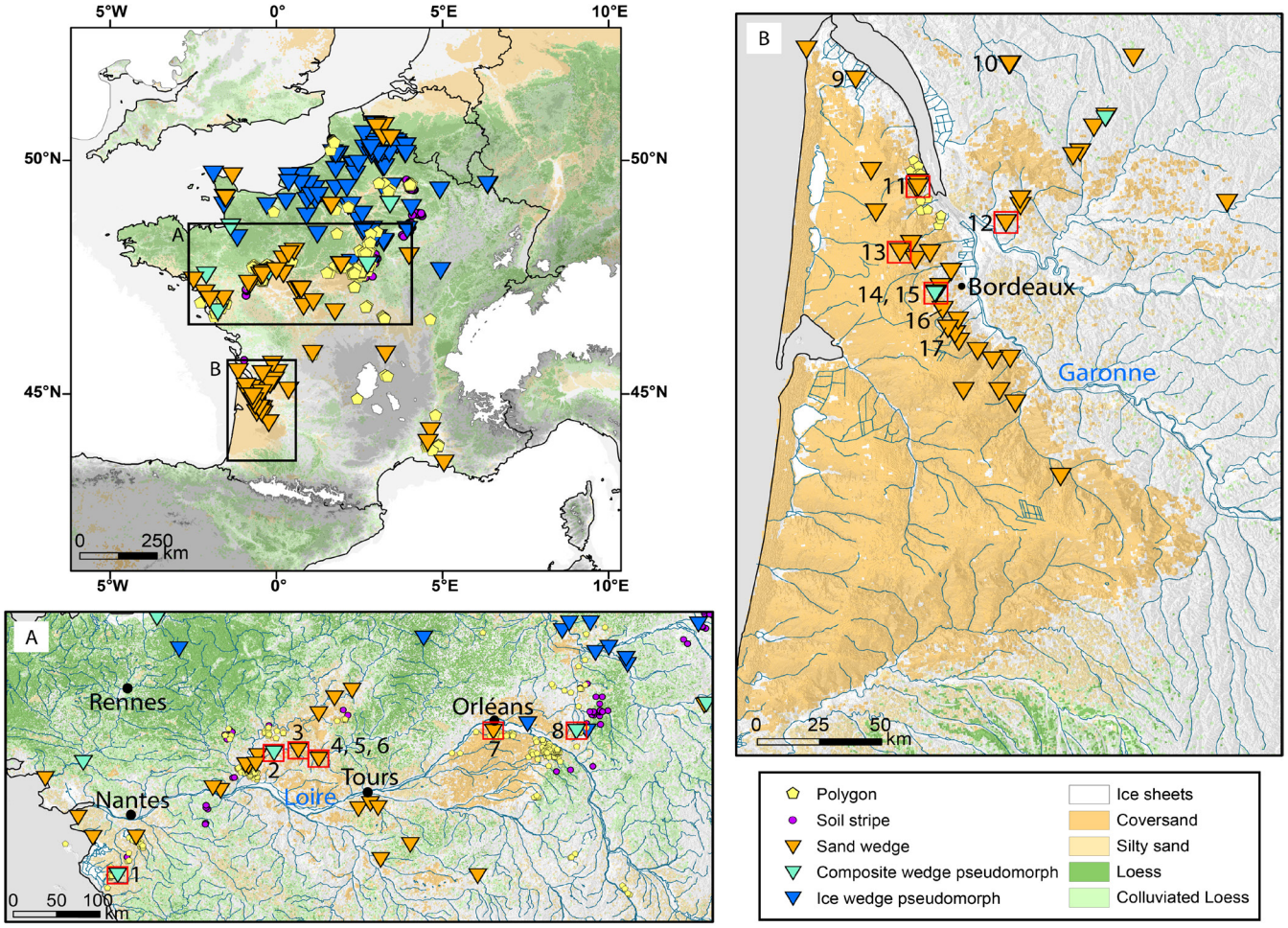

Figure 1: Spatial distribution of periglacial features in France with zooms on A) Loire valley and B) Northern Aquitaine. OSL dating was carried out on the numbered features, the ones dated therein are highlighted with a red square. 1 Challans; 2 Durtal; 3 La Flèche; 4, 5, 6 La-Chapelle-aux-Choux; 7 Olivet; 8 Sainte-Geneviève-des-Bois; 9 Jau-Dignac; 10 Jonzac (Guhl et al., 2013); 11 Cussac-Fort-Médoc; 12 Saint-André-de-Cubzac; 13 Salaunes; 14, 15 Mérignac; 16 Pessac Cap-de-Bos, 17 Lac Bleu (Lenoble et al., 2012).

Background

Relict periglacial wedge structures and pseudomorphs created by thermal contraction cracking in areas that underwent permafrost and/or deep seasonal freezing of the ground have been widely reported in France. Ice-wedge pseudomorphs characterised by a secondary infilling replacing ice have been described in alluvial deposits of the Paris basin and in loess of northern France (e.g. Michel, 1969, 1975; Sommé and Tuffreau, 1971; Lautridou, 1985; Antoine, 1988, 1990; Lécolle, 1989; Deschodt et al., 1998; Sellier and Coutard, 2007; Feray, 2009; Moine et al., 2011; Andrieux et al., 2016a,b). These features are only found north of 47°N, and demonstrate that part of the territory was affected by permafrost during the coldest periods of the Pleistocene (Andrieux et al., 2016a). Relict epigenetic sand wedges have been discovered between 47 and 43.5°N in the vicinity of coversands in the Loire valley, Northern Aquitaine and Provence (Bouteyre and Allemann, 1964; Arnal, 1971; Antoine et al., 2005; Lenoble et al., 2012; Bertran et al., 2014; Andrieux et al., 2016a,b). Unlike ice-wedge pseudomorphs, they show a laminated or massive primary infilling of aeolian sand. Composite wedge pseudomorphs that have both primary and secondary infilling have also been described (Antoine et al., 2005; Andrieux et al., 2016a,b) but difficulties in identifying secondary infillings in sandy sedimentary contexts may have lead to the classification of a large number of these features as 'sand wedges' (Andrieux et al., 2016b).

In Europe, North America and Asia, thermoluminescence (TL), infrared-stimulated luminescence (IRSL) and optically-stimulated luminescence (OSL) have been already applied for dating sand wedges on K-feldspars, polymineral fine grains or quartz, using multiple aliquots or single aliquots approaches. Although different techniques were used that does not ensure data homogeneity, the calculated ages provide a first chronological framework for sand wedge development during the Late Pleistocene. The largest set of OSL ages has been obtained by Buylaert et al. (2009) from 14 sand and composite wedges in Flanders, Belgium. The results suggest that most wedges (i.e. 12 out of 14) were active between 21.8 ± 1.2 and 13.9 ± 1.0 ka. This is in agreement with the previously published ages for northern Europe (Böse, 1992, 2000; Briant et al., 2005; Kjaer et al., 2006; Kasse et al., 2007), which show that the features mostly formed during the late Pleniglacial and the Lateglacial. Few ages fall within MIS 3 (Kolstrup and Mejdhal, 1986; Kolstrup, 2007; Christiansen, 1998). More to the south (47.64°N), two sand wedges also yielded late MIS 2 ages in Hungary (Kovàcs et al., 2007; Fàbiàn et al., 2014). The published OSL ages for French sand wedges (ca. 45°N) are on average older and cluster between 37 and 23 ka (Guhl et al., 2013; Lenoble et al., 2012; Bertran et al., 2014). Although being part of the same polygonal network visible in aerial photographs, all the investigated wedges yielded different ages which cannot be explained by

luminescence dating uncertainties. This strongly suggested that sand wedge growth was asynchronous and controlled by local conditions rather than global.

A number of cross-sections in loess from northern France, Belgium and Germany show networks of ice-wedge pseudomorphs which open generally in iron-depleted and cryoturbated horizons referred to as “tundra gleys” (i.e. Haplic Cryosols according to Kadereit et al., 2013). These serve as benchmark levels for the correlation between sections at a regional scale in northern France (Antoine and Locht, 2015). The few reliable numerical ages in direct association with the pseudomorphs highlight six events of permafrost development. The main phase is characterized by two levels of large ice wedge pseudomorphs, sometimes slotted together, and dated to ca. 25 and 30 ka respectively (Frechen et al., 2001; Locht et al., 2006; Kreutzer et al., 2012; Meszner et al., 2013; Antoine et al., 2015). This period stretches over GS 3, 4 and 5 and can be interpreted as the Last Permafrost Maximum (LPM, Vandenberghe et al., 2014). Three other levels of ice-wedge pseudomorphs associated with tundra gleys have been identified in France at Havrincourt (Antoine et al., 2014): (1) small pseudomorphs at the top of the sequence, which remain undated but are stratigraphically younger than the LPM, (2) pseudomorphs in between two soil complexes dated respectively to 42.1 ± 2.8 and 51.5 ± 3.2 ka, and (3) small pseudomorphs bracketed between 61.7 ± 4 and 65 ± 3.8 ka.

These ages depict a complex formation history and differ from those published for sand wedges in Northern Europe, which are unexpectedly much younger.

Study sites

The precise location of the studied features, the sample name and the lab codes are given in table 1. The sites of Salaunes (Château Montgaillard), Cussac-F”” width, and have either a massive or a laminated sandy infilling (Figure 2). In total, 17 samples were gathered from 5 sand wedges in these sites.

In the Loire valley 16 samples were taken from 6 epigenetic sand wedges (Olivet, La Flèche, La-Chapelle-aux-Choux, Challans) and 2 composite wedge pseudomorphs (Durtal, Sainte-Geneviève-des-Bois) (table 1, Figure 2). The wedges develop within Pleistocene alluvial terraces composed of sandy gravel, in close proximity of rivers which provided abundant aeolian sand during the glacials. The wedges are 0.3 to 1 m wide and 1 to 2.5 m in depth. At Durtal a primary laminated sandy infill (0.3 m wide, 1.7 m depth) cross-cuts a previous secondary infill composed of massive sandy gravel (1 m wide, 2 m in depth).

The composite wedge at Sainte-Geneviève-des-Bois, 1.2 m wide and 1.7 m in depth, shows a primary massive sandy infill cross-cut by a secondary silty infill which exhibits U-shaped lamination. The site of Saint-Christophe-du-Ligneron (Challans) is located south of the Loire estuary in the vicinity of a small coversand area.

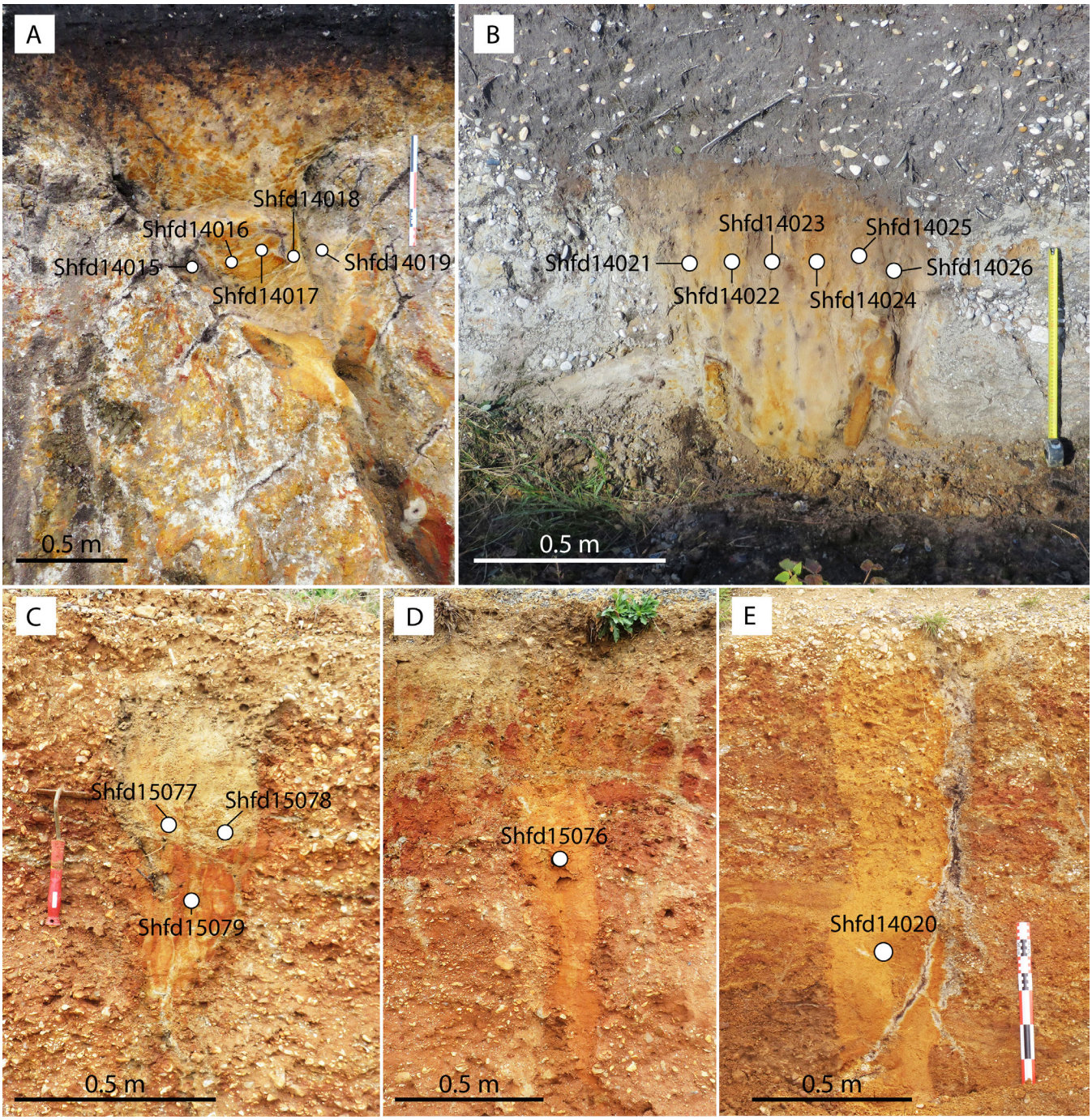

Figure 2: Relict sand-wedges in A) Mérignac (Chronopost; 44.83°N, 0.69°W), B) Cussac-Fort-Médoc (Parcelle Lagrange, 45.11°N, 0.75°W), C) and D) La Chapelle-aux-Choux (47.62°N, 0.21°E), E) Saint-Christophe-du-Ligneron (Challans; 46.8°N, 1.76°W)

Area	Site	Sample	Lab code	Latitude (°)	Longitude (°)	Altitude (m a.s.l.)
Northern Aquitaine	Salaunes - Château Montgaillard	Montg13.1	Shfd14011	44.935	-0.821	49
		Montg13.2	Shfd14012			
		Montg13.3	Shfd14013			
		Montg13.4	Shfd14014			
	Cussac-Fort Médoc - Parcelle Lagrange	Cu13.1	Shfd14021	45.114	-0.75	38
		Cu13.2	Shfd14022			
		Cu13.3	Shfd14023			
		Cu13.4	Shfd14024			
		Cu13.5	Shfd14025			
		Cu13.6	Shfd14026			
	Mérignac - Chronopost	MC13.1	Shfd14015	44.827	-0.689	47
		MC13.2	Shfd14016			
		MC13.3	Shfd14017			
		MC13.4	Shfd14018			
		MC13.5	Shfd14019			
		Chronopost 1	Shfd12099-1			
	Saint-André-de-Cubzac	St André 2	Shfd12098-1	45.01	0.26	52
Loire valley	La Chapelle-aux-Choux	CAH1.1	Shfd15076	47.617	0.211	69
		CAH2.1	Shfd15077			
		CAH2.2	Shfd15078			
		CAH2.3	Shfd15079			
		CAH4.1	Shfd15083			
		CAH4.2	Shfd15084			
	Olivet	O1	Shfd15085	47.815	1.927	114
		O2	Shfd15086			
	Sainte-Geneviève-des-Bois - Les Bézards	B1	Shfd15087	47.81	2.742	145
		B2	Shfd15088			
		B3	Shfd15089			
		B4	Shfd15090			
	Durtal	Durtal	Shfd14028	47.66	-0.231	39
		Durtal 3	Shfd13040			
	Saint-Christophe-du-Ligneron - Challans	Challans 2	Shfd14020	46.8	1.76	32
	La Flèche - La Louverie	Lou3	Shfd14027	47.685	-0.01	34

Table 1: Location of the studied features

Methodology

Sample collection and preparation

Thirty-three samples were collected for OSL from the sandy infillings of freshly exposed sand wedges or composite wedge pseudomorphs by hammering in the sections opaque PVC tubes or metal tubes (60 mm in diameter, 250 mm long). To get a better chance of recording different events potentially preserved in the wedges multiple samples were taken along a horizontal line in the infilling of each wedge when possible. Vertical samples were taken within the primary infillings to check for the influence of depth on doses. The host sediments were also sampled for gamma dose rate modelling purposes.

The samples were prepared under subdued red light conditions at the Sheffield Luminescence

Laboratory. To avoid any potential light contamination that may have occurred during sampling, 2 cm of sediment located at the ends of the PVC tubes was removed and used for estimations of palaeomoistures. The light-unexposed material was treated with hydrochloric acid (1m, HCl) and hydrogen peroxide (H_2O_2) to remove carbonates and organic matter. To ensure that only one grain will fit into each hole when mounted on discs for single grain analysis and to minimise intra-sample variability dry sieving of the sediment was performed, and the 180-250 µm fraction size was kept for OSL measurement. Heavy liquid treatment with sodium polytungstate at 2.67 $g.cm^{-3}$ allowed the separation of quartz from sediment of higher specific gravity (i.e heavy minerals). The remaining sediment was then treated with hydrofluoric acid (HF) to etch the grain surface and to remove residual feldspars and light minerals other than quartz. Once dry, the sediment was treated again with HCl, and then re-sieved at 180 µm to remove acid-soluble fluorides and any grains that have been significantly reduced in size by etching.

Dose rate determination

Dose rates to individual samples are based on elemental measurements made using inductively-coupled plasma mass spectrometry (ICP-MS) as in situ gamma-spectrometer were not possible. This was carried out at the laboratories of SGS Canada (www.sgs.ca). Insofar as most wedges are less than 0.5 m in width, it was generally not possible to sample 0.3 m away from the host sediment. Therefore, the adjacent different lithostratigraphic units of host sediment were also measured to establish their contribution to the gamma dose rate. Gamma dose rates were modelled and corrected using the scaling factors of Aitken (1985) and had little impact on the total doses. Elemental concentrations were converted to annual dose rates using data from Guérin et al. (2011). In order to adjust the dose rates, the following attenuation factors were used: (i) alpha and beta grain size attenuation effects from Bell (1980), Mejdhal (1979) and Readhead (2002), (ii) an a-value of 0.10 ± 0.02 for coarse grain quartz (Olley et al. 1998), (iii) an etch attenuation factor after Duller (1992), and (iv) an attenuation for palaeomoisture content based on moisture content at time of sampling with an absolute error of ± 5% incorporated to allow for past changes. The contribution to dose rates from cosmic sources is a function of geographic location, burial depth and altitude and was calculated using the algorithms published in Prescott and Hutton (1994). An internal quartz dose rate of 10 µGy/ka was added to the total dose rate as done by Vandenberghe et al. (2008). The dosimetry results are available in table 2.

Lab code	K (%)	U (ppm)	Th (ppm)	Rb (ppm)	Alpha (uGy/ka)	Beta (uGy/ka)	Gamma (uGy/ka)	O. (m)	Cosmic (uGy/ka)	Water content (%)	Dose rate (µGy/a)
Shfd14011	0.4 ± 0.02	0.87 ± 0.087	3.7 ± 0.37	26 ± 2.6	22 ± 4	589 ± 40	337 ± 22	1.1	182 ± 9	8.7 ± 5	1130 ± 46
Shfd14012	0.4 ± 0.02	0.67 ± 0.067	3 ± 0.3	21.8 ± 2.18	20 ± 4	563 ± 39	304 ± 20	1.1	182 ± 9	3.8 ± 5	1070 ± 44
Shfd14013	0.4 ± 0.02	0.67 ± 0.067	3 ± 0.3	19.9 ± 1.99	20 ± 3	552 ± 38	305 ± 20	1	184 ± 9	3.7 ± 5	1062 ± 44
Shfd14014	0.4 ± 0.02	0.63 ± 0.063	2.8 ± 0.28	21.1 ± 2.11	19 ± 2	535 ± 37	283 ± 18	0.85	188 ± 9	6 ± 5	1026 ± 42
Shfd14021	0.4 ± 0.02	0.61 ± 0.061	2 ± 0.2	19 ± 1.9	18 ± 4	531 ± 37	258 ± 17	0.61	193 ± 10	1.8 ± 5	1001 ± 42
Shfd14022	0.5 ± 0.025	1.73 ± 0.173	4.2 ± 0.42	27.1 ± 2.71	28 ± 3	802 ± 55	487 ± 31	0.61	193 ± 10	5.5 ± 5	1510 ± 48
Shfd14023	0.4 ± 0.02	0.59 ± 0.059	2 ± 0.2	16.6 ± 1.66	18 ± 3	516 ± 37	257 ± 16	0.61	193 ± 10	1.4 ± 5	984 ± 32
Shfd14024	0.4 ± 0.02	0.72 ± 0.072	1.9 ± 0.19	16.2 ± 1.62	18 ± 3	520 ± 37	263 ± 17	0.61	193 ± 10	2.5 ± 5	995 ± 41
Shfd14025	0.5 ± 0.025	0.61 ± 0.061	2.4 ± 0.24	20.4 ± 2.04	19 ± 4	623 ± 44	302 ± 19	0.61	193 ± 10	1.6 ± 5	1138 ± 49
Shfd14026	0.6 ± 0.03	0.75 ± 0.075	2.9 ± 0.29	29.7 ± 2.97	21 ± 4	770 ± 54	359 ± 23	0.61	193 ± 10	3 ± 5	1343 ± 59
Shfd14015	0.4 ± 0.02	0.99 ± 0.099	4.2 ± 0.42	22.3 ± 2.23	22 ± 2	501 ± 34	318 ± 20	0.9	187 ± 9	20.4 ± 5	1221 ± 50
Shfd14016	0.5 ± 0.03	1.04 ± 0.104	5.2 ± 0.52	27.7 ± 2.77	24 ± 4	623 ± 42	389 ± 25	0.9	187 ± 9	18.5 ± 5	1357 ± 56
Shfd14017	0.4 ± 0.02	0.88 ± 0.088	4.3 ± 0.43	24.6 ± 2.46	22 ± 3	552 ± 37	340 ± 22	0.9	187 ± 9	14.1 ± 5	1189 ± 48
Shfd14018	0.4 ± 0.02	0.71 ± 0.071	3.1 ± 0.31	20.7 ± 2.07	19 ± 4	455 ± 31	257 ± 16	0.9	187 ± 9	19.3 ± 5	1060 ± 43
Shfd14019	0.4 ± 0.02	0.85 ± 0.085	3.7 ± 0.37	22.3 ± 2.23	20 ± 2	474 ± 32	284 ± 18	0.9	187 ± 9	21.2 ± 5	1139 ± 46
Shfd12099	0.3 ± 0.02	0.88 ± 0.088	3.4 ± 0.34	24.1 ± 2.41	23 ± 2	567 ± 51	336 ± 22	2	161 ± 8	5.2 ± 5	1029 ± 42
Shfd12098	1.2 ± 0.06	0.95 ± 0.095	3.8 ± 0.38	53.8 ± 5.38	23 ± 2	1311 ± 95	535 ± 34	1.8	165 ± 8	7.8 ± 5	2034 ± 102
Shfd15076	0.4 ± 0.02	0.87 ± 0.087	4.4 ± 0.44	27.8 ± 2.78	24 ± 2	639 ± 43	382 ± 25	1.2	180 ± 9	5.6 ± 5	1225 ± 50
Shfd15077	0.5 ± 0.03	1.42 ± 0.142	7.1 ± 0.71	46.1 ± 4.61	30 ± 2	825 ± 55	518 ± 33	0.6	196 ± 10	15.16 ± 5	1569 ± 66
Shfd15078	0.4 ± 0.02	1.1 ± 0.11	5.6 ± 0.56	40.5 ± 4.05	26 ± 2	702 ± 47	423 ± 27	0.6	196 ± 10	12.29 ± 5	1347 ± 56
Shfd15079	0.4 ± 0.02	0.99 ± 0.099	5.7 ± 0.57	46.1 ± 4.61	26 ± 2	740 ± 50	426 ± 28	0.8	190 ± 10	10.62 ± 5	1382 ± 58
Shfd15083	0.2 ± 0.01	0.56 ± 0.056	2 ± 0.2	7.2 ± 0.72	18 ± 3	303 ± 22	203 ± 13	0.6	196 ± 10	2 ± 5	720 ± 27
Shfd15084	0.2 ± 0.01	0.44 ± 0.044	1.5 ± 0.15	6.6 ± 0.66	16 ± 2	272 ± 19	166 ± 11	0.9	188 ± 9	2.5 ± 5	642 ± 24
Shfd15085	2.5 ± 0.13	1.25 ± 0.125	4.5 ± 0.45	110 ± 11	27 ± 2	2789 ± 211	962 ± 64	1	187 ± 9	1.4 ± 5	3689 ± 202
Shfd15086	2.7 ± 0.14	1.64 ± 0.164	6.5 ± 0.65	126 ± 12.6	33 ± 2	2969 ± 218	1094 ± 72	1.4	177 ± 9	5.5 ± 5	4483 ± 241
Shfd15087	2.4 ± 0.12	1.38 ± 0.138	7.7 ± 0.77	119 ± 11.9	34 ± 2	2713 ± 197	1051 ± 68	1.5	175 ± 9	5.5 ± 5	3973 ± 209
Shfd15088	2.2 ± 0.11	1.36 ± 0.136	7.1 ± 0.71	110 ± 11	31 ± 2	2343 ± 171	917 ± 59	1.2	183 ± 9	10.5 ± 5	3695 ± 193
Shfd15089	1.2 ± 0.06	1.47 ± 0.147	8.1 ± 0.81	77.7 ± 7.77	35 ± 2	1589 ± 109	772 ± 49	1	188 ± 9	8.2 ± 5	2583 ± 121
Shfd15090	2.5 ± 0.13	1.31 ± 0.131	7 ± 0.7	121 ± 12.1	32 ± 2	2779 ± 204	1038 ± 68	1	188 ± 9	5.3 ± 5	4037 ± 215
Shfd14028	0.3 ± 0.02	0.5 ± 0.05	2.3 ± 0.23	14.7 ± 1.47	18 ± 3	320 ± 25	228 ± 15	0.8	189 ± 9	3.9 ± 5	755 ± 30
Shfd13040	0.2 ± 0.01	0.45 ± 0.045	1.6 ± 0.16	14.1 ± 1.41	16 ± 2	310 ± 22	165 ± 11	1.1	181 ± 9	5.6 ± 5	673 ± 25
Shfd14020	0.8 ± 0.04	1.24 ± 0.124	5.3 ± 0.53	43.4 ± 4.34	28 ± 2	1051 ± 73	543 ± 35	1.1	181 ± 9	7.2 ± 5	1803 ± 81
Shfd14027	0.2 ± 0.01	0.42 ± 0.042	1.8 ± 0.18	11.7 ± 1.17	16 ± 3	236 ± 19	178 ± 11	0.6	194 ± 10	1.6 ± 5	626 ± 24

Table 2: Elemental and associated data used to calculate OSL sample dose rates.

Luminescence measurements

Luminescence measurements were performed on a Risø reader TL-DA-15 equipped with a 90Sr/90Y beta source for irradiation (Bøtter-Jensen et al., 2003). The reader was fitted with a single grain attachment that used a 10 mW Nd:YVO4 solid state diode-pumped laser emitting at 532 nm, which produced a spot approximately 50 µm in diameter (Duller et al., 1999), allowing simulation of individual grains. The luminescence emissions were detected through a Hoya U-340 filter. The purity of extracted quartz was tested for each sample by stimulation with infra-red light as per Duller (2003). No samples showed signs of feldspar contamination. Single grains were measured on 9.6 mm diameter aluminium discs containing 100 holes.

Equivalent dose (D_e) determination was carried out using the Single-Aliquot Regenerative-dose (SAR; Murray and Wintle, 2000, 2003; Table S1). A four point SAR protocol was employed to bracket the expected

palaeodoses with an additional recycling point to check for uncorrected sensitivity changes (Figure S1). Preheat temperatures were determined using a dose recovery preheat plateau test (Murray and Wintle, 2003). The samples displayed OSL decay curves dominated by the fast (bleachable) component, had good dose recovery, low thermal transfer and good recycling (Figure S2). D_e values were only accepted when the recycling ratio was comprised between 0.8 and 1.2, recuperation on zero dose was lower than 5%, and the error on the D_e was less than 30%. The grains exhibiting a signal that was not possible to fit by an exponential, or exponential plus linear growth curve were rejected. However, when the palaeodose could not be ascertained for a grain due to saturation it was recorded as it gives important information on the sample. A minimum of 50 D_e values which met the quality acceptance criteria were measured for each sample to ensure a representative spread in D_e values and to assess the degree of scatter and skewness of the data. Only 2 to 4% of the grains had a measurable OSL signal that met the selection criteria. The samples CAH2.1, CAH2.2, CAH2.3, CAH4.1 and CAH4.2 from the Loire valley had between 10 to 20% saturated grains, whereas the samples from Northern Aquitaine do not show any saturation. Potential contamination by host material was checked during sampling and preparation. No evidence for mixing of different material was found.

The measurements of the OSL signal at single grain level show a large D_e heterogeneity with high overdispersion (Figure 3; Figure S3). As for the sand wedge investigated by Bateman et al. (2008, 2010) the scatter of the D_e values cannot be explained by poor recycling, recuperation problems, or sensitivity changes. In few sampled wedges sand lamination was visible, which testifies to the lack of post-depositional perturbation of the primary infilling. However, a significant amount of the samples were taken from massive sand bodies or from infillings where lamination was only locally preserved, which probably indicate that subsequent mixing occurred due to ice thaw, bioturbation and other pedoturbations (Murton et al., 2000). Such processes may have lead to the inclusion of partially bleached grains in the wedges coming from the surrounding ground surface or from the host sediment, which can result in long tails of D_e or in broad distributions rather than in discrete peaks. The scatter of data is thus assumed to be caused either by poor bleaching of grains prior burial or by the mixing of different age deposits.

An averaging issue would arise if the Central Age model (CAM; Galbraith et al 1999, Roberts et al., 2000) was used to extract the D_e values since this model is designed for well-bleached samples. The

standard approaches are to use either the Minimum Age Model (MAM; Galbraith and Laslett, 1993) or the Finite Mixture Model (FMM; Galbraith and Green 1990) to calculate age estimates. FMM allows the extraction of De components within De distributions and MAM extract the component that provide the minimum age. In our case this means that FMM date the different periods of periglacial wedge infilling while MAM gives the estimate of the last time the wedge was active. Both models were used to calculate the age estimates of the wedges. However, FMM was considered more appropriate because of the potential multi-phased nature of sand-wedges. As the CAM is the model used in previous dating of sand-wedges, the CAM ages were calculated for comparison purposes.

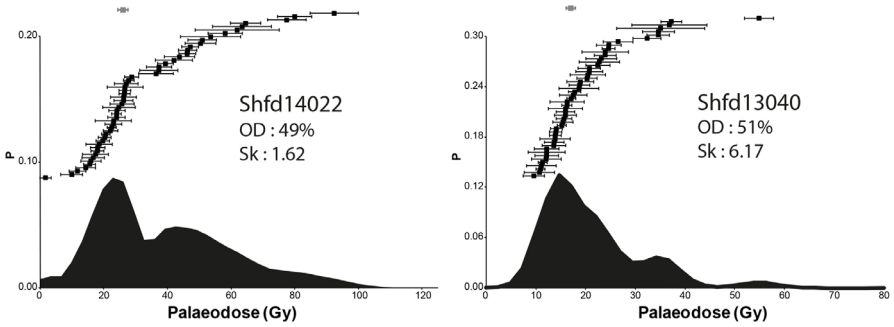

Figure 3: Examples of probability density functions (pdf) plotted for the single grain samples Shfd13040 and Shfd14022 with the individual grain results above (Black) and mean (grey) showing multiple De components. Overdispersion values (OD) were calculated as per Galbraith et al., (1999), skewness (Sk) as per Bailey and Arnold (2006).

For FMM a σ_b value of 0.15 was chosen based on dose recovery tests. The best fit was assessed by iteratively increasing the number (k) of components until the closest to zero value of the Bayesian Information Criterion (BIC) was reached. To avoid the influence of potential post-contamination the D_e components were considered only when exceeding 10% of the total D_e values for each sample (Bateman et al., 2007).

Results

FMM analysis allowed extraction of two to four components for each of the 33 samples from which a total of 86 age estimates were calculated, 47 in the Loire valley and 39 in Northern Aquitaine respectively (table 3). The OSL ages range between 337 ± 40 ka and 7.5 ± 1.2 ka.

In order to test the assumption that wedge activity was not random during the last glacial but rather occurred during specific, climate-controlled periods, the cumulated probability density of the ages was calculated using Oxcal 4.2 (Bronk Ramsey, 2013) with the expectation that peaks would emerge from

the probability distribution. As this was the case, the distribution was adjusted to a combination of Gaussian functions using the software Fityk 0.9.8 (Wojdyr, 2010) and their respective contribution was calculated. The goodness of fit was assessed using R^2, which reached almost unity (R^2=0.9999). The standard deviation of the distribution around the centre of each Gaussian function was estimated from the Full Width at Half Maximum (FWHM). The PDF was plotted together with the NGRIP δO^{18} data over the last 100 ka tuned to the revised Greenland Ice Core Chronology proposed by Rasmussen et al. (2014) to compare the thermal contraction cracking events with known cooling occurrences over Europe (Figure 4).The results suggest the following:

- The sand wedges and composite wedge pseudomorphs were repeatedly active during the Pleistocene up to the beginning of the Holocene.

- The oldest events are recorded in the Loire valley where 71% of OSL ages fall within MIS 3, 4 and 5. In contrast, MIS 2 represent up to 54% of the total OSL ages in Northern Aquitaine. In the latter area, the oldest age falls within MIS 4.

- A total of 11 peaks of wedge activity have been extracted from the 86 ages provided by the samples from the whole dataset during the last 100 ka, i.e. 8.5 ± 0.6, 11.9 ± 0.5, 15.3 ± 0.4, 17.4 ± 0.7, 20.7 ± 0.7, 24 ± 1.1, 30 ± 2.5, 42.5 ± 1.9, 56.2 ± 4, 71.4 ± 1.8, 86 ± 4.2 ka

- Seven OSL ages are older than 100 ka and may correspond to cracking events that occurred during MIS 6, 8 or 10.

The PDFs of the estimates calculated with the different age models (i.e. CAM, MAM, and FMM) allow for comparisons (Figure 5).Differences between the models are evident. As expected the CAM based dataset by averaging all grains from samples identifies fewer more prominent phases of wedge activity during MIS 2. The MAM based dataset by selecting only the youngest component of grains from a sample, under-estimates the earlier phases of wedging. The FMM datasets by attempting to isolate similar age components within samples provides a longer record with more phases within it.

As shown on a representative case study in figure 6, the calculated ages are much younger than the host material of the wedges. They overlap from one sample to another within the same wedge, and between different wedges, and they are not dependent on depth.

Site	Lab code	Central Age Model		Minimum Age Model		Finite Mixture Model		
		De (Gy)	Age (ka)	De (Gy)	Age (ka)	De Component (Gy)	De Component (%)	Age (ka)
Salaunes - Château Montgaillard	Shfd14011	27.11 ± 1.56	23.98 ± 1.69	21.5 ± 1.27	19.02 ± 1.37	17.5161 ± 1.513	25	15.58 ± 1.49
						29.9071 ± 1.708	57	26.46 ± 1.86
						52.324 ± 4.285	17	46.29 ± 4.24
	Shfd14012	16.19 ± 0.92	15.13 ± 1.06	15.29 ± 0.58	14.29 ± 0.81	16.6355 ± 0.541	74	15.55 ± 0.82
						34.8896 ± 2.547	18	32.61 ± 2.74
	Shfd14013	16.68 ± 0.85	15.71 ± 1.03	16.82 ± 0.31	15.84 ± 0.72	16.401 ± 0.709	72	15.45 ± 0.92
						27.092 ± 3.021	17	25.52 ± 3.03
	Shfd14014	20.88 ± 0.92	20.36 ± 1.23	20.09 ± 1.16	19.59 ± 1.39	8.872 ± 1.189	10	8.65 ± 1.21
						21.4495 ± 0.719	76	20.91 ± 1.11
						40.6771 ± 3.384	14	39.66 ± 3.68
Cussac-Fort Médoc - Parcelle Lagrange	Shfd14021	56.09 ± 3.51	56.05 ± 4.22	41.97 ± 1.95	41.94 ± 2.63	30.5052 ± 1.968	27	30.49 ± 2.35
						72.4853 ± 2.392	73	72.44 ± 3.87
	Shfd14022	27.87 ± 1.88	18.45 ± 1.37	22.69 ± 0.73	15.02 ± 0.68	22.51 ± 0.887	63	14.9 ± 0.75
						53.684 ± 2.443	37	35.55 ± 2.21
	Shfd14023	15.5 ± 0.7	15.75 ± 0.97	16.08 ± 0.31	16.33 ± 0.76	14.8822 ± 0.588	80	15.12 ± 0.77
						22.4762 ± 2.434	18	22.83 ± 2.65
	Shfd14024	15.81 ± 0.98	15.89 ± 1.19	14.3 ± 0.75	14.37 ± 0.97	15.0239 ± 0.793	62	15.1 ± 1.02
						25.5927 ± 2.111	30	25.72 ± 2.38
	Shfd14025	17.37 ± 0.91	15.27 ± 1.04	17.68 ± 0.29	15.54 ± 0.72	18.3634 ± 0.562	73	16.14 ± 0.86
						56.3969 ± 4.67	11	49.58 ± 4.64
	Shfd14026	26.01 ± 2.38	19.36 ± 1.97	20.01 ± 0.81	14.89 ± 0.9	15.0251 ± 1.127	25	11.18 ± 0.97
						24.4409 ± 1.347	37	18.19 ± 1.29
						58.2539 ± 4.905	16	43.36 ± 4.13
						156.2825 ± 13.925	22	116.33 ± 10.91
Mérignac - Chronopost	Shfd14015	20.83 ± 1.38	20.27 ± 1.57	14.64 ± 0.69	14.25 ± 0.88	8.4222 ± 0.824	13	8.18 ± 0.87
						19.2245 ± 1.321	39	18.71 ± 1.48
						30.4879 ± 1.747	41	29.67 ± 2.07
	Shfd14016	17.3 ± 0.93	13.93 ± 0.95	14.48 ± 0.51	11.84 ± 0.64	14.7663 ± 0.534	68	12.08 ± 0.66
						29.001 ± 1.529	32	23.72 ± 1.58
	Shfd14017	16.41 ± 0.77	14.9 ± 0.92	12.51 ± 0.61	11.36 ± 0.72	13.3105 ± 1.762	36	12.09 ± 1.67
						19.3465 ± 2.3	55	17.57 ± 2.21
	Shfd14018	14.07 ± 0.68	15.33 ± 0.96	14.5 ± 0.20	15.8 ± 0.67	13.8868 ± 0.507	84	15.13 ± 0.82
						23.1301 ± 2.8843	13	25.2 ± 3.3
	Shfd14019	14.92 ± 0.96	15.46 ± 1.17	11.78 ± 0.59	12.21 ± 0.79	7.4434 ± 0.913	17	7.71 ± 0.99
						17.2444 ± 0.607	79	17.87 ± 0.95
	Shfd12099-2	18.98 ± 0.75	18.44 ± 1.05	17.72 ± 0.39	17.21 ± 0.8	17.6972 ± 0.676	65	17.19 ± 0.97
						28.9987 ± 2.329	22	28.17 ± 2.54
Saint-André-de-Cubzac	Shfd12098-2	25.91 ± 1.17	12.74 ± 0.86	20.44 ± 0.80	10.05 ± 0.64	18.7443 ± 1.336	31	9.21 ± 0.81
						32.5813 ± 1.287	66	16.02 ± 1.02
La Chapelle-aux-Choux	Shfd15076	63.54 ± 3.03	51.86 ± 3.27	53.41 ± 2.69	43.59 ± 2.84	54.0867 ± 2.921	46	44.14 ± 3.01
						83.078 ± 4.81	45	67.8 ± 4.82
	Shfd15077	94.8 ± 5.7	60.42 ± 4.42	60.98 ± 3	38.87 ± 2.51	47.8942 ± 3.7692	21	30.53 ± 2.73
						94.3216 ± 6.244	46	60.12 ± 4.71
						176.7245 ± 11.027	33	112.64 ± 8.46
	Shfd15078	122.91 ± 8.11	91.22 ± 7.1	84.98 ± 4.53	63.07 ± 4.25	91.0753 ± 6.639	36	67.59 ± 5.66
						180.2477 ± 8.2192	53	133.78 ± 8.22
	Shfd15079	113.09 ± 9.12	81.8 ± 7.44	64.96 ± 3.21	46.99 ± 3.05	60.8352 ± 4.417	21	44 ± 3.69
						125.3123 ± 8.421	43	90.64 ± 7.18
						220.7999 ± 13.182	31	159.71 ± 11.66
	Shfd15083	99.22 ± 8.19	137.81 ± 12.5	65.06 ± 3.93	90.36 ± 6.43	67.4209 ± 4.355	29	93.64 ± 7.01
						116.2007 ± 10.528	34	161.39 ± 15.84
						228.8668 ± 18.035	28	317.88 ± 27.76
	Shfd15084	53.62 ± 3.79	83.57 ± 6.7	31.67 ± 1.43	49.36 ± 2.91	25.4295 ± 2.2454	14	39.64 ± 3.81
						54.726 ± 2.501	49	85.3 ± 5.05
						113.4103 ± 10.037	24	176.77 ± 17.01
						216.1 ± 24.657	10	336.82 ± 40.48
Olivet	Shfd15085	118.83 ± 8	29.97 ± 2.6	73.42 ± 3.39	18.52 ± 1.33	69.5658 ± 4.153	27	17.55 ± 1.43
						132.4353 ± 10.833	41	33.4 ± 3.29
						208.6423 ± 16.942	32	52.62 ± 5.16
	Shfd15086	112.92 ± 7.6	26.43 ± 2.28	83.81 ± 4.13	19.61 ± 1.43	48.236 ± 4.703	12	11.29 ± 1.26
						97.257 ± 5.68	40	22.76 ± 1.81
						176.3477 ± 8.288	47	41.27 ± 2.95
Sainte-Geneviève-des-Bois - Les Bézards	Shfd15087	103.4 ± 7.86	26.03 ± 2.41	75.38 ± 5.09	18.97 ± 1.63	69.475 ± 5.44	42	17.49 ± 1.66
						124.2104 ± 13.806	31	31.26 ± 3.62
						239.435 ± 15.016	28	60.27 ± 4.93
	Shfd15088	125.09 ± 11.83	36.01 ± 3.89	90.07 ± 5.65	25.93 ± 2.12	39.7643 ± 4.2667	12	11.45 ± 1.37
						90.2591 ± 10.569	26	25.98 ± 3.33
						203.9413 ± 10.707	62	58.71 ± 4.34
	Shfd15089	109.71 ± 10.71	42.47 ± 4.6	71.25 ± 5.28	27.58 ± 2.42	54.2115 ± 7.1722	19	20.98 ± 2.94
						102.8782 ± 9.382	39	39.82 ± 4.08
						208.1408 ± 12.988	38	80.57 ± 6.58
	Shfd15090	90.88 ± 10.09	22.51 ± 2.77	70.65 ± 5.95	17.5 ± 1.75	30.3856 ± 4.376	12	7.53 ± 1.16
						71.5037 ± 8.623	32	17.71 ± 2.34
						133.2005 ± 12.547	36	33 ± 3.57
						278.2291 ± 34.389	20	68.92 ± 9.28
Durtal	Shfd14028	40.82 ± 2.39	54.06 ± 3.84	28.02 ± 1.16	37.1 ± 2.14	18.1332 ± 1.3274	14	24.01 ± 2
						40.3646 ± 1.954	51	53.45 ± 3.36
						64.0464 ± 4.221	32	84.81 ± 6.54
	Shfd13040-2	16.92 ± 0.74	25.15 ± 1.45	16.54 ± 0.46	24.58 ± 1.16	14.7938 ± 0.928	56	21.99 ± 1.62
						21.9162 ± 2.834	27	32.57 ± 4.39
						37.7118 ± 3.2319	13	56.05 ± 5.25
Saint-Christophe-du-Ligneron - Challans	Shfd14020	56.05 ± 2.01	31.08 ± 1.78	55.49 ± 2.56	30.77 ± 1.98	57.9666 ± 2.73	79	32.14 ± 2.1
						89.328 ± 11.371	12	49.53 ± 6.68
La Flèche - La Louverie	Shfd14027	39.86 ± 2.02	63.71 ± 4.06	30.92 ± 1.32	49.42 ± 2.85	13.0501 ± 1.163	14	20.86 ± 2.03
						36.3304 ± 2.478	45	58.07 ± 4.55
						54.1907 ± 3.251	42	86.62 ± 6.18

Table 3: Finite Model Mixture (FMM) ages in comparison with the estimates calculated from the Central Age Model (CAM) and Minimum Age Model (MAM)

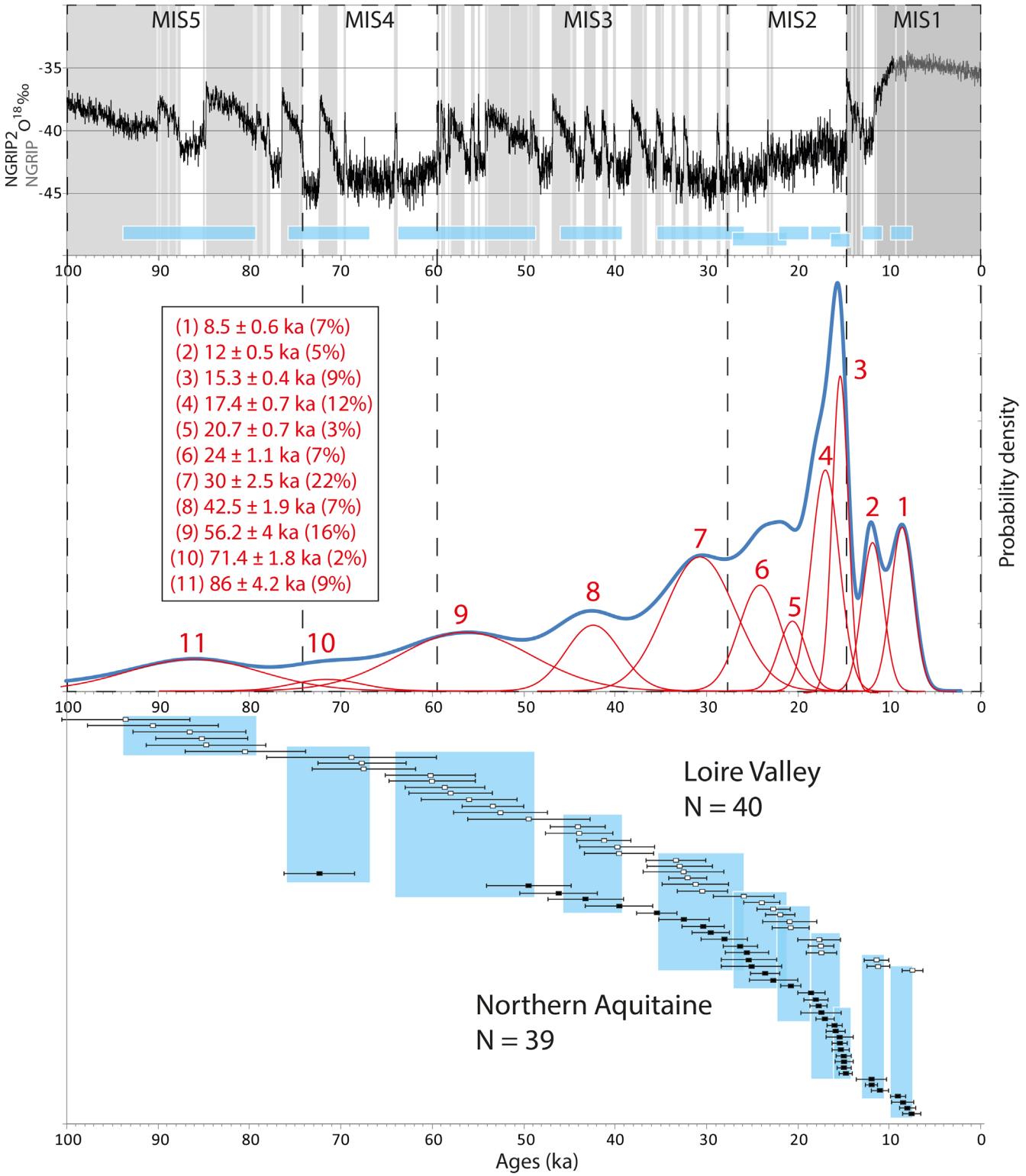

Figure 4: Probability density of the FMM ages and FMM estimates of the Loire valley (white) and Northern Aquitaine (black),plotted together with the NGRIP δO18 data over the last 100 ka tuned to the revised Greenland Ice Core Chronology proposed by Rasmussen et al. (2014). The distribution of the probability density function was adjusted to a combination of Gaussian functions using the software Fityk 0.9.8 (Wojdyr, 2010) and their respective contribution was calculated in percentages of the complete dataset. The goodness of fit was assessed using R^2, which reached almost unity (R^2=0.9999). Blue boxes in the Ngrip curve and over the age estimates represent the Full Width at Half Maximum (FWHM) of each Gaussian function fitted.

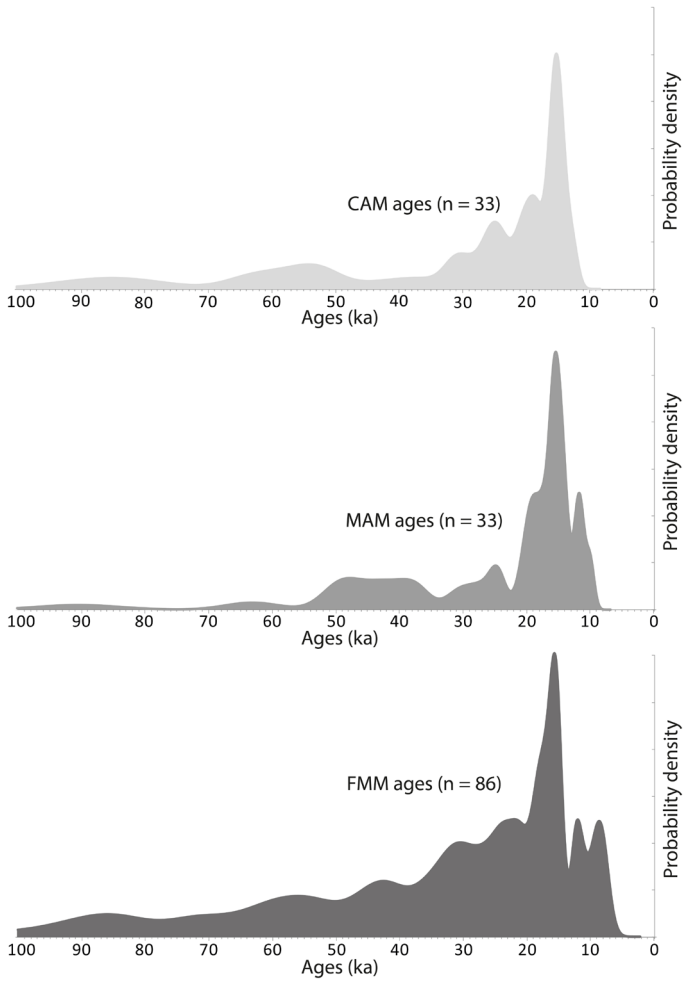

Figure 5: Probability density function of the ages calculated from A) CAM, B) MAM, and C) FMM.

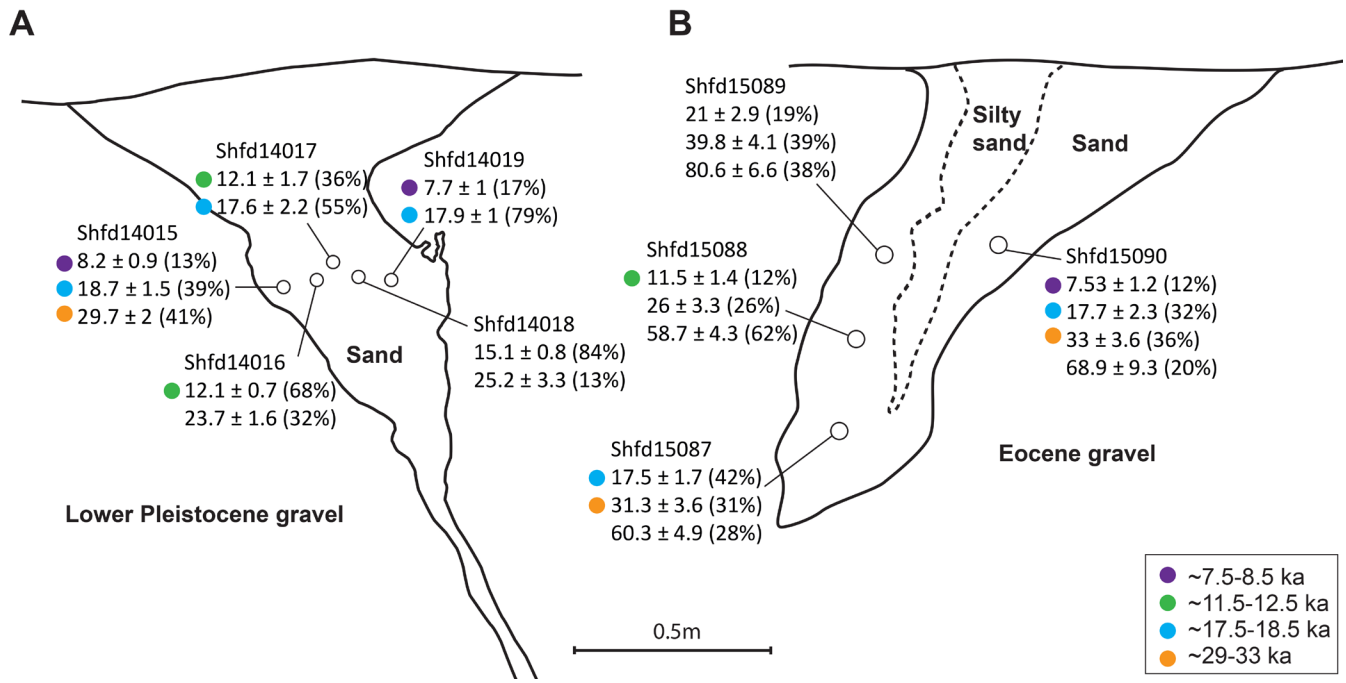

Figure 6: Representative case study of two wedges sampled A) Mérignac (Chronopost) and B) Sainte-Genevieve-des-bois (Les Bézards). OSL ages are calculated from FMM components which contribution in the sample is shown in percentage. Coloured circles show the overlap of ages between the samples and their belonging to an age cluster.

Discussion

The overall age distribution of periglacial wedges shows repetitive thermal contraction cracking over the last 100 ka. However, substantial differences emerge from the comparison between the two regions. Two main factors may be involved, which include:

(1) The latitude of the investigated wedges. As expected, the Loire valley yields a larger number of ages falling into MIS 5 to 3 than does Northern Aquitaine which is located at lower latitude. Overall, the first area is assumed to have been more frequently affected by deep seasonal freezing and/or permafrost during the Late Pleistocene.

(2) The sand availability. In addition to the temperature drop that triggers thermal contraction cracking, the main limiting factor in the growth of sand-wedges is the sand supply. In the Loire valley the sand has a fluvial origin, and sand drifting was probably active during the stadials all along the last glacial on bare alluvial deposits exposed to deflation. In contrast, the location of the sand wedges of Northern Aquitaine near the margin of the coversands ("Sables des Landes" Formation, Sitzia et al., 2015) strongly suggests that this formation, which was fed by deflation on the continental plateau exposed during sea-level lowstands, was the main sand source that filled the contraction cracks. Available chronological data (Bertran et al., 2011; Sitzia et al., 2015) show that the coversands built up mostly between ca. 24 and 14 ka. Comparison between the distribution of ages for coversands and sand wedges points to strong similarity, suggesting that the latter primarily record periods where thermal contraction cracking and huge sand drifting in the coversand area occurred at once (Figure 7). To a certain extent, this record may, therefore, be biased toward MIS 2 which corresponds to the main phase of coversand emplacement.

Age clusters were identified in both areas within the Lateglacial (12 ka, i.e. Younger Dryas, 5 dates in whole data set) and, more surprisingly, within the early Holocene at 8.5 ka (5 dates). Wedge activity during these periods, which were typified by mean annual air temperatures too high for permafrost development in France (Renssen and Isarin, 1998; Simonis et al., 2012), reinforces the assumption that these features are poor indicators of past permafrost as already suggested by Andrieux et al. (2016a) and Wolfe et al. (2016). However, as reconstructed by some proxies, particularly beetles (Ponel et al., 2007), mean January air temperatures remained very low (up to -10°C in the Paris basin) during the Younger Dryas due to low winter insulation (Berger, 1978) allowing deep seasonal ground freezing to occur. Sand drifting was still active in European coversand areas during the Younger Dryas (Kasse, 2002; Sitzia et al., 2015). In Aquitaine, fields of parabolic dunes developed on large areas at that time (Bertran et al., 2011).

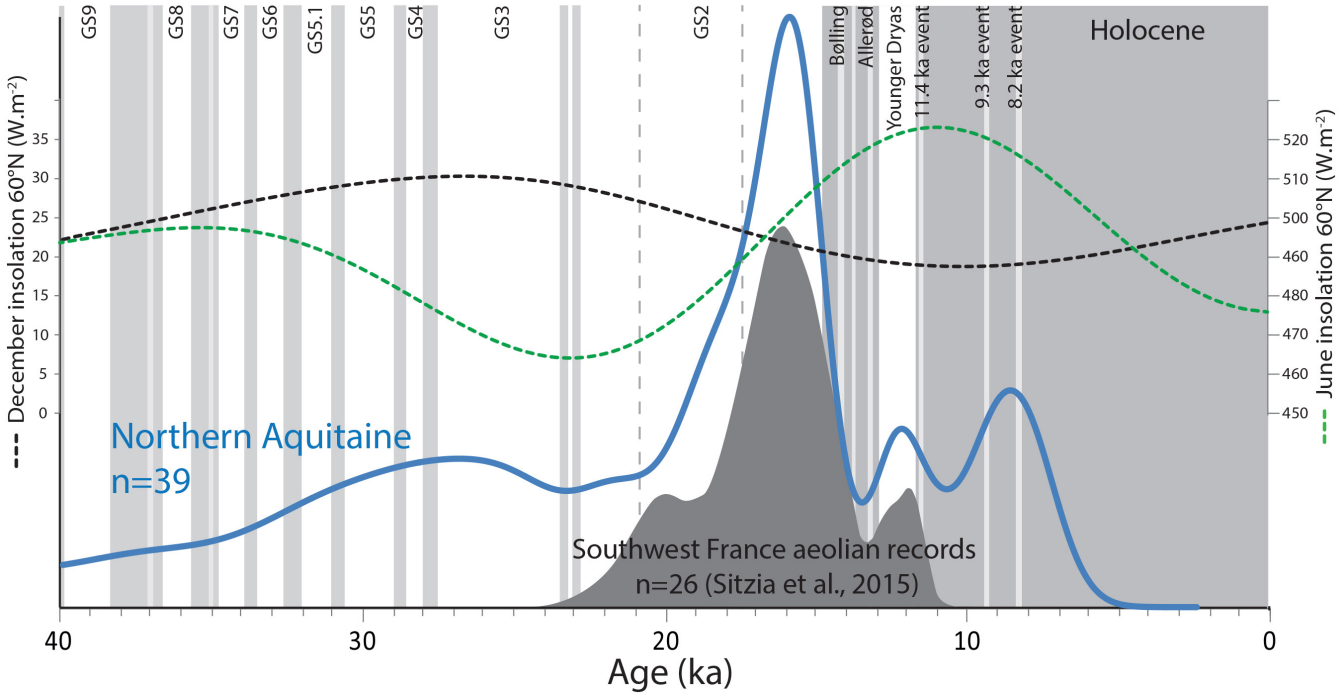

Figure 7: Probability density of the sand wedge ages in Northern Aquitaine compared with the aeolian records from southwest France (Sitzia et al., 2015) and the insolation in June and December at 60°N (Berger, 1978). Interstadials are illustrated by grey shading and light grey indicates cold sub-events (Rasmussen et al., 2014)

MIS 2 is a period characterized by strong wedge activity, and includes up to 54% of the ages (i.e. 21 dates) of the Northern Aquitaine data set. Both regions record wedging at the beginning and in the middle of Greenland Stadial 2 (GS 2.1) around respectively 17.5 ka (GS 2.1a) and 21 ka (GS 2.1c), and around 24 ka at the end of GS 3. Another cluster is identified at 15.5 ka (late GS 2.1) only in Northern Aquitaine. The absence of this phase of contraction cracking in the Loire valley may be explained as follows:

(1) Sand availability and/or deflation were limited in regions distant from the main coversand areas. However, the reason why this occurred specifically during this period remains hard to explain.

(2) The higher number of ages obtained in Northern Aquitaine allows better precision in the calculation of peaks, which are typified by low FWHM. This highlights the sensitivity of the method used for identifying the major phases of wedge growth to the size of the data set. Further dating will make it possible to improve the representativeness of the identified phases.

A period of widespread thermal contraction cracking which is common to both study areas is also recorded during the end of MIS 3 at approximately 30 ka (GS 5). Older wedge activity is mostly detected in the Loire valley. Clustering of ages appears less obvious, however, and the identified phases have to be considered with caution. The most preeminent phase took place at ~56 ka, i.e. probably at the very end

of MIS 4 taking into account the luminescence dating uncertainties. It is worth noting that a significant number of ages (6 dates) fall within late MIS 5 which was typified on average by a mild climate. PDF analysis suggests that they cluster around ~86 ka, i.e. during the stadial GS 22. As for the early Holocene, this period coincides with a minimum in winter insolation (Berger, 1978).

Although it is not possible to define D_e values for saturated grains, their presence within the investigated wedges is interpreted as reflecting phases of thermal contraction cracking that are beyond the limit of the luminescence dating method on quartz. The saturated grains come from samples that provided the oldest ages, i.e. MIS 8 or 10.

In some wedges (Salaunes, Mérignac and Cussac-Fort-Médoc) the samples taken from the sides of the infilling have yielded older ages than those from the middle. This has to be interpreted as the preferred preservation of early phases of activity in the sides of the wedges.

Comparisons with the records of Northern Europe

The analysis presented here show that the permafrost events previously identified in the loess deposits of northern France were also recorded in the sand wedges and composite wedge pseudomorphs from southwest France and the Loire valley. Particularly, the two main levels of large ice-wedge pseudomorphs dated to 30 and 25 ka in the loess sequences have their counterparts in sand wedges (ca. 30 and 24 ka respectively). Such a synchronicity testifies to widespread events of thermal contraction cracking in France, which are thought to coincide with the last maximum of permafrost extension. Because of the scarcity of available ages, more in detail fitting of the records remains impossible both for older and younger phases. Overall, the number of the phases of wedge development appears to be larger in the sand wedges than in loess. The following factors may be involved:

(1) Poor preservation of ice-wedge pseudomorphs due to thermokarst processes (Locht et al., 2006). Strong pedoturbation at the top of loess sequences during the Holocene may also have obscured or made illegible Late Pleniglacial features.

(2) Lack of permafrost and associated growth of large ice bodies susceptible to produce pseudomorphs. Thermal contraction cracking in the context of deep seasonal freezing of the ground created sand wedges where sand drifting was active, but only tiny fissures elsewhere. This was especially the case for Late

MIS 5 and the Lateglacial.

Using a same approach to that used here on periglacial patterned ground (polygons and stripes) found in East Anglia, UK, Bateman et al. (2014) found similar phases of activity during the last 90 ka at 55–60 ka (MIS 4), 31–35 ka (MIS 3), 20–22 ka (GS2.1c) and 11–12 ka (GS1). However, most of the previous age estimates for sand wedges from northern Europe fall within late MIS 2 and the Lateglacial, i.e. during the main periods of coversand emplacement. In contrast to loess sequences, almost no wedge activity is recorded within late MIS 3 and early MIS 2. In the light of our data, this pattern has to be interpreted as reflecting two main factors: (1) limited record of thermal contraction phases during periods with low sand availability, (2) the use of aliquot and/or CAM analysis for the calculation of age estimates, which led to averaging the signal. This skewed the ages in favour of the most prominent phases of activity and hampered identification of the multiple events of sand wedge growth. Although a few studies in North America have suggested that distinct generations of sand wedges or multi-phased wedges occurred, multiple-dose populations within wedges in Europe (Kolstrup, 2004) or unexpected ages were often attributed to partial bleaching of the sand grains due to sediment mixing and were thus rejected.

Conclusion

The application of single grain OSL to 33 samples taken from sand and composite wedges in France allowed identifying of multi-phased thermal contraction events within single preserved wedge features. FMM analysis identified two to four components for each sample and resulted in the calculation of 86 age estimates, each corresponding to a period of ground cracking. These show that wedges were active during Late Pleistocene cooling periods when thermal contraction and sand drifting in the coversand areas occurred at the same time, i.e. dominantly during MIS 2. Synchronicity between the ages provided by ice-wedge pseudomorphs, sand-wedges and composite-wedges in France testifies to widespread events of thermal contraction cracking between ca. 30 and 24 ka (Last Permafrost Maximum). Late MIS 5 and Early Holocene events also suggest that wedging occurred in connection with deep seasonal ground freezing during phases with marked seasonality. In comparison, the mainly late MIS2 – Younger Dryas ages yielded by North-European sand wedges are interpreted as reflecting poor record of the periods with low sand supply. In addition, the potential averaging issue inherent with the use of aliquots and CAM analysis for the dating of sand-wedges may have biased the ages towards the major phases of

activity and have hampered the identification of multiple periods of opening.

By providing the first chronological framework for thermal contraction cracking in France, this study shows that sand-wedges and composite-wedge pseudomorphs are significant, but complex archives of the Pleistocene periglacial environments. Our results allow reassessing the periglaciation of France and its timing across Western Europe. However, owing to OSL uncertainties more effort in dating is required to improve the accuracy of the identified phases of thermal contraction cracking. The multiplication of study areas in Europe should also make it possible to highlight the latitudinal fluctuations of periglacial processes during the last glacial.

Aknowledgements

This work benefitted from funds provided by the INRAP, the Lascarbx (program of the Agence National de la Recherche ANR-10-LABX-52), the University of Bordeaux, and the UMR-5199 PACEA. EA whishes to aknowledge the department of Geography Univesity of Shefiield whilst a visiting scientist, Mark Bateman, Robert Ashurst and Alicia Medialdea for their assistance in prepraring and dating the samples.

References

Aitken, M.J., 1985. Thermoluminescence dating. Academic Press, Orlando, Florida, 359p.

Andrieux, E., Bertran, P., Saito K., 2016a. Spatial analysis of the French Pleistocene permafrost by a GIS database. Permafrost and Periglacial Processes, 27 (1), 17-30.

Andrieux, E., Bertran, P., Antoine, P., Deschodt, L., Lenoble, A., Coutard, S., 2016b. Database of pleistocene periglacial features in France: description of the online version », Quaternaire, 27/4, 329-339.

Antoine, P., 1988. Contribution à l'étude des loess du Pléistocène supérieur du bassin de la Somme. Revue Archéologique de Picardie 1-2, 25-44.

Antoine, P., 1990. Chronostratigraphie et environnement du Paléolithique du Bassin de la Somme. Publication du centre d'Etude et de Recherches Préhistoriques de Lille (CERP) 2, 231 pp.

Antoine, P., Marchiol, A., Brocantel, M., Gros Y., 2005. *Découverte de structures périglaciaires (*sand-wedges et composite-wedges) sur le site de stockage de déchets radioactifs de l'Aube (France). Comptes Rendus Géosciences, 337 (16), 1462-1473.

Antoine, P., Goval, E., Jamet, G., Coutard, S., Moine, O., Hérisson, D., Auguste, P., Guérin, G., Lagroix,

F., Schmidt, E., Robert, V., Debenham, N., Meszner, S., Bahain, J.J., 2014. Les séquences Loessiques Pléistocène supérieur d'Havrincourt (Pas-de-Calais, France) : stratigraphie, paléoenvironnements, géochronologie et occupations paléolithiques. Quaternaire, 4, p. 321-368.

Antoine, P., Locht, J.L., 2015. Chronostratigraphie, paléoenvironnements et peuplements au Paléolithique moyen : les données du nord de la France. Mémoire de la Société Préhistorique Française , 59 , 11-23.

Antoine, P., Moncel, M.H., Locht, J.L., Limondin-Lozouet, N., Auguste, P., Stoetzel, E., Dabkowski, J., Voinchet, P., Bahain, J.J., Falgueres, C., 2015. Dating the earliest human occupation of Western Europe: New evidence from the fluvial terrace system of the Somme basin (Northern France). Quaternary International, 370, 77-99.

Arnal, H., 1971. Les sols polygonaux étirés et sols striés d'âge würmien de Laudun (Gard). Bulletin de l'Association Française pour l'Etude du Quaternaire, 8 (3), 151-160.

Bailey, R.M., Arnold, L.J., 2006. Statistical modelling of single grain quartz De distributions and an assessment of procedures for estimating burial dose. Quaternary Science Reviews, 25, 2475-2502.

Bateman, M.D., 2008. Luminescence dating of periglacial sediments and structures: a review. Boreas 37, 574-588.

Bateman, M.D., Boulter, C.H., Carr, A.S., Frederick, C.D., Peter, D., Wilder, M., 2007. Preserving the palaeoenvironmental record in Drylands: Bioturbation and its significance for luminescence derived chronologies. Sediment Geology, 195, 5-19.

Bateman, M.D., Hitchens, S., Murton, J.B., Lee, J.R., Gibbard, P.L., 2014. The evolution of periglacial patterned ground in East Anglia, UK. Journal of Quaternary Science, 29, 301–317.

Bateman, M.D., Murton, J.B., Boulter, C., 2010. The source of De variability in periglacial sand wedges: Depositional processes versus measurement issues. Quaternary Geochronology, 5, 250-256.

Bell, W.T., 1980. Alpha attenuation in Quartz grains for Thermoluminescence Dating. Anc. TL 12, 4-8.

Berger, A., 1978. Long-term variations of daily insolation and Quaternary climatic changes. J. Atmos. Sci., 35(12), 2362–2367.

Bertran, P., Bateman, M., Hernandez, M., Lenoir, M., Mercier, N., Millet, D., Tastet, J.P., 2011. Inland aeolian deposits of southwest France: facies, stratigraphy and chronology, Journal of Quaternary Science, 26, 374-388.

Bertran, P., Andrieux, E., Antoine, P., Coutard, S., Deschodt, L., Gardère, P., Hernandez, M., Legentil, C., Lenoble, A., Liard, M., Mercier, N., Moine, O., Sitzia, L., Van Vliet-Lanoë, B., 2014. Distribution and chronology of Pleistocene permafrost features in France: database and first results. Boreas, 43 (3), 699-711.

Böse, M., 1992: Late Pleistocene sand-wedge formation in the hinterland of the Brandenburg stade. Sveriges Geologiska Undersökning Series Ca 81, 59-63

Böse, M., 2000. Gravel analysis of Weichselian tills and OSL dates of sand wedges in western Poland. Quaestiones Geographicae 21, 39-44.

Bøtter-Jensen, L., Andersen, C.E., Duller, G.A.T., Murray, A.S., 2003. Developments in radiation, stimulation and observation facilities in luminescence measurements. Radiation Measurement 37, 535-541.

Bouteyre G., Allemann M., 1964. Sur quelques phénomènes périglaciaires en Costières du Gard. Un réseau polygonal de fentes en coin. Bulletin de la Société des Sciences Naturelles de Nimes L, 84-96.

Briant, R.M., Bateman, M.D., Russell Coope, G., Gibbard, P.L., 2005. Climatic control on Quaternary fluvial sedimentology of a Fenland Basin river, England. Sedimentology, 52, 1397-1423.

Bronk Ramsey, C., Lee, S., 2013. Recent and Planned Developments of the Program OxCal. Radiocarbon, 55(2-3), 720-730.

Buylaert, J.P., Ghysels, G., Murray, A.S., Thomsen, K.J., Vandenberghe, D., De Corte, F., Heyse, I., Van den Haute, P., 2009. Opticla dating of relict sand wedges and composite-wedge pseudomorphs in Flandders, Belgium. Boreas, 38, 160-175.

Christiansen, H.H., 1998. Periglacial sediments in an Eemian–Weichselian succession at Emmerlev Klev, southwestern Jutland, Denmark. Palaeogeography, Palaeoclimatology, Palaeoecology 138, 245–258.

Deschodt, L., Djemmali, N., Drwila, G., Feray, P., Teheux, E., 1998. Onnaing (59), usine Toyota. 62 pp. Rapport des sondages archéologiques profonds, Inrap, Amiens.

Duller, G.A.T., 1992. Luminescence Chronology of Raised Marine Terraces, South-West North Island, New Zealand. PhD thesis. University of Wales, Aberystwyth.

Duller, G.A.T., 2003. Distinguishing quartz and feldspar in single grain luminescence measurements. Radiation Measurements 37, 161-165

Duller, G.A.T., Bøtter-Jensen, L., Murray, A.S., Truscott, A.J., 1999. Single grain laser luminescence (SGLL) measurements using a novel automated reader. Nuclear Instruments and Methods in Physics Reseach B 155, 506-514.

Fàbiàn, S.A., Kovàcs, J., Varga, G., Sipos, G., Horvàth, Z., Thamo_Bozso, E., Toth, G., 2014. Distribution of relict permafrost features in the Pannonian Basin, Hungary. Boreas, Vol. 43, pp. 722-732.

Feray, P., 2009. Feignies (59), « Les Mottes », « Queue Bizenne » et « Grand Bray » : Extensio ‘’

Frechen, M., Van Vliet-Lanoë, B., Van den Haute, P., 2001. The Upper Pleistocene loess record at Harmignies/Belgium - High resolution terrestrial archive of climate forcing. Palaeogegraphy, Palaeoclimatology, Palaeoecology 173, 175-195.

Galbraith, R.F., Green, P.F., 1990. Estimating the component ages in a finite mixture. International Journal of Radiation Applications and Instrumentation. Part D. Nuclear Tracks and Radiation Measurements 17, 197-206.

Galbraith, R.F., Laslett, G.M., 1993. Statistical models for mixed fission track ages. Nuclear Tracks and Radiation Measurements 21, 459-470.

Galbraith, R.F., Roberts, R.G., Laslett, G.M., Yoshida, H., Olley, J.M., 1999. Optical dating of single and multiple grains of quartz from Jinmium Rock Shelter, Northern Australia: Part I, Experimental design and statistical models. Archaeometry 41, 339-364.

Guérin, G., Mercier, N., Adamiec, G., 2011. Dose-rate conversion factors: update. Anc.TL, 29, 5-8

Guhl, A., Bertran, P., Fitzsimmons, K.E., Zielhofer, C., 2013. Optically stimulated luminescence (OSL) dating of sand-filled wedges structures and their alluvial host sediments from Jonzac, SW France. Boreas 42, 317-332.

Huijzer, B., Vandenberghe, J., 1998. Climatic reconstruction of the Weichselian Pleniglacial in northwestern and central Europe. Journal of Quaternary Science, 13(5), 391–417.

Isarin, R., Huijzer, B., van Huissteden, K., 1998. Time-slice oriented multiproxy database (MPDB) for palaeoclimatie reconstruction. National Snow and Ice Data Center, University of Boulder, Colorado. http://nsidc.org/data/ggd248.html

Kadereit, A., Kind, C.J., Wagner, G.A., 2013. The chronological position of the Lohne Woil in the Nussloch loess section – re-evaluation for a European loess-marker horizon. Quaternary Science Reviews 59, 67-89.

Kasse, C., 2002. Sandy aeolian deposits and environments and their relation to climate during the Last Glacial Maximum and Lateglacial in northwest and central Europe. Progress in Physical Geography 26, 4, 507-532.

Kasse, C., Vandenberghe, J., 1998. Topographic and drainage control on Weichselian ice-wedge and sand-wedge formation, Vennebrügge, German–Dutch border. Permafrost and Periglacial Processes 9, 95–106.

Kasse, C., Vandenberghe, J., de Corte, F., van den Haute, P., 2007. Late Weichselian fluvio-aeolian sands and coversands of the type locality Grubbenvorst (southern Netherlands): sedimentary environments, climate record and age. Journal of Quaternary Science 22, 7, 695–708.

Kjaer, K.H., Lagerlun, E., Adrielsson, L., Thomas, P.J., Murray, A., Sandgren, P., 2006. The first independent chronology of Middle and Late Weichselian sediments from southern Sweden and the island of Bornholm. GFF, 128, 209-220.

Kolstrup, E., 2004. Stratigraphic and Environmental Implications of a large ice-wedge cast at Tjaereborg, Denmark. Permafrost and Periglacial Processes, 15, 31-40.

Kolstrup, E., 2007. OSL dating in palaeoenvironmental reconstructions. A discussion from a user's perspective. Estonian Journal of Earth Sciences, 56, 157-166.

Kolstrup, E., Mejdhal, V., 1986. Three frost wedge casts from Jutland (Denmark) and TL dating of their infill. Boreas 15, 311-321.

Kovàcs, J., Fàbiàn, S.A., Schweitzer, F., Varga, G., 2007. A relict sand-wedge polygon site in north-central Hungary. Permafrost and Periglacial Procecesses. 18, 379-384.

Kreutzer, S., Lauer, T., Meszner, S., Krbetschek, M.R., Faust, D., Fuchs, M., 2012. Chronology of the Quaternary profile Zeuchfeld in Saxony-Anhalt / Germany – a preliminary luminescence dating study. Zeitschrift für Geomorphologie fast track, 1–21.

Lautridou, J.P., 1985. Le cycle périglaciaire pléistocène en Europe du nord-ouest et plus particulièrement en Normandie. Thèse d'Etat, Université de Caen, 487 pp.

Lécolle, F., 1989. Le cours moyen de la Seine au Pléistocène moyen et supérieur. Thèse, Caen et Université de Rouen, 549 pp.

Lenoble, A., Bertran, P., Mercier, N., Sitzia L., 2012. Le site du Lac Bleu et la question de l'extension du pergélisol en France au Pléistocène supérieur. Quaternaire continental d'Aquitaine : un point sur les travaux récents. Livret-guide de l'excursion AFEQ-ASF 2012, Université de Bordeaux, AFEQ, 107-121.

Locht, J. L., Antoine, P., Auguste, P., Bahain, J.J., Debeham, N., Falguères, C., Farkh, S., Tissoux, H., 2006. La séquence lœssique Pléistocène supérieur de Savy (Aisne, France): stratigraphie, datations et

occupations paléolithiques. Quaternaire, 17, 269–275.

Maarleveld, G.C., 1976. Periglacial phenomena and the mean annual air temperature during the last glacial time in The Netherlands. Biuletyn Periglacjalny, 26, 57–78.

Mackay, J.R., 1993. Air temperature, snow cover, creep of frozen ground, and the time of ice-wedge cracking, western Arctic coast. Canadian Journal of Earth Sciences, 30 (8), 1720-1729.

Mejdhal, V., 1979. Thermoluminescence dating: Beta-dose attenuation in quartz grains. Archaeometry 21, 61-72.

Meszner, S., Kreutzer, S., Fuchs M., Faust, D., 2013. Late Pleistocene landscape dynamics in Saxony, Germany: Paleoenvironmental reconstruction using loess-paleosol sequences. Quaternay International, 296, 94-107.

Michel, J. P., 1969. Divers types de phénomènes périglaciaires et leur répartition dans les alluvions quaternaires de la Seine et de ses affluents. Supplément du Bulletin de l'Association Française pour l'Etude du Quaternaire 2, 721-735.

Michel, J.P., 1975. Périglaciaires des environs de Paris. Biuletyn Peryglacjalny, 24, 259-352.

Moine, O., Antoine, P., Deschodt, L., Sellier-Segard, N., 2011. Enregistrements malacologiques à haute résolution dans les loess et les gleys de toundra du Pléniglaciaire weichsélien supérieur: premiers exemples du nord de la France. Quaternaire 22, 307-325.

Murray, A.S., Wintle, A.G., 2000. Luminescence dating of quartz using an improved single- aliquot regenerative-dose protocol. Radiation Measurements 32, 57-73.

Murray, A.S., Wintle, A.G., 2003. The single aliquot regenerative dose protocol: Potential for improvements in reliability. Radiation Measurements, 37, 377-381.

Murton, J.B., 2013. Permafrost and Periglacial Features. Ice Wedges and Ice-Wedge Casts. In Encyclopedia of Quaternary Science (Second Edition), Elsevier, Amsterdam, 436-451.

Murton, J.B., Worsley, P., Gozdzik, J., 2000. Sand veins and wedges in cold Aeolian environments. Quaternary Science Reviews, 19 (9), 899-922.

Olley, J., Caitcheon, G., Murray, A., 1998. The distribution of apparent dose as determined by optical stimulated luminescence in small aliquots of uvial quartz: Implications for dating young sediments. Quaternary Geochronology, 17, 1033-1040.

Péwé, T.L., 1966. Palaeoclimatic significance of fossil ice wedges. Biuletyn Peryglacjalny, 5, 65-72.

Ponel, P., Gandouin, E., Russell Coope, G., Andrieu-Ponel, V., Guiter, F., Van Vliet-Lanoë, B., Franquet, E., Brocandel, M., Brulhet, J., 2007. Insect evidence for environmental and climate changes from Younger Dryas to Sub-Boreal in a river floodplain at St-Momelin (St-Omer basin, northern France), Coleoptera and Trichoptera. Palaeogepgraphy, Palaeoclimatology, Palaeoecology 245, 483-504.

Prescott, J.R., Hutton, J.T., 1994. Cosmic-ray contributions to dose-rates for luminescence and ESR dating – Large depths and long-term time variations. Radiation Measurements 23, 497-500.

Rasmussen, S. O., Bigler, M., Blockley, S. P., Blunier, T., Buchardt, S. L., Clausen, H. B., Cvijanovic, I., Dahl-Jensen, D., Johnsen, S. J., Fischer, H., Gkinis, V., Guillevic, M., Hoek, W. Z., Lowe, J. J., Pedro, J., Popp, T. J., Seierstad, I. K., Steffensen, J. P., Svensson, A., Vallelonga, P. T., Vinther, B. M., Walker, M. J. C., Wheatley, J. J, Winstrup, M., 2014. A stratigraphic framework for abrupt climatic changes during the

Last Glacial period based on three synchronized Greenland ice-core records: refining and extending the INTIMATE event stratigraphy. Quaternary Science Reviews, 106, pp 14-28.

Readhead, M.L., 2002. Absorbed dose fraction for 87Rb beta particles. Anc. TL 20, 25-29.

Renssen, H., Isarin, R.F.B., 1998. Surface temperature in NW Europe during the Younger Dryas: AGCM simulation compared with climate reconstructions. Climate Dynamics, 14, 33-44.

Roberts, R.G., Galbraith, R.F., Yoshida, H., Laslett, G.M., Olley, J.M., 2000. Distinguishing dose populations in sediment mixtures: a test of optical dating procedures using mixtures of laboratory-dosed quartz. Radiation Measurements, 32, 459-465.

Sellier, N., Coutard, S., 2007. Données récentes sur le Paléolithique moyen de l'Aisne : une occupation du Weichselien ancien à Courmelles. Revue archéologique de Picardie 3-4, 5-16.

Sommé, J., Tuffreau., A., 1971. Stratigraphie du Pléistocène récent et Moustérien de Tradition Acheuléenne à Marcoing (Cambresis – nord de la France). Bulletin de l'Association Française pour l'Etude du Quaternaire 2, 57-74.

Simonis, D., Hense, A., Litt, T., 2012. Reconstruction of late Glacial and Early Holocene near surface temperature anomalies in Europe and their statistical interpretation. Quaternary International, 274, 233-250.

Sitzia, L., Bertran, P., Bahain, J.J., Bateman, M.D., Hernandez, M., Garon, H., De Lafontaine, G., Mercier, N., Leroyer, C., Queffelec A., Voinchet, P., 2015. The quaternary coversands of southwest France. Quaternary Science Reviews, 124, 84-105.

Tricart, J., 1956. Carte des phénomènes périglaciaires quaternaires en France. Mémoire pour servir à l'explication de la carte géologique détaillée de la France. Ministère de l'Industrie et du Commerce: Paris.

Vandenberghe, D., De Corte, F., Buylaert, J.-P., Kucera, J., Van Den Haute, P., 2008. On the internal radioactivity in quartz. Radiation Measurements, 43, 771-775.

Vandenberghe, J., 1983. Ice-wedge casts and involutions as permafrost indicators and their stratigraphic position in the Weichselian. Proceedings of the 4th International Conference on Permafrost, Fairbanks, Alaska, 1, 1298-1302.

Vandenberghe, J., French, H., Gorbunov, A., Marchenko, S., Velichko, A.A., Jin, H., Cui, Z., Zhang, T., Wan, X., 2014. The Last permafrost Maximum (LPM) map of the Northern Hemisphere: permafrost extent and mean annual air temperatures, 25-17 ka. Boreas, 43, 652–666.

Van Vliet-Lanoë, B., Hallégouët, B., 2001. European permafrost at the LGM and at its maximal extent. The geological approach. In Permafrost Response on Economic Development, Environmental Security and Natural Resources, Paepe R, Melnikov V (eds). Kluwer Academic Publishers: Dordrecht, 195–213.

Wanner, H., Solomina, O., Grosjean, M., Ritz, S.P., Markéta, J., 2011. Structure and origin of Holocene cold events. Quaternary Science reviews, 30, 3109-3123.

Williams, R.B.G., 1968. Periglacial climate and its relation to landforms: a study of southern and eastern England during the Last Glacial Period. PhD Thesis, University of Cambridge.

Wojdyr, M.J., 2010. Fityk: a general-purpose peak fitting program. Journal of Applied Crystallography 43, 1126-1128.

Wolfe, S.A., Morse, P.D., Kokelj, S.V., Neudorf, C.M., Lian, O.B., 2016. Contrasting environments of

sand wedge formation in discontinuous permafrost, Great Slave High Boreal Plains, Northwest Territories, Canada. Abstracts, 11th international conference on permafrost, 20-24 June 2016, Potsdam, Germany, 112.

Appendix

Step	Treatment
1	Give dose*
2	Pre-heat (160-220°C for 10s, heating at a rate of 2°C/s)
3	Stimulation of single grains with green laser light (90% power) for 1s at 125°C
4	Test dose
5	Cut-heat (160°C for 0s, heating at a rate of 2°C/s)
6	Stimulation of single grain with green laser light (90% power) for 1s at 125°C
7	Return to step 1

Table S1: The Single-Aliquot Regenerative-dose (SAR) protocol used in this study. * The final dose given is equal to the first regeneration dose allowing the calculation of a recycling ratio. The third or fourth regeneration point is always 0 Gy allowing recuperation to be observed.

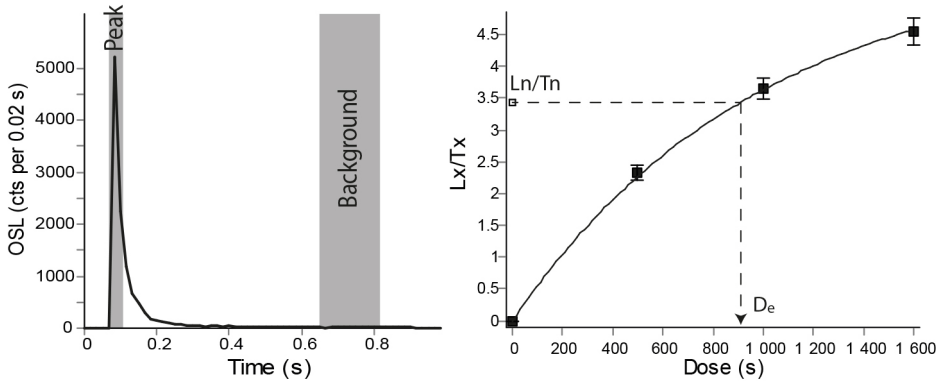

Figure S1: Single-aliquot regenerative dose (SAR) OSL decay curves and dose response curves for a single grain of sample Shfd14022. The used signal and background intervals are highlighted in grey.

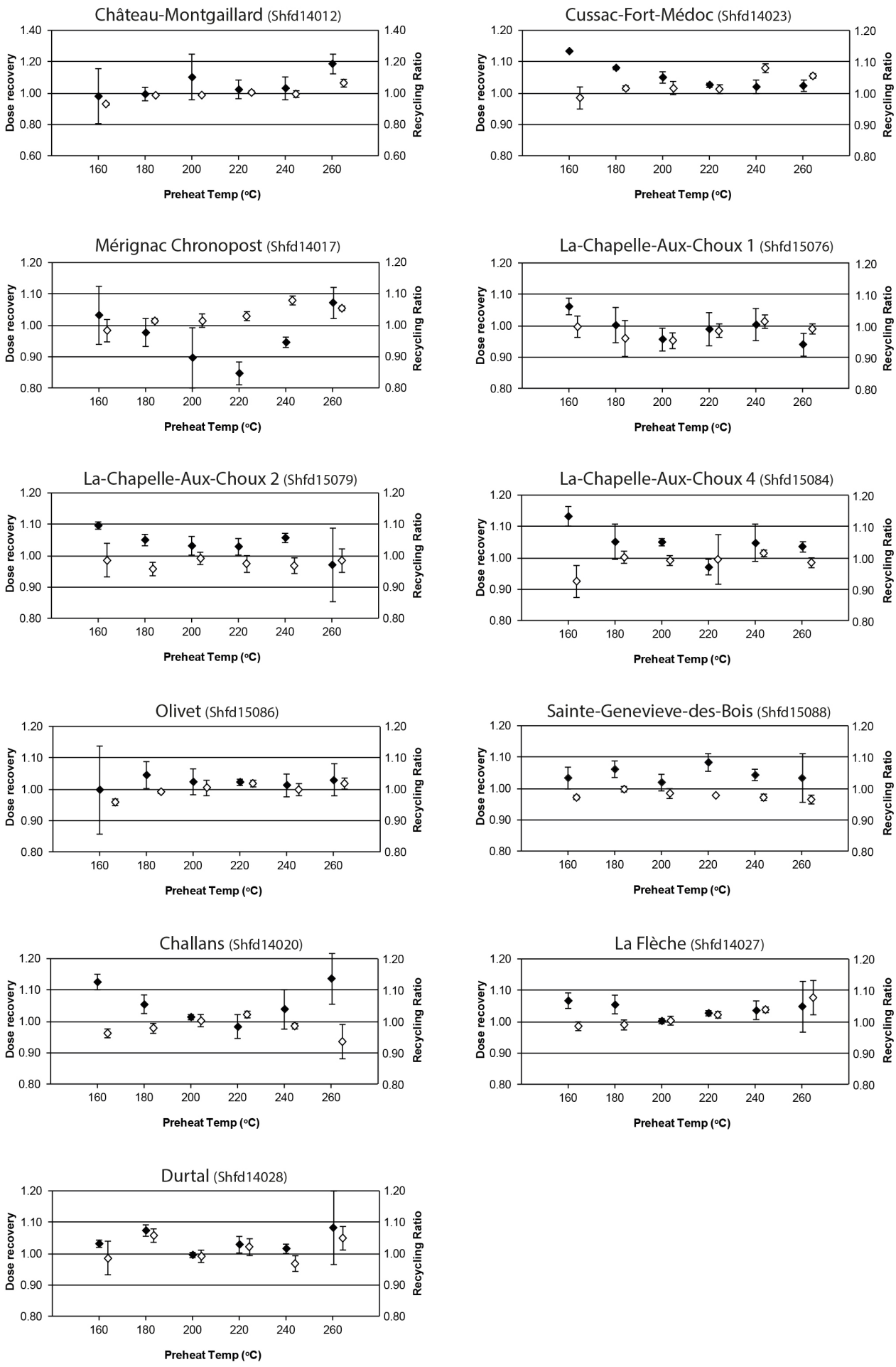

Figure S2: Dose-recovery preheat plateau test performed on three small aliquots at each temperature. The average values of the dose recovery (black) and the recycling ratio (white) are presented with standard deviation. The solid line indicates the ideal values.

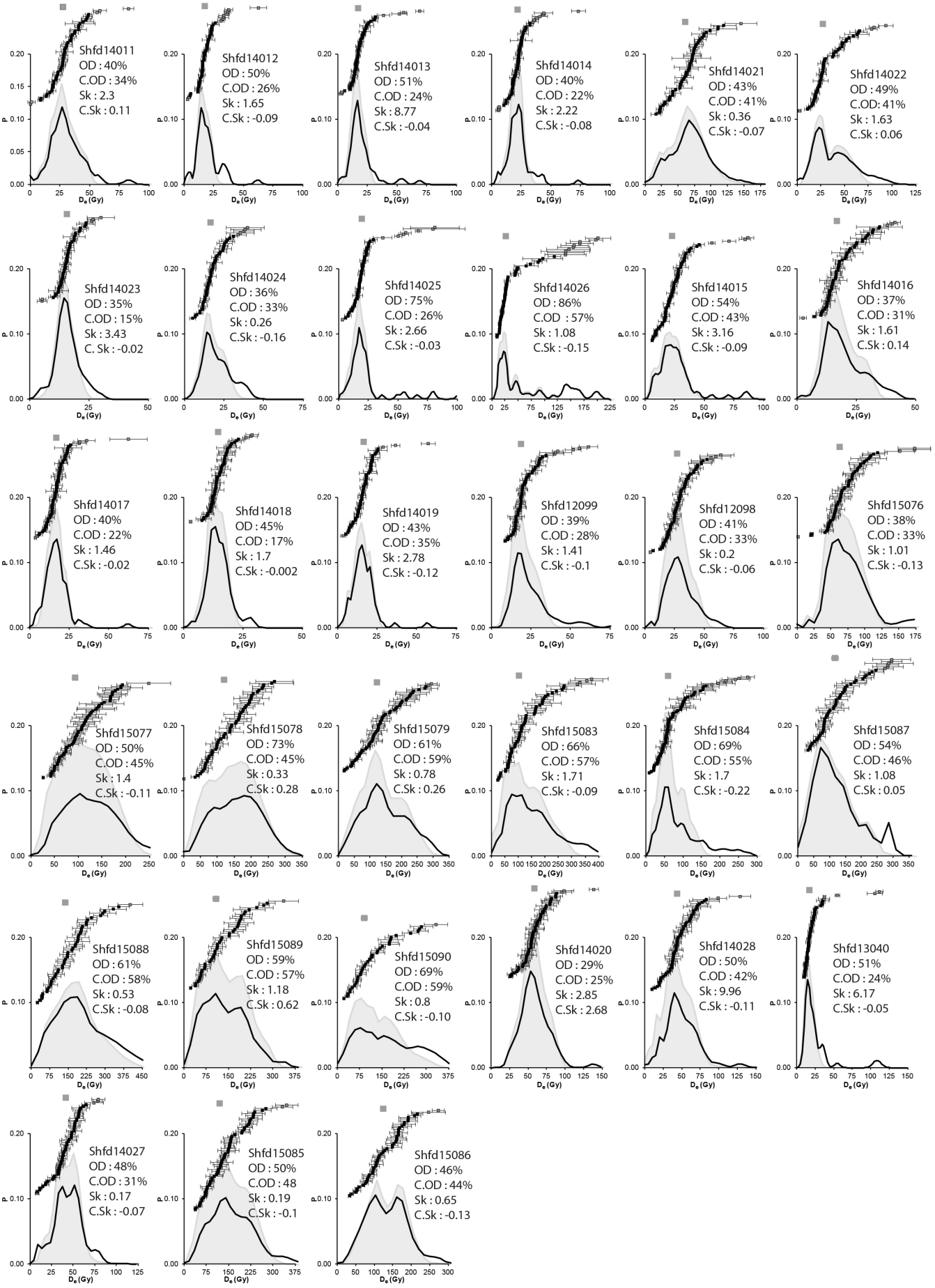

Figure S3: Probability density functions (pdf, solid line) plotted for all samples with the individual grain results above (Black) and mean (dark grey) compared with the pdf (grey filled curv) of the same data without outliers. Overdispersion values (OD), and OD without outliers (C.OD) were calculated as per Galbraith et al., (1999), skewness (Sk) and Sk without outliers (C.Sk) as per Bailey and Arnold (2006).

7. Synthesis

At the start of our study on the extent and chronology of the Late Pleistocene permafrost in France, the already existing reconstructions based on field evidence showed that large parts of France were affected by permafrost during the Late Pleistocene and attributed its maximum extent to the Last Glacial Maximum (LGM). However, the discrepancies between the overviews that were done for almost a century highlighted that the occurrence of certain features gave rise to different interpretations. The different overviews, produced from periglacial field evidence, highlight the poor agreement of the scientific community on the palaeoclimatic significance of certain periglacial features. In addition, the chronological framework used for the different reconstructions was mostly based on relative ages and/or on the assumption that the coldest period of the Pleistocene was reached during the LGM. In this context, it was critical to re-evaluate the field evidence of periglaciation in France to the light of the present knowledge and to look for new datable features. The approach developed to solve these issues was divided into three parts. First of all, it was necessary to provide a homogenised and easy to access dataset of features that would allow a site or an occurrence of periglacial features to be placed in a broader regional context. This will avoid the pitfalls of simplistic local environmental interpretations, and instead, will make it possible to provide a more accurate regional synopsis. This has led to the creation of the database of the French periglacial features that compiles data from cross-sections, i.e. relict sand-wedges, ice-wedge pseudomorphs, composite-wedge pseudomorphs, and data from aerial photographs, i.e. polygonal networks and soil stripes. Other patterned ground such as small nets, thermokarst, and involutions in cross-section will be added in the future. This database is available online at https://afeqeng.hypotheses.org/48. The second part of our work aimed at processing the gathered data. GIS-based analysis gave us information on the influence of different factors on the development of periglacial features. Comparison with a dataset from northern Europe made it possible to propose a new map of the permafrost boundaries based on field evidence in Western Europe. The map was then compared with an improved set of modelled permafrost distributions to delineate the issues in the reconstruction methods. Finally the third part of the thesis provides the first chronological framework for thermal contraction cracking in France that relies on OSL dating of sand-wedges.

7.1. Geographical extent of periglacial features in France

The distribution of the identified features clearly indicates that large areas in France were affected by periglacial phenomena, apart from the south-westernmost part of France and the Languedoc that are

the only regions free of periglaciation evidence. The relict features are mainly located in sedimentary basins, and particularly in Early to Middle Pleistocene alluvial deposits.

Ice-wedge pseudomorphs are only found north of 47°N, preferably on poorly drained flat terrains. Their occurrence proves that the regions where these features are found were affected by at least widespread discontinuous permafrost during the Pleistocene, in environments similar to those actual where regional MAATs are lower than or equal to -4 to -5°C. The distribution of ice-wedge pseudomorphs correlates strongly with that of loess deposits. However, their absence below 47°N cannot be explained only by difficulties in identifying secondary infillings in more heterogeneous materials, and rather shows that the growth of large ice bodies was not possible south of 47°N. The composite-wedge pseudomorphs that have been described below this latitude have small secondary infillings which suggest that at least locally ice veins formed at lower latitudes, but probably during exceptionally cold winters.

Relict epigenetic sand wedges are mainly located between 47 and 43.5°N in the vicinity of coversands in the Loire valley, Northern Aquitaine and Provence. GIS analysis shows that they are mostly present in well-drained terrains, often times at a higher altitude than the surroundings terrains. Interpretations of their presence is more controversial since in modern environments they are rare, and were mainly described in very dry areas within continuous permafrost where thermal contraction cracking is associated with sand drifting (e.g. Antarctica; Bockheim et al., 2009). This has led many researchers to consider that these particular features formed only under continuous permafrost, and outside misinterpretations of features it is probably the main reason behind the contradictory reconstructions of past permafrost that have been made in France. However, in the Pleistocene context that is characterised by greater aridity at mid-latitudes and the extension of cold deserts, we proposed that these features should only be used to infer the boundaries of thermal contraction cracking since the sand availability was more important than in modern arctic milieus. This is particularly relevant in France when considering the location of sand-wedges that are mostly on the margins of coversands and where old sandy formations are cropping out. Thermal contraction cracking occurs in current environments in areas that undergo deep seasonal freezing of the ground or permafrost where MAATs are lower or equal to -1/0°C (Washburn et al., 1963; Friedman et al., 1971) and up to 2°C in hyper-continental areas (Romanovskij, 1976). According to observations in the Canadian Arctic, cracking is favoured by sharp temperature drops and a mean thermal gradient in the active layer higher than ca. -10°C/meters (Fortier and Allard, 2005). The recent discovery of active sand-wedges in areas subject to deep seasonal freezing of the ground (Wolffe et al., 2016) supports our assumption.

Since ice-wedge pseudomorphs are indicative to at least widespread discontinuous permafrost, it was expected to find features that form in similar conditions in northern France. Possible examples of pingo and lithalsa scars were described in the literature, but the lack of description and observation in cross-section made their classification as cryogenic mounds difficult (Michel, 1967; Lécolle, 1998) and the origin of many depressions has been reinterpreted as karstic (Boyé, 1958; Courbouleix and Fleury, 1996; Texier, 2011; Becheler, 2014). Recently, ductile and brittle deformations that may result from the development of an open-system pingo and thermokarst have been observed in Pleistocene alluvial deposits at Gourgançon (France) (Van Vliet-Lanoë et al., 2016; Jolivel et al., 2016). In addition, the aerial photographs and the Digital Elevation Model (DEM) of the area revealed rounded depressions in alluvial deposits that could correspond to thermokarstic features (Figure 27). Erosion events in loess sequences that are characterized in the sediment by lateral undercutting are also described in the literature and are thought to be of thermokarstic origin (Antoine et al., 2001; Antoine et al., 2008). In northern France, two main thermokarst events were identified in the Villiers-Adam loess sequence at the base and the top of the Middle pleniglacial. These events suggest rapid thawing of permafrost and are interpreted as a potential marker for Dansgaard-Oeschger events (Antoine et al., 2013). Similar features were identified in other parts of northern France in aerial photographs (Figure 28), their identification and dating could potentially provide data to better constrain extreme cold phases.

No closed-system pingo scar has been observed in France. In modern environment, these features are limited to continuous permafrost, i.e. at MAATs lower than -6/-8°C. Based on our current state of knowledge, there is no evidence showing that continuous permafrost has affected France.

Most of small nets and soil stripes are located at latitude greater than 47°N, which corresponds to the southern boundary of ice-wedge pseudomorphs, and can therefore be interpreted as deformations of an active layer on permafrost. Cross-sections in areas covered by small nets showed involutions. Their origin is controversial since periglacial processes and earthquakes can form similar features (Jolivel et al., 2016). However, Bertran et al. (submitted) show that there is no clear relationship between their distribution and known faults and the earthquakes listed in available databases, which suggest mostly a periglacial origin. No correlation has been found between the size of the polygons, which are interpreted as networks of thermal contraction cracks, and other parameters such as ground composition. The average polygon diameter rather suggests that the polygons in France reached a steady-state after their subdivision during multiple or long periods of activity.

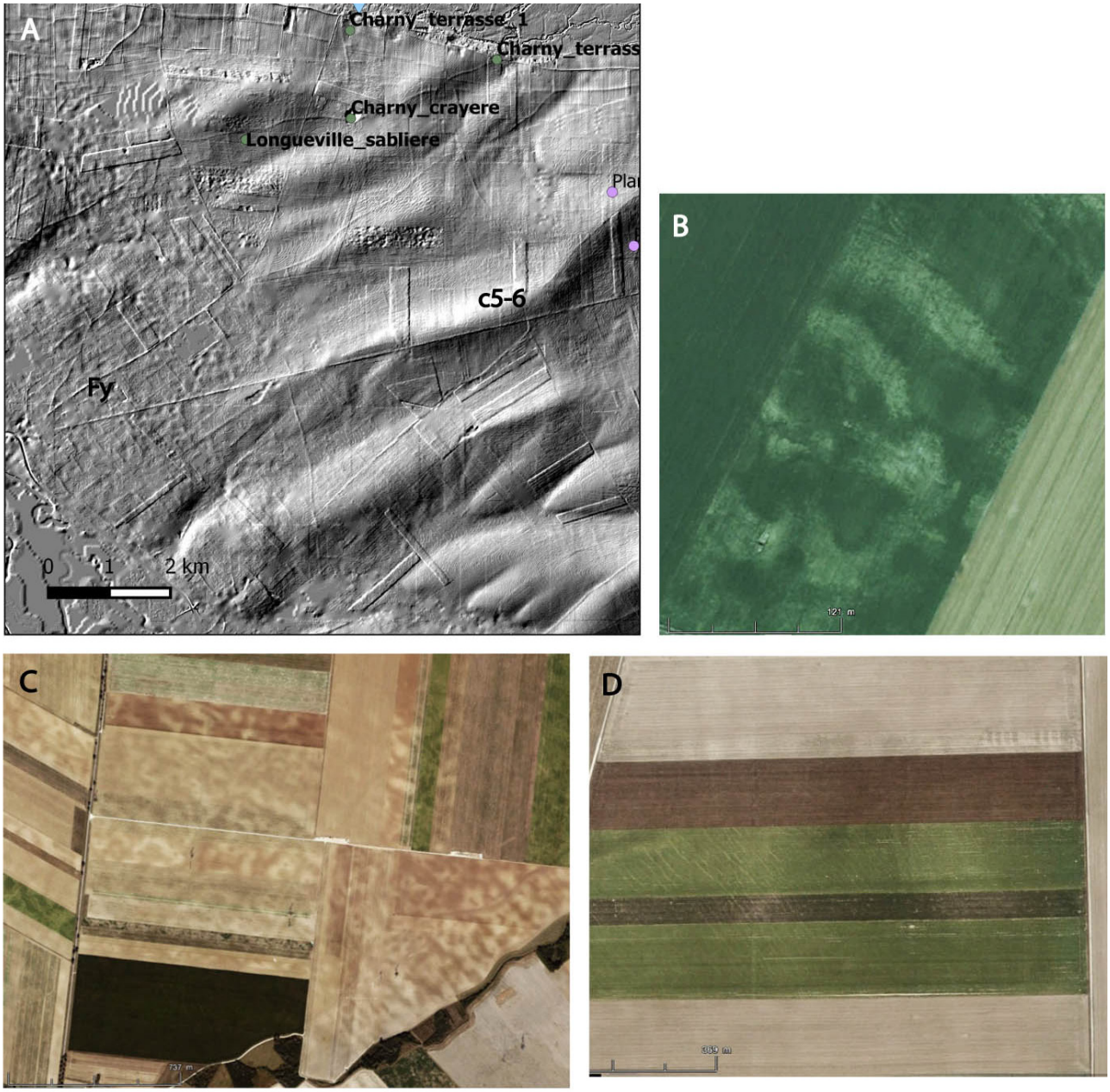

Figure 27: Features visible in aerial photographs near Gourgançon - Charny-le-Bachot; A - DEM with a 5m resolution show depression in the alluvial deposits; B, C - aerial photographs of the depression visible in the alluvial deposits, potentially of thermokarstic origin.; D - soil stripes are visible in the same area on a slope

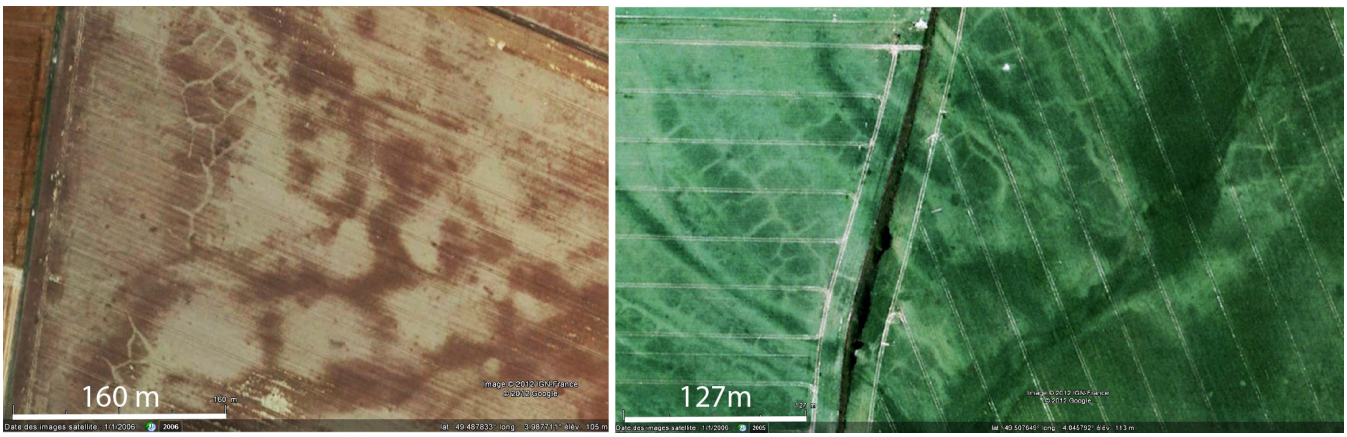

Figure 28: Potential thermokarst in Northern France (Sissonne, 49.5°N, 4°E)

The permafrost extent that is inferred from these results is in line with data on western European deep aquifers that show an uninterrupted recharge even during the coldest periods of the Late Pleistocene in most part of France (Jirakova et al., 2011; Saltel et al., 2016), and in agreement with previous 'warmer' reconstructions made, e.g. Lautridou and Sommé (1981) or Huijzer and Vandenberghe (1998). Climatic simulations still show, however, discrepancies between field data and the reconstructed extent of permafrost (Saito et al., 2013; Andrieux et al., 2016b). The reasons for such a difference is not fully assessed, but can partly be explained by a time lag between the LGM (21 ka) used for modelling and the LPM (31-24 ka), or by a warm winter bias of the models as already noticed by Kageyama et al. (2006).

7.2. Chronological framework

The chronological data available to define the chronology of periglaciation in France is scarce because periglacial features have rarely been dated.

In the loess deposits of northern France, six main levels of ice-wedge pseudomorphs have been described. To the exception of a few OSL bracketing ages, the researchers often rely on correlations between different cross-sections to provide the relative ages of the features. The levels of ice-wedge pseudomorphs show a complex formation history during the Late Pleistocene with multiple periods of permafrost aggradation and degradation. This differs from the ages of sand-wedges obtained in Northern Europe that in contrary suggest a main phase of activity during the Late Pleniglacial. The few French sand-wedges that were already dated not only yielded older estimates than those in Northern Europe, but also showed that several wedges belonging to the same polygonal network gave different ages. These results suggested that sand-wedge growth was asynchronous and controlled by local conditions rather than global. However, recent luminescence dating in Canada demonstrated that multiple paleodose populations within sand-wedges could be the result of multiple periods of activity. Further research was needed to firmly establish whether it was the case or not. Investigating the French sand-wedges gave that opportunity, and allowed us to provide the first chronological framework for thermal contraction cracking in France.

Three areas were surveyed in order to sample sand-wedges, namely the northern Aquitaine, the Loire valley and the lower Rhone valley. These regions were in the vicinity of coversand or alluvial sand that could have provided sufficient aeolian sand for the growth of sand-wedges during the Pleistocene. The survey of the lower Rhone valley did not provide features to be sampled, but 17 samples were

taken from 5 wedges in Northern Aquitaine and 16 samples from 8 wedges in the Loire valley. The application of single grain OSL to the collected samples allowed multi-phased thermal contraction events within each wedge to be identified. The 86 calculated age estimates cluster around 11 periods of wedge activity during the Late Pleistocene, which is more in line with the apparent number of ice-wedge pseudomorph events. Wedges were active during most Late Pleistocene cooling periods when thermal contraction cracking was concomitant with sand drifting. Most of thermal contraction activity, let it be for ice-wedges or sand-wedges, occurred between ca. 30 and 24 ka which likely corresponds to the Last Permafrost Maximum. More surprisingly it appears that wedging occurred also during Late MIS 5 and the Early Holocene, for which other proxies (e.g. beetles, pollens) clearly indicate that MAATs were too high for permafrost to develop. These periods are characterized by low winter insolation causing a strong seasonality and subsequent deep seasonal freezing of the ground. Sand-wedges were able to form in this context which supports the assumption that they have formed outside permafrost during the Pleistocene.

Previous dating obtained on sand-wedges fall mainly during the MIS 3/2 in northern Aquitaine and late MIS 2 - Younger Dryas in northern Europe. This correlates well with the main phases of coversand emplacement in both areas, and reflect a poor record in the wedges of the periods with low sand supply. Since averaging methods were used for the dating, the estimates are probably biased towards the most prominent phases of wedging, which hampers the identification of multiple periods of activity.

7.3. Outlook and future prospects

The ongoing acquisition of data on periglacial features and the mapping of their distribution across Europe are necessary. Approximate zones sharing similar climatic conditions during the LGM were defined by K. Saito using MAATs given by the Global Climate Models (GCMs) involved in the Paleoclimate Model Intercomparison Project (PMIP3) (Figure 29; Jolivel et al., 2016; Saito et al., 2013). The resultant maps potentially highlight areas that were affected by similar periglacial processes, which can ease the finding of periglacial features.

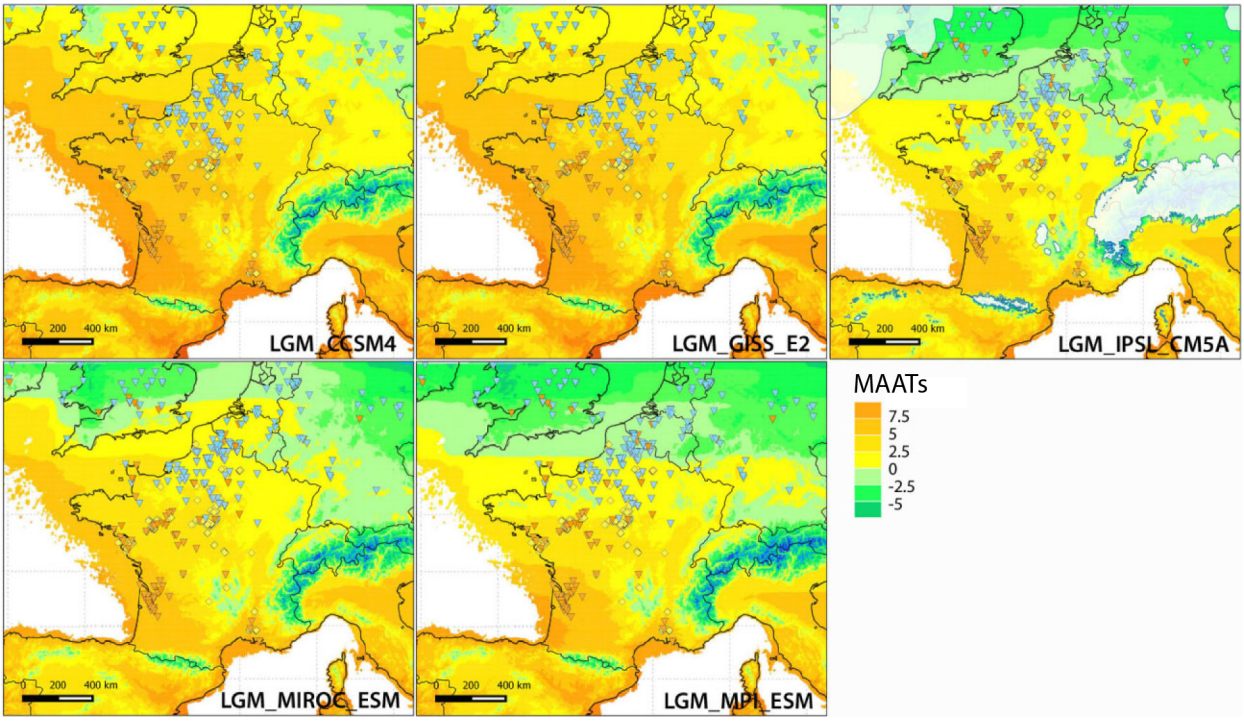

Figure 29: Simulations of the Mean Annual Air Temperatures (MAATS) from the different Global Climate Models (GCMs) (source K. Saito; Jolivel et al., 2016), in comparison with the distribution of sand wedges (orange triangle) and ice-wedge pseudomorphs from the French database of periglacial features (see chapter 4, 5) and from the Northern Europe database (Isarin et al., 1998). GCMs : CCSM4 = National Center for Atmospheric Research, USA; GISS8_E2 = NASA Goddard Institute for Space Studies, USA; IPSL_CM5A = Institut Pierre-Simon Laplace, France; MIROC_ESM = Japan Agency for Marine-Earth Science and Technology, Japan; MPI_ESM = Max Planck Institute for Meteorology, Germany

The analysis of these maps and the distribution of the periglacial features from the French database and northern Europe database (Isarin et al., 1998) stressed the following points:

The coldest models are those from Institut Pierre-Simon Laplace (IPSL, France), and Max Planck Institute for Meteorology (MPI, Germany) and have a difference of ca. 5°C with the warmer model (National Center for Atmospheric Research, CCSM4, USA). All the simulations show MAATs isotherms parallel to the latitudes in northern France and that become slanted near the Bay of Biscay.

Considering the coldest model (IPSL) the distribution of ice-wedge pseudomorphs correlates roughly with the 0°C isotherm. Because ice-wedges in modern environments can form at MAATs of -4°C, the bias of this model is evaluated to at least 4°C. Part of Normandy, Champagne-Ardenne, Alsace, and Lorraine are amongst the areas that have potentially been affected by the growth of ice-wedges.

The southernmost sand-wedges in northern Aquitaine and the lower Rhône valley are located in areas subjected to similar climatic conditions that correspond to the 6°C isotherm in the IPSL model. Since

thermal contraction cracking can occur in MAATs up to +2°C in hyper-continental milieus (Romanovskij, 1976) the bias is also evaluated to at least 4°C.

The IPSL model suggests that France was not affected by continuous permafrost, even with a 4°C bias taken into account. In contrary, the simulation suggests that continuous permafrost affected England, the Netherlands, and the north of Germany. This is in agreement with the LPM map proposed (Chapter 5).

Dating of French sand-wedges shows an intricate thermal contraction cracking chronology, which question the model of periglaciation across France and Europe. Wedges inactivity should be taken with caution since numerous factors contribute to wedging that are not necessarily related to temperature (e.g. snow or vegetation cover, sand input). It is thus difficult to map the extent of permafrost or deep seasonal freezing during distinct periods of the Pleistocene with the data available, only broad trends can be identified as for example the LPM. In addition, more datings are needed to make up for the luminescence dating resolution. It is especially the case for the identified periods of wedging that are older than 35 ka, for which the amount of ages remains too low to be statistically significant. Further dating is also needed in direct association with ice-wedge pseudomorph levels in loess deposits to better understand the permafrost events. The implementation of an approach based on Bayesian chronological modelling that takes into account the stratigraphical constraints should also improve the representativeness and the accuracy of the identified phases of thermal contraction cracking or permafrost (Lanos and Dufresne, 2012).

Although quartz has proved to be a reliable dosimeter for dating sand-wedges, the saturated grains identified during our measurements indicate that other methods of dating should be considered in northern France where it is likely that MIS 8-10 wedging has been recorded. K- Feldspars have a higher saturation dose, which allows the potential to date much older deposits than quartz. However, feldspars are far from being readily datable because they often suffer from anomalous fading and consistent under-estimation of ages (e.g. Wintle, 1997). Despite methodological doubts raised (Buylaert et al., 2012), Infrared Radiofluorescence (IR-RF) of K-feldspar (Trautmann et al., 1999; Frouin et al., 2015, 2017) have a great potential to overcome these issues. Single-grain feldspar IRSL (Rhodes, 2015) also shows promising results.

A particular intention of this thesis was to combine the results of geomorphological work with GIS analysis and the OSL dating of features, in order ultimately to shed new light on how periglaciation

occurred in France. Such an interdisciplinary approach should be used and intensified in other regions to allow geographical and temporal comparisons. The advances in remote sensing analysis, luminescence and simulation methodologies hold a lot of promises, and should further ease the reconstructions and understanding of Pleistocene environments. Having a better grasp of the past is the key to better anticipate and adapt to the future.

References

Aitken, M.J., 1998. *An introduction to optical dating: The dating of Quaternary sediments by the use of photon-stimulated luminescence*. Oxford, Oxford University Press.

Allard, M., Seguin, M.K., 1987. The Holocene evolution of permafrost near the tree line, on the eastern coast of Hudson Bay (northern Quebec). *Canadian journal of Earth Sciences* 24, 11, 2206-2222.

Andrieux, E., Bertran, P., Saito K., 2016a. Spatial analysis of the French Pleistocene permafrost by a GIS database. *Permafrost and Periglacial Processes*, 27 (1), 17-30.

Andrieux, E., Bertran, P., Antoine, P., Deschodt, L., Lenoble, A., Coutard, S., 2016b. Database of pleistocene periglacial features in France: description of the online version », *Quaternaire*, 27/4, 329-339.

Andrieux, E., Bateman M., Bertran, P., 2017. The chronology of Late Pleistocene thermal contraction cracking in France. submitted

Antoine, P., 1989. Le complexe de sols de Saint-Sauflieu (Somme), micromorphologie et stratigraphie d'une coupe type du Début Weichsélien. *Publ. du Centre d'Etudes et de Recherches Préhistoriques* 1, 51-59.

Antoine, P., Rousseau, D.D., Zöller, L., Lang, A., Munaut, A.V., Hatté, C., Fontugne, M., 2001. High resolution record of the last Interglacial-glacial cycle in the Nussloch loess-palaeosol sequences, Upper Rhine Area Germany. *Quaternary International* 76-77, 211-229.

Antoine, P., Goval, E., Jamet, G., Coutard, S., Moine, O., Hérisson, D., Auguste, P., Guérin, G., Lagroix, F., Schmidt, E., Robert, V., Debenham, N., Meszner, S., Bahain, J.J., 2014. Les séquences Loessiques Pléistocène supérieur d'Havrincourt (Pas-de-Calais, France) : stratigraphie, paléoenvironnements, géochronologie et occupations paléolithiques. *Quaternaire*, 4, p. 321-368.

Antoine P., Locht J.L., 2015. Chronostratigraphie, paléoenvironnements et peuplements au Paléolithique moyen : les données du nord de la France. Les plaines du Nord-Ouest : carrefour de l'Europe au Paléolithique moyen? Actes de la table-ronde d'Amiens, 28-29 mars 2008, Depaepe, P., Goval, E., Koehler, H., Locht, J.L., *Mémoire de la Société Préhistorique Française*, 59 ,11-23.

Antoine, P., Coutard, S., Guerin, G., Deschodt, L., Goval, E., Locht, J.L., Paris, C., 2016. Upper Pleistocene loess-palaeosol records from Northern France in the European context: Environmental background and dating of the Middle Palaeolithic, *Quaternary International*, 411, A, 4-24.

Ballantyne CK, Harris C. 1994. T*he Periglaciation of Great Britain.* Cambridge University Press: Cambridge.

Becheler, P., 2014. L'origine tectono-karstique des lagunes de la region Villagrains-Landiras. *L'écho des Faluns, Saucats*, 35-36, 11-17.

Bertran, P., Andrieux, E., Antoine, P., Coutard, S., Deschodt, L., Gardère, P., Mercier, N., 2014. Distribution and chronology of Pleistocene permafrost features in France: database and first results. *Boreas* 43(3), 699-711

Bertran, P., Andrieux, E., Antoine, P., Deschodt, L., Font, M., Sicilia, D., 2017. Pleistocene involutions and patterned ground in France : examples and analysis using a GIS database. submitted.

Black, R.F., 1976. Periglacial features indicative of permafrost: ice and soil wedges. *Quaternary Research*, 6 (1), 3-26.

Bockheim, J.G., Kurz, M.D., Soule, S.A., Burke, A., 2009. Genesis of active sand-filled polygons in lower and central Beacon Valley, Antarctica. *Permafrost and Periglacial Processes*, 20, 295–308.

Böse, M., 1992: Late Pleistocene sand-wedge formation in the hinterland of the Brandenburg stade. *Sveriges Geologiska Undersökning Series Ca* 81, 59-63

Böse, M., 2000. Gravel analysis of Weichselian tills and OSL dates of sand wedges in western Poland. *Quaestiones Geographicae* 21, 39-44.

Boyé, M., 1958. Les lagunes du plateau landais. *Biuletyn Peryglacjalny* 26, 195–225.

Briant, R.M., Bateman, M.D., Russell Coope, G., Gibbard, P.L., 2005. Climatic control on Quaternary fluvial sedimentology of a Fenland Basin river, England. *Sedimentology,* 52, 1397-1423.

Büdel, J., 1960. Die Frostschott-zone Südost Spitzbergen. *Colloquium Geographica*, 6, 105 pp.

Buylaert, J.P., Ghysels, G., Murray, A.S., Thomsen, K.J., Vandenberghe, D., De Corte, F., Heyse, I., Van den Haute, P., 2009. Opticla dating of relict sand wedges and composite-wedge pseudomorphs in Flandders, Belgium. *Boreas*, 38, 160-175.

Buylaert, J.P., Jain, M., Murray, A.S., Thomsen, K.J., Lapp, T., 2012. IR-RF dating of sand-sized K-feldspar extracts: A test of accuracy. *Radiation Measurements* 47, 759–765.

Cailleux, A., 1948. Carte des actions périglaciaires quaternaires en France. *Bulletin du Service de la Carte Géologique de France*, 224, 33-39.

Calmels, F., Allard, M., Delisle, G., 2007. Development and decay of a lithalsa in Northern Quebec : a

geomorphological history. *Geomorphology* 97, 3, 287-289.

Christiansen, H.H., 1998. Periglacial sediments in an Eemian–Weichselian succession at Emmerlev Klev, southwestern Jutland, Denmark. *Palaeogeography, Palaeoclimatology, Palaeoecology* 138, 245–258.

Christiansen, H.H., Matsuoka, N., Watanabe, T., 2016. Progress in understanding the dynamics, internal structure and palaeoenvironmental potential of ice wedges and sand wedges. *Permafrost and Periglacial processes*, 27, 365–376.

Courbouleix, S., Mouroux, B., 1994. Les phénomènes périglaciaires en France: inventaire et intérêt en géoprospective. *Environnements périglaciaires, Association Française du Périglaciaire* 1, 109–114.

Courbouleix, S., Fleury, R., 1996. Mares, mardelles et pergélisol: exemple des dépressions circulaires de Sologne. *Environnements Périglaciaires* 3, 63–70.

Dubreuilh J., 1976. *Contribution à l'étude sédimentologique du système fluviatile Dordogne-Garonne dans la région bordelaise. Les ressources en matériaux alluvionnaires du département de la Gironde.* These, 273p.

Duller, G.A.T., 1991. Equivalent dose determination using single aliquots. *Nuclear Tracks and Radiation Measurements* 18, 371–378.

Ewertowski M., Kijowski A., Szuman, I., Tomczyk A.M., Kasprzak, L., 2016. Low-altitude remote sensing and GIS-based analysis of cropmarks: classification of past thermal-contraction-crack polygons in central western Poland. *Geomorphology*, in press.

Fàbiàn, S.A., Kovàcs, J., Varga, G., Sipos, G., Horvàth, Z., Thamo_Bozso, E., Toth, G., 2014. Distribution of relict permafrost features in the Pannonian Basin, Hungary. *Boreas*, 43, 722-732.

Feray, P., Coutard, S., Créteur, Y., Debenham, N., Deschodt, L., Lantoine, J., 2013. S*aint-Hilaire-sur-Helpe (Nord), «La Grande Pièce», carrière des Ardennes. Une série lithique du Début Glaciaire weichsélien*. 80 p. Rapport Final d'Opération de fouille, Inrap, Amiens.

Fortier, D., Allard, M., 2005. Frost-cracking conditions, Bylot Island, eastern Canadian Arctic archipelago. *Permafrost Periglac. Process.*, 16, 145-161

Frechen, M., Van Vliet-Lanoë, B.,Van den Haute, P., 2001. The Upper Pleistocene loess record at Harmignies/Belgium – High resolution terrestrial archive of climate forcing. *Palaeogeography, Palaeoclimatology, Palaeoecology* 173, 175–195.

French, H.M., 2007. *The Periglacial Environment, 3rd edition*. John Wiley & Sons: Chichester.

French, H.M., Demitroff, M., Forman, S.L., 2003. Evidence for late-Pleistocene permafrost in the New Jersey Pine Barrens (latitude 39°N), eastern USA. *Permafrost Periglac. Process.*, 14, 259–274.

Friedman, J.D, Johansson, C.E., Oskarsson, N., Svesson, H., Thorarinsson, S., Williams, J.R., 1971.

Observations on Icelandic polygon surfaces and palsa areas, photo interpretation and field studies. *Geografiska Annaler,* 53A, 3-4, 115–145.

Frouin, M., Huot, S., Mercier, N., Lahaye, C., Lamothe, M., 2015. The issue of laboratory bleaching in the infrared-radiofluorescence dating method. *Radiation Measurements* 81, 212–217.

Frouin, M., Huot, S., Kreutzer, S., Lahaye, C., Lamothe, M., Philippe, A., Mercier, N., 2017. An improved radiofluorescence single-aliquot regenerative dose protocol for K-feldspars. *Quaternary Geochronology* 38, 13–24.

Geyer, A., Folch, A., Marti, J., 2006. Relationship between caldera collapse and magma chamber withdrawal: an experimental approach. *Journal of Volvanology and Geothermal Research*, 157, 375-386.

Goval, E., Locht, J. L., 2009. Remontages, systèmes techniques et répartitions spatiales dans l'analyse du site weichselien ancien de Fresnoy-au-Val (Somme, France), *Bulletin de la Société préhistorique française*, 106, 4, 653-678.

Guhl, A., Bertran, P., Fitzsimmons, K.E., Zielhofer, C., 2013. Optically stimulated luminescence (OSL) dating of sand-filled wedges structures and their alluvial host sediments from Jonzac, SW France. *Boreas* 42, 317-332.

Haase, D., Fink, J., Haase, G., Ruske, R., Pecsi, M., Richter, H., Alterman, M., Jager, K.H., 2007.Loess in Europe: its spatial distribution based on a European loess map, scale 1–2 500 000. *Quaternary Science Reviews,* 26, 1301–1312.

Haesaerts, P., Juvigne, E., Kuyl, O., Mücher, H., Roebroeks, W., 1981. Compte rendu de l'excursion du 13 juin 1981, en Hesbaye et au Limbourg Néerlandais, consacrée à la chronostratigraphie des loess du Pléistocène supérieur, *Annales de la Société géologique de Belgique*, 104, p. 223-240.

Haesaerts, P., Damblon, F., Gerasimenko, N., Spagna, P., Pirson, S., 2016. The Late Pleistocene loess-palaeosol sequence of Middle Belgium. *Quaternary International*, 411, 25-43.

Harris, C., Murton, J.B., 2005. Experimental simulation of ice-wedge casting: Processes, products and palaeoenvironmental significance. In: Harris C., and Murton J.B., (eds.) *Cryospheric Systems: Glaciers and Permafrost*, 131–143. *London: Geological Society Special Publication* 242.

Huijzer, A.S., Vandenberghe, J., 1998. Climatic reconstruction of the Weichselian Pleniglacial in northwestern and central Europe. *Journal of Quaternary Science*, 13 (5), 391-417.

Isarin, R., Huijzer, B., van Huissteden, K., 1998. *Time-slice oriented multiproxy database (MPDB) for palaeoclimatie reconstruction.* National Snow and Ice Data Center, University of Boulder, Colorado. http://nsidc.org/data/ggd248.html

Jiraková, H., Huneau, F., Celle-Jeanton, H., Hrkal, Z., Le Coustumer, P., 2011. Insights into palaeorecharge conditions for European deep aquifers. *Hydrology Journal* 19, 1545–1562.

Jolivel, M., Bertran, P., Sicilia, D., 2016. *Projet SISMOGEL : Déformations des sols d'origine périglaciaire et sismique. Revue de littérature et exemples français.*

Kadereit, A., Kind, C.J., Wagner, G.A., 2013. The chronological position of the Lohne Woil in the Nussloch loess section – re-evaluation for a European loess-marker horizon. *Quaternary Science Reviews* 59, 67-89.

Kageyama, M., Laîné, A., Abe-Ouichi, A., Braconno, P., Cortijo, E., Crucifix, M., de Vernal, A., Guiot, J., Hewitt, C.D., Kitoh, A., Kucera, M., Marti, O., Ohgaito, R., Otto-Bliesner, B., Peltier, W.R., Rosell-Melé, A., Vettoretti, G., Weber, S.L., Yu, Y., MARGO Project Members. 2006. Last Glacial Maximum temperatures over the North Atlantic, Europe and western Siberia: a comparison between PMIP models, MARGO sea-surface temperatures and pollen-based reconstructions. *Quaternary Science Reviews* 25, 2082-2102.

Kasse, C.K., Bohncke, S., 1992. Weichselian Upper Pleniglacial aeolian and ice-cored morphology in the southern Netherlands (Noord-Brabant, Groote Peel). *Permafrost and Periglacial Processes* 3, 327–342.

Kasse, C., Vandenberghe, J., 1998. Topographic and drainage control on Weichselian ice-wedge and sand-wedge formation, Vennebrügge, German–Dutch border. *Permafrost and Periglacial Processes* 9, 95–106.

Kasse, C., Vandenberghe, J., de Corte, F., van den Haute, P., 2007. Late Weichselian fluvio-aeolian sands and coversands of the type locality Grubbenvorst (southern Netherlands): sedimentary environments, climate record and age. *Journal of Quaternary Science* 22, 7, 695–708.

Kitover, D.C., van Balen, R.T., Roche, D.M., Vandenberghe, J., Renssen, H., 2013. New estimates of permafrost evolution during the last 21 k years in Eurasia using numerical modelling. *Permafrost and Periglacial Processes* 24, 286–303.

Kjaer, K.H., Lagerlun, E., Adrielsson, L., Thomas, P.J., Murray, A., Sandgren, P., 2006. The first independent chronology of Middle and Late Weichselian sediments from southern Sweden and the island of Bornholm. *GFF*, 128, 209-220.

Kolstrup, E., 2004. Stratigraphic and Environmental Implications of a large ice-wedge cast at Tjaereborg, Denmark. *Permafrost and Periglacial Processes*, 15, 31-40.

Kolstrup, E., 2007. OSL dating in palaeoenvironmental reconstructions. A discussion from a user's perspective. *Estonian Journal of Earth Sciences*, 56, 157-166.

Kolstrup, E., Mejdhal, V., 1986. Three frost wedge casts from Jutland (Denmark) and TL dating of their infill. *Boreas* 15, 311-321.

Kovàcs, J., Fàbiàn, S.A., Schweitzer, F., Varga, G., 2007. A relict sand-wedge polygon site in north-central Hungary. *Permafrost and Periglacial Procecesses*. 18, 379-384.

Kreutzer, S., Lauer, T., Meszner, S., Krbetschek, M.R., Faust, D., Fuchs, M., 2012. Chronology of the

Quaternary profile Zeuchfeld in Saxony-Anhalt / Germany – a preliminary luminescence dating study. *Zeitschrift für Geomorphologie fast track,* 1–21.

Lachenbruch, A.H., 1962. Mechanics of the thermal contraction cracks and ice-wedge polygons in permafrost. *Geological Society of America Special Paper* 70.

Lachenbruch, A.H., 1966. Contraction theory of ice-wedge polygons: A qualitative discussion. In: *Permafrost International Conference, Proceedings, Lafayette, Indiana, 11–15 November 1963*, 63–71. Washington, DC: National Academy of Sciences. *National Research Council Publication* 1287.

Lanos, P., Dufresne, P., 2012. Modélisation statistique bayésienne des données chronologiques. In S. Archambault de Beaune, H.P. Francfort (eds.), *L'Archéologie à découvert.* CNRS Editions, Paris, 238-248.

Lautridou, J.P., 1985. *Le cycle périglaciaire pléistocène en Europe du nord-ouest et plus particulièrement en Normandie.* Thèse d'Etat, Université de Caen, 487 pp.

Lautridou, J.P., Sommé, J., 1981. L'extension des niveaux repères périglaciaires à grandes fentes de gel de la stratigraphie du Pléistocène récent dans la France du Nord-Ouest. *Biuletyn Peryglacjalny*, 28, 179-185.

Lautridou, J.P., Coutard, J.P., 1995. Le problème de l'extension et de la profondeur du pergélisol pléistocène en Normandie (France du Nord-Ouest). *Quaestiones Geographicae 4*, 201-203.

Lécolle, F., 1998. Que faire des dépressions fermées. *Quaternaire* 9, 101–104.

Lenoble, A., Bertran, P., Mercier, N., Sitzia L., 2012. *Le site du Lac Bleu et la question de l'extension du pergélisol en France au Pléistocène supérieur. Quaternaire continental d'Aquitaine: un point sur les travaux récents. Guidebook of the field excursion AFEQ-ASF 2012*. University of Bordeaux, AFEQ: 107–121.

Levavasseur, G., Vrac, M., Roche, D.M., Paillard, D., Martin, A., Vandenberghe, J., 2011. Present and LGM permafrost from climate simulations: contribution of statistical downscaling Climate of the Past, *Discussions* 7, 1647-1962.

Liard M., Tissoux, H., Deschamps, S., 2017. Les alluvions anciennes de la Loire en Orléanais (France, Loiret), une relecture à l'aune de travaux d'archéologie préventive et d'un programme de datations ESR. *Quaternaire*, 28 (1), 105-128.

Locht, J.L., Antoine, P., Bahain, J.J., Limondin-Lozouet, N., Gauthier, A., Debenham, N., Frechen, M., Dwrila, G., Raymond, P., Rousseau, D.D., Hatté, C., Haesaerts, P., Metsdagh, H., 2003. Le gisement paléolithique moyen et les séquences pléistocènes de Villiers-Adam (Val-d'Oise, France) : chronostratigraphie, Environnement et Implantations humaines, *Gallia Préhistoire*, 45, 1-111.

Locht, J. L., Antoine, P., Auguste, P., Bahain, J.J., Debeham, N., Falguères, C., Farkh, S., Tissoux, H., 2006. La séquence lœssique Pléistocène supérieur de Savy (Aisne, France): stratigraphie, datations et occupations paléolithiques. *Quaternaire*, 17, 269–275.

Maarleveld, G.C., 1976. Periglacial phenomena and the mean annual air temperature during the last glacial time in The Netherlands. *Biuletyn Periglacjalny,* 26, 57–78.

Mackay, J.R., 1993. Air temperature, snow cover, creep of frozen ground, and the time of ice-wedge cracking, western Arctic coast. *Canadian Journal of Earth Sciences*, 30 (8), 1720-1729.

Mejdahl, V., 1988. The plateau method for dating partially bleached sediments by thermoluminescence. *Quaternary Science Reviews* 7, 347-348.

Mejdahl, V., 1991. Thermoluminescence dating of Late Glacial sand sediments. Nuclear Tracks and *Radiation Measurements* 18, 71-75.

Mejdhal, V., Shlukov, A.I., Shakovets, S.A., Voskoskaya, L.T., Lyashenko, M.G., 1992. The effect of shallow traps: a possible source of error in TL dating of sediments. *Ancient TL* 10, 22-25.

Mejdahl, V., Bøtter-Jensen, L., 1994. Luminescence dating of archaeological materials using a new technique based on single aliquot measurements. *Quaternary Science Reviews (Quaternary Geochronology)* 7, 551–554.

Meszner, S., Kreutzer, S., Fuchs M., Faust, D., 2013. Late Pleistocene landscape dynamics in Saxony, Germany: Paleoenvironmental reconstruction using loess-paleosol sequences. *Quaternay International*, 296, 94-107.

Michel, J.P., 1967. Dépressions fermées dans les alluvions anciennes de la Seine à 100 km au S-E de Paris. *Bulletin de l'Association Française pour l'Etude du Quaternaire* 2, 131–134.

Murray, A.S., Olley, J.M. 2002. Precision and accuracy in the optically stimulated luminescence dating of sedimentary quartz: A status review. *Geochronometria* 21, 1-16

Murton, J.B., 2013. *Permafrost and Periglacial Features. Ice Wedges and Ice-Wedge Casts*. In Encyclopedia of Quaternary Science (Second Edition), Elsevier, Amsterdam, 436-451.

Murton, J.B., French, H.M., Lamothe, M., 1997. Late Wisconsinan erosion and eolian deposition, Summer Island area, Pleistocene Mackenzie Delta, Northwest Territories: Optical dating and implications for glacial chronology. *Canadian Journal of Earth Sciences* 34, 190–199.

Murton, J.B., Worsley, P., Gozdzik, J., 2000. Sand veins and wedges in cold aeolian environments. *Quaternary Science Reviews* 19, 899-922.

Murton, J., Kolstrup, E., 2003. Ice-wedge casts as indicators of palaeotemperatures: precise proxy or wishful thinking? *Progress in Physical Geography* 27, 155–170.

Murton, J. B., Bateman, M.D., 2007. Syngenetic sand veins and anti-syngenetic sand wedges, Tuktoyaktuk Coastlands, western Arctic Canada. *Permafrost and Periglacial Processes* 18, 33–47.

Owen, L.A., Richards, B., Rhodes, E.J., Cunningham, W.D., Windley, B.F., Badamgarav, J., Dorjnamjaa, D., 1998. Relic permafrost structures in the Gobi of Mongolia: Age and significance. *Journal of Quaternary*

Science 13, 539–547.

Péwé, T.L., 1959. Sand-wedge polygons (tessellations) in the McMurdo Sound Region, Antarctica a progress report. *American Journal of Science,* 257, 545-552.

Péwé, T.L., 1966. Palaeoclimatic significance of fossil ice wedges. *Biuletyn Peryglacjalny*, 5, 65-72.

Pissart A., 2002. Palsas, lithalsas and remnants of these periglacial mounds. A progress report. *Progress in Physical Geography* 26 (4), 605-621.

Poser, H., 1948. Boden- und Klimaverhältnisse im Mittle- und Westeuropa während der Würmeiszeit. *Erdkunde* 2, 53-68.

Remillard, A.M., Hetu, B., Bernatchez, P., Buylaert, J.P., Murray, A.S., St-Onge, G., Geach, M., 2015. Chronology and palaeoenvironmental implications of the ice-wedge pseudomorphs and compositewedge casts on the Magdalen Islands (eastern Canada). *Boreas* 44, 658-675.

Renssen, H.,Vandenberghe, J., 2003. Investigation of the relationship between permafrost distribution in NW Europe and extensive winter sea-ice cover in the NorthAtlantic Ocean during the cold phases of the Last Glaciation. *Quaternary Science Reviews* 22, 209–223.

Rhodes E.J., 2015. Dating sediments using potassium feldspar single-grain IRSL : Initial methodological considerations. *Quaternary International,* 362, 14-22.

Romanovskij, N.N., 1976. The scheme of correlation of polygonal wedge structures. *Biuletyn Peryglacjalny,* 26, 287-294.

Ross, N., Harris, C., Brabham, P.J., Sheppard, T.H., 2011. Internal structure and geological context of ramparted depressions, Llanpumsaint, Wales. *Permafrost and Periglacial Processes* 22, 4, 291-305.

Saito, K., Sueyoshi, T., Marchenko, S., Romanovsky, V., Otto-Bliesner, B., Walsh, J., Bigelow, N., Hendricks, A., Yoshikawa, K., 2013. LGM permafrost distribution: how well can the latest PMIP multi-model ensembles perform reconstruction? *Climate of the Past* 9, 1697–1714.

Saltel, M., Lavielle, B., Thomas, B., Rebeix, R., Franceschi, M., 2016. Etude sur la paléo-recharge des aquifères du nord du Bassin aquitain par l'utilisation de traceurs isotopiques et des gaz rares. Application à la paléoclimatologie. *Résumés du Colloque Q10, AFEQ-CNF INQUA, Bordeaux,* p. 37.

Sitzia, L., 2014. *Chronostratigraphie et distribution spatiale des dépôts éoliens du Bassin Aquitain.* Université de Bordeaux, Bordeaux. PhD thesis.

Sitzia, L., Bertran, P., Bahain, J.J., Bateman, M.D., Hernandez, M., Garon, H., De Lafontaine, G., Mercier, N., Leroyer, C., Queffelec A., Voinchet, P., 2015. The quaternary coversands of southwest France. *Quaternary Science Reviews*, 124, 84-105.

Texier, J.P., 2011. Genèse des lagunes landaises: un point sur la question. In : De la lagune à l'airial: le peuplement de la Grande Lande, Merlet, J.C., Bost, J.P. (eds). *Aquitania suppl.* 24. Pessac; 23-42.

Texier, J.P., Bertran, P., 1993: Données nouvelles sur la présence d'un pergélisol en Aquitaine au cours des dernières glaciations. Permafrost and Periglacial Processes 4, 183–198.

Tissoux, H., Prognon, F., Martelet, G., Tourliere, B., Despriée, J., Liard, M., Lacquement, F., 2017. Contribution de la spectrométrie gamma aéroportée à la caractérisation et à la cartographie des dépôts silico-clastiques fluviatiles dans le val de Loire et en Sologne (Centre, France). *Quaternaire,* 28 (1), 87-103.

Trautmann, T., Krbetschek, M.R., Dietrich, A., Stolz, W., 1999. Feldspar radioluminescence: a new dating method and its physical background. *Journal of Luminescence* 85, 45–58.

Tricart, J., 1956. *Carte des phénomènes périglaciaires quaternaires en France.* 40 p. Mémoire pour servir à l'explication de la carte géologique détaillée de la France, Ministère de l'Industrie et du Commerce, Paris.

Tuffreau, A., Revillion, S., Sommé, J., Van Vliet-Lanoë, B., 1994. Le gisement paléolithique moyen de Seclin (Nord), *Bulletin de la Société préhistorique française*, 91, 1, 23-46.

Vandenberghe, J., 1983. Ice-wedge casts and involutions as permafrost indicators and their stratigraphic position in the Weichselian. *Proceedings of the 4th International Conference on Permafrost, Fairbanks, Alaska,* 1, 1298-1302.

Vandenberghe J., Kasse, C., 1993. Periodic ice-wedge formation and weichselian cold-climate floodplain sedimentation in the Netherlands. *Proceedings of 6th International Conference on Permafrost 1, Beijing*, 643–647.

Vandenberghe, J., Pissart, A., 1993. Permafrost changes in Europe during the last glacial. *Permafrost and Periglacial Processes*, 4 (2), 121-135.

Vandenberghe, J., Renssen, H., Roche, D.M., Goose, H., Velichko, A.A., Gorbunov, A., Levavasseur, G., 2012. Eurasian permafrost instability constrained by reduced sea-ice cover. *Quaternary Science Reviews* 34, 16–23.

Vandenberghe, J., French, H., Gorbunov, A., Marchenko, S., Velichko, A.A., Jin, H., Cui, Z., Zhang, T., Wan, X., 2014. The Last permafrost Maximum (LPM) map of the Northern Hemisphere: permafrost extent and mean annual air temperatures, 25-17 ka. *Boreas* 43, 652-666.

Van Vliet-Lanoë, B., 1989. Dynamics and extent of the Weichselian permafrost in western Europe (substage 5e to stage 1). *Quaternary International,* 3-4, 109-113.

Van Vliet-Lanoë, B., 1996. Relations entre la contraction thermique des sols en Europe du Nord-Ouest et la dynamique de l'inlandsis weichselien. Comptes-rendus de l'Académie des Science Paris, 322 (série IIa), 461-468.

Van Vliet-Lanoë, B., Hallégouët, B., 2001. European permafrost at the LGM and at its maximal extent. The geological approach. In: Permafrost Response on Economic Development, Environmental Security

and Natural Resources, Paepe, R., Melnikov, V. (eds). *Kluwer Academic Publishers: Dordrecht*, 195–213.

Van Vliet-Lanoë, B., Brulhet, J., Combes, P., Duvail, C., Ego, F., Baize, S., Cojan, I. 2016. Quaternary thermokarst and thermal erosion features in northern France: origin and palaeoenvironments. *Boreas.* 10.1111/bor.12221. ISSN 0300-9483.

Velichko, A.A. 1982. *Palaeogeography of Europe during the Last One Hundred Thousand Years.* Nauka, Moscow.

Washburn, A.L., 1979. *Geocryology - A survey of periglacial processes and environment*. Arnold Publications: London.

Washburn, A.L., Smith, D., Goddard, R., 1963. Frost cracking in a Middle Latitude climate. *Biuletyn Peryglacjalny*, 12, 175-189.

Watson, E., Watson, S., 1974. Remains of pingos in the Cletwr basin, south-west Wales. *Geografiska Annaler* 56A, 213–225.

Wintle, A.G., 1997. Luminescence dating: Laboratory procedures and protocols. *Radiation Measurements* 27, 769-817.

Wolfe, S.A., Morse, P.D., Kokelj, S.V., Neudorf, C.M., Lian, O.B., 2016. Contrasting environments of sand wedge formation in discontinuous permafrost, Great Slave High Boreal Plains, Northwest Territories, Canada. *Abstracts, 11th international conference on permafrost, 20-24 June 2016, Potsdam, Germany,* 112.

Zielinski, P., Sokołowski, R.J., Fedorowicz, S., Zaleski, I. 2014. Periglacial structures within fluvio-aeolian successions of the end of the Last Glaciation - examples from SE Poland and NW Ukraine. *Boreas,* 43, 712–721.

Appendix

Figure S1: Schematic diagram of the Mérignac Parking Chronopost cross-section (44.827°N, 0.689°W). Fm=alluvial loam, Gp=Oblique gravel beds, Gh=horizontal gravel beds